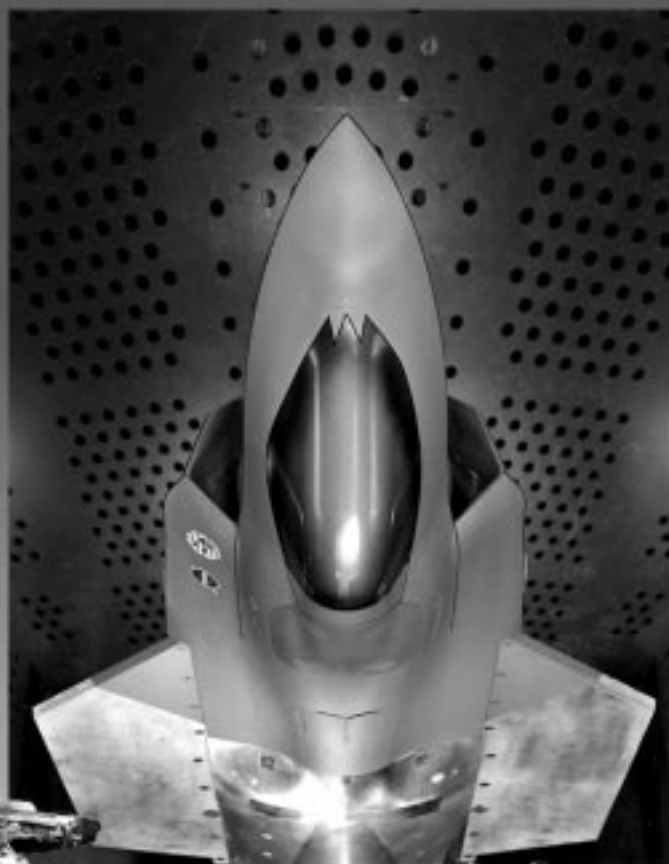
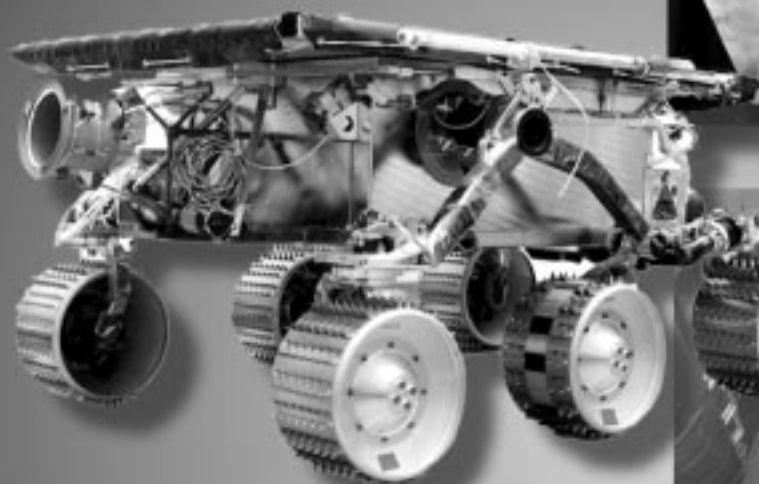


# R&T

## 1997

Research &  
Technology



NASA Lewis  
Research Center  
Cleveland, Ohio



NASA/TM—1998-206312

**About the cover:**

Left: Mars Pathfinder Sojourner rover showing Lewis' Wheel Abrasion Experiment (p. 31) on a special section of the center wheel. This experiment measured abrasion to analyze the consistency of the Martian soil. Two other Lewis experiments were conducted on the Sojourner rover: electrostatic charging experiments (p. 32), which measured the accumulation of static charge, and the Materials Adherence Experiment, which measured dust accumulation (p. 34) to assess its potential interference on solar panels. In addition, Lewis helped test the air-bag landing system for the Mars Pathfinder, modeled solar energy on Mars to determine solar panel requirements, and provided tungsten points for removing potentially damaging electrostatic charge from the rover. Visit Lewis on the World Wide Web to find out more about our involvement in the Mars Pathfinder mission (<http://www.lerc.nasa.gov/WWW/PAO/html/marspath.htm>).

Top right: Joint Strike Fighter model installed in Lewis' 8- by 6-Foot Supersonic Wind Tunnel (p. 87).

Bottom right: Astronaut crew training performed onboard Lewis' DC-9 aircraft (p. 134) in preparation for the Microgravity Science Laboratory missions flown on the Space Shuttle Columbia in April and July of 1997.

# Research & Technology 1997



National Aeronautics and  
Space Administration

**Lewis Research Center**  
Cleveland, Ohio 44135

NASA/TM—1998-206312

Trade names or manufacturers' names are used in this report for identification only. This usage does not constitute an official endorsement, either expressed or implied, by the National Aeronautics and Space Administration.

Available from

NASA Center for Aerospace Information  
Parkway Center  
7121 Standard Drive  
Hanover, MD 21076-1320

National Technical Information Service  
5287 Port Royal Road  
Springfield, VA 22100  
Price Code: A08



# Introduction

NASA Lewis Research Center is responsible for developing and transferring critical technologies that address national priorities in aeropropulsion and space applications in partnership with U.S. industries, universities, and Government institutions.

As NASA's designated Lead Center for Aeropropulsion, our role is to develop, verify, and transfer aeropropulsion technologies to U.S. industry. As NASA's designated Center of Excellence in Turbomachinery, our role is to develop new and innovative turbomachinery technology to improve the reliability, performance, efficiency and affordability, capacity, and environmental compatibility of future aerospace vehicles. We also maintain a science and

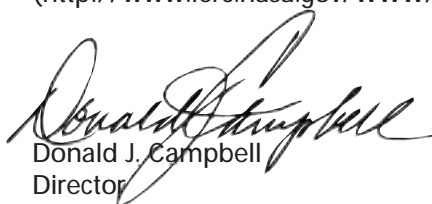
technology development role in aeropropulsion, communications, space power and onboard propulsion, and microgravity fluid physics and combustion. We are committed to enabling nonaerospace U.S. industries to benefit directly from the technologies developed through our programs to maximize the benefit to the Nation and the return on each taxpayer's investment. In addition, we are aggressively pursuing continuous improvement in our management and business practices and striving for diversity in our workforce as together we push the edge of technology in space and aeronautics.

The Lewis Research Center is a unique facility located in an important geographical area, the southwest corner of Cleveland, Ohio. Situated on 350 acres of land adjacent to the Cleveland Hopkins International Airport, Lewis comprises more than 140 buildings that include 24 major facilities and over 500 specialized research and test facilities. Additional facilities are located at Plum Brook Station, which is about 50 miles west of Cleveland.

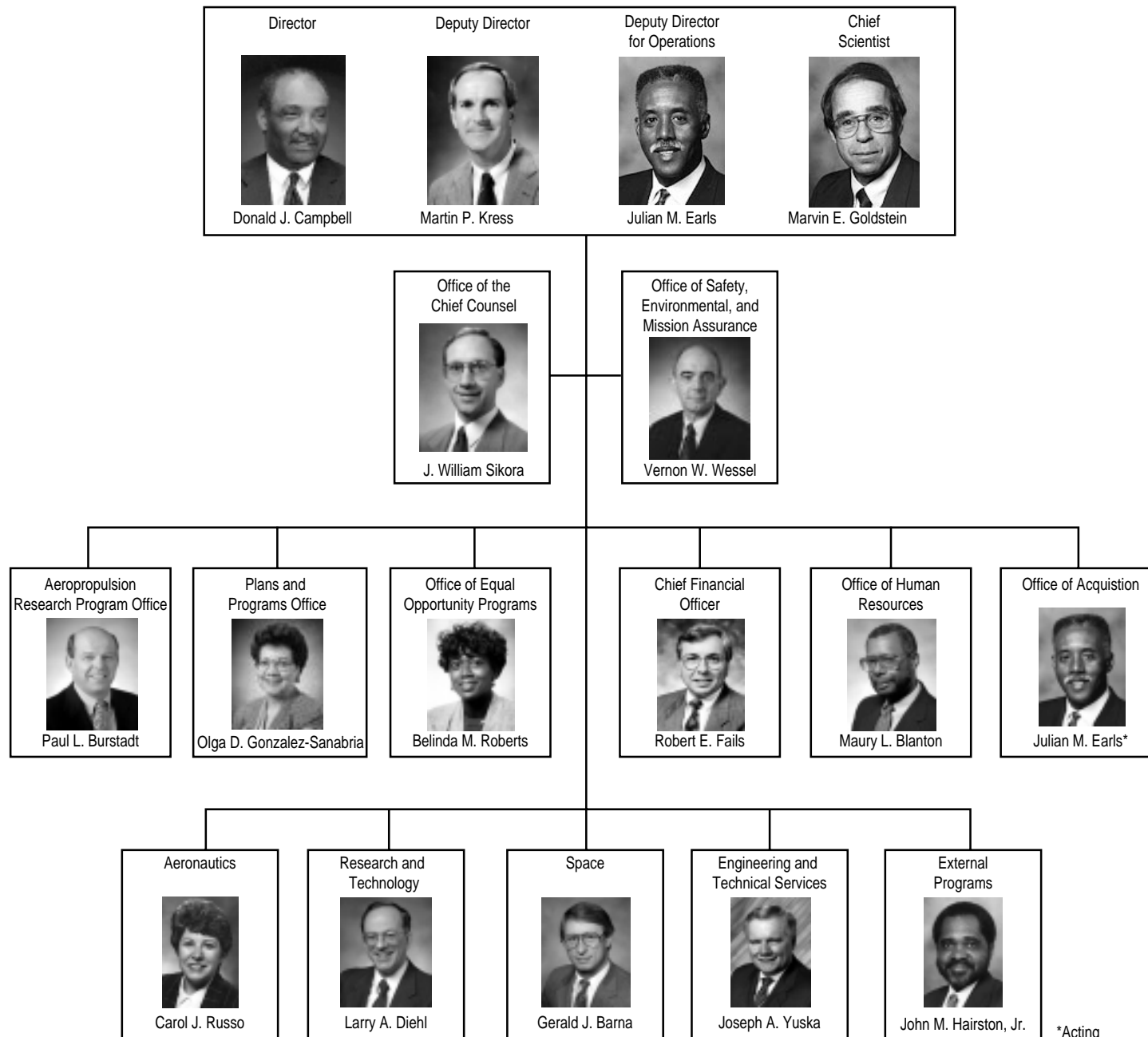
Over 3700 people staff Lewis, including civil service employees and support service contractors. Over half of them are scientists and engineers, who plan, conduct or oversee, and report on our research tasks and projects. They are assisted by technical specialists, skilled workers, and an administrative staff.

Our end product is knowledge. This report is designed to help us make this knowledge fully available to potential users—the aircraft engine industry, the energy industry, the automotive industry, the aerospace industry, and others. It is organized so that a broad cross section of the community can readily use it. Each article begins with a short introductory paragraph that should prove to be a valuable tool for the layperson. These articles summarize the progress made during the year in various technical areas and portray the technical and administrative support associated with Lewis' technology programs.

We hope that the information is useful to all. If additional information is desired, readers are encouraged to contact the researchers identified in the articles and to visit Lewis on the World Wide Web (<http://www.lerc.nasa.gov/>). This document is available on the World Wide Web (<http://www.lerc.nasa.gov/WWW/RT/>).

  
Donald J. Campbell  
Director

# NASA Lewis Research Center Senior Management

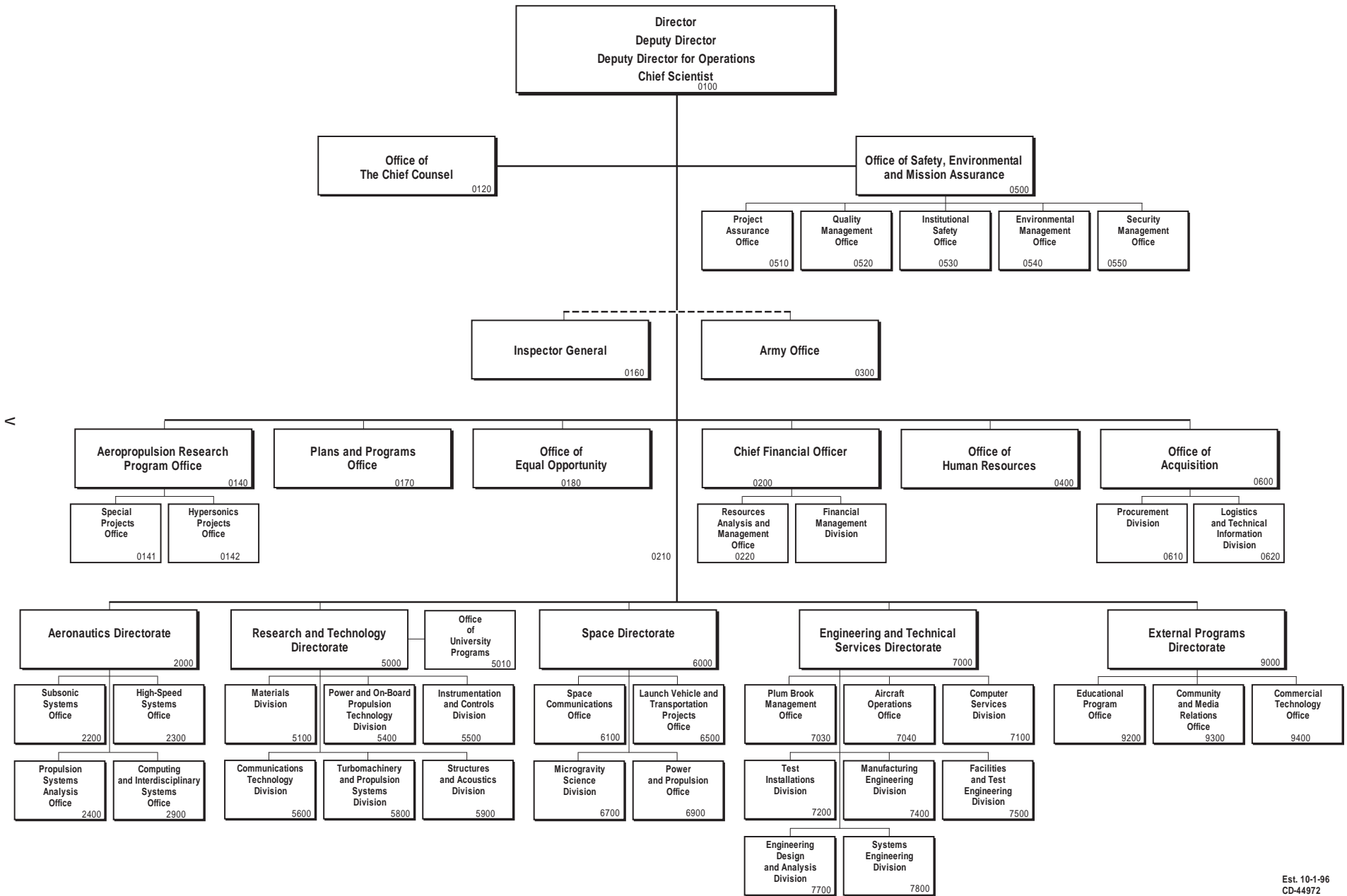


\*Acting

CD-48534

December 1997

# NASA Lewis Research Center





The Quality Council was established in October 1992 to adopt and implement a Total Quality (TQ) plan for Lewis. It is composed of Executive Council members as well as the president of the American Federation of Government Employees (AFGE), Local 2812, and the president of the Lewis Engineers and Scientists Association (LESA), IFPTE Local 28. A representative of major onsite support service contractors serves as a liaison.



# Contents

## Aeronautics

### *High Speed Systems*

High Speed Research—Propulsion Project Accomplishments .....	2
--	---

### *Propulsion Systems Analysis*

Minimum Climb to Cruise Noise Trajectories Modeled for the High Speed Civil Transport .....	3
Inlet Performance Analysis Code Developed .....	4
Conceptual Design Method Developed for Advanced Propulsion Nozzles .....	5

### *Computing and Interdisciplinary Systems*

Multiphysics Code Demonstrated for Propulsion Applications .....	6
Flow of a Gas Turbine Engine Low-Pressure Subsystem Simulated .....	8

## Research and Technology

### *Materials*

Assessing the Resistance of $\gamma$ -Ti-47Al-2Nb-2Cr (at.%) to Foreign Object Damage .....	12
Strengthening Precipitate Morphologies Fully Quantified in Advanced Disk Superalloys .....	13
High-Temperature Compressor Material Development .....	15
Method Developed for the High-Temperature Nondestructive Evaluation of Fiber-Reinforced Silicon Carbide Ceramic Matrix Composites .....	16
Interfacial Thickness Guidelines for SiC <sub>Fiber</sub> /SiC <sub>Matrix</sub> Composites .....	17
Stable Boron Nitride Interphases for Ceramic Matrix Composites .....	18
Cyclic Fiber Push-In Test Monitors Evolution of Interfacial Behavior in Ceramic Matrix Composites .....	19
Tribometer for Lubrication Studies in Vacuum .....	20
Computational Chemistry and Lubrication .....	22
“Green” High-Temperature Polymers .....	23
Low-Cost Manufacturing of High-Temperature Polymer Composites .....	24
Residual Stresses Modeled in Thermal Barrier Coatings .....	25
Oxidation of Boron Nitride in Composites .....	27
Carbon-13 Labeling Used to Probe Cure and Degradation Reactions of High-Temperature Polymers .....	28
Thermal High- and Low-Cycle Fatigue Behavior of Thick Thermal Barrier Coating Systems .....	30

### *Power and On-Board Propulsion Technology*

Wheel Abrasion Experiment Conducted on Mars .....	31
Results From Mars Show Electrostatic Charging of the Mars Pathfinder Sojourner Rover .....	32
Measuring Dust on Mars .....	34
Lightweight Nickel Electrode Development Program .....	35
Systems Analysis in Support of the NASA Fuel Cell Upgrade Program for the Space Shuttle Orbiter .....	36
Bipolar Nickel-Metal Hydride Battery Being Developed .....	37
Electrolysis Propulsion Provides High-Performance, Inexpensive, Clean Spacecraft Propulsion .....	38
“Green” Monopropellant Developed for Spacecraft .....	40
Power Management and Distribution System Developed for Thermionic Power Converters .....	41
Advanced Electric Distribution, Switching, and Conversion Technology for Power Control .....	42
Soft X-Ray Exposure Testing of FEP Teflon for the Hubble Space Telescope .....	43
Evaluation of Low-Earth-Orbit Environmental Effects on International Space Station Thermal Control Materials .....	44

Integrated Solar Upper Stage Technical Support .....	46
High-Voltage 1-kW dc/dc Converter Developed for Low-Temperature Operation .....	47
Atomic Oxygen Cleaning Shown to Remove Organic Contaminants at Atmospheric Pressure ..	48
Refractive Secondary Solar Concentrator Being Designed and Developed .....	49
Aerospace Power Systems Design and Analysis (APSDA) Tool .....	51

### ***Instrumentation and Controls***

Drag Force Anemometer Used in Supersonic Flow .....	52
Attachment of Free Filament Thermocouples for Temperature Measurements on Ceramic Matrix Composites .....	53
Silicon Carbide Mixers Demonstrated to Improve the Interference Immunity of Radio-Based Aircraft Avionics .....	54
Silicon Carbide Junction Field Effect Transistor Digital Logic Gates Demonstrated at 600 °C ...	56
Chemical Mechanical Polishing of Silicon Carbide .....	57
Model-Trained Neural Networks and Electronic Holography Demonstrated to Detect Damage in Blades .....	58
Particle Imaging Velocimetry Used in a Transonic Compressor Facility .....	59
Jet Injection Used to Control Rotating Stall in a High-Speed Compressor .....	60
Distortion Tolerant Control Demonstrated In Flight .....	61
Active Pattern Factor Control for Gas Turbine Engines .....	62
Real-Time Sensor Validation System Developed .....	64

### ***Communications Technology***

Asynchronous Transfer Mode Quality-of-Service Testing .....	65
Satellite-Terrestrial Network Interoperability .....	66
High-Temperature Superconducting/Ferroelectric, Tunable, Thin-Film Microwave Components .....	67
Reflectarray Demonstrated to Transform Spherical Waves Into Plane Waves .....	69

### ***Turbomachinery and Propulsion Systems***

Wave Rotor Research and Technology Development .....	70
Low-Pressure Turbine Flow Physics Program .....	72
LSPRAY: Lagrangian Spray Solver for Applications With Parallel Computing and Unstructured Gas-Phase Flow Solvers .....	73
EUPDF: Eulerian Monte Carlo Probability Density Function Solver for Applications With Parallel Computing, Unstructured Grids, and Sprays .....	74
Three-Dimensional Measurements of Fuel Distribution in High-Pressure, High-Temperature, Next-Generation Aviation Gas Turbine Combustors .....	75
Mixing of Multiple Jets With a Confined Subsonic Crossflow .....	77
Advanced Subsonic Combustion Rig .....	78
Time-Resolved Optical Measurements of Fuel-Air Mixedness in <i>Windowless</i> High Speed Research Combustors .....	79
Advanced Fuels Can Reduce the Cost of Getting Into Space .....	80
Metallized Gelled Propellants: Heat Transfer of a Rocket Engine Fueled by Oxygen/RP-1/ Aluminum Was Measured by a Calorimeter .....	82
F100 Engine Emissions Tested in NASA Lewis' Propulsion Systems Laboratory .....	84
Microblowing Technique Demonstrated to Reduce Skin Friction .....	85
Effect of Installation of Mixer/Ejector Nozzles on the Core Flow Exhaust of High-Bypass-Ratio Turbofan Engines .....	86
Forebody/Inlet of Joint Strike Fighter Tested at Low Speeds .....	87
Lift Fan Nozzle for Joint Strike Fighter Tested in NASA Lewis' Powered Lift Rig .....	88
New Nozzle Test Rig Developed .....	89
Resonance of Twin Jet Plumes Studied .....	90
Design Concepts Studied for the Hydrogen On-Orbit Storage and Supply Experiment .....	91

Vented Tank Resupply Experiment Demonstrated Vane Propellant Management Device for Fluid Transfer .....	93
Recent Advancements in Propellant Densification .....	94
Parametric Study Conducted of Rocket-Based, Combined-Cycle Nozzles .....	95

### ***Structures and Acoustics***

Design Process for High Speed Civil Transport Aircraft Improved by Neural Network and Regression Methods .....	97
Thermal Effects Modeling Developed for Smart Structures .....	98
Procedure Developed for Ballistic Impact Testing of Composite Fan Containment Concepts ..	99
Mechanical Characterization of the Thermomechanical Matrix Residual Stresses Incurred During MMC Processing .....	100
Test Standard Developed for Determining the Slow Crack Growth of Advanced Ceramics at Ambient Temperature .....	102
Accelerated Testing Methodology Developed for Determining the Slow Crack Growth of Advanced Ceramics .....	103
Constitutive Theory Developed for Monolithic Ceramic Materials .....	104
Noncontact Determination of Antisymmetric Plate Wave Velocity in Ceramic Matrix Composites .....	105
Experimental Techniques Verified for Determining Yield and Flow Surfaces .....	108
Cares/ <i>Life</i> Ceramics Durability Evaluation Software Used for Mars Microprobe Aeroshell ...	109
Continuum Damage Mechanics Used to Predict the Creep Life of Monolithic Ceramics ....	110
Single-Transducer, Ultrasonic Imaging Method for High-Temperature Structural Materials Eliminates the Effect of Thickness Variation in the Image .....	111
Neural Network Control of a Magnetically Suspended Rotor System .....	112
Feasibility of Using Neural Network Models to Accelerate the Testing of Mechanical Systems .....	114
Magnetic Suspension for Dynamic Spin Rig .....	115
High-Temperature Magnetic Bearings Being Developed for Gas Turbine Engines .....	117
Integrated Fiber-Optic Light Probe: Measurement of Static Deflections in Rotating Turbomachinery .....	118
Damping Experiment of Spinning Component Plates With Embedded Viscoelastic Material .	118
Lewis-Developed Seal Is a Key Technology for High-Performance Engines .....	119

## **Space**

### ***Microgravity Science***

Droplet Combustion Experiment .....	122
Fiber-Supported Droplet Combustion Experiment-2 .....	124
Laminar Soot Processes Experiment Is Shedding Light on Flame Radiation .....	125
Structure of Flame Balls at Low Lewis-Number .....	127
Physics of Hard Spheres Experiment (PhaSE) or "Making Jello in Space" .....	128
Liquid-Vapor Interface Configurations Investigated in Low Gravity .....	130
NASA Lewis' Telescience Support Center Supports Orbiting Microgravity Experiments ....	131
Capillary-Driven Heat Transfer Experiment: Keeping It Cool in Space .....	132
Ground-Based Reduced-Gravity Facilities .....	134

### ***Power and Propulsion***

Pulsed Plasma Thruster Technology Development and Flight Demonstration Program ....	136
Liquid Motion Experiment Flown on STS-84 .....	138
Closed Cycle Engine Program Used in Solar Dynamic Power Testing Effort .....	139
Dark Forward Electrical Test Techniques Developed for Large-Area Photovoltaic Arrays ....	140
On-Orbit Electrical Performance of a Mir Space Station Photovoltaic Array Predicted .....	142
Radiation Heat Transfer Modeling Improved for Phase-Change, Thermal Energy Storage Systems .....	143

High-Temperature, High-Flux Multifoil Shield Developed for Space Applications .....	145
Solar Electric Propulsion for Mars Exploration .....	146
Space Station Radiator Test Hosted by NASA Lewis at Plum Brook Station .....	147
Improving Safety and Reliability of Space Auxiliary Power Units .....	148

## Engineering and Technical Services

### *Computer Services*

Antiterrorist Software .....	152
Worldwide Research, Worldwide Participation: Web-Based Test Logger .....	154
Real-Time, Interactive Echocardiography Over High-Speed Networks: Feasibility and Functional Requirements .....	155

### *Manufacturing Engineering*

Electron Beam Welder Used to Braze Sapphire to Platinum .....	156
---	-----

### *Facilities and Test Engineering*

New Spray Bar System Installed in NASA Lewis' Icing Research Tunnel .....	157
Luminescent Paints Used for Rotating Temperature and Pressure Measurements on Scale-Model High-Bypass-Ratio Fans .....	158
New Model Exhaust System Supports Testing in NASA Lewis' 10- by 10-Foot Supersonic Wind Tunnel .....	160
Process Developed for Forming Urethane Ice Models .....	161

### *Engineering Design and Analysis*

Manipulating Liquids With Acoustic Radiation Pressure Phased Arrays .....	162
Statistical Treatment of Earth Observing System Pyroshock Separation Test Data .....	163
New Test Section Installed in NASA Lewis' 1- by 1-Foot Supersonic Wind Tunnel .....	164
Embedded Web Technology: Internet Technology Applied to Real-Time System Control ...	165

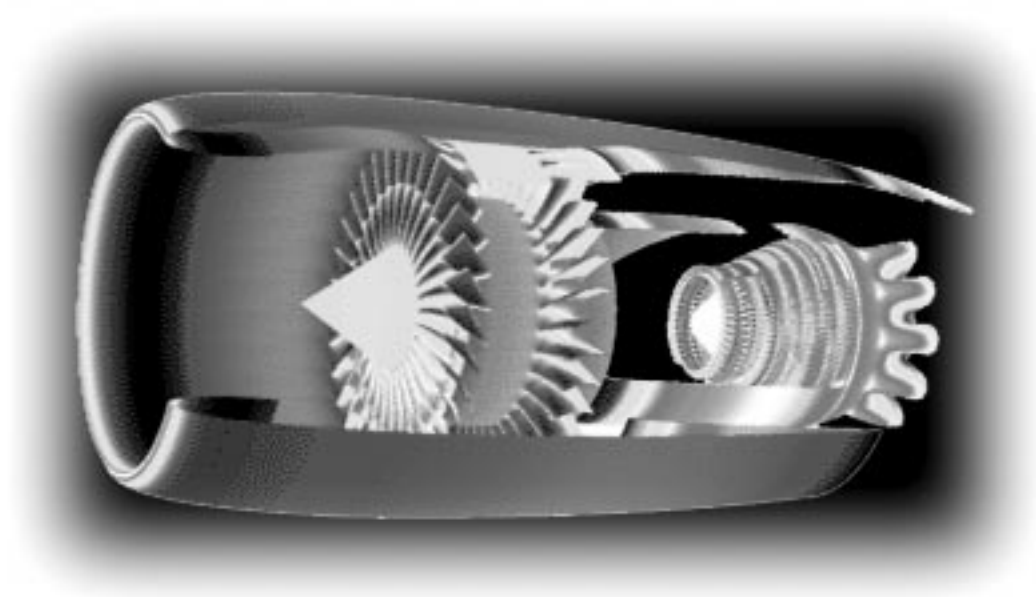
## Commercial Technology

NASA Lewis Helps Company With New Single-Engine Business Turbojet .....	168
NASA Lewis Helps Develop Advanced Saw Blades for the Lumber Industry .....	169
Modeling Code Is Helping Cleveland Develop New Products .....	170
Electronics Manufacturer Provided With Testing and Evaluation Data Necessary to Obtain Additional Orders .....	171
NASA Lewis' Icing Research Tunnel Works With Small Local Company to Test Coatings ....	172
NASA Lewis and Ohio Company Hit Hole in One .....	173
New Research Methods Developed for Studying Diabetic Foot Ulceration .....	174

## Appendixes

NASA Headquarters Program Offices .....	175
Programs and Projects That Support or Will Benefit From This Research .....	176
Index of Authors and Contacts .....	178

# Aeronautics



# High Speed Systems

## High Speed Research—Propulsion Project Accomplishments

This past year has been one of great accomplishment for the propulsion element of NASA's High Speed Research (HSR) Program. The HSR Program is a NASA/industry partnership to develop the high-risk/high-payoff air-frame and propulsion technologies applicable to a second-generation supersonic commercial transport, or High Speed Civil Transport (HSCT). The propulsion element, which also involves industry partners, is managed by the NASA Lewis Research Center. These technologies will contribute greatly to U.S. industry's ability to make an informed product launch decision for an HSCT vehicle. Specific NASA Lewis accomplishments in 1997 include

- Small-scale combustor sector tests conducted in Lewis' Engine Research Building contributed to the evolution of approaches to developing a combustor with ultralow NO<sub>x</sub> emissions.
- Components were tested in Lewis' CE-9 facility (in Lewis' Engine Research Building) to assess the performance of candidate ceramic matrix composite (CMC) materials in this realistic combustion environment. Test results were promising, and acceptable levels of structural durability were demonstrated for the ceramic matrix composite material tested. Ceramic matrix composites continue to show great promise for use in HSCT combustor liners.
- Engine emissions tests in Lewis' Propulsion Systems Laboratory provided insight into other classes of emissions (e.g., particulates and aerosols) which will be important to control in HSCT propulsion system designs.
- Small-scale nozzle tests conducted in Lewis' Aero-Acoustic Propulsion Laboratory are contributing to the design of a low-noise, high-performance mixer/ejector nozzle configuration for HSCT engines.
- Over 18,000 hours of durability testing were completed in Lewis' materials laboratories to evaluate superalloy and  $\gamma$ -titanium aluminide performance for HSCT nozzle applications.
- A two-dimensional supersonic inlet concept was tested in Lewis' 10- by 10-Foot Supersonic Wind Tunnel. The extensive database and the knowledge gained contributed to the selection of a two-dimensional inlet as the preferred inlet concept for the HSR Program.

**For more information, visit Lewis' HSR and aeropropulsion facility sites on the World Wide Web:**

**HSR:** <http://www.lerc.nasa.gov/WWW/HSR/>

**Engine Research Building:** <http://www.lerc.nasa.gov/WWW/AFED/facilities/erb.html>

**Propulsion Systems Laboratory:** <http://www.lerc.nasa.gov/WWW/AFED/facilities/psl.html>

**Aero-Acoustic Propulsion Laboratory:** <http://www.lerc.nasa.gov/WWW/AFED/facilities/aapl.html>

**10- by 10-Foot Supersonic Wind Tunnel:** <http://www.lerc.nasa.gov/WWW/AFED/facilities/10x10.html>

**Lewis contacts:**

Dr. Robert J. Shaw, (216) 977-7135, [Robert.J.Shaw@lerc.nasa.gov](mailto:Robert.J.Shaw@lerc.nasa.gov), and  
Lori A. Manthey, (216) 433-2484, [Lori.A.Manthey@lerc.nasa.gov](mailto:Lori.A.Manthey@lerc.nasa.gov)

**Author:** Dr. Robert J. Shaw

**Headquarters program office:** OASTT

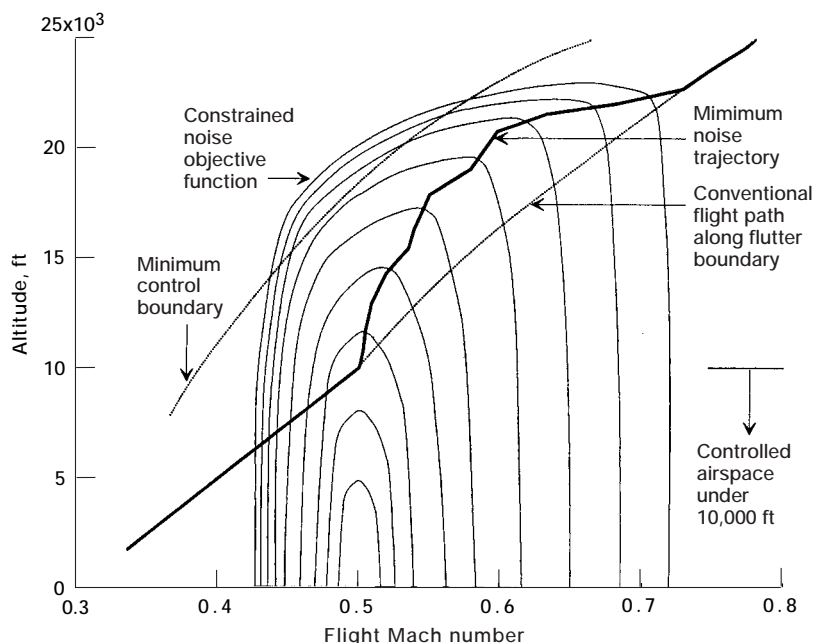
**Programs/Projects:** HSR, HSCT



# Propulsion Systems Analysis

## Minimum Climb to Cruise Noise Trajectories Modeled for the High Speed Civil Transport

The proposed U.S. High Speed Civil Transport (HSCT) will revolutionize commercial air travel by providing economical supersonic passenger service to destinations worldwide. Unlike the high-bypass turbofan engines that propel today's subsonic airliners, HSCT engines will have much higher jet exhaust speeds. Jet noise, caused by the turbulent mixing of high-speed exhaust with the surrounding air, poses a significant challenge for HSCT engine designers. To resolve this challenge, engineers have designed advanced mixer-ejector nozzles that reduce HSCT jet noise to airport noise certification levels by entraining and mixing large quantities of ambient air with the engines' jet streams. Although this works well during the first several minutes of flight, far away from the airport, as the HSCT gains speed and climbs, poor ejector inlet recovery and ejector ram drag contribute to poor thrust, making it advantageous to turn off the ejector. Doing so prematurely, however, can cause unacceptable noise levels to propagate to the ground, even when the aircraft is many miles from the airport.



*Optimized HSCT flight path for minimum noise (not to scale).*

This situation lends itself ideally to optimization, where the aircraft trajectory, throttle setting, and ejector setting can be varied (subject to practical aircraft constraints) to minimize the noise propagated to the ground. A method was developed at the NASA Lewis Research Center that employs a variation of the classic energy state approximation: a trajectory analysis technique historically used to minimize climb time or fuel burned in many aircraft problems. To minimize the noise on the ground at any given throttle setting, high aircraft altitudes are desirable; but the HSCT may either climb quickly to high altitudes using a high, noisy throttle setting or climb more slowly at a lower, quieter throttle setting. An optimizer has been

programmed into NASA's existing aircraft and noise analysis codes to balance these options by dynamically choosing the best altitude-velocity path and throttle setting history.

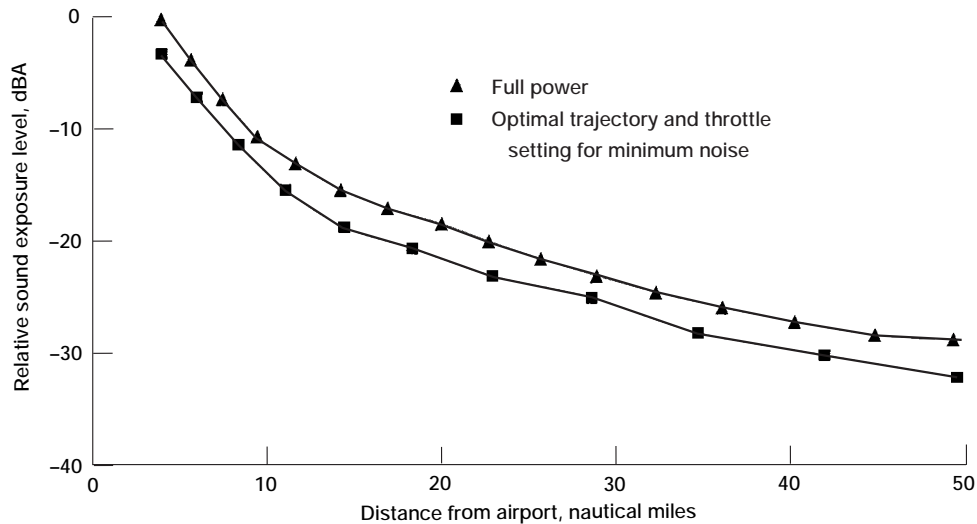
The noise level standard, or metric, used in the optimizer should be one that accurately reflects the subjective annoyance levels of ground-based observers under the flight path. A variety of noise metrics are available, many of which are practical for airport-adjacency noise certification. Unlike airport noise, however, the HSCT's climb noise will be characterized by relatively low noise levels, long durations, and low-frequency spectra. The noise metrics used in these calculations are based on the recommendations of researchers at the NASA Langley Research Center, who have correlated the flyover noise annoyance levels of actual laboratory subjects with a variety of measurements (ref. 1).

Analysis of data from this optimizer has shown that significant reductions in noise may be obtained with trajectory optimization. And since throttling operations are performed in the subsonic portion of the climb path (where thrust is plentiful), only small penalties in HSCT range or fuel performance occur.

### Reference

1. McCurdy, D.A.: Annoyance Caused by Aircraft En Route Noise. NASA TP-3165, 1992.

**For more information about this research, visit our web site:**  
<http://www.lerc.nasa.gov/WWW/HSR/>



*Relative noise at ground level for various trajectories.*

**Lewis contact:** Jeffrey J. Berton, (216) 977-7031, Jeffrey.J.Berton@lerc.nasa.gov

**Author:** Jeffrey J. Berton

**Headquarters program office:** OASTT

**Programs/Projects:** HSR

## Inlet Performance Analysis Code Developed

The design characteristics of an inlet very much depend on whether the inlet is to be flown at subsonic, supersonic, or hypersonic speed. Whichever the case, the primary function of an inlet is to deliver free-stream air to the engine face at the highest stagnation pressure possible and with the lowest possible variation in both stagnation pressure and temperature. At high speeds, this is achieved by a system of oblique and/or normal shock waves, and possibly some isentropic compression. For both subsonic and supersonic flight, current design practice indicates that the inlet should deliver the air to the engine face at approximately Mach 0.45. As a result, even for flight in the high subsonic regime, the inlet must retard (or diffuse) the air substantially.

Second, the design of an inlet is influenced largely by the compromise between high performance and low weight. This compromise involves tradeoffs between the mission requirements, flight trajectory, airframe aerodynamics, engine performance, and weight—all of which, in turn, influence each other. Therefore, to study the effects of some of these influential factors, the Propulsion System Analysis Office of the NASA Lewis Research Center developed the Inlet Performance Analysis Code (IPAC).

This code uses oblique shock and Prandtl-Meyer expansion theory to predict inlet performance. It can be used to predict performance for a given inlet geometric design such as pitot, axisymmetric, and two-dimensional. IPAC also can be used to design preliminary inlet systems and to make

subsequent performance analyses. It computes the total pressure, the recovery, the airflow, and the drag coefficients. The pressure recovery includes losses associated with normal and oblique shocks, internal and external friction, the sharp lip, and diffuser components. Flow rate includes captured, engine, spillage, bleed, and bypass flows. The aerodynamic drag calculation includes drags associated with spillage, cowl lip suction, wave, bleed, and bypass.

**Lewis contact:**

Kenol Jules, (216) 977-7016, Kenol.Jules@lerc.nasa.gov

**Authors:** Kenol Jules and Paul J. Barnhart

**Headquarters program office:** OASTT

**Programs/Projects:**

Methods Development, AST, HSR



# Conceptual Design Method Developed for Advanced Propulsion Nozzles

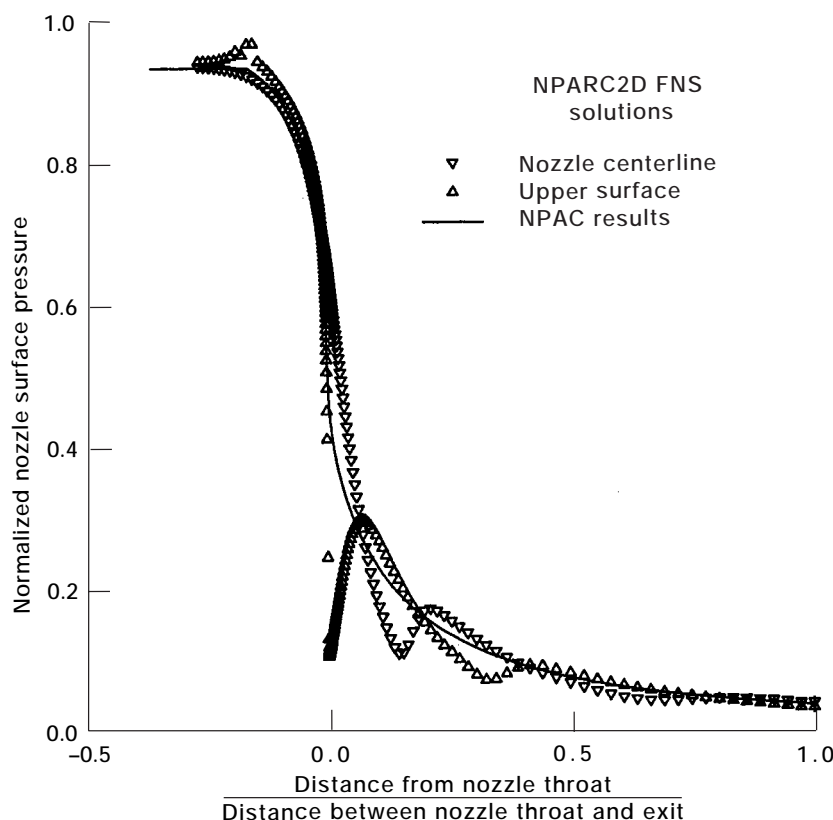
As part of a contract with the NASA Lewis Research Center, a simple, accurate method of predicting the performance characteristics of a nozzle design has been developed for use in conceptual design studies. The Nozzle Performance Analysis Code (NPAC) can predict the on- and off-design performance of axisymmetric or two-dimensional convergent and convergent-divergent nozzle geometries. NPAC accounts for the effects of overexpansion or underexpansion, flow divergence, wall friction, heat transfer, and small mass addition or loss across surfaces when the nozzle gross thrust and gross thrust coefficient are being computed. NPAC can be used to predict the performance of a given nozzle design or to develop a preliminary nozzle system design for subsequent analysis.

The input required by NPAC consists of a simple geometry definition of the nozzle surfaces, the location of key nozzle stations (entrance, throat, exit), and the nozzle entrance flow properties. NPAC performs three analysis "passes" on the nozzle geometry. First, an isentropic control volume analysis is performed to determine the gross thrust and gross thrust coefficient of the nozzle. During the second analysis pass, the skin friction and heat transfer losses are computed. The third analysis pass couples the effects of wall shear and heat transfer with the initial internal nozzle flow solutions to produce a system of equations that is solved at steps along the nozzle

geometry. Small mass additions or losses, such as those resulting from leakage or bleed flow, can be included in the model at specified geometric sections. A final correction is made to account for divergence losses that are incurred if the nozzle exit flow is not purely axial.

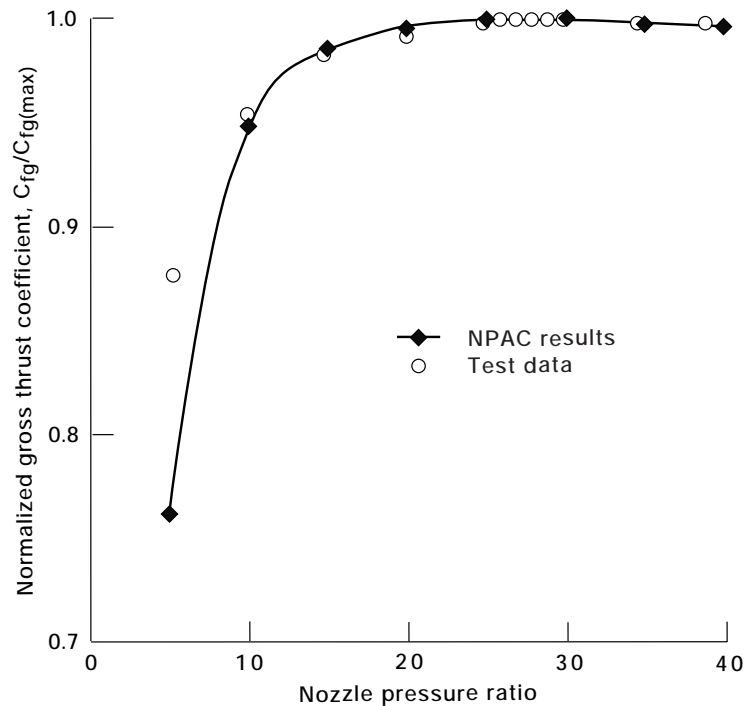
NPAC has been validated with various nozzle test data. In addition, NPAC results have been compared with computational fluid dynamics (CFD) solutions. Results are presented here for a two-dimensional nozzle test model.

The first figure compares the nozzle surface pressure distribution computed by NPAC with that computed by a CFD solution. The NPAC solution corresponds very closely to an average of the upper and center-line surface solutions from the CFD analysis. The second figure compares the normalized gross thrust coefficient  $C_{fg}$  computed for this nozzle by NPAC with those from model test data. This figure indicates good agreement between the computed and measured values of  $C_{fg}$  over most of the range of nozzle pressure ratios. The numbers diverge at lower nozzle pressure ratios, however. This is a result of the separation that can result inside a greatly overexpanded nozzle. NPAC does not include the ability to model this separation, and will, therefore, predict a  $C_{fg}$  significantly lower than that seen in actual nozzles.



Surface pressure comparison of NPAC results with a full Navier-Stokes (FNS) flow field solution for a two-dimensional test model nozzle.

The Nozzle Performance Analysis Code is a simple method for predicting nozzle performance. NPAC enables nozzle trade and design studies to be performed quickly and accurately. It is, therefore, a valuable tool in the conceptual design process of advanced propulsion systems.



*Comparison of normalized gross thrust coefficient from NPAC results with that from experimental data for a two-dimensional test model nozzle at various nozzle pressure ratios.*

**Lewis contact:**

Shari-Beth Nadell, (216) 977-7035,  
Shari-Beth.Nadell@lerc.nasa.gov

**Authors:** Shari-Beth Nadell and  
Paul J. Barnhart

**Headquarters program office:** OASTT

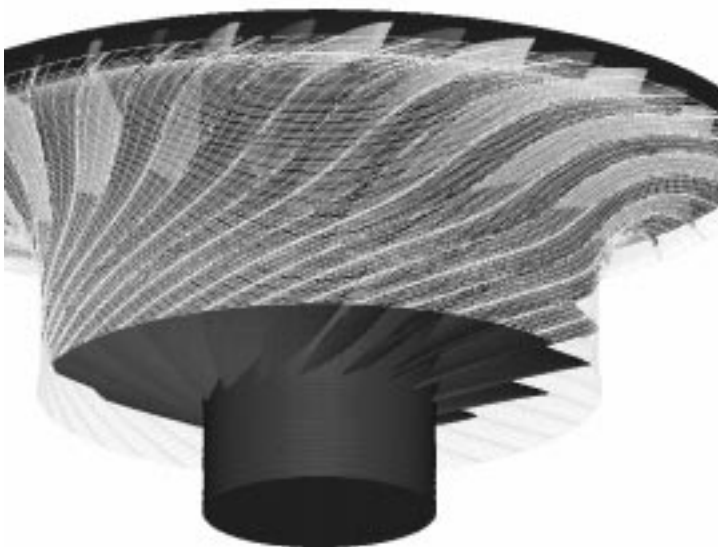
**Programs/Projects:** AST, HSR

## Computing and Interdisciplinary Systems

### Multiphysics Code Demonstrated for Propulsion Applications

The utility of multidisciplinary analysis tools for aeropropulsion applications is being investigated at the NASA Lewis Research Center. The goal of this project is to apply Spectrum, a multiphysics code developed by Centric Engineering Systems, Inc., to simulate multidisciplinary effects in turbomachinery components. Many engineering problems today involve detailed computer analyses to predict the thermal, aerodynamic, and structural response of a mechanical system as it undergoes service loading. Analysis of aerospace structures generally requires attention in all three disciplinary areas to adequately predict component service behavior, and in many cases, the results from one discipline substantially affect the outcome of the other two. There are numerous computer codes currently available in the engineering community to perform such analyses in each of these disciplines. Many of these codes are developed and used in-house by a given organization, and many are commercially available. However, few, if any, of these codes are designed specifically for multidisciplinary analyses.

The Spectrum code has been developed for performing fully coupled fluid, thermal, and structural analyses on a mechanical system with a single simulation that accounts for all simultaneous interactions, thus eliminating the requirement for running a large number of sequential, separate, disciplinary analyses. The Spectrum code has a true multiphysics analysis capability, which improves analysis efficiency as well as accuracy.



*Computational grid overlaid on geometry of centrifugal impeller.*

Centric Engineering, Inc., working with a team of Lewis and AlliedSignal Engines engineers, has been evaluating Spectrum for a variety of propulsion applications including disk quenching, drum cavity flow, aeromechanical simulations, and a centrifugal compressor flow simulation.

For centrifugal compressor simulations, AlliedSignal provided a mesh of the computational domain for a cyclic symmetry sector of the main gas path for one of their production compressors. A viscous, steady, compressible

flow finite element analysis was performed for the AlliedSignal centrifugal compressor. This is the first successful application of this technology to three-dimensional turbomachinery fluid flow. Centric Engineering performed the flow analyses, and results from the simulations were forwarded to AlliedSignal Engines and NASA for comparison with test data and other computational fluid dynamics (CFD) results. Deliverables included the values of the fluid pressure, velocity, temperature, density, and turbulence intensity computed by the Spectrum solver at the mesh nodes.

The successful application of the Spectrum multiphysics code to turbomachinery fluid flow simulations provides opportunities for performing full-system multidisciplinary simulations. Since this code already has demonstrated capabilities for thermal and structural analysis, establishing its ability to analyze turbomachinery fluids would provide a complete foundation for multidisciplinary aeropropulsion simulations. Opportunities for follow-on work include adding the back cavity flow and the solid casing to the main gas path model. In addition, several opportunities exist for accelerating the simulation run times to bring them to within acceptable design constraints.

**Lewis contacts:**

Dr. Charles Lawrence, (216) 433-6048, Charles.Lawrence@lerc.nasa.gov, and Matthew E. Melis, (216) 433-3322, Matthew.E.Melis@lerc.nasa.gov

**Authors:** Dr. Charles Lawrence and Matthew E. Melis

**Headquarters program office:** OASTT  
**Programs/Projects:** HPCCP

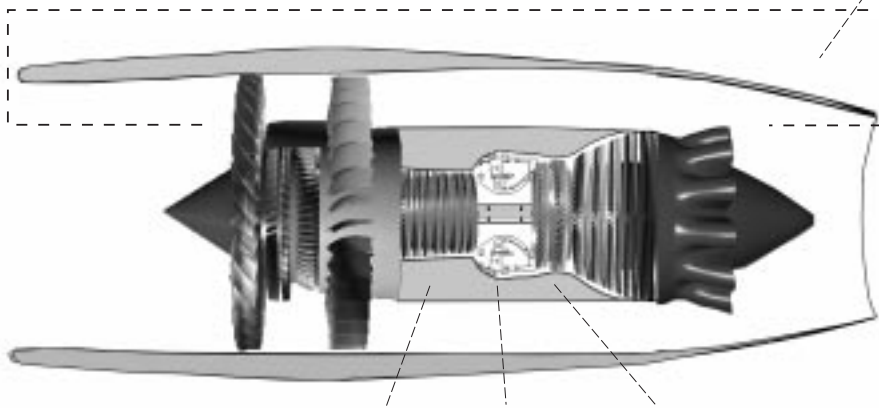


*Pressure results for single blade passage of centrifugal impeller.*

# Flow of a Gas Turbine Engine Low-Pressure Subsystem Simulated

The NASA Lewis Research Center is managing a task to numerically simulate overnight, on a parallel computing testbed, the aerodynamic flow in the complete low-pressure subsystem (LPS) of a gas turbine engine. The model solves the three-dimensional Navier-Stokes flow equations through all the components within the LPS, as well as the external flow around the engine nacelle. The LPS modeling task is being performed by Allison Engine Company under the Small Engine Technology contract. The large computer simulation was evaluated on networked computer systems using 8, 16, and 32 processors, with the parallel computing efficiency reaching 75 percent when 16 processors were used.

Low-pressure subsystem (LPS) model—ADPAC Navier-Stokes model including fan, booster, bypass duct, low-pressure turbine, mixer, and external flow



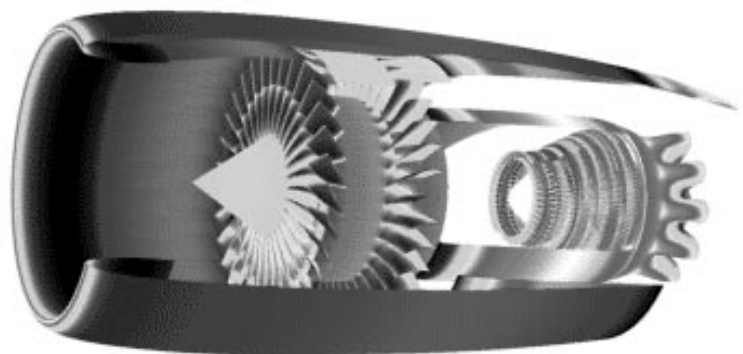
Core engine cycle model: NEPP thermodynamic cycle code including high-pressure compressor, combustor, and high-pressure turbine

*Gas turbine engine geometry and flow simulation of the low-pressure subsystem.*

The three-dimensional Navier-Stokes flow code for this LPS simulation is the Advanced Ducted Propeller Analysis Code (ADPAC), and the engine geometry being modeled is the Energy Efficient Engine designed by GE Aircraft Engines. The three-dimensional flow model of the LPS provides a tightly coupled aerodynamic analysis that captures the quasi-steady interaction effects between the components. The high-pressure core engine is simulated with the NASA Engine Performance Program (NEPP) thermodynamic cycle code, and the LPS flow model is linked to the NEPP core engine model by sharing common boundary conditions. Together, the three-dimensional LPS model and the thermodynamic model of the core engine form a hybrid model of the complete engine.

By varying the speed of rotation, researchers were able to use a coarse mesh grid solution to obtain the torque balance between the compression system and the turbine to within 1 percent in a few iterations. Balancing the torque with the ADPAC solution obtained from the coarse mesh enabled the fine mesh numerical solution to be run to full convergence. The large-scale (74-block, 6.7-million-grid-point) simulation of the complete LPS was successfully run on networked workstation clusters on Davinci and Babbage (Ames), on LACE (Lewis Advanced Cluster Environment), and at Allison. The interaction between components within LPS, as well as between LPS and the core engine were evaluated at various engine operating conditions: that is, the design point at takeoff, and the altitude cruise condition.

The hybrid engine model can be used to evaluate the detailed interactions between LPS components while considering the lumped-parameter performance of the core engine. The flow model enables critical engine component



*Gas turbine engine Navier-Stokes flow simulation.*

interactions to be quantified early in the design phase, reducing the costs associated with numerous engine configuration tests in an engine design program. For capturing detailed propulsion/airframe integration effects on vehicle performance, the model can be coupled to an external aerodynamic simulation of the airframe. The large-scale simulation also helps define the requirements for the computer architecture and simulation environment for the Numerical Propulsion System Simulation (NPSS) project.

Plans in the LPS modeling task include replacing the NEPP engine model with the National Cycle Program (NCP) model, thereby integrating its detailed flow modeling capability into NPSS, which will serve as a “numerical test cell” for turbine engines. The goal of NPSS is to provide a tool that can significantly reduce the design time, risk, and cost associated with designing advanced gas turbine engines.

**More information about this research is available on the World Wide Web:**  
<http://hpcc/lpsubs/>

**Lewis contact:** Joseph P. Veres, (216) 433–2436, [Joseph.P.Veres@lerc.nasa.gov](mailto:Joseph.P.Veres@lerc.nasa.gov)

**Author:** Joseph P. Veres

**Headquarters program office:** OASTT

**Programs/Projects:** HPCCP, NPSS, NCP

# Research and Technology





# Materials

## Assessing the Resistance of $\gamma$ -Ti-47Al-2Nb-2Cr (at.%) to Foreign Object Damage

A team consisting of GE Aircraft Engines, Precision Cast Parts, Oremet, and Chromalloy were chosen for a NASA-sponsored Aerospace Industry Technology Program (AITP) to develop a design and manufacturing capability that will lead to an engine test demonstration and the eventual implementation of a titanium-aluminide (TiAl) low-pressure turbine blade into commercial service. One of the main technical risks of implementing TiAl low-pressure turbine blades is the poor impact resistance of TiAl in comparison to the currently used nickel-based superalloy. The impact resistance of TiAl is being investigated at the NASA Lewis Research Center as part of this program.

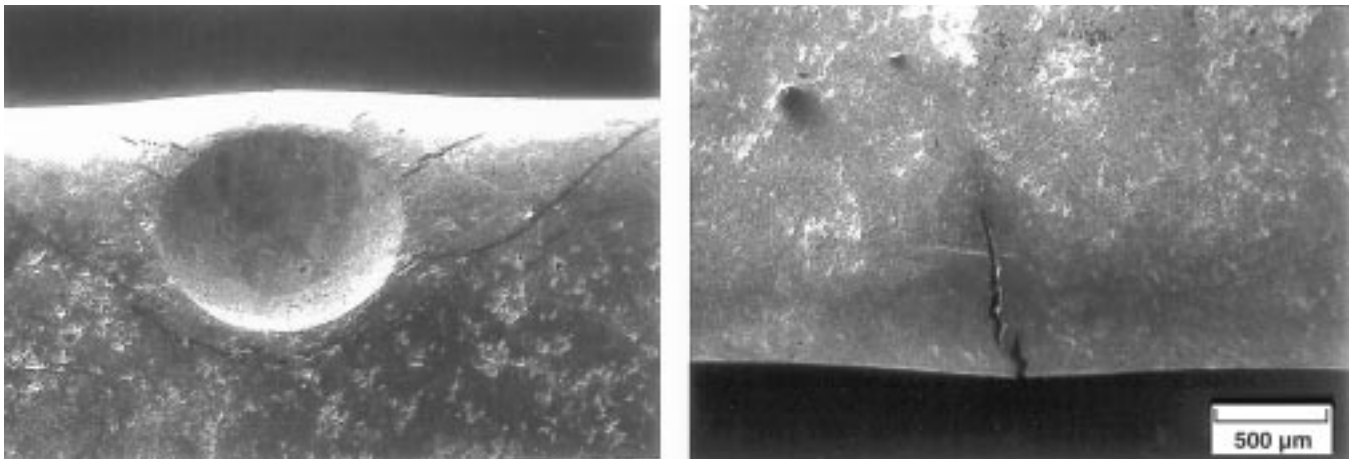
The overall objective of this work is to determine the influence of impact damage on the high-cycle fatigue life of TiAl simulated low-pressure turbine blades. To minimize the quantity of high-cycle fatigue tests required, a design of experiments was initiated to determine the level of importance of various impact variables based on a microstructural analysis. The variables studied included energy, specimen thickness, hardness of projectile, and impact temperature.

Impact specimens were cast to size in a dog-bone configuration and given a typical processing sequence followed by an exposure at 650 °C for 20 hr to simulate embrittlement at service conditions. The specimens were impacted at 260 °C under a 69-MPa load. Steel projectiles with diameters of 1.6 and 3.2 mm and Rockwell hardnesses of 20 and 60  $R_c$  were impacted at 90° to the leading edge. Backside crack lengths were emphasized in the analysis, but cracks on the front (impact) side were also characterized.

The experimental impact conditions chosen produced a spectrum of damage from minor denting to major cracking. The backside crack length was strongly dependent on the projectile energy, but the projectile hardness

had no effect on crack length. Thin specimens and medium thickness specimens exhibited similar crack resistance for low and medium energies, but the crack lengths increased substantially for thin specimens impacted at high energies. Thick specimens exhibited improved impact resistance at all energy levels. Temperature had no effect on the backside crack length when either hard or soft projectiles impacted the specimens at the medium energy.

This study is being used by the industry-NASA team to determine the technical risks associated with impact issues, as well as the design and processing methods that could minimize such risks. The actual damage tolerable for the low-pressure turbine blade application will be determined by a combination of fatigue testing and consideration of actual engine conditions. Current evaluations indicate that Ti-47Al-2Nb-2Cr possesses the level of damage tolerance required for implementation. These results



*Damage as a result of high-energy impacts ( $E = 0.33$  joules) with 1.6-mm projectiles. Left: Front. Right: Back.*

were incorporated into the selection of an airfoil design that balanced impact resistance with component weight.

### Bibliography

Draper, S.L.; Pereira, J.M.; and Nathal, M.V.: Impact Resistance of  $\gamma$ -Ti-48Al-2Nb-2Cr. HITEMP Review 1997. NASA CP-10192, Vol. II, 1997, paper 25, pp. 1-13.  
(Permission to cite this material was granted by Carol A. Ginty, February 19, 1998.)

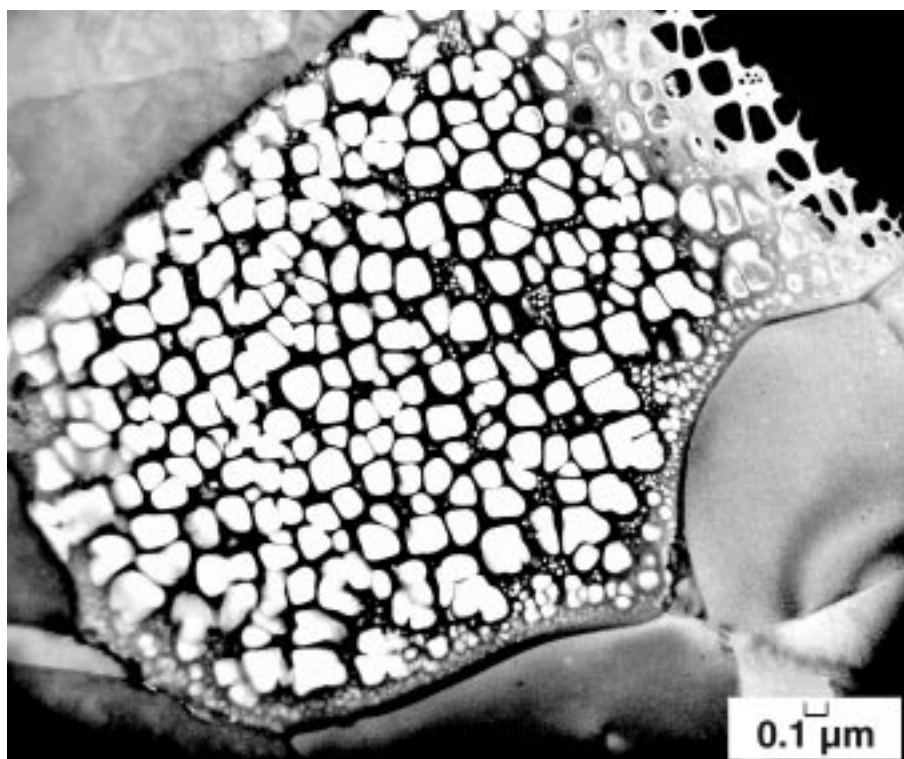
**Lewis contact:** Susan L. Draper, (216) 433-3257, Susan.L.Draper@lerc.nasa.gov

**Authors:** Susan L. Draper, Dr. J. Michael Pereira, and Dr. Michael V. Nathal

**Headquarters program office:** OASTT

**Programs/Projects:** Propulsion Systems R&T, HITEMP, AITP

## Strengthening Precipitate Morphologies Fully Quantified in Advanced Disk Superalloys



*Disk superalloy showing various sizes of  $\gamma'$  precipitates*

Advanced aviation gas turbine engines will require disk superalloys that can operate at higher temperatures and stresses than current conditions. Such applications will be limited by the tensile, creep, and fatigue mechanical properties of these alloys. These mechanical properties vary with the size, shape, and quantity of the  $\gamma'$  precipitates that strengthen disk superalloys. It is therefore important to quantify these precipitate parameters and relate them to mechanical properties to improve disk superalloys. Favorable precipitate morphologies and practical processing approaches to

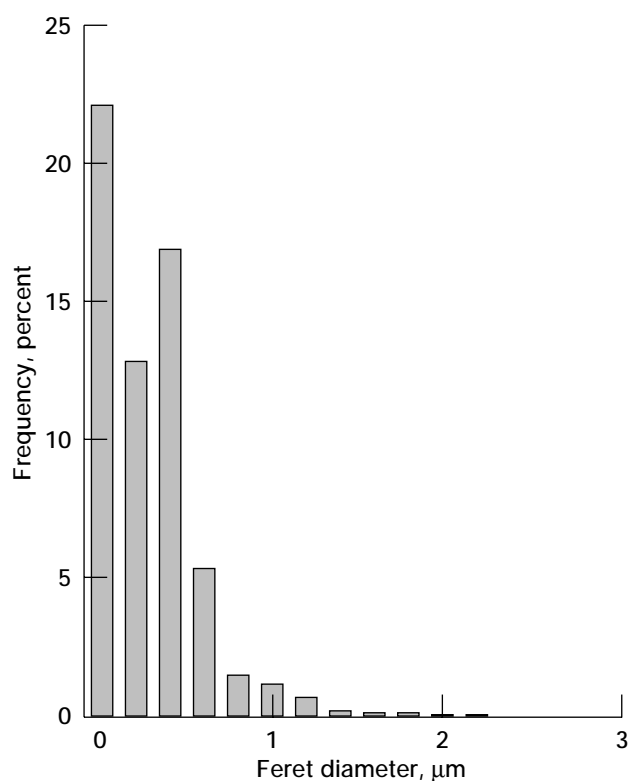
achieve them can then be determined. A methodology has been developed at the NASA Lewis Research Center to allow the comprehensive quantification of the size, shape, and quantity of all types of  $\gamma'$  precipitates.

Disk superalloys can contain micrometer, submicrometer, and fine aging  $\gamma'$  precipitates, as in this photo. Micrometer-size  $\gamma'$  precipitates with a diameter greater than 1  $\mu\text{m}$  can survive from the original solidification structure ("primary  $\gamma'$ ") or grow during low-temperature solution heat treatments. These precipitates were observed by optical and scanning electron microscopy of metallographically mounted, polished, and etched sections. Submicrometer-size  $\gamma'$  precipitates between 0.1 and 1  $\mu\text{m}$  in diameter often form during quenching from solution heat treatments. These precipitates often grow with their edges approximately aligned along preferred crystallographic planes to produce regularly aligned rounded cubes or connected rectangles. In general, transmission electron microscopy (TEM) of thin foils obtained consistently oriented,

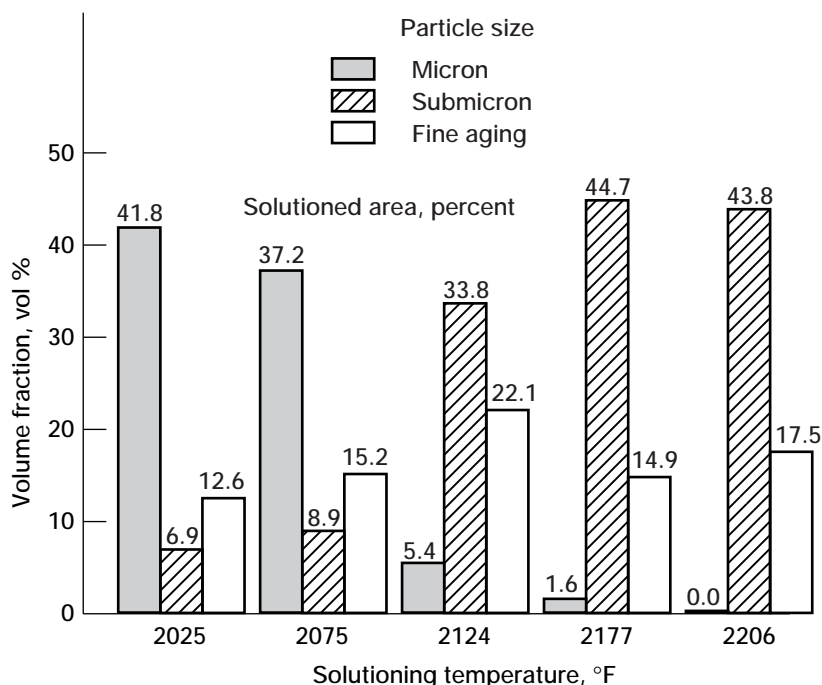


high-resolution images of the aligned morphology. Fine aging  $\gamma'$  precipitates less than 0.1  $\mu\text{m}$  in diameter formed later during solution quenching and subsequent lower temperature heat treatments. These very small, nearly spherical precipitates also had to be imaged by transmission electron microscopy to be accurately quantified.

The delicate balance between superior disk mechanical properties and practical processing approaches requires unprecedented levels of  $\gamma'$  microstructural quantification. Therefore, SigmaScan image analysis software was used to determine the size, shape, and volume fraction of each type of  $\gamma'$  precipitate. A typical measured distribution of  $\gamma'$  feret diameter versus frequency is shown in the bar graph to the right for a disk alloy specimen solution heat treated at 2124 °F for 1 hr and cooled in the furnace, then subsequently heat treated at 1550 °F for 2 hr and at 1400 °F for 8 hr. Micrometer, submicrometer, and fine aging  $\gamma'$  precipitates were present in this specimen's microstructure. The volume fractions of micrometer, submicrometer, and fine aging  $\gamma'$  precipitates for specimens of the same disk alloy solution heat treated from 2025 to 2206 °F are compared in the following figure. Increasing the solution heat treatment temperature reduced micrometer  $\gamma'$  content and increased submicrometer  $\gamma'$  content. These changes can affect the strength and creep resistance of this disk alloy.



Size distribution of  $\gamma'$  precipitates in a disk alloy specimen that was first solution heat treated at 2124 °F.



$\gamma'$  volume fractions of heat-treated disk alloy specimens.

The accurate quantification of  $\gamma'$  morphology and associated mechanical properties for different disk alloy microstructures can enable modeling of processing-microstructure-property relationships in advanced disk alloys. This can aid in obtaining improved mechanical properties in advanced disk alloys by using practical processing to achieve favorable  $\gamma'$  morphologies.

#### Lewis contacts:

Dr. Timothy P. Gabb, (216) 433-3272, Timothy.P.Gabb@lerc.nasa.gov;  
 Dr. John Gayda, (216) 433-3273, John.Gayda@lerc.nasa.gov;  
 David L. Ellis, (216) 433-8736, David.L.Ellis@lerc.nasa.gov; and  
 Dr. Anita Garg, (216) 433-8908, Anita.Garg@lerc.nasa.gov

**Author:** Dr. Timothy P. Gabb

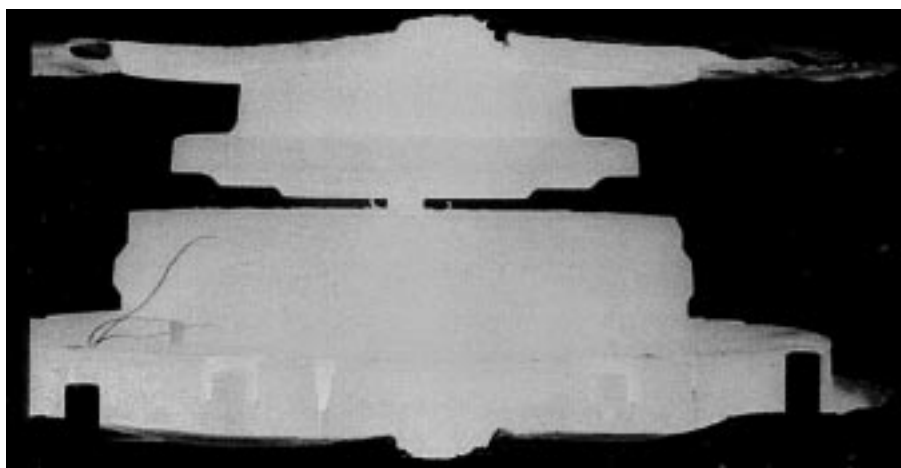
**Headquarters program office:** OASTT

**Programs/Projects:** Propulsion  
 Systems R&T, AST, EPM, P&PM, HITEMP

# High-Temperature Compressor Material Development

The next generation of subsonic commercial aircraft will require engines with improved efficiency and greater durability at lower costs. To help achieve these goals, manufacturing technologies for the disks, airfoils, and impellers in the compressors of these advanced turbine engines are being developed by a team representing all four U.S. aircraft engine companies—GE Aircraft Engines, Pratt & Whitney, AlliedSignal Inc., and Allison Engine Company. This work is being funded by NASA's Advanced Subsonic Technology (AST) project.

For axial compressors, manufacturing technologies are being developed for advanced nickel-base superalloy disks with improved creep strength and slower crack growth rates. Statistically designed experiments are being employed to develop the optimal compaction, forging, and heat treatment of these advanced disk alloys for large and small turbine engines. For large turbine engines, emphasis will be directed at developing the manufacturing technologies for an advanced disk alloy developed under NASA's Enabling Propulsion Materials (EPM) program. A wide processing window will be needed because of the thick bores and large diameters of these disks. For small turbine engines, emphasis will be directed at optimizing the processing window of alloys specifically tailored for the more aggressive heat treatments obtainable in smaller disk sizes. The disk manufacturing technologies will be developed on subscale disks and verified on full-scale disks, with a goal of increasing the operating temperatures by as much as 200 °F or extending life at current operating temperatures up to 2 times. Furthermore, the cost of manufacturing these advanced disk alloys should be no greater than that for current disk alloys.



*Forging of nickel-base superalloy disk.*

To realize increased operating temperatures in advanced axial compressors, researchers must also improve airfoil alloys since current forged airfoils will not meet the projected life requirements of future compressors. To overcome this deficiency, the AST engine team is also developing casting technologies for "razor" thin compressor airfoils. Cast nickel-base superalloy airfoils will match the enhanced temperature capability of the advanced disk alloys and at the same time reduce the cost of compressor airfoils once the casting process is developed and optimized.

Although the disk and airfoil effort will enable higher operating temperatures in axial compressors, many smaller turbine engines utilize a centrifugal compressor that is limited by the speed and temperature of the impeller. Current impellers, which use only a single alloy (titanium or superalloy), will not meet projected operating conditions for future designs. Instead, using a dual-alloy titanium impeller appears to be the only way future requirements can be met. In this part of the program, AlliedSignal and GE have formed a team to develop a dual-alloy titanium impeller for future commercial turbine engines. The impeller will use a high-temperature, creep-resistant titanium alloy in the airfoil section bonded to a high-strength, fatigue-resistant titanium alloy in the hub. As with the disk program, subscale impellers will be used to develop manufacturing technologies, such as the bonding process. After development is completed, a full-scale impeller will be produced and spin tested to prove the design.

Development and demonstration of all three technology items—disk, airfoil, and impeller—are scheduled to be completed by 2001. If successful, they will be available to all four U.S. engine companies at that time to help them maintain a competitive position in the global market.

**Lewis contact:**

Dr. John Gayda, (216) 433-3273,  
John.Gayda@lerc.nasa.gov

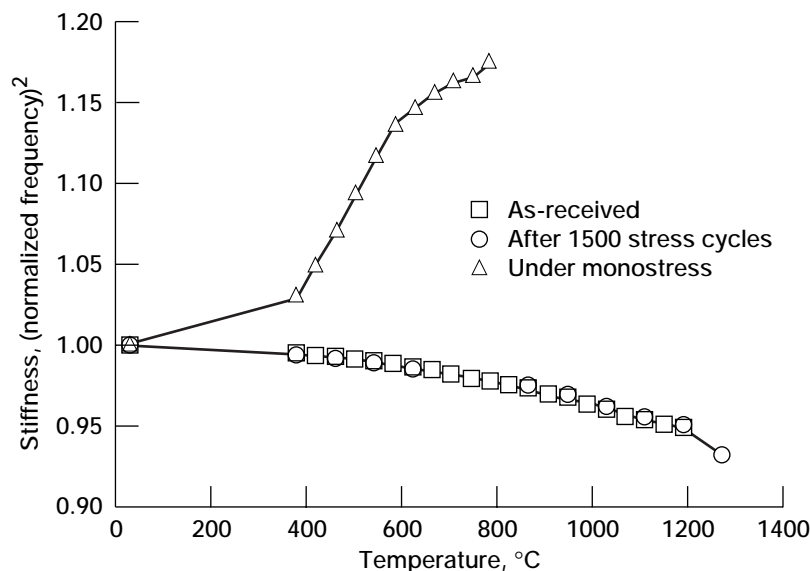
**Author:** Dr. John Gayda

**Headquarters program office:** OASTT  
**Programs/Projects:** AST, EPM

# Method Developed for the High-Temperature Nondestructive Evaluation of Fiber-Reinforced Silicon Carbide Ceramic Matrix Composites

Ceramic matrix composites have emerged as candidate materials to allow higher operating temperatures (1000 to 1400 °C) in gas turbine engines (ref. 1). A need, therefore, exists to develop nondestructive methods to evaluate material integrity at the material operating temperature by monitoring thermal and mechanical fatigue. These methods would also have potential as quality inspection tools. The goal of this investigation at the NASA Lewis Research Center is to survey and correlate the temperature-dependent damping and stiffness of advanced ceramic composite materials with imposed thermal and stress histories that simulate in-service turbine engine conditions.

A typical sample size of 100 by 4 by 2 mm<sup>3</sup>, along with the specified stiffness and density, placed the fundamental vibration frequencies between 100 and 2000 Hz. A modified Forster apparatus seemed most applicable to simultaneously measure both damping and stiffness. Testing in vacuum reduced the effects of air on the measurements. In this method, a single composite sample is vibrated at its fundamental tone; then suddenly, the mechanical excitation is removed so that the sample's motion freely decays with time.



*Effects of various thermal and mechanical histories on temperature-dependent stiffness for a SiC/SiC fiber-reinforced ceramic composite.*

The figure illustrates typical results. Notice the dramatic difference in behavior between composite samples with different thermal and stress histories. When its relative stiffness, as a function of temperature, is increased, the silicon-carbide-fiber-reinforced silicon carbide (SiC/SiC) composite under constant stress (monostress) at room temperature behaves differently from samples exposed to repeated stresses (1500 cycles) at 1200 °C in air and

from the as-received composite. This indicates that combined thermally and mechanically induced oxidation is integral to understanding advanced composite material fatigue and ultimate performance.

This system was used to measure temperature-dependent damping and stiffness of advanced ceramic composites for Lewis' Advanced High Temperature Engine Materials Technology Program (HITEMP) and for Marshall Space Flight Center's Simplex Turbopump Project.

## References

1. Ginty, C.A.: Overview of NASA's Advanced High Temperature Engine Materials Technology Program. HITEMP Review 1997. NASA CP-10192, Vol. I, 1997, paper 2, pp. 1-19. (Permission to cite this material was granted by Carol A. Ginty, February 19, 1998.)

## Lewis contact:

Dr. Jon C. Goldsby, (216) 433-8250, Jon.C.Goldsby@lerc.nasa.gov

**Author:** Dr. Jon C. Goldsby

**Headquarters program office:** OASTT

**Programs/Projects:** Propulsion Systems R&T, HITEMP, Simplex Turbopump

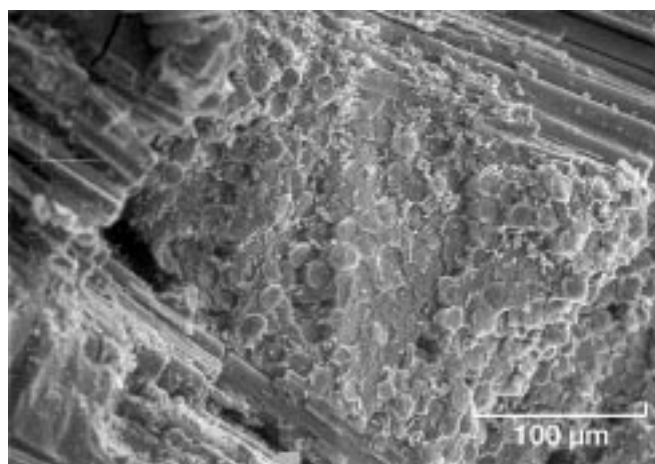
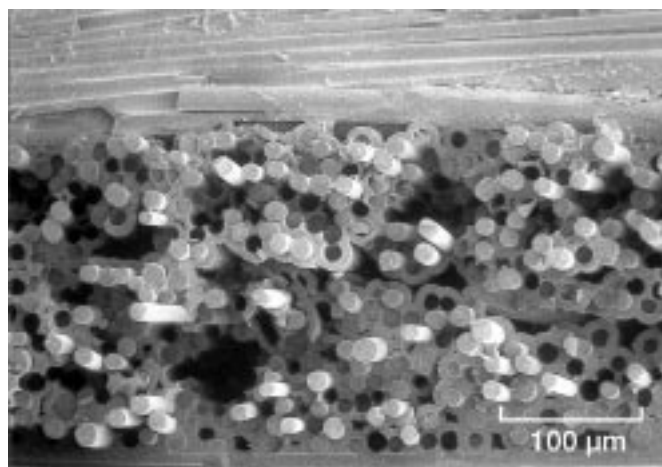
## Interfacial Thickness Guidelines for SiC<sub>Fiber</sub>/SiC<sub>Matrix</sub> Composites

Researchers at the NASA Lewis Research Center have developed a guideline for the interface thickness necessary for SiC<sub>Fiber</sub>/SiC<sub>Matrix</sub> composites to demonstrate good composite properties. These composite materials have potential commercial applications for high-temperature structural components such as engine hot sections. Several samples of each were composed from three different small-diameter (less than 20  $\mu\text{m}$ ), polymer-derived SiC fibers that were woven into two-dimensional cloths and laid up as preforms. The preforms were treated with a chemical-vapor-infiltrated boron nitride layer as an interfacial coating on the fiber surfaces to provide the necessary debonding characteristics for successful composite behavior. Then, the preforms were filled with additional SiC as a matrix phase.

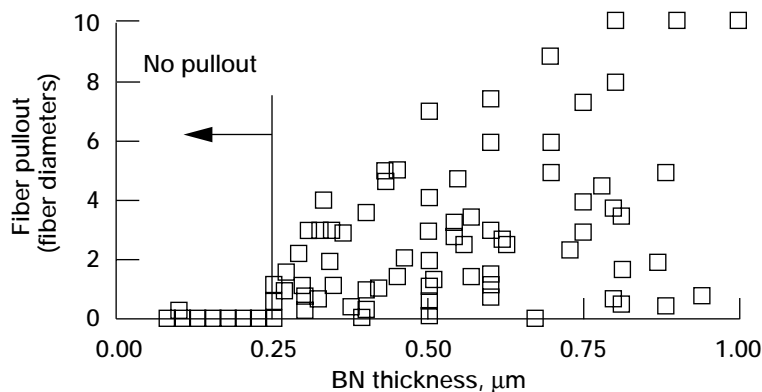
We found that the interface thickness must be at least 0.25  $\mu\text{m}$  for the fiber to decouple from the surrounding matrix. An example of this decoupling is shown in the top photo. When the interface was less than 0.25  $\mu\text{m}$ , the fracture front passed through both the fiber and matrix as a unit, as shown in the bottom photo. The fiber was bonded within the matrix and behaved as a brittle monolithic material. Both fiber debonding and brittle fracture may occur within the same specimen and often within immediately adjacent areas.

In addition, we found that an interface thickness greater than 0.5  $\mu\text{m}$  did not provide a substantial benefit. Investigations of the microstructure and fracture surfaces of numerous samples containing fibers made by different manufacturers and by different processes all required the same interface thickness of 0.25  $\mu\text{m}$  of boron nitride to assure that fibers would decouple from the matrix. Measurements of fiber pullout length versus interface thickness shown in the following graph illustrate the 0.25- $\mu\text{m}$ -thickness requirement.

We also found that the surface roughness of the fiber did not affect the required interface thickness. It had been previously proposed that a rough fiber surface might require a thicker interface thickness to overcome potential mechanical interlocking of adjacent fiber surfaces. Samples containing fibers with the greatest degree of surface roughness still required a thickness of 0.25  $\mu\text{m}$  for decoupling to occur.



*Top: Good fiber pullout from the matrix. Bottom: Brittle fracture of fiber and matrix.*



Interface thickness guideline. Pullout lengths for small-diameter SiC fibers.

### Bibliography

Hurst, J.B.; Freedman, M.R.; Kiser, J.D.: Fracture Surface Observations for SiC Fiber/SiC Matrix Composites. Paper presented at the 20th Annual Conference on Composites, Materials & Structures, Cocoa Beach, Florida, Jan. 1997.

### Lewis contact:

Janet B. Hurst, (216) 433-3286,  
Janet.B.Hurst@lerc.nasa.gov

**Author:** Janet B. Hurst

**Headquarters program office:** OASTT

**Programs/Projects:** EPM

## Stable Boron Nitride Interphases for Ceramic Matrix Composites

Ceramic matrix composites (CMC's) require strong fibers for good toughness and weak interphases so that cracks which are formed in the matrix debond and deflect around the fibers. If the fibers are strongly bonded to the matrix, CMC's behave like monolithic ceramics (e.g., a ceramic coffee cup), and when subjected to mechanical loads that induce cracking, such CMC's fail catastrophically. Since CMC's are being developed for high-temperature corrosive environments such as the combustor liner for advanced High Speed Civil Transport aircraft, the interphases need to be able to withstand the environment when the matrix cracks.

The state-of-the-art interphase for silicon carbide (SiC) fiber-reinforced SiC matrix composites is boron nitride (BN). Unfortunately, in the presence of oxygen and water vapor at temperatures ranging from 600 to 1000 °C, composites made with these interphases have severe embrittlement problems because of environmental attack of the interphase. A liquid or solid reaction product is formed that attacks the fibers and/or strongly bonds the fibers to the matrix. The stability of the BN interphases in water-containing environments can be improved by processing the interphases at higher temperatures or by doping the BN with silicon (ref. 1). However, it is a costly process to develop interphase coatings and incorporate them into large composite pieces suitable for testing.

The basic environmental degradation processes are known: the oxidation of BN and volatilization of the liquid oxidation product due to its reaction with water vapor. A simple test was developed at the NASA Lewis Research Center to compare the durability of different BN interphases subjected to severe environments. The different interphases were made on a small scale and composited as single-tow minicomposites. These minicomposites were then cut to lengths of about 2 cm and subjected to temperatures of 700 or 800 °C and different environmental conditions

ranging from 0.2 to 90 percent H<sub>2</sub>O (the balance being O<sub>2</sub>). The minicomposites were then polished along their lengths, and the distance that the BN interphase receded from the exposed end was measured for a number of different fiber/matrix interphases.

The figure shows the results for a test performed at 800 °C for 88 hr with an environment of 10 percent O<sub>2</sub> and 90 percent H<sub>2</sub>O (a total pressure of 1 atm). The BN interphases usually used in CMC's are the low-temperature variety. Environmental durability is improved dramatically by increasing the processing temperature of BN deposition and/or by doping the BN with Si. Unfortunately, in order to get very durable BN interphases by processing at higher temperatures, the BN has to be processed at temperatures greater than 1800 °C. This is impractical because BN deposition at these temperatures is nonuniform, resulting in poor composite mechanical properties.



The most promising interphase was the Si-doped BN interphase. This interphase had three orders of magnitude improvement over the low-temperature BN. The Si-doped BN interphases in this study were processed at 1400 °C, yet they even outperformed the undoped BN interphases processed at 1800 °C. Work is continuing to assess the mechanical behavior of composites with Si-doped interphases as well as to determine the optimum Si content for mechanical properties and environmental durability.

#### Reference

1. Moore, A.W., et al.: Improved Interface Coatings for SiC Fibers in Ceramic Composites. *Ceram. Eng. Sci. Proc.*, vol. 6, no. 4, 1995, pp. 409–416.

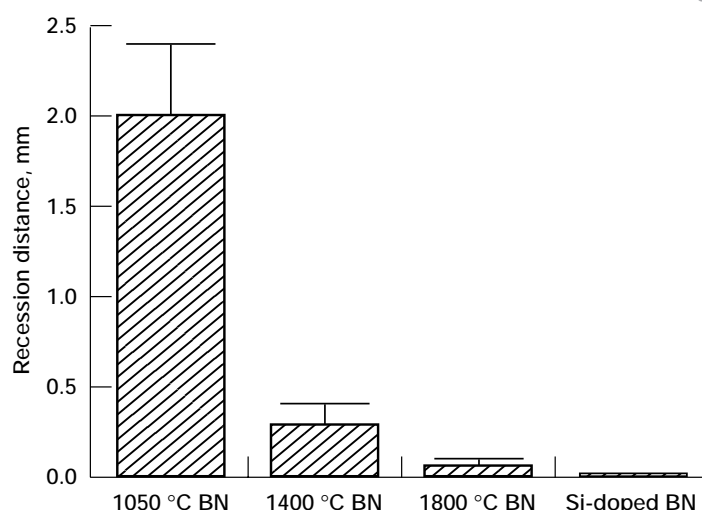
**Lewis contact:** Gregory N. Morscher, (216) 433–5512, Gregory.N.Morscher@lerc.nasa.gov

**Author:** Gregory N. Morscher

**Headquarters program office:** OASTT

**Programs/Projects:**

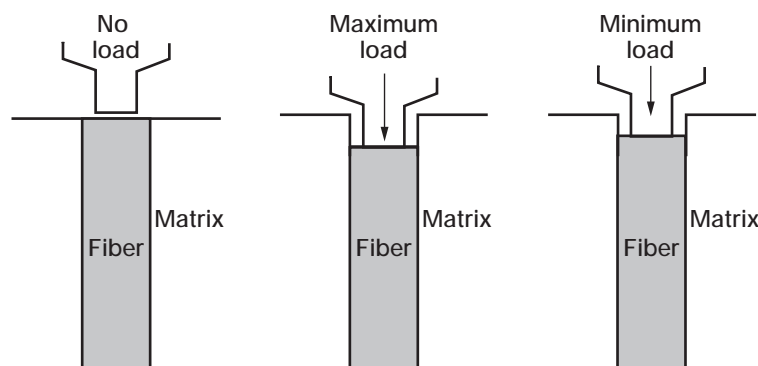
Propulsion Systems R&T, HSR, HITEMP



*Recession distance of different BN interphases in single-tow SiC/SiC minicomposites. The BN interphases were either processed at different temperatures or doped with Si (~20 wt %).*

## Cyclic Fiber Push-In Test Monitors Evolution of Interfacial Behavior in Ceramic Matrix Composites

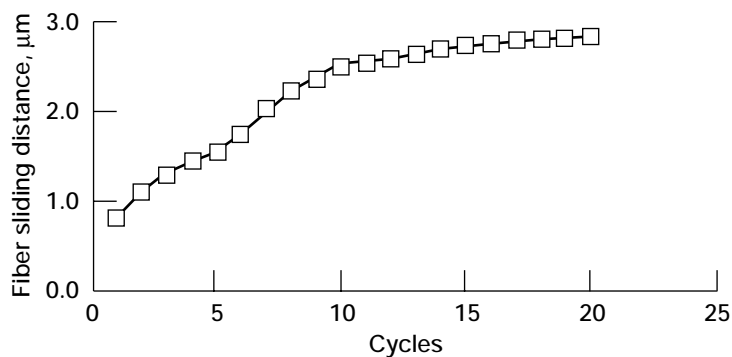
SiC fiber-reinforced ceramic matrix composites are being developed for high-temperature advanced jet engine applications. Obtaining a strong, tough composite material depends critically on optimizing the mechanical coupling between the reinforcing fibers and the surrounding matrix material. This has usually been accomplished by applying a thin C or BN coating onto the surface of the reinforcing fibers. The performance of these fiber coatings, however, may degrade under cyclic loading conditions or exposure to different environments. Degradation of the coating-controlled interfacial behavior will strongly affect the useful service lifetime of the composite material.



*Cyclic fiber push-in test approach.*

Cyclic fiber push-in testing was applied to monitor the evolution of fiber sliding behavior in both C- and BN-coated small-diameter (15- $\mu$ m) SiC-fiber-reinforced ceramic matrix composites. The cyclic fiber push-in tests were performed using a desktop fiber push-out apparatus. At the beginning of each test, the fiber to be tested was aligned underneath a 10- $\mu$ m-diameter diamond punch; then, the applied load was cycled between selected maximum and minimum loads. From the measured response, the fiber sliding distance and frictional sliding stresses were determined for each cycle. Tests were performed in both room air and nitrogen.

Cyclic fiber push-in tests of C-coated, SiC-fiber-reinforced SiC showed progressive increases in



*Variation in fiber sliding distance with continued cycling for 23- $\mu\text{m}$ -diameter, C-coated SiC fiber in SiC matrix. 20 cycles up to 1.4 N.*

fiber sliding distances along with decreases in frictional sliding stresses for continued cycling in room air. This rapid degradation in interfacial response was not observed for cycling in nitrogen, indicating that moisture exposure had a large effect in immediately lowering the frictional sliding stresses of C-coated fibers. These results indicate that matrix cracks bridged by C-coated fibers will not be stable, but will rapidly grow in moisture-containing environments.

In contrast, cyclic fiber push-in tests of both BN-coated, SiC-fiber-reinforced SiC and BN-coated, SiC-fiber-reinforced barium strontium aluminosilicate showed no significant changes in fiber sliding behavior with continued

short-term cycling in either room air or nitrogen. Although the composites with BN-coated fibers showed stable short-term cycling behavior in both environments, long-term (several-week) exposure of debonded fibers to room air resulted in dramatically increased fiber sliding distances and decreased frictional sliding stresses. These results indicate that although matrix cracks bridged by BN-coated fibers will show short-term stability, such cracks will show substantial growth with long-term exposure to moisture-containing environments. Newly formulated BN coatings, with higher moisture resistance, will be tested in the near future.

**Lewis contact:**

Dr. Jeffrey I. Eldridge, (216) 433-6074, [Jeffrey.I.Eldridge@lerc.nasa.gov](mailto:Jeffrey.I.Eldridge@lerc.nasa.gov)

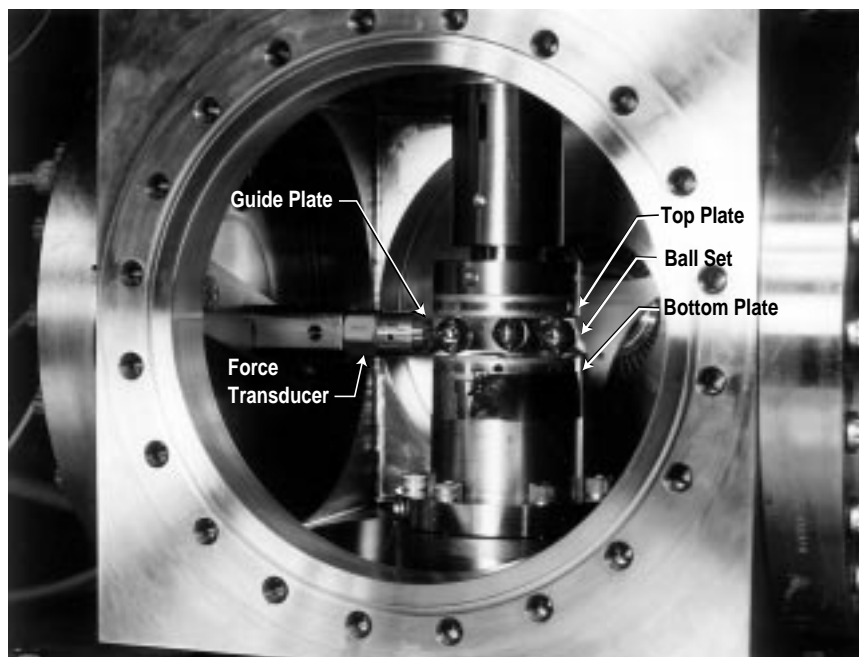
**Author:** Dr. Jeffrey I. Eldridge

**Headquarters program office:** OASTT

**Programs/Projects:**

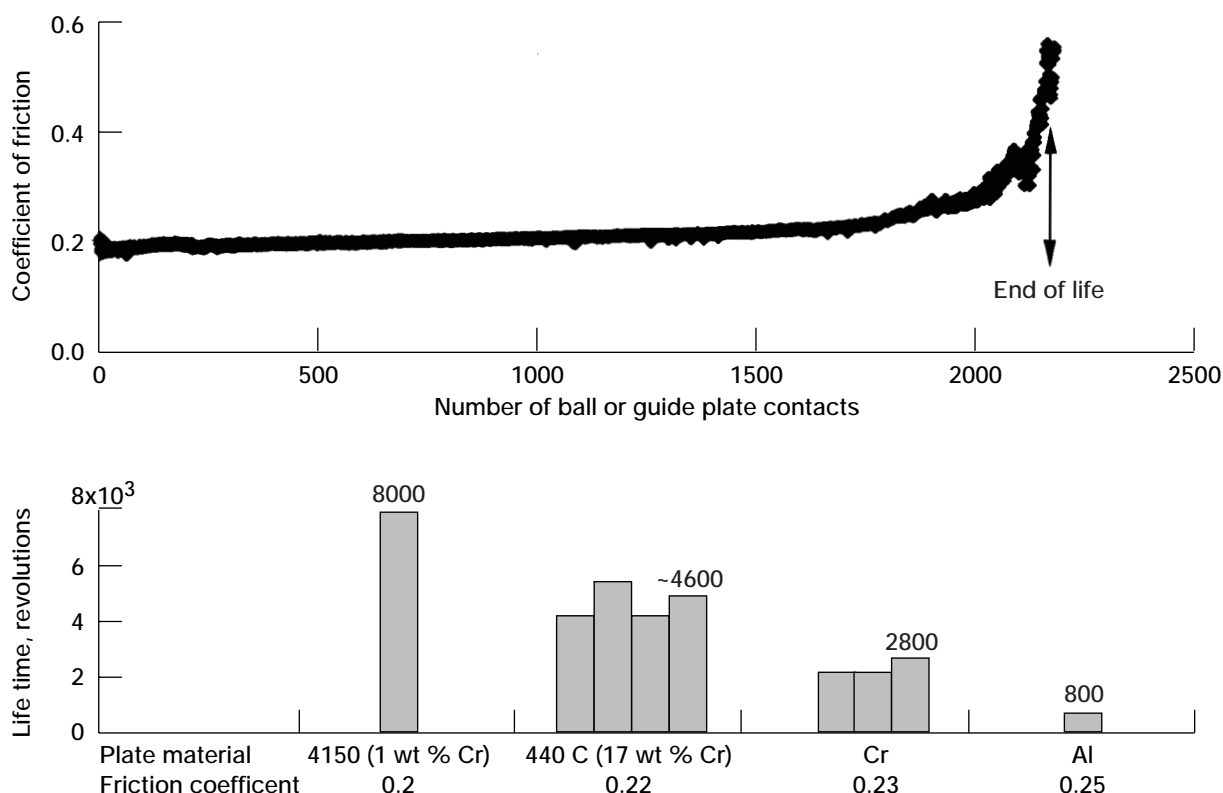
Propulsion Systems R&T, HITEMP

## Tribometer for Lubrication Studies in Vacuum



*Ball-on-plate tribometer.*

The NASA Lewis Research Center has developed a new way to evaluate the liquid lubricants used in ball bearings in space mechanisms. For this evaluation, a liquid lubricant is exercised in the rolling contact vacuum tribometer shown in the photo. This tribometer, which is essentially a thrust bearing with three balls and flat races, has contact stresses similar to those in a typical preloaded, angular contact ball bearing. The rotating top plate drives the balls in an outward-winding spiral orbit instead of a circular path. Upon contact with the "guide plate," the balls are forced back to their initial smaller orbit radius; they then repeat this spiral orbit thousands of times. The orbit rate of the balls is low enough, 2 to 5 rpm, to allow the



Top: Test of Fomblin Z-25 on 440C steel. Bottom: Response of Fomblin Z-25 showing dependence on plate material. (Fomblin Z-25 is a tradename owned by the Montefluos, Montedison Group, of Milan, Italy.)

system to operate in the boundary lubrication regime that is most stressful to the liquid lubricant.

This system can determine the friction coefficient, lubricant lifetime, and species evolved from the liquid lubricant by tribo-degradation. The lifetime of the lubricant charge is only a few micrograms, which is "used up" by degradation during rolling. As shown in the top graph, the friction increases when the lubricant is exhausted. The species evolved by the degrading lubricant are determined by a quadrupole residual gas analyzer that directly views the rotating elements. The flat races (plates) and 0.5-in.-diameter balls are of a configuration and size that permit easy posttest examination by optical and electron microscopy and the full suite of modern surface and thin-film chemical analytical techniques, including infrared and Raman microspectroscopy and x-ray photoelectron spectroscopy. In addition, the simple sphere-on-a-flat-plate geometry allows an easy analysis of the contact stresses at all parts of the ball orbit and an understanding of the frictional energy losses to the lubricant. The analysis showed that when the ball contacts the guide plate, gross sliding occurs between the ball and rotating upper plate as the ball is forced back to a smaller orbit radius. The friction force due to gross sliding is sensed by the piezoelectric force transducer behind the guide plate and furnishes the coefficient of friction for the system.

This tribometer has been used to determine the relative lifetimes of Fomblin Z-25, a lubricant often used in space mechanisms, as a function of the material of the plates against which it was run. The balls were 440C

steel in all cases; the plate materials were aluminum, chromium (Cr), 440C steel (17 wt % Cr), and 4150 steel (1 wt % Cr). As shown in the bar graph, the lifetime is greatest for the plate material with least chromium, thus implicating chromium as a tribochemically active element attacking Fomblin Z-25.

### Bibliography

Pepper, S.V.; Ebihara, B.T.; and Kingsbury, E.: A Rolling Element Tribometer for the Study of Liquid Lubricants in Vacuum. NASA TP-3629, 1996.

### Lewis contact:

Dr. Stephen V. Pepper,  
(216) 433-6061,  
Stephen.V.Pepper@lerc.nasa.gov

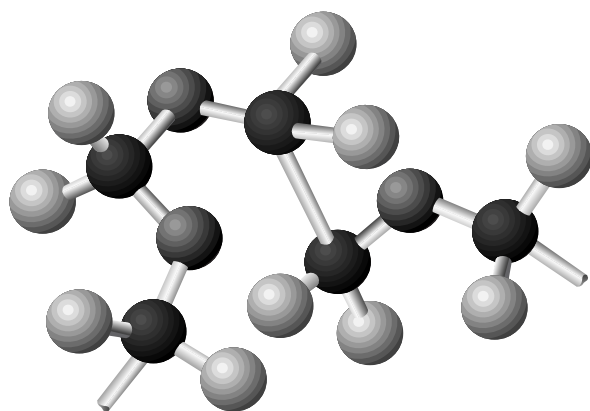
**Author:** Dr. Stephen V. Pepper

**Headquarters program office:** OSS

**Programs/Projects:** AXAF

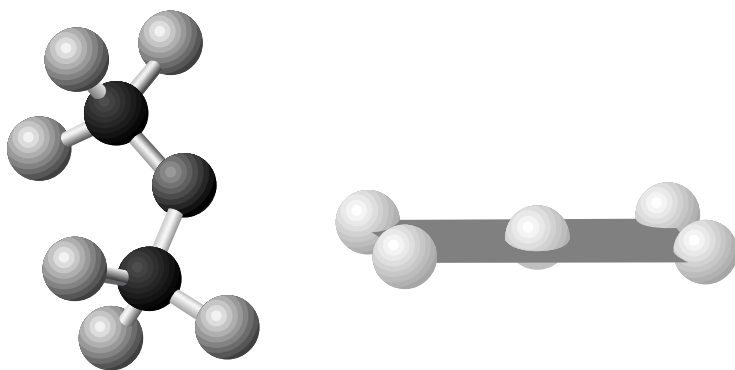
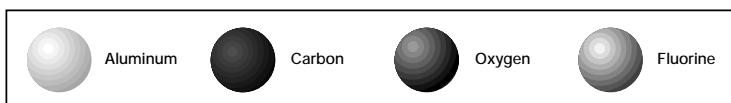


# Computational Chemistry and Lubrication



*Chemical composition of one typical commercial perfluorinated polyalkyl ether lubricant. Molecular weight, 10,000 to 50,000.*

Members of NASA Lewis Research Center's Tribology and Surface Science Branch are applying high-level computational chemistry techniques to the development of new lubrication systems for space applications and for future advanced aircraft engines. The next generation of gas turbine engines will require a liquid lubricant to function at temperatures in excess of 350 °C in oxidizing environments. Conventional hydrocarbon-based lubricants are incapable of operating in these extreme environments, but a class of compounds known as the perfluoropolyether (PFAE) liquids (see the top illustration; figures are shown in color in the online version of this article—<http://www.lerc.nasa.gov/WWW/RT1997/5000/5140zehe.htm>) shows promise for such applications. These commercially available products are already being used as lubricants in conditions where low vapor



*Nondissociative binding site (edge site) of five-atom Al cluster/perfluorodimethyl ether complex. Ether oxygen is directed toward the aluminum atoms.*

pressure and chemical stability are crucial, such as in satellite bearings and composite disk platters. At higher temperatures, however, these compounds undergo a decomposition process that is assisted (catalyzed) by metal and metal oxide bearing surfaces. This decomposition process severely limits the applicability of PFAE's at higher temperatures. A great deal of laboratory experimentation has revealed that the extent of fluid degradation depends on the chemical properties of the bearing surface materials. Lubrication engineers would like to understand the chemical breakdown mechanism to design a less vulnerable PFAE or to develop a chemical additive to block this degradation.

The chemical reactions that take place between the PFAE chain and the surface are being studied successfully with quantum chemical techniques in which all "experiments" are done on the computer. A cluster of metal atoms representing the surface is approached by a molecule of lubricant, and the detailed chemistry that takes place is accurately computed (see the bottom illustration). By adjusting the relative orientation of the approaching ether and the surface, and by changing the chemical makeup of the surface cluster, one can begin to understand what factors influence the lubricant decomposition. This understanding will help us design a surface-lubricant-additive combination that is stable at high temperatures.

**Lewis contact:**

Dr. Michael J. Zehe, (216) 433-5833,  
[Michael.J.Zehe@lerc.nasa.gov](mailto:Michael.J.Zehe@lerc.nasa.gov)

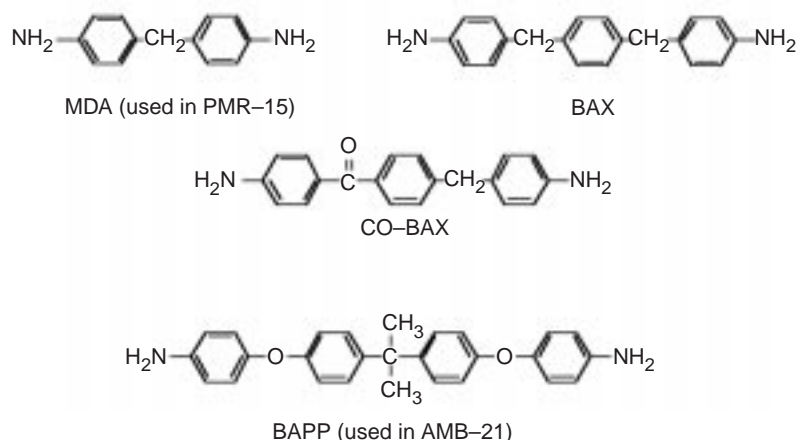
**Author:** Dr. Michael J. Zehe

**Headquarters Program Office:** OASTT

**Programs/Projects:**

Aeronautics Base R&T

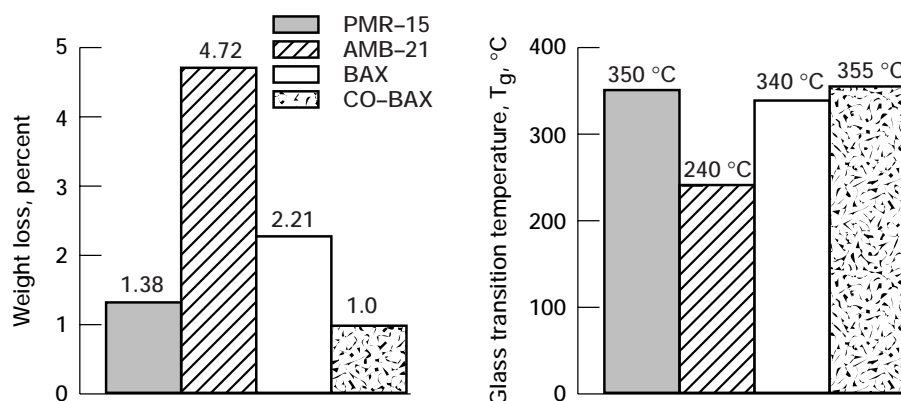
## "Green" High-Temperature Polymers



Some candidate diamines for replacing MDA (top left) in PMR-15.

PMR-15 is a processable, high-temperature polymer developed at the NASA Lewis Research Center in the 1970's principally for aeropropulsion applications. Use of fiber-reinforced polymer matrix composites in these applications can lead to substantial weight savings, thereby leading to improved fuel economy, increased passenger and payload capacity, and better maneuverability. PMR-15 is used fairly extensively in military and commercial aircraft engines components seeing service temperatures as high as 500 °F (260 °C), such as the outer bypass duct for the F-404 engine. The current world-wide market for PMR-15 materials (resins, adhesives, and composites) is on the order of \$6 to 10 million annually.

PMR-15 is prepared with a monomer, methylenedianiline (MDA), which is a known animal and suspect human carcinogen. The Occupational Safety and Health Administration (OSHA) and the Environmental Protection Agency (EPA) heavily regulate the use of MDA in the workplace and require certain engineering controls be used whenever MDA-containing materials (e.g., PMR-15) are being handled and processed. Implementation of these safety measures for the handling and disposal of PMR-15 materials costs the aircraft engine manufacturing industry millions of dollars annually.



Comparison of the glass-transition temperature and thermal-oxidative stability of graphite-reinforced composites prepared with non-MDA PMR-15 replacements. Left: Weight loss after 125 hr in air at 316 °C and 5 atm. Right: Glass-transition temperature.

Under the Advanced Subsonic Technology (AST) Program, researchers at NASA Lewis, General Electric, DuPont, Maverick Composites, and St. Norbert College have been working to develop and identify replacements for PMR-15 that do not rely upon the use of carcinogenic or mutagenic starting materials. This effort involves toxicological screening (Ames' testing) of new monomers as well as an evaluation of the properties and high-temperature performance of polymers and composites prepared with these materials. A number of diamines have been screened for use in PMR-15 replacements. Three diamines, BAX, CO-BAX, and BAPP (see the chemical diagram), passed the Ames' testing. Graphite-reinforced composites prepared with polyimides containing these diamines were evaluated against a PMR-15 control in terms of their high-temperature stability (weight loss after 125 hr in air at 316 °C and 5-atm pressure) and glass-transition temperature (an indication of high-temperature mechanical performance). Of these three materials systems, both the BAX and CO-BAX composites had stabilities and glass-transition temperatures comparable to those of PMR-15 (see the graphs). Further evaluation of the processability of these materials as well as their long-term stability and mechanical performance at 288 °C (550 °F) is in progress.

### Lewis contacts:

Dr. Peter Delvigs, (216) 433-3225, Peter.Delvigs@lerc.nasa.gov;  
Raymond D. Vannucci, (216) 433-3202, Raymond.D.Vannucci@lerc.nasa.gov;  
and Dr. Michael A. Meador, (216) 433-9518, Michael.A.Meador@lerc.nasa.gov

**Author:** Dr. Michael A. Meador

**Headquarters program office:** OASTT

**Programs/Projects:** AST, F-404 engine

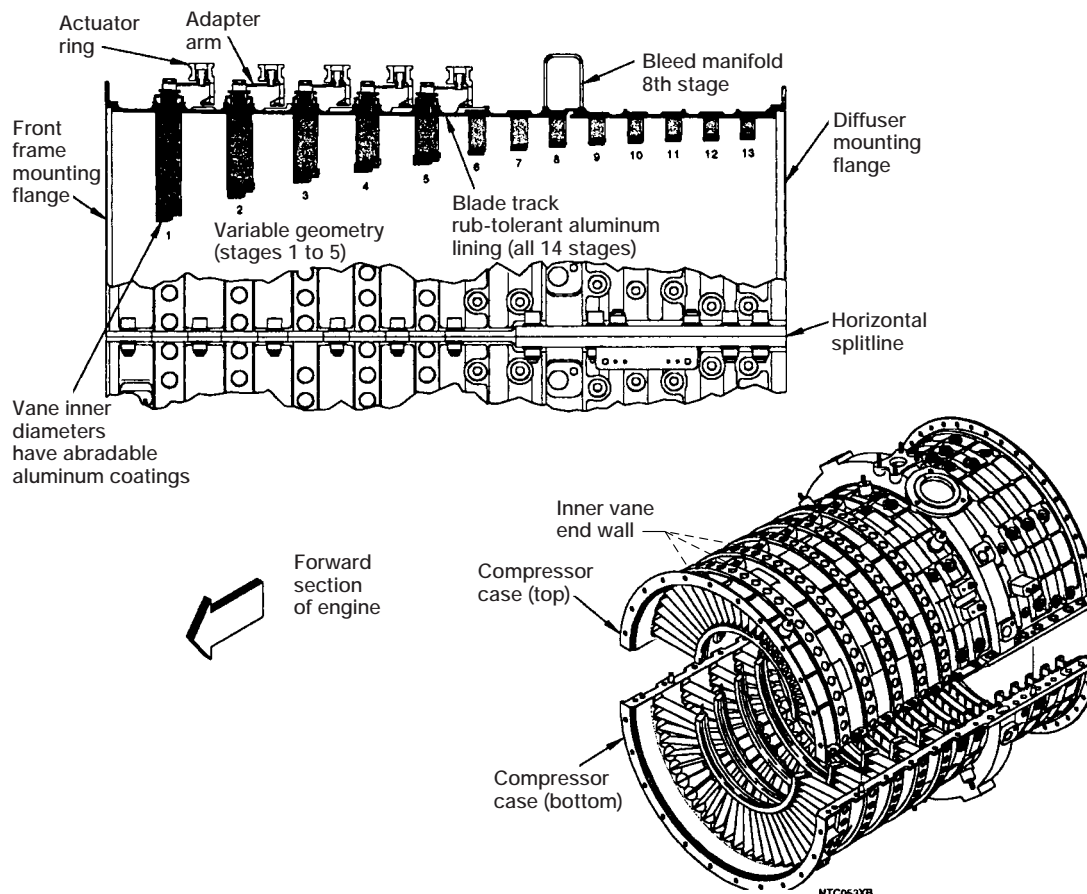
# Low-Cost Manufacturing of High-Temperature Polymer Composites

Major goals of NASA and the Integrated High Performance Turbine Engine Technology (IHPTET) initiative include improvements in the affordability of propulsion systems, significant increases in the thrust/weight ratio, and increases in the temperature capability of components of gas turbine engines. Members of NASA Lewis Research Center's HITEMP project worked cooperatively with Allison Advanced Development Corporation to develop a manufacturing method to produce low-cost components for gas turbine engines. Affordability for these polymer composites is defined by the savings in acquisition and life-cycle costs associated with engine weight reduction. To lower engine component costs, the Lewis/Allison team focused on chopped graphite fiber/polyimide resin composites. The high-temperature polyimide resin chosen, PMR-II-50, was developed at NASA Lewis.

The current generation of high-temperature polymer composites is primarily limited to engine components operating up to 260 °C and manufacturing techniques requiring labor-intensive hand layup molding procedures. The Lewis/Allison team is investigating alternative fabrication techniques, such as compression molding, combined with high-temperature polymer composites that can operate in engine environments up to 316 °C. Compression molding offers a more rapid, cost effective manufacturing

approach for smaller turbine engine components than hand layup methods. In addition, compression molding reduces manufacturing costs of polymer composites by (1) reducing component mold time in comparison to autoclave processing, (2) reducing fabrication time by minimizing labor intensive hand layup operations associated with autoclaving and individual ply fabrication techniques (such as ply orientation and ply count), and (3) reducing machining costs after component fabrication because of the use of match metal molding tools.

The 1-in. chopped graphite fiber and PMR-II-50 resin were mixed



*Allison AE3007 compressor case and vane assembly. (Copyright Allison Advanced Development Company; used with permission.)*

together through a technique called prepregging. Standard commercial prepregging equipment was used to produce a continuous sheet of chopped fiber/PMR-II-50 prepreg. The resin's viscosity and concentration were optimized to produce a PMR-II-50 prepreg with constant proportions of resin and graphite fiber throughout its length. It was critical that the prepreg have a random distribution of graphite fiber throughout the components' thicknesses so that the chopped fiber/resin engine components would not warp during their production. The Lewis/Allison team successfully produced PMR-II-50 chopped graphite fiber prepreg at Quantum Composites in Midland, Michigan.

Allison is currently evaluating these chopped-fiber polymer composites by molding and testing compressor components for both IHPTET and commercial engine applications. An inner vane endwall used to secure and align stator vanes was chosen as a demonstration component; it is shown in the illustration on the top section of Allison's 3007 compressor. Previously, these endwalls were made from stainless steel, which weighed more than two times the polymer composite and required extensive machining to produce a smooth surface finish. Allison will further reduce the cost of

the endwall by reducing the part count of the metallic components by a factor of three when using the chopped graphite fiber/PMR-II-50 composite.

**Lewis contacts:**

Dr. James K. Sutter, (216) 433-3226, James.K.Sutter@lerc.nasa.gov, and Dr. William B. Alston, (216) 433-3220, William.B.Alston@lerc.nasa.gov

**Allison contacts:**

Kevin Kannmacher, (317) 230-8113, John A. Spees, (317) 230-6953, and Frank Macri, (317) 230-3281

**Author:** Dr. James K. Sutter

**Headquarters program office:** OASTT

**Programs/Projects:** Propulsion Systems R&T, HITEMP, IHPTET

## Residual Stresses Modeled in Thermal Barrier Coatings

Thermal barrier coating (TBC) applications continue to increase as the need for greater engine efficiency in aircraft and land-based gas turbines increases. However, durability and reliability issues limit the benefits that can be derived from TBC's. A thorough understanding of the mechanisms that cause TBC failure is a key to increasing, as well as predicting, TBC durability.

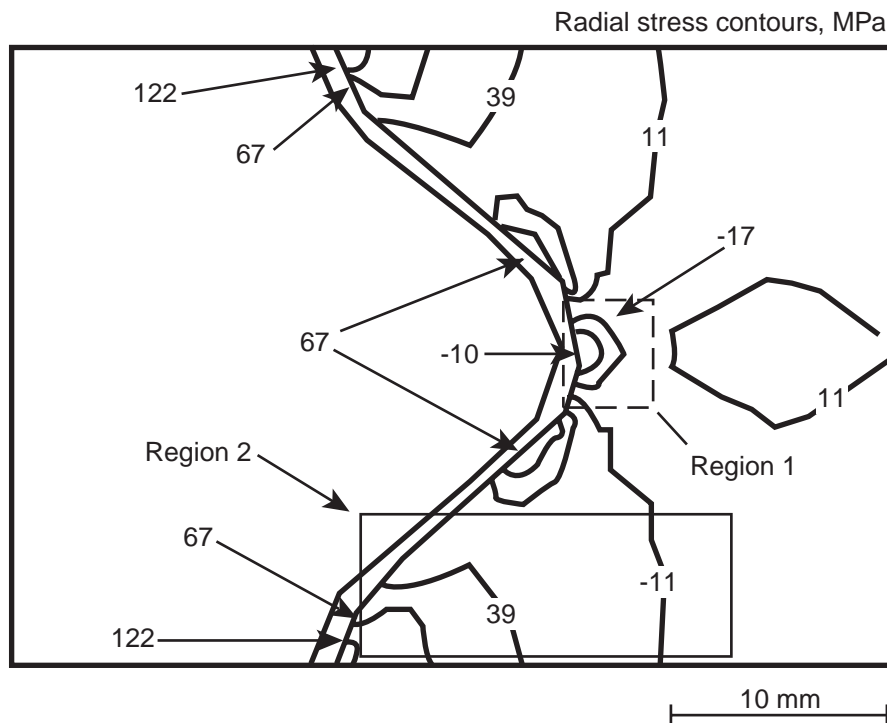
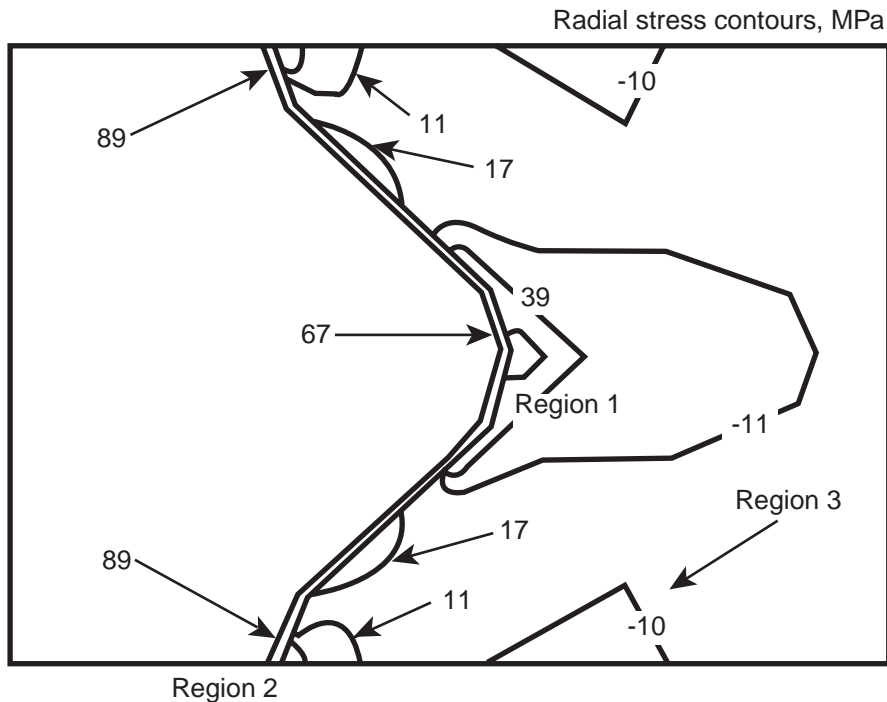
Oxidation of the bond coat has been repeatedly identified as one of the major factors affecting the durability of the ceramic top coat during service. However, the mechanisms by which oxidation facilitates TBC failure are poorly understood and require further characterization. In addition, researchers have suspected that other bond coat and top coat factors might influence TBC thermal fatigue life, both separately and through interactions with the mechanism of oxidation. These other factors include the bond coat coefficient of thermal expansion, the bond coat roughness, and the creep behavior of both the ceramic and bond coat layers.

Although it is difficult to design an experiment to examine these factors unambiguously, it is possible to design a computer modeling "experiment" to examine the action and interaction of these factors, as well as to determine failure drivers for TBC's. Previous computer models have examined some of these factors separately to determine their effect on coating residual stresses, but none have examined all the factors concurrently. The purpose of this research, which was performed at DCT, Inc., in contract with the NASA Lewis Research Center, was to develop an inclusive finite element model to characterize the effects of oxidation on the residual

stresses within the TBC system during thermal cycling as well as to examine the interaction of oxidation with the other factors affecting TBC life.

The plasma sprayed, two-layer thermal barrier coating that was modeled incorporated a superalloy substrate, a NiCrAlY bond coat, and a  $\text{ZrO}_2$ -8 wt %  $\text{Y}_2\text{O}_3$  ceramic top coat. We examined the effect on stress during burner rig thermal cycling of the following independent variables: creep in the bond coat and top coat, oxidation, bond coat coefficient of thermal expansion, number of thermal cycles, and interfacial roughness. All these factors were suspected of influencing TBC failure.

The model showed that all the material properties studied had a significant effect on the coating's residual stresses if the interface of the bond coat was rough. Bond



Contour plot showing the change in stress distribution with increasing oxide thickness at increased numbers of cycles. Top: At four cycles, the bond coat peak region (region 1) is primarily tensile, while the tensile region in the valley (region 2) is quite small and adjacent to a compressive region (region 3). Bottom: At 51 cycles, the tensile region over the valley has grown substantially (region 2), while the peak region has become compressive (region 1). These plots are shown in color in the online version of this article (<http://www.lerc.nasa.gov/WWW/RT1997/5000/5160brindley.htm>).

coat expansion, bond coat oxidation, and bond coat creep had the highest effect on coating stresses, and these were highly interactive. The model also showed that the mechanism of stress generation during thermal cycling changed with the number of thermal cycles. Bond coat and top coat creep dominated stress generation during early thermal cycles, greatly increasing delamination stresses at the peaks of the bond coat. Therefore, creep is the prime driver for delamination cracking early in life, but cracking is limited to the bond coat peak region. Oxidation of the bond coat, on the other hand, tended to dominate stress generation during later cycles by greatly increasing delamination stresses over bond coat valleys. These results indicate that oxidation is the driver for the continued cracking necessary to cause ceramic layer spallation.

**Lewis contact:**

Dr. William J. Brindley, (216) 433-3274, William.J.Brindley@lerc.nasa.gov

**Authors:** A.M. Freborg, B.L. Ferguson, G.J. Petrus, DCT, Inc. (440) 234-8477; and W.J. Brindley

**Headquarters program office:** OASTT

**Programs/Projects:** Propulsion Systems R&T, HITEMP



# Oxidation of Boron Nitride in Composites

Boron nitride (BN) is a prime candidate for fiber coatings in silicon carbide (SiC) fiber-reinforced SiC matrix composites. The properties of BN allow the fiber to impart beneficial composite properties to the matrix, even at elevated temperatures.

The problem with BN is that it is readily attacked by oxygen. Although BN is an internal component of the composite, a matrix crack or pore can create a path for hot oxygen to attack the BN. This type of attack is not well understood. A variety of phenomena have been observed. These include borosilicate glass formation, volatilization of the BN, and under some conditions, preservation of the BN. In this study at the NASA Lewis Research Center, a series of BN materials and BN-containing model composites were methodically examined to understand the various issues dealing with the oxidation of BN in composites.

Initial studies were done with a series of monolithic BN materials prepared by hot pressing and chemical vapor deposition (CVD). From these studies, we found that BN showed a strong orientation effect in oxidation and was extremely sensitive to the presence of water vapor in the environment. In addition, CVD material deposited at a high temperature showed much better oxidation behavior than CVD material deposited at a lower temperature.

With this information we were able to examine BN oxidation in a composite. Borosilicate glass formation, the most common behavior, occurred when the BN coatings were exposed to oxygen at intermediate temperatures. In these cases, the BN oxidizes to boric oxide ( $B_2O_3$ ), which enhances SiC oxidation to silica ( $SiO_2$ ). The two oxidation products react to form borosilicate. It was also observed that as the reaction progressed the  $B_2O_3$  was leached out of the glass by residual water vapor.

Another observation was the volatilization of the BN fiber coatings. This was observed in water-vapor-containing environments. Volatilization is caused by oxidation of BN to  $B_2O_3$  and the subsequent reaction with water to form highly stable species of the form  $H_xB_yO_z(g)$ . We have developed some models to describe this process and predict recession, based on simple diffusion through pores.

Finally, in some cases the BN remained intact. This occurred primarily in model composites with the CVD BN deposited at very high temperatures. Currently, it is not feasible to make commercial materials with this type of BN. In such cases, BN is preserved because of the high stability of these BN materials as well as the gettering of oxygen by SiC, which effectively lowers the oxygen potential below that at which  $B_2O_3$  forms.

The data from this series of experiments is being used to understand the issues necessary to improve the properties of BN—such as processing and additives. Current work is focusing on the effectiveness of additives in improving BN oxidation properties.

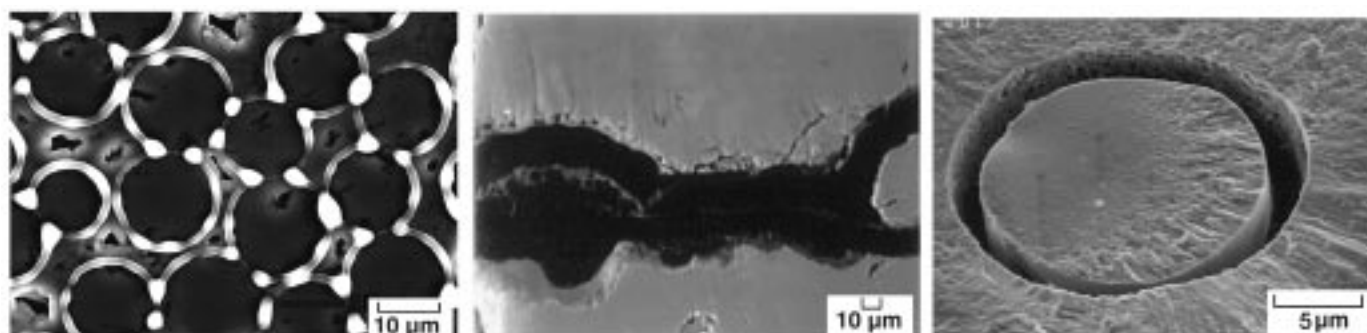
## Lewis contact:

Dr. Nathan S. Jacobson,  
(216) 433-5498,  
Nathan.S.Jacobson@lerc.nasa.gov

**Author:** Dr. Nathan S. Jacobson

**Headquarters program office:** OASTT

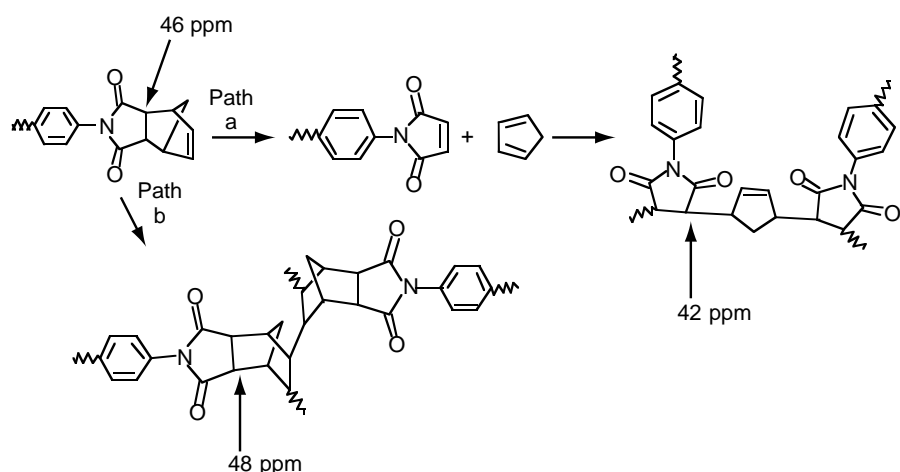
**Programs/Projects:** Propulsion  
Systems R&T, HITEMP, HSR, EPM



*Oxidation behavior of model composites with BN layers. Left: At 816 °C for 100 hr with low water vapor, BN deposited at a low temperature forms borosilicate. Middle: At 900 °C for 140 hr with low water vapor, BN deposited at a high temperature remains intact. Right: At 500 °C for 100 hr with water vapor, BN deposited at a low temperature is volatilized.*

# Carbon-13 Labeling Used to Probe Cure and Degradation Reactions of High-Temperature Polymers

High-temperature, crosslinked polyimides are typically insoluble, intractable materials. Consequently, in these systems it has been difficult to follow high-temperature curing or long-term degradation reactions on a molecular level. Selective labeling of the polymers with carbon-13, coupled with solid nuclear magnetic resonance spectrometry (NMR), enables these reactions to be followed (ref. 1). We successfully employed this technique to provide insight into both curing and degradation reactions of PMR-15, a polymer matrix resin used extensively in aircraft engine applications (refs. 2 and 3).

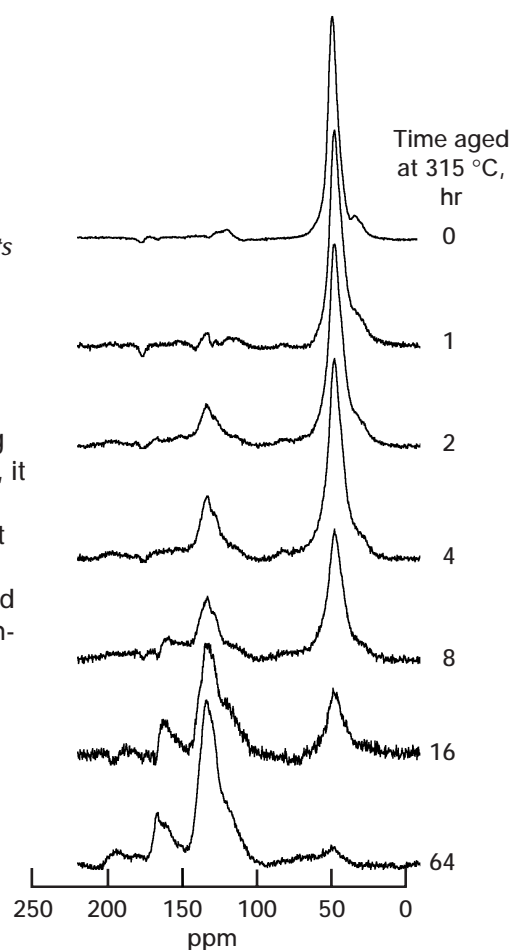


*Possible crosslinking pathways for the endcap with the carbon-13 chemical shifts of labeled carbons predicted from model compounds.*

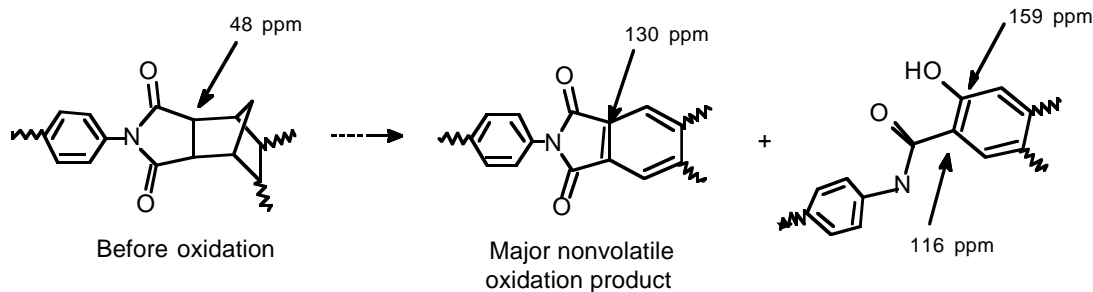
PMR-15 is prepared via a two-step approach involving the initial formation of an endcapped prepolymer followed by crosslinking through the endcaps, producing a void-free network. Though the polymer has been studied extensively for more than 20 years, the nature of the crosslinking step has not been well-understood (see the preceding figure). Originally, it was thought that crosslinking occurred through cleavage of the endcap, followed by copolymerization, path a (ref. 4). Later, others suggested that the endcap simply homopolymerized through the double bond, path b (ref. 5). Solid nuclear magnetic resonance of selectively carbon-13 labeled endcap allowed researchers at the NASA Lewis Research Center to unambiguously distinguish between the two pathways (ref. 6).

For each step of curing or aging, the solid nuclear magnetic resonance spectrum of natural abundance PMR-15 powder, as well as that of the labeled analog, was determined. Carefully matched experimental conditions allowed the natural abundance spectra to be subtracted from the labeled to obtain difference spectra containing only labeled resonances. In this way, it was possible to follow the transformations of only the labeled carbon. The difference spectrum of the prepolymer consists of a single peak at 46 ppm. On crosslinking, the peak shifts downfield to 48 ppm, indicating that polymerization takes place mainly through path b.

Knowledge of the crosslinking mechanism and the resulting molecular structure is not merely important for understanding how the polymer cures. We can now begin interpreting the degradation reactions occurring in the endcap during long-term aging (ref. 7). The next figure shows difference spectra for endcap-labeled PMR-15 powder aged at 315 °C. After 64 hr, nearly all the peak at 48 ppm is gone. In its place, three broad peaks for labeled carbons grew in at 110 to 120, 125 to 140, and 155 to 165 ppm.



*Carbon-13 difference spectra of labeled carbons on nadic endcap shown before and after aging at 315 °C for up to 64 hr.*



*Possible products of the oxidation of nadic crosslinks shown with chemical shifts predicted from model compounds.*

Though the spectra are complex, these broad peaks suggest (see the final figure) that degradation involves oxidation of the bridging methylene followed by carbon monoxide extrusion to lead to substituted phenyl rings (130 ppm). Further oxidation might lead to breakage of the imide bond and give rise to structures with oxygen directly attached to one of the labeled carbons (159 ppm), with the other labeled carbon at 116 ppm. These results represent the first molecular level evidence of the formation of nonvolatile degradation products from the endcaps, and they give insight into ways to stabilize the endcap for a new generation of cross-linked polyimides.

## References

1. Swanson, S.A.; Fleming, W.W.; and Hofer, D.C.: Acetylene-Terminated Polyimide Cure Studies Using  $^{13}\text{C}$  Magic-Angle Spinning NMR on Isotopically Labeled Samples. *Macromol.*, vol. 25, 1992, pp. 582–588.
2. Serafini, T.T.; Delvigs, P.; and Lightsey, G.R.: Thermally Stable Polyimides From Solutions on Monomeric Reactants. *J. Appl. Polym. Sci.*, vol. 16, 1972, pp. 905–915.
3. Meador, M.A.; Cavano, P.J.; and Malarik, D.C.: High-Temperature Polymer Matrix Composites for Extreme Environments. *Proceedings of the Sixth Annual Advanced Composites Conference*, ASM International, Metals Park, Ohio, 1990, pp. 529–539.
4. Burns, E.A., et al.: Thermally Stable Laminating Resins. NASA CR-72633, 1970.
5. Wong, A.C.; and Ritchey, W.M.: Nuclear Magnetic-Resonance Study of Norbornene End-Capped Polyimides. *Macromol.*, vol. 14, no. 3, 1981, pp. 825–831.
6. Meador, M.A.B.; Johnston, J.C.; and Cavano, P.: Elucidation of the Cross-Link Structure of Nadic-End-Capped Polyimides Using NMR of  $^{13}\text{C}$ -Labeled Polymers. *J. Macromol.*, vol. 30, no. 3, 1997, pp. 515–519.
7. Meador, M.A.B., et al.: Oxidative Degradation of Nadic-End-Capped Polymides. Evidence for Reactions Occurring at High Temperatures. *Macromol.*, vol. 30, no. 11, 1997, pp. 3215–3223.

## Lewis contacts:

Dr. Mary Ann B. Meador, (216) 433–3221, Maryann.Meador@lerc.nasa.gov, and  
Dr. J. Christopher Johnston, (216) 433–5029, James.C.Johnston@lerc.nasa.gov

**Authors:** Dr. Mary Ann B. Meador and Dr. J. Christopher Johnston

**Headquarters program office:** OASTT

**Programs/Projects:** Propulsion Systems R&T, HITEMP



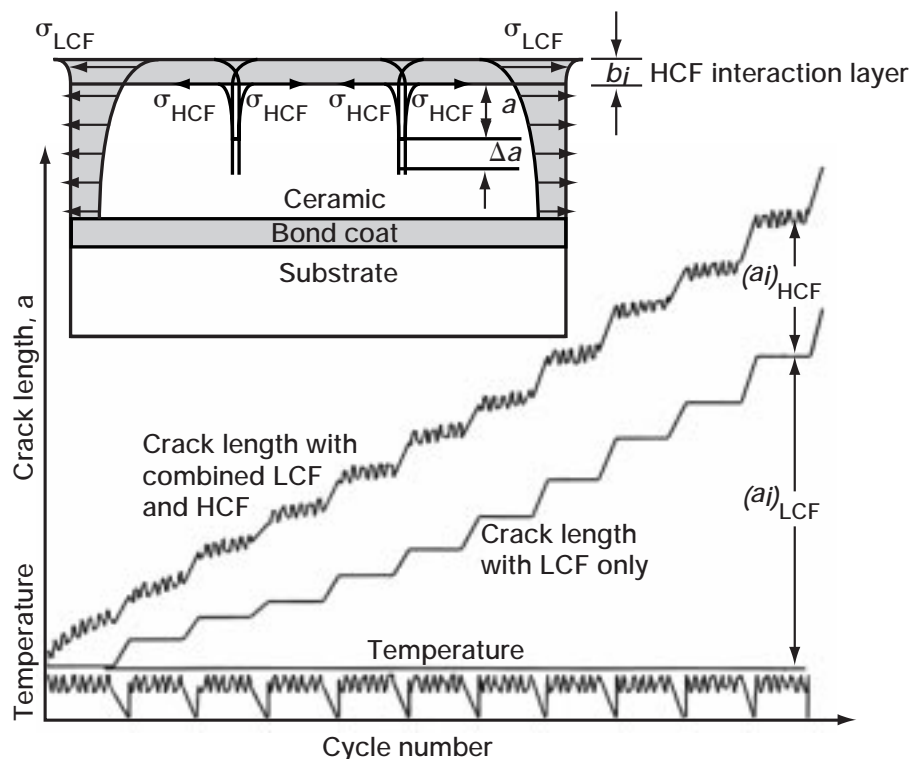
# Thermal High- and Low-Cycle Fatigue Behavior of Thick Thermal Barrier Coating Systems

Ceramic thermal barrier coatings have received increasing attention for advanced gas turbine and diesel engine applications because of their ability to provide thermal insulation to engine components. However, the durability of these coatings under the severe thermal cycling conditions encountered in a diesel engine (ref. 1) still remains a major issue. In this research at the NASA Lewis Research Center, a high-power laser was used to investigate the thermal fatigue behavior of a yttria-stabilized zirconia coating system under simulated diesel engine conditions. The mechanisms of fatigue crack initiation and propagation, and of coating failure under complex thermal low-cycle fatigue (LCF, representing stop/start cycles) and thermal high-cycle fatigue (HCF, representing operation at 1300 rpm) are described.

Continuous wave and pulse laser modes were used to simulate pure LCF and combined LCF/HCF, respectively (ref. 2). The LCF mechanism was found to be closely related to the coating sintering and creep at high temperatures. These creep strains in the ceramic coating led to a tensile stress state during cooling, thus providing the major driving force for crack growth under LCF conditions. The combined LCF/HCF tests induced more severe coating surface cracking, microspallation, and accelerated crack growth than did the pure LCF test. HCF thermal loads also facilitated lateral crack branching and ceramic/bond coat interface delaminations.

HCF is associated with the cyclic stresses originating from the high-frequency temperature fluctuation at the ceramic coating surface. The HCF thermal loads act on the crack by a wedging mechanism (ref. 1), resulting in continuous crack growth at temperature. The HCF stress intensity factor amplitude increases with the interaction depth and temperature swing, and decreases with the crack depth. HCF damage also increases with the thermal expansion coefficient and the Young's modulus of the ceramic coating (refs. 1 and 3).

LCF/HCF interactions are expected to be complex. As illustrated in the figure for the proposed LCF/HCF mechanisms, alternating HCF and LCF loading ( $\sigma_{HCF}$  and  $\sigma_{LCF}$  stresses) at temperature and during cooling would increase the overall crack growth rate in the combined LCF/HCF tests. In addition, because of the ceramic-bond coat elastic mismatch, the stress intensity factor amplitudes tend to drop to zero when the crack approaches the ceramic/bond coat interface because of the relatively stiff bond coat (ref. 4). Therefore, the crack will be expected to deflect along the interface, thus leading to interface delamination under subsequent LCF and HCF loading. The thermal LCF and HCF crack growth is also greatly influenced by the HCF loading-unloading process.



Proposed thermal LCF and HCF mechanisms;  $a_i$ , crack length at any given cycle.

## References

1. Zhu, D.; and Miller, R.A.: Influence of High Cycle Thermal Loads on Thermal Fatigue Behavior of Thick Thermal Barrier Coatings. NASA TP-3676, 1997. Available online: <http://letrs.lerc.nasa.gov/cgi-bin/LeTRS/browse.pl?1997/TP-3676.html>

2. Zhu, D.; and Miller, R.A.: Thermal Fatigue Testing of  $\text{ZrO}_2\text{-Y}_2\text{O}_3$  Thermal Barrier Coating Systems Using a High Power  $\text{CO}_2$  Laser. NASA TM-107439, 1997. Available online: <http://letrs.lerc.nasa.gov/cgi-bin/LeTRS/browse.pl?1997/TM-107439.html>
3. Zhu, D.; and Miller, R.A.: Investigation of Thermal Low Cycle and High Cycle Fatigue Mechanisms of Thick Thermal Barrier Coatings. *Surface and Coatings Technology*, vol. 94-95, pp. 94-101.
4. Zhu, D.; and Miller, R.A.: Investigation of Thermal Low Cycle and High Cycle Fatigue Mechanisms of Thick Thermal Barrier Coatings. The 3rd Thermal Barrier Coating Workshop, sponsored by the TBC Interagency Coordination Committee (W. J. Brindley, ed.), (also *Materials Science and Engineering*, in press) 1997, pp. 139-150.

**Lewis contact:**

Dr. Robert A. Miller, (216) 433-3298,  
Robert.A.Miller@lerc.nasa.gov

**Authors:**

Dongming Zhu and Dr. Robert A. Miller

**Headquarters program offices:**

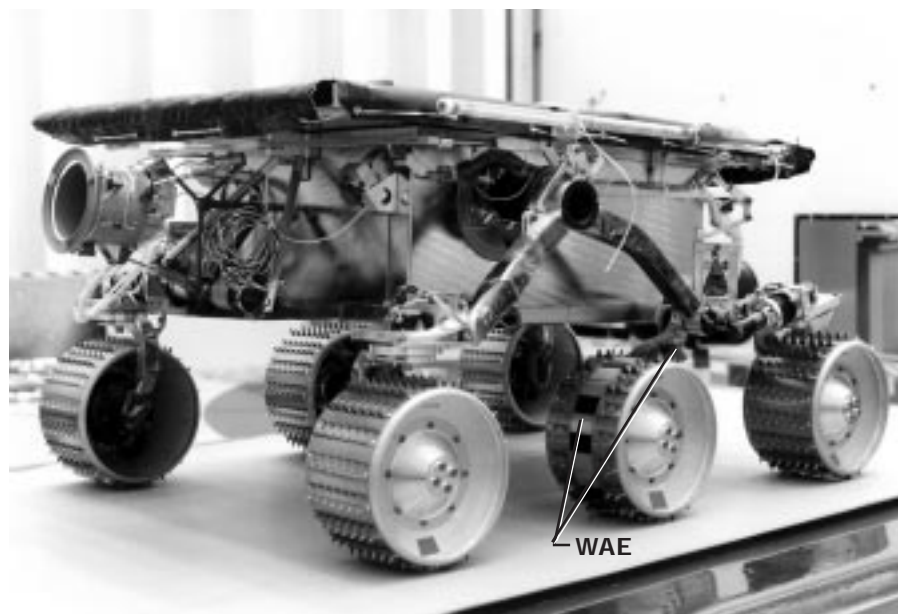
OASTT, ARL

**Programs/Projects:**

Propulsion Systems R&T, HITEMP

## Power and On-Board Propulsion Technology

### Wheel Abrasion Experiment Conducted on Mars



*Sojourner rover showing Lewis' wheel abrasion experiment.*

The Mars Pathfinder spacecraft soft-landed on Mars on July 4, 1997. Among the many experiments on its small Sojourner rover are three technology experiments from the NASA Lewis Research Center, including the Wheel Abrasion Experiment (WAE). The WAE was designed, built, delivered, and operated on Mars by a team of engineers and scientists from Lewis' Photovoltaics and Space Environments Branch. This experiment collected data to assess wheel surface wear on the Sojourner. It used a specially designed rover wheel, with thin films (200 to 1000 angstroms) of aluminum, nickel, and platinum deposited on black, anodized aluminum strips attached to the rover's right center wheel. As the wheel spun in the Martian soil, a photovoltaic sensor monitored changes in film reflectivity. These changes indicated abrasion of the metal films by Martian surface material. Rolling wear data were accumulated by the WAE. Also, at frequent intervals, all the

rover wheels, except the WAE test wheel, were locked to hold the rover stationary while the test wheel alone was spun and dug into the Martian regolith. These tests created wear conditions more severe than simple rolling.

The WAE will contribute substantially to our knowledge of Martian surface characteristics. Marked abrasion would indicate a surface composed of hard, possibly sharply edged grains, whereas lack of abrasion would suggest a somewhat softer surface. WAE results will be correlated with ground simulations to determine which terrestrial materials behave most like those on Mars. This knowledge will enable a deeper understanding of erosion processes on Mars and the role they play in Martian surface evolution.

Preliminary results show that electrostatic charging of the rover wheels sometimes caused dust to accumulate on the WAE wheel, making interpretation of the reflectance data problematic. If electrostatic charging is the mechanism for dust attraction, this indicates that the Martian dust has a size somewhat smaller than 40  $\mu\text{m}$  in

diameter. The WAE experiment has detected electrostatic charging in the Martian environment for the first time; however, under conditions when the wheel is relatively clean of Martian dust, flight data now indicate that abrasion has also been detected. Crude limits so far place the hardness of the Martian dust at harder than aluminum but softer than nickel, and place the grain size at somewhat smaller than 40  $\mu\text{m}$ .

**Lewis contact:**

Dr. Dale C. Ferguson, (216) 433-2298,  
Dale.C.Ferguson@lerc.nasa.gov

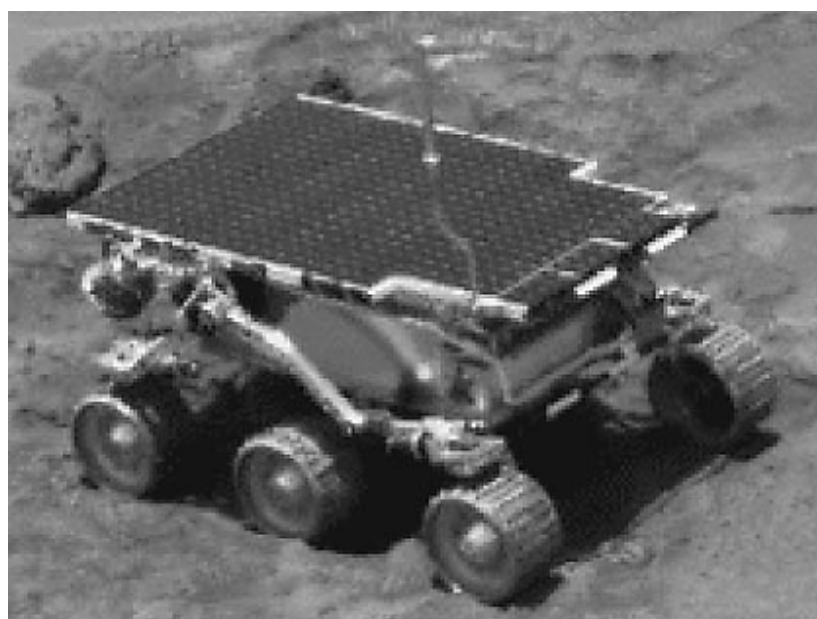
**Author:** Dr. Dale C. Ferguson

**Headquarters program office:** OSS

**Programs/Projects:**

Mars Pathfinder Sojourner

## Results From Mars Show Electrostatic Charging of the Mars Pathfinder Sojourner Rover



*Sojourner rover at the end of sol 22. Fine dust shows around the wheel edges.*

Indirect evidence (dust accumulation) has been obtained indicating that the Mars Pathfinder rover, Sojourner, experienced electrostatic charging on Mars. Lander camera images of the Sojourner rover provide distinctive evidence of dust accumulation on rover wheels during traverses, turns, and crabbing maneuvers. The sol 22 (22nd Martian "day" after Pathfinder landed) end-of-day image (shown above) clearly shows fine red dust concentrated around the wheel edges with additional accumulation in the wheel hubs (images are shown in color in the online version of this article—<http://www.lerc.nasa.gov/WWW/RT1997/5000/5410kolecki.htm>). A sol 41 image of the rover near the rock "Wedge" (see the next image) shows a more uniform coating of dust on the wheel drive surfaces with accumulation in the hubs similar to that in the previous image. In the sol 41 image, note particularly the loss of black-white contrast on the Wheel Abrasion Experiment strips (center wheel). This loss of contrast was also seen when dust accumulated on test wheels in the laboratory (see the last image and ref. 1).

We believe that this accumulation occurred because the Martian surface dust consists of clay-sized particles, similar to those detected by Viking, which have become electrically charged. By adhering to the wheels, the charged dust carries a net nonzero charge to the rover, raising its electrical potential relative to its surroundings. Similar charging behavior was routinely observed in an experimental facility at the NASA Lewis Research Center, where a Sojourner wheel was driven in a simulated Martian surface environment. There, as the wheel moved and accumulated dust (see the third image), electrical potentials in excess of 100 V (relative to the chamber ground) were detected by a capacitively coupled electrostatic probe located 4 mm from the wheel surface. The measured wheel capacitance was approximately 80 picofarads (pF), and the calculated charge,  $8 \times 10^{-9}$  coulombs (C) (ref. 1). Voltage differences of 100 V and greater are believed sufficient to produce Paschen electrical discharge in the Martian atmosphere (ref. 2). With an accumulated net charge of  $8 \times 10^{-9}$  C, and average arc time of 1 msec, arcs can also occur with estimated arc currents approaching 10 milliamperes (mA). Discharges of this magnitude could interfere



*Sojourner rover on sol 41. Dust is uniform on the wheel drive surface.*

with the operation of sensitive electrical or electronic elements and logic circuits.

Before launch, we believed that the dust would become triboelectrically charged as it was moved about and compacted by the rover wheels. In all cases observed in the laboratory, the test wheel charged positively, and the wheel tracks charged negatively. Dust samples removed from the laboratory wheel averaged a few ones to tens of micrometers in size (clay size). Coarser grains were left behind in the wheel track. On Mars, grain size estimates of 2 to 10  $\mu\text{m}$  were derived for the Martian surface materials from the Viking Gas Exchange Experiment. These size estimates approximately match the laboratory samples. Our tentative conclusion for the Sojourner observations is that fine clay-sized particles acquired an electrostatic charge during rover traverses and adhered to the rover wheels, carrying electrical charge to the rover. Since the Sojourner rover carried no instruments to measure this mission's onboard electrical charge, confirmatory measurements from future rover missions on Mars are desirable so that the physical and electrical properties of the Martian surface dust can be characterized.

Sojourner was protected by discharge points, and Faraday cages were placed around sensitive electronics. But larger systems than Sojourner are being contemplated for missions to the Martian surface in the foreseeable future. The design of such systems will require a detailed knowledge of how they will interact with their environment. Validated environmental interaction models and guidelines for the Martian surface must be developed so that design engineers can test new ideas prior to cutting hardware. These models and guidelines cannot be validated without actual flight data. Electrical charging of vehicles and, one day, astronauts moving across the Martian surface may have

moderate to severe consequences if large potential differences develop. The observations from Sojourner point to just such a possibility. It is desirable to quantify these results. The various lander/rover missions being planned for the upcoming decade provide the means for doing so. They should, therefore, carry instruments that will not only measure vehicle charging but characterize all the natural and induced electrical phenomena occurring in the environment and assess their impact on future missions.

#### References

1. Siebert, M.; and Kolecki, J.: Electrostatic Charging of the Mars Pathfinder Rover. AIAA Paper 96-0486, 1996.
2. Leach, R.N.: Effect of Pressure on Electrostatic Processes on Mars. Sand and Dust on Mars. NASA CP-10074, 1991, p. 36.

#### Lewis contacts:

Joseph C. Kolecki, (216) 433-2296, Joseph.C.Kolecki@lerc.nasa.gov, and Mark W. Siebert, (216) 433-6012, Mark.W.Siebert@lerc.nasa.gov

**Authors:** Joseph C. Kolecki and Mark W. Siebert

**Headquarters program office:** OSS

**Programs/Projects:**

Mars Pathfinder Sojourner

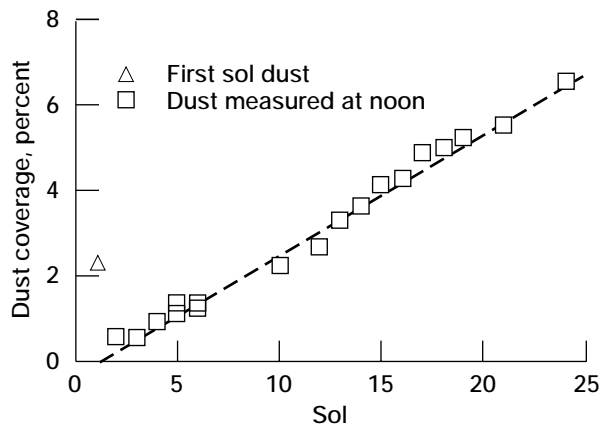


*Sojourner rover wheel tested in laboratory before launch to Mars.*



# Measuring Dust on Mars

Mars is a dusty planet. Will dust accumulation on solar arrays be a problem for large solar power systems used on long-duration future missions on Mars? NASA Lewis Research Center's Materials Adherence Experiment (MAE) on the Mars Pathfinder Sojourner rover was designed to find out. It measured the dust deposited on the rover's solar array by measuring the change in transparency of a movable glass cover as dust settled on it. This graph shows the results from the first 2½ weeks of operation on Mars.



*Dust deposition on the Sojourner rover. Slope, 0.28 percent per day.*

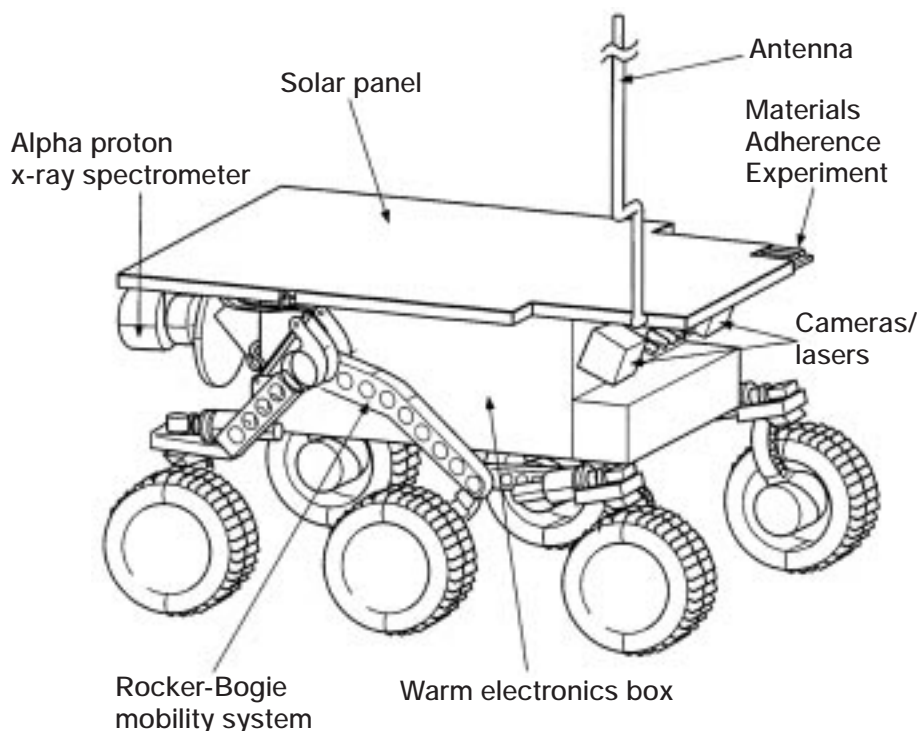
The rover solar array accumulated dust at a rate of about a quarter of a percent of coverage per day (see the graph). This is very close to the coverage of 0.22 percent predicted before the mission (ref. 1). The deposition rate seemed to be the same on the sols (Martian "days") when the rover was in motion as it was on sols when the rover remained in place, indicating that the deposition was probably due to dust settling out of the atmosphere, not dust kicked up by the Sojourner Rover's motion.

The illustration shows the location of the MAE on the Sojourner rover, and the photo shows the experiment mounted on the corner of the rover during a prelaunch test. Information on the new design of lightweight nitinol actuator used for the experiment can be found in a paper describing the experiment (ref. 2). The MAE solar cell experiment was built by Geoffrey Landis of the Ohio Aerospace Institute and Phillip Jenkins of Essential Research, Inc.

**More discussion of solar energy on Mars and the Materials Adherence Experiment is available on the World Wide Web:**

<http://powerweb.lerc.nasa.gov/pv/SolarMars.html>

<http://powerweb.lerc.nasa.gov/pv/landis.html>



*Sojourner Rover showing location of the Materials Adherence Experiment.*

## References

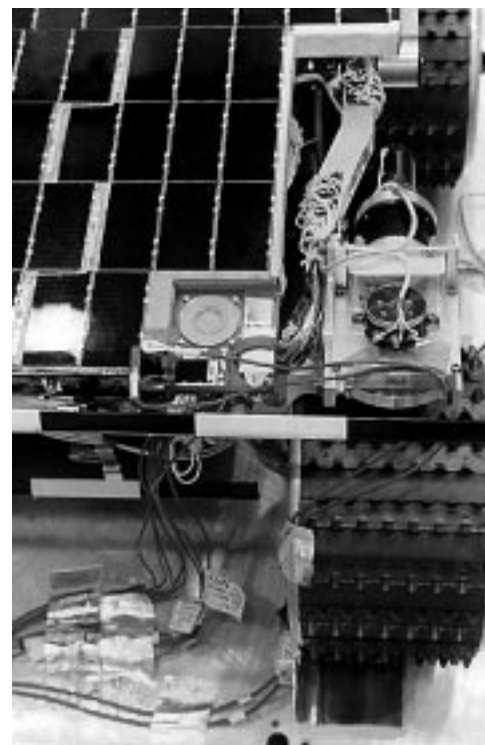
1. Landis, G.A.: Dust Obscuration of Mars Solar Arrays. *Acta Astronaut.*, vol. 38, no. 11, 1996, pp. 885–891.
2. Jenkins, P.P.; Landis, G.A.; and Oberle, L.G.: Materials Adherence Experiment—Technology. IECEC–97339, Proceedings of the 32nd Intersociety Energy Conversion Engineering Conference, Vol. 1, 1997, pp. 728–731. Available online: <http://powerweb.lerc.nasa.gov/pv/techn.html>
3. Landis, G.A.: Mars Dust Removal Technology. IECEC–97345, Proceedings of the 32nd Intersociety Energy Conversion Engineering Conference, Vol. 1, 1997, pp. 764–767. Available online: <http://powerweb.lerc.nasa.gov/pv/removal.html>

**Lewis contact:** Geoffrey A. Landis, (216) 433–2238, [Geoffrey.A.Landis@lerc.nasa.gov](mailto:Geoffrey.A.Landis@lerc.nasa.gov)

**Author:** Geoffrey A. Landis

**Headquarters program office:** OSS

**Programs/Projects:** Mars Pathfinder Sojourner



*Materials Adherence Experiment shown mounted on the Sojourner rover.*

## Lightweight Nickel Electrode Development Program



*Nickel-hydrogen boilerplate cell.*

Because of its relatively high specific energy and excellent cycling capability, the nickel-hydrogen (Ni-H<sub>2</sub>) cell is used extensively to store energy in aerospace systems. For the past several years, the NASA Lewis Research Center has been developing the Ni-H<sub>2</sub> cell to improve its components, design, and operating characteristics. The battery size and weight are crucial parameters in aerospace and spacecraft power systems for applications such as the International Space Station, space satellites, and space telescopes. The nickel electrode has been identified as the heaviest and most critical component of the Ni-H<sub>2</sub> cell. Consequently, Lewis began and is leading a program to reduce the electrode's weight by using lightweight plaques.

Using a lightweight nickel plaque in place of a heavy sintered nickel plaque is expected to improve the specific energy, weight, and performance of the nickel electrode. The three nickel fiber plaques used in this development program were developed by Memtec America Corporation, Ribbon Technology Corporation, and Auburn University. These new materials enable plaques to be made with reduced pore sizes as well as with increased surface area, conductivity, strength, and porosity. The plaques are fabricated into nickel electrodes by electrochemically impregnating them with nickel hydroxide active material.



A boilerplate Ni-H<sub>2</sub> cell with a lightweight nickel electrode was fabricated and is currently being tested in-house at Lewis at a 60-percent depth of discharge. So far, the cell has accumulated over 1000 cycles with stable voltage.

In this combined effort, Lewis has a contract with Hughes Space and Communications Company to transfer the technology and is working with Eagle Picher Industries to commercially develop the lightweight nickel electrode. Lewis also has a grant with the Space Power Institute (Auburn University) to develop a high-performance nickel-hydroxide electrode with composite microstructure nickel-fiber electrodes. These electrodes are being tested in boilerplate Ni-H<sub>2</sub> cells both at Hughes and Lewis.

Improving the lightweight Ni-H<sub>2</sub> cell will benefit NASA (exploratory platforms and rovers) as well as commercial aerospace companies (communi-

cation satellites). It will also benefit commercial battery companies that use nickel-based electrodes (e.g., nickel-metal-hydride and nickel-cadmium systems).

**Lewis contact:**

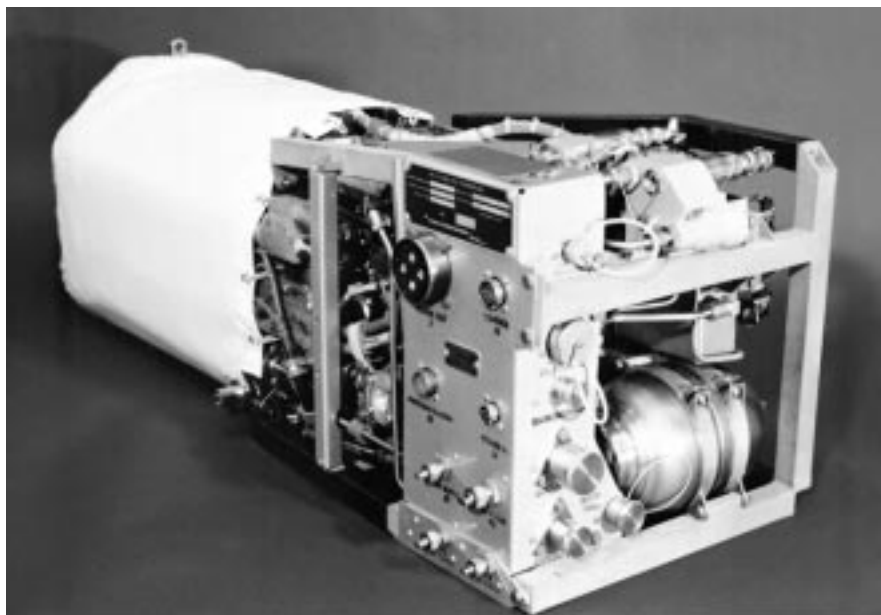
Doris L. Britton, (216) 433-5246,  
dbritton@lerc.nasa.gov

**Author:** Doris L. Britton

**Headquarters program office:** OSS

**Programs/Projects:** HST, Communications Satellites, commercial batteries, ISS, space telescopes

## Systems Analysis in Support of the NASA Fuel Cell Upgrade Program for the Space Shuttle Orbiter



*Existing alkaline fuel cell power plant for shuttle orbiter.*

In early 1996 as part of NASA's overall efforts to improve space shuttle operations, NASA undertook an internal assessment of the shuttle to identify subsystems in the greatest need of upgrading. The criteria used to rank the candidate subsystems were safety improvement, reduction in acquisition and operational costs, improvement in fleet supportability, improvement in mission effectiveness, implementation risk, and commonality with future NASA missions. On the basis of the preliminary results of the NASA assessment, the Fuel Cell Power Plant (FCP) for the shuttle orbiter was among those subsystems selected for further consideration.

The FCP upgrade will involve replacing the existing alkaline fuel cell system with an advanced proton exchange membrane (PEM) fuel cell system. Development of the PEM system for the shuttle will also support a number of other important future space applications. Among these are Moon and Mars surface and transportation power, International Space Station emergency power and/or energy storage, reusable launch vehicle power, and various portable power applications. In carrying out its shuttle FCP upgrade program, NASA is leveraging its own technology development efforts by capitalizing on all of the large-scale PEM fuel cell technology development activities that have been conducted for the Department of Energy, the Department of Defense, and commercial users.

A team comprising members from NASA's Johnson Space Center, Lewis Research Center, Jet Propulsion Laboratory, and Kennedy Space Center has been working on

a plan to upgrade the shuttle orbiter FCP. Key elements of the plan include (1) systems analysis to assure compatibility and the maximum utilization by the shuttle of the best PEM fuel cell characteristics, (2) testing of both short stacks and water separators from the leading PEM fuel cell manufacturers, (3) a flight experiment to verify PEM system thermal and water management under zero-gravity conditions, (4) selection of the best PEM system, and (5) development of flight hardware for both the power and accessory subsystems. NASA Lewis is leading the systems analysis effort in concert with the Jet Propulsion Laboratory. Important subtasks of this effort include defining conceptual design options, configuring computer models for the design, conducting performance parametric analyses, developing system packaging configurations, and ranking conceptual design options. Data derived from the systems analysis task will help guide both the team and our contractor partners as we work toward developing the flight hardware.

**Lewis contact:**

Mark A. Hoberecht, (216) 433-5362,  
Mark.A.Hoberecht@lerc.nasa.gov

**Author:** Mark A. Hoberecht

**Headquarters program office:** OSS

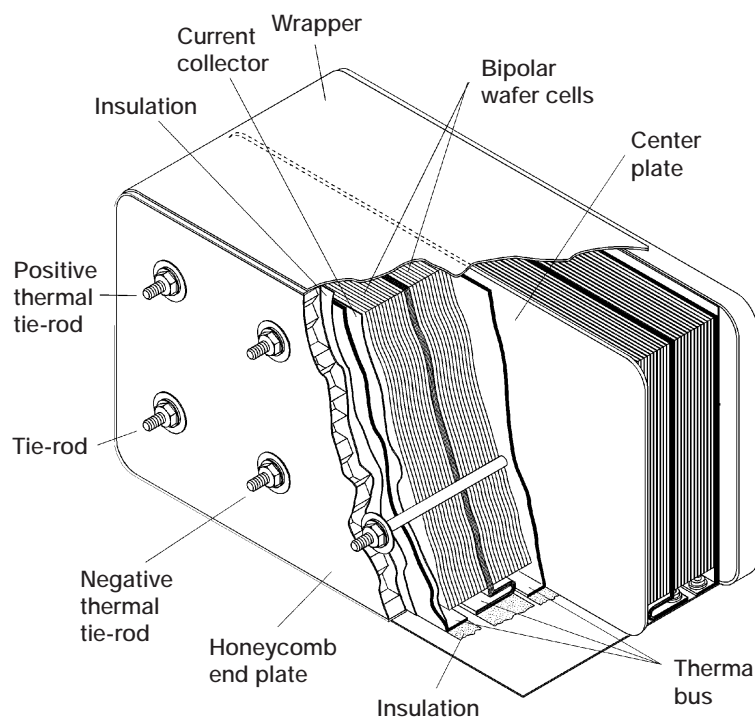
**Programs/Projects:** ATMS, space shuttles, ISS, Moon and Mars surface and transportation power

## Bipolar Nickel-Metal Hydride Battery Being Developed

The NASA Lewis Research Center has contracted with Electro Energy, Inc., to develop a bipolar nickel-metal hydride battery design for energy storage on low-Earth-orbit satellites (NASA contract NAS3-27787). The objective of the bipolar nickel-metal hydride battery development program is to approach advanced battery development from a systems level while incorporating technology advances from the lightweight nickel electrode field, hydride development, and design developments from nickel-hydrogen systems. This will result in a low-volume, simplified, less-expensive battery system that is ideal for small spacecraft applications. The goals of the program are to develop a 1-kilowatt, 28-volt (V), bipolar nickel-metal hydride battery with a specific energy of 100 watt-hours per kilogram (W-hr/kg), an energy density of 250 W-hr/liter and a 5-year life in low Earth orbit at 40-percent depth-of-discharge.

Electro Energy has teamed with Rhône-Poulenc, Eagle-Picher Industries, Inc., Rutgers University, and Design Automation Associates to provide a well-integrated battery design.

Electro Energy is the prime contractor responsible for the overall management of the program, battery design and development, component development and testing, and cell and battery testing. Rhône-Poulenc is responsible for the metal hydride component development and improvement. Eagle-Picher is supporting component and hardware development, battery design, fabrication procedures, trade studies, and documentation.



*Electro Energy's bipolar nickel-metal hydride battery design layout—two parallel, 24-cell stacks. (Copyright Electro Energy; used with permission.)*

Rutgers is providing treated material for the nickel electrodes in the batteries as well as analytical support for new and cycled cell components. Design Automation Associates is developing a

rules-based technology program to aid in trade studies integrating battery design and thermal and structural analyses. This tool will be used to identify areas where development is required to meet the program goals. In addition, the rules-based technology program could be used in the design of bipolar nickel-metal hydride batteries for specific applications.

The program is beginning the third year of a 4-year effort. The baseline battery is a rectangular design that uses two substacks with a 26-ampere-hour (A-hr) capacity each, which are connected in parallel to yield a total capacity of 52 A-hr. Each substack contains 24 cells that measure 6 by 12 in., and the cells are connected in series to provide the required 28 V. The Electro Energy design uses wafer cells to encase the electrochemical cell components. These wafer cells are made of nickel foil and sealed with epoxy. The electrochemical cell components are composed of a lightweight nickel electrode, a Pellon separator, a plastic-bonded metal hydride electrode using AB<sub>5</sub> alloy material from Rhône-Poulenc, and an electrolyte solution of potassium hydroxide. The current version of the design is projected to have a specific energy of 69.5 W-hr/kg and an energy density of 128.3 W-hr/liter. The nickel and hydride electrodes and the battery packaging and housing have been targeted for further development to achieve the program goals of 100 W-hr/kg and 250 W-hr/liter. Preliminary cost

estimates predict an 80-percent cost reduction compared with a similarly sized, state-of-the-art, individual pressure vessel nickel-hydrogen battery system.

**More information about Design Automation Associates is available on the World Wide Web:**  
<http://www.daasolutions.com/>

**Lewis contacts:**

Michelle A. Manzo, (216) 433-5261, [Michelle.A.Manzo@lerc.nasa.gov](mailto:Michelle.A.Manzo@lerc.nasa.gov), and Thomas B. Miller, (216) 433-6300, [Thomas.B.Miller@lerc.nasa.gov](mailto:Thomas.B.Miller@lerc.nasa.gov)

**Author:** Michelle A. Manzo

**Headquarters program office:** OSS

**Programs/Projects:** ATMS

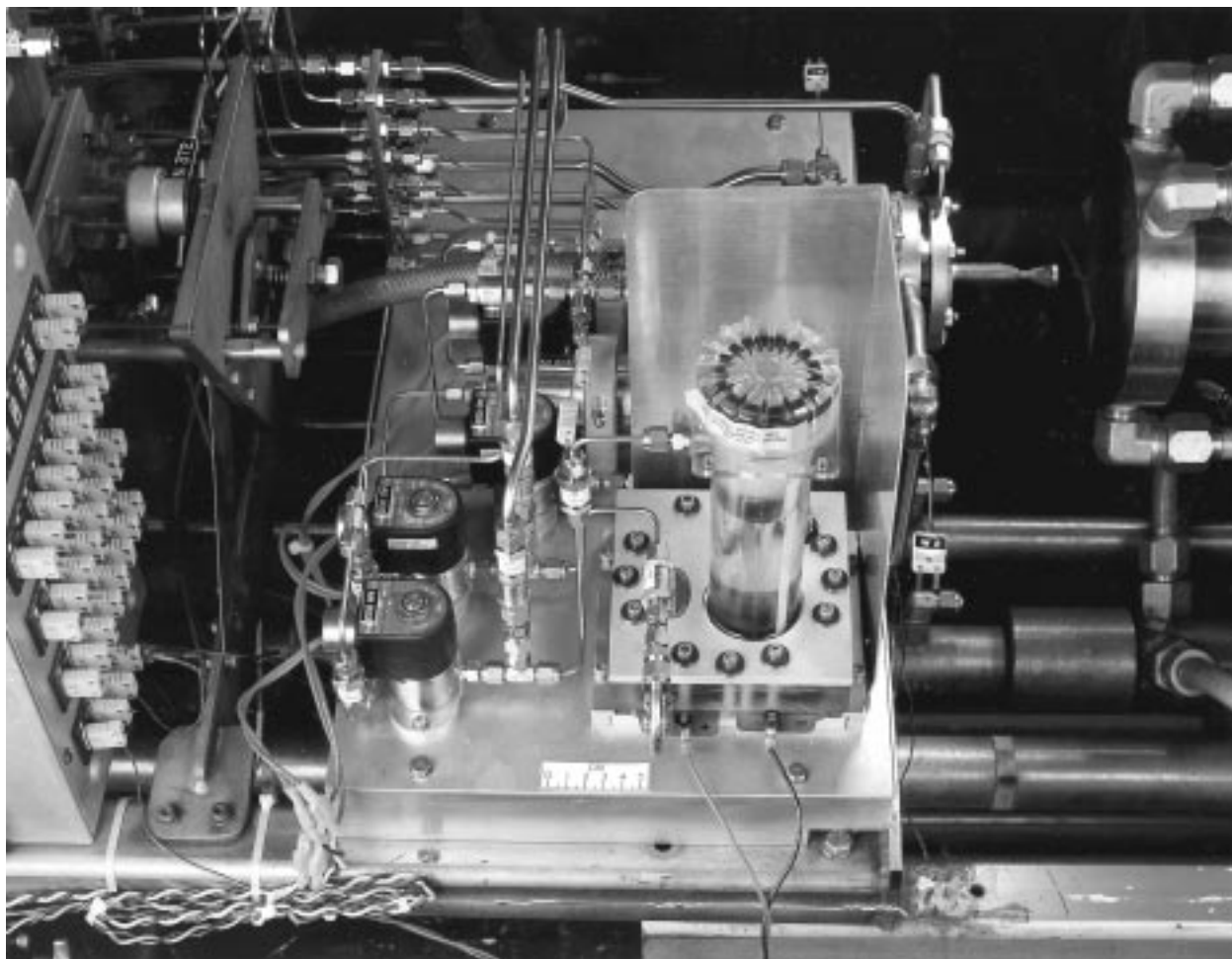
## Electrolysis Propulsion Provides High-Performance, Inexpensive, Clean Spacecraft Propulsion

An electrolysis propulsion system consumes electrical energy to decompose water into hydrogen and oxygen. These gases are stored in separate tanks and used when needed in gaseous bipropellant thrusters for spacecraft propulsion. The propellant and combustion products are clean and nontoxic. As a result, costs associated with testing, handling, and launching can be an order of magnitude lower than for conventional propulsion systems, making electrolysis a cost-effective alternative to state-of-the-art systems. The electrical conversion efficiency is high (>85 percent), and maximum thrust-to-power ratios of 0.2 newtons per kilowatt (N/kW), a 370-sec specific impulse, can be obtained. A further advantage of the water rocket is its dual-mode potential. For relatively high thrust applications, the system can be used as a bipropellant engine. For low thrust levels and/or small impulse bit requirements, cold gas oxygen can be used alone. An added innovation is that the same hardware, with modest modifications, can be converted into an energy-storage and power-generation fuel cell, reducing the spacecraft power and propulsion system weight by an order of magnitude.

In a cooperative NASA Lewis Research Center, Hamilton Standard, and Lawrence Livermore National Laboratory effort, an electrolysis propulsion testbed was assembled. It consisted of a gravity-fed percolating water electrolysis system, storage tanks for hydrogen and oxygen with a volume ratio of approximately 2:1, and a 1.1-N rhenium/iridium high-temperature, oxidation-resistant temperature thruster. The feed system was designed to

operate in a blowdown mode in order to limit weight and complexity. Calibrated flow venturis determined the propellant mass flow rates. The testbed was installed in a high-altitude simulation chamber for cycle testing, as shown in the photo.

Parameters recorded during testing were the electrolysis unit supply current and voltage, and temperatures and pressures inside the electrolysis unit, near the storage tanks, and in the 1.1-N thruster. Quantities derived from these data were the propellant generation rate as a function of supplied power and electrolysis unit gas pressure, thruster mass flow rates, and propellant mixture ratios. The test bed was cycled with input powers varying from 1 to 18 W. Results showed a high degree of repeatability.



*Electrolysis propulsion breadboard installed inside a high-altitude simulation chamber.*

Combustion chamber oxygen-to-fuel mass flow rates varied from 7 to 9 during blowdown tests. Combustion chamber outer wall temperatures did not exceed 1600 °F for the duration of the thruster firings, which lasted between 2.5 and 4.5 seconds.

In a flight system, the gravity-fed electrolyzer utilized for these experiments is replaced with a vapor-feed electrolyzer. Neither mechanical pumps nor pressurant gas is required to feed a water electrolysis rocket system because electrolyzers are able to electrochemically “pump” water decomposition products from ambient pressure up to pressures of at least 20 MPa. The absence of a pressurization system simplifies the propellant feed significantly and eliminates components that must have long-term compatibility with propellants. For deep space missions, water is significantly easier to contain than hypergolic Earth storables (those that can ignite without an outside source of ignition), offering stability over a relatively wide temperature range.

#### **Bibliography**

McElroy, J.F.; and Butler, L.B.: Integrated Modular Propulsion and Regenerative Electro-Energy Storage System (IMPRESS) for Small Satellites. 10th Annual AIAA/USU Conference on Small Satellites, 1996.

de Groot, W.A., et al.: Electrolysis Propulsion for Spacecraft Applications. AIAA Paper 97-2948, 1997.

#### **Lewis contact:**

Dr. Wim A. de Groot, (216) 977-7485, Wilhelmus.A.Degroot@lerc.nasa.gov

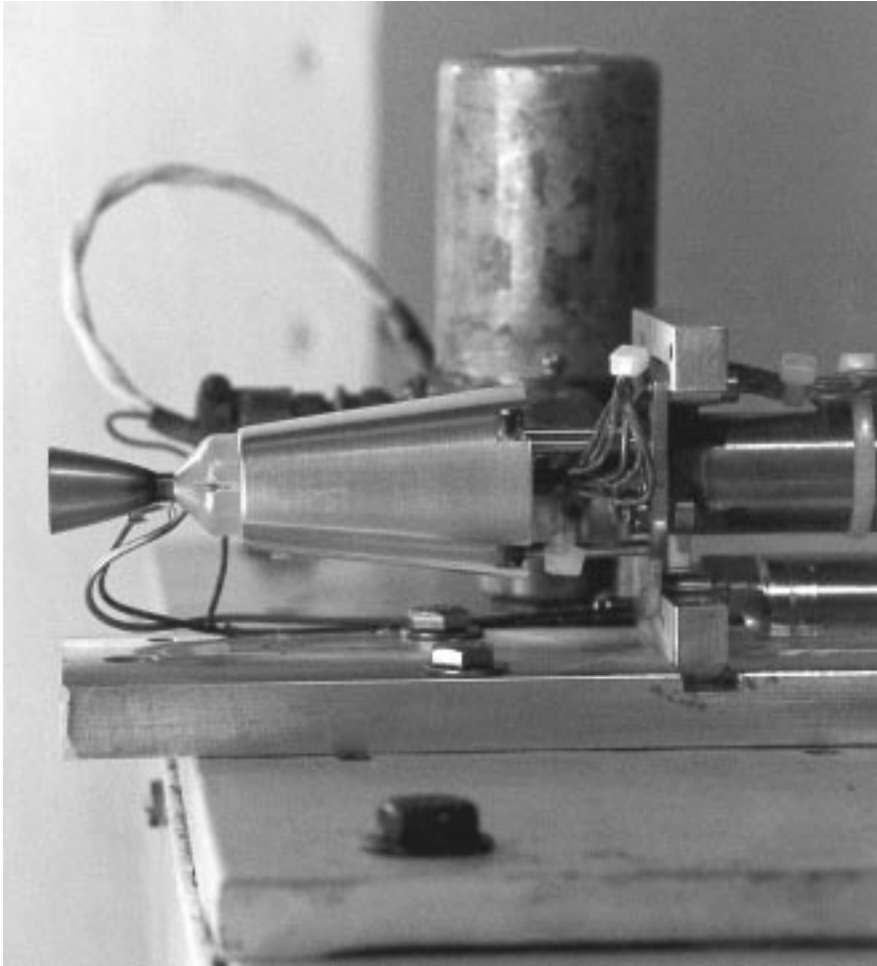
**Author:** Dr. Wim A. de Groot

**Headquarters program office:** OSS

**Programs/Projects:** ATMS



## “Green” Monopropellant Developed for Spacecraft



*Hydroxylammonium nitrate (HAN)-based monopropellant thruster test at Primex Aerospace. (Copyright Primex Aerospace Company; used with permission.)*

The NASA Lewis Research Center and Primex Aerospace Company have developed a “green” monopropellant and thruster for replacement of the toxic hydrazine thrusters presently being used on most spacecraft. The thruster developed is a derivative of the Primex 1-lbf hydrazine MR-111C and operates on a hydroxylammonium nitrate (HAN)-based monopropellant. Initial thruster tests have resulted in a specific impulse of 195 sec and a density-specific impulse of 275 g-sec/cm<sup>3</sup> (which is 25-percent greater than for state-of-the-art hydrazine thrusters).

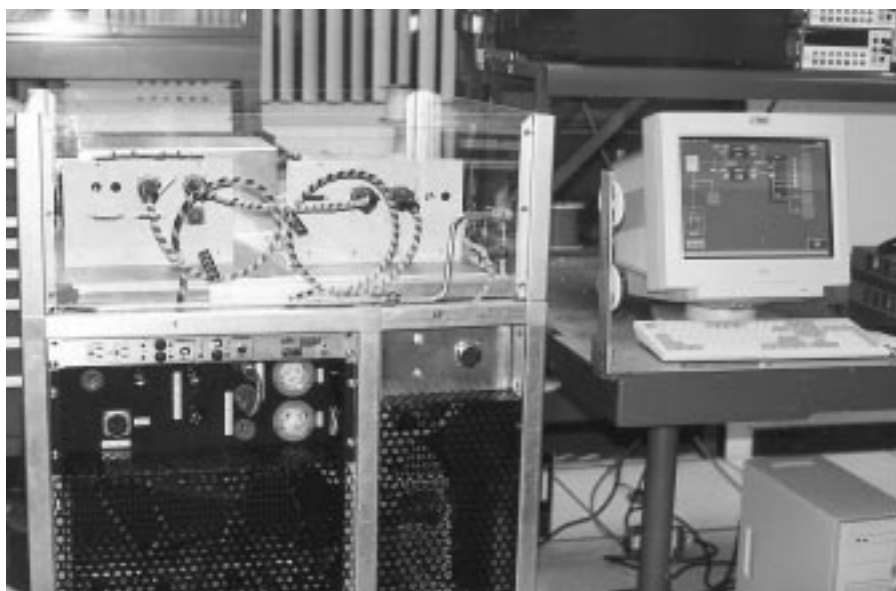
**Lewis contact:** Robert S. Jankovsky, (216) 977-7515,  
Robert.S.Jankovsky@lerc.nasa.gov

**Author:** Robert S. Jankovsky

**Headquarters program office:** OSS

**Programs/Projects:** Projects that use hydrazine or cold gas thrusters

## Power Management and Distribution System Developed for Thermionic Power Converters



*Thermionic power management and distribution hardware.*

A spacecraft solar, bimodal system combines propulsion and power generation into a single integrated system. An Integrated Solar Upper Stage (ISUS) provides orbital transfer capabilities, power generation for payloads, and onboard propulsion to the spacecraft. A key benefit of a bimodal system is a greater payload-to-spacecraft mass ratio resulting in lower launch vehicle requirements. Scaling down to smaller launch vehicles increases space access by reducing overall mission cost. NASA has joined efforts with the Air Force Phillips Laboratory to develop enabling technologies for such a system. The NASA/Air Force bimodal concept uses solar concentrators to focus energy into an integrated power plant. This power plant consists of a graphite core that stores thermal energy within a cavity. An array of thermionic converters encircles the graphite cavity and provides electrical energy conversion functions. During the power generation phase of the bimodal system, the thermionic converters are exposed to the heated cavity and convert the thermal energy to electricity. Near-term efforts of the ISUS bimodal program are focused on a ground demonstration of key technologies in order to proceed to a full space flight test. Thermionic power generation is one key technology of the bimodal concept.

Thermionic power converters impose unique operating requirements upon a power management and distribution (PMAD) system design. Single thermionic converters supply large currents at very low voltages. Operating voltages can vary over a range of up to 3 to 1 as a function of operating temperature. Most spacecraft loads require regulated 28-volts direct-current (Vdc) power. A combination of series-connected converters and power-processing boosters is required to deliver power to the spacecraft's payloads at this level.

The NASA Lewis Research Center developed the PMAD system for the ISUS bimodal thermionic converters. In-house development activities included

design, analysis, fabrication, and tests of all major components. These include two series-connected boost regulators, a power distribution and control unit, and a data acquisition system. The series-connected boost regulators are based on the principle of adding a biasing isolated voltage on top of the power source. Changes in the power source voltage are compensated for by adjusting the bias voltage.

This unique interconnect topology developed by Lewis has been demonstrated for various power system architectures. System efficiencies of up to 97 percent and power densities above 1000 watts per kilogram (W/kg) are just a few benefits of this technology. Of the additional hardware and software developed by NASA, the thermionic converter electronic simulator and thermionic performance evaluation system are noteworthy. Electrical characteristics of thermionic converters can be evaluated with this unique system. This capability enhances the NASA/Air Force team's ability to investigate the performance of spacecraft systems powered by thermionic converters. The PMAD system includes a graphical user interface for easy operation and can supply a maximum of 1500 W at 28 Vdc. Fabrication and test of the PMAD system was completed in August 1997.

### **Lewis contact:**

Anastacio N. Baez, (216) 433-5318,  
A.Baez@lerc.nasa.gov

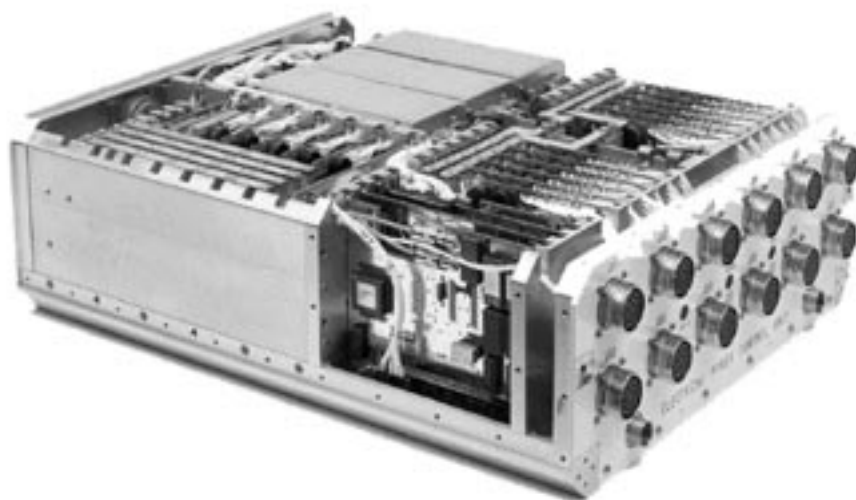
**Author:** Anastacio N. Baez

**Headquarters program office:** USAF

**Programs/Projects:** ISUS, ISS, HEDS



# Advanced Electric Distribution, Switching, and Conversion Technology for Power Control



*Engineering model of Electrical Power Control Unit. (Copyright Sundstrand Aerospace; used with permission.)*

The Electrical Power Control Unit currently under development by Sundstrand Aerospace for use on the Fluids Combustion Facility of the International Space Station is the precursor of modular power distribution and conversion concepts for future spacecraft and aircraft applications. This unit combines modular current-limiting flexible remote power controllers and paralleled power converters into one package.

Each unit includes three 1-kW, current-limiting power converter modules designed for a variable-ratio load sharing capability. The flexible remote power controllers can be used in parallel to match load requirements and can be programmed for an initial ON or OFF state on powerup. The unit contains an integral cold plate.

The modularity and hybridization of the Electrical Power Control Unit sets the course for future spacecraft electrical power systems, both large and small. In such systems, the basic hybridized converter and flexible remote power controller building blocks could be configured to match power distribution and conversion capabilities to load requirements. In addition, the flexible remote power controllers could be configured in assemblies to feed multiple individual loads and could be used in parallel to meet the specific current requirements of each of those loads.

Ultimately, the Electrical Power Control Unit design concept could evolve to a common switch module hybrid, or family of hybrids, for both converter and switchgear applications. By assembling hybrids of a common current rating and voltage class in parallel, researchers could readily adapt these units for multiple applications.

## FLEXIBLE REMOTE POWER CONTROLLER SPECIFICATIONS

Voltage rating, Vdc . . . 120/28
Current rating, A . . . . . 4

## CONVERTER SPECIFICATIONS

Nominal input voltage, Vdc . . . . 120
Nominal output voltage, Vdc . . . . 28
Total converter output rating, kW . . . 3

The Electrical Power Control Unit concept has the potential to be scaled to larger and smaller ratings for both small and large spacecraft and for aircraft where high-power-density, remote power controllers or power converters are required and a common replacement part is desired for multiples of a base current rating.

### **Lewis contact:**

James V. Soltis, (216) 433-5444,  
James.V.Soltis@lerc.nasa.gov

**Author:** James V. Soltis

**Headquarters program office:** OLMSA

**Programs/Projects:** ISS, HEDS, NSTS,  
Commercial Communications

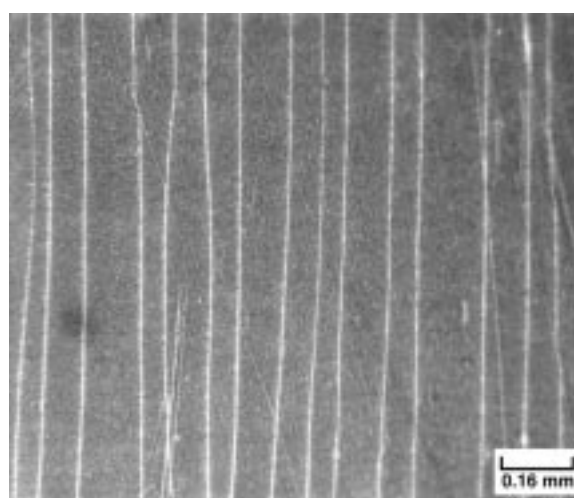
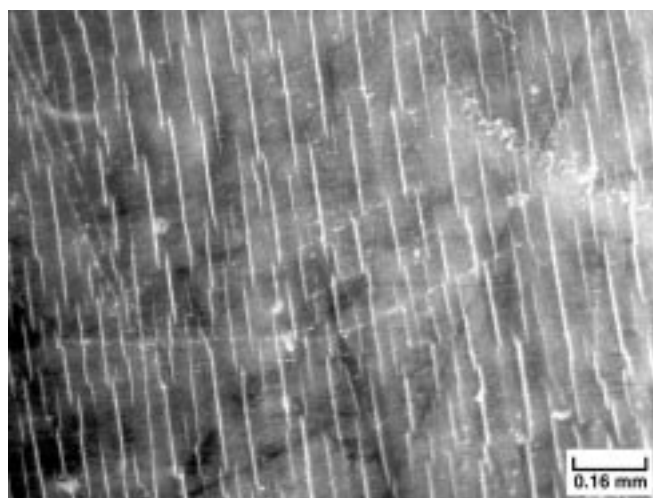
## Soft X-Ray Exposure Testing of FEP Teflon for the Hubble Space Telescope

The FEP Teflon (DuPont) multilayer insulation (MLI) thermal-control blanket material on the Hubble Space Telescope is degrading in the space environment. During the first Hubble servicing mission in 1993, after 3.6 years in low Earth orbit, aluminized and silvered FEP Teflon MLI thermal-control blanket materials were retrieved. These materials have been jointly analyzed by the NASA Lewis Research Center and the NASA Goddard Space Flight Center for degradation induced in the space environment (ref. 1). Solar-facing blanket materials were found to be embrittled with through-the-thickness cracking in the 5-mil FEP. During the second Hubble servicing mission in 1997, astronauts noticed that several blankets had large areas with tears. The torn FEP was curled up in some areas, exposing the underlying materials to the space environment. This tearing problem, and the associated curling up of torn areas, could lead to over-heating of the telescope and to particulate contamination.

A Hubble Space Telescope MLI Failure Review Board was assembled by Goddard to investigate and identify the degradation mechanism of the FEP, to identify and characterize replacement materials, and to estimate the extent of damage at the time of the third servicing mission in 1999. A small piece of FEP retrieved during the second servicing mission is being evaluated by this failure review board along with materials from the first servicing mission. Since the first servicing mission, and as part of the failure review board, Lewis has been exposing FEP to soft x-rays to help determine the damage mechanisms of FEP in the space environment. Soft x-rays, which can penetrate into the bulk of FEP, are generated during solar flares and appear to be contributing to the degradation of the Hubble MLI.

Lewis researchers exposed FEP Teflon to soft x-ray radiation in an electron beam facility. In this facility, different target materials can be irradiated with an 8- to 10-kiloelectronvolts (keV) electron beam producing soft x-rays with different characteristic lines and continuous spectrums.

Samples of FEP exposed to 5 hr of aluminum soft x-rays (characteristic and continuous spectrum radiation) were found to be embrittled to a similar extent as the materials retrieved from the first Hubble servicing mission. The photos show cracking of first servicing mission FEP and FEP exposed to aluminum soft x-rays after bending in tension. Tensile testing of first servicing mission samples produced significant decreases in the percent elongation as compared to unexposed FEP because of space-induced embrittlement. The elongation of the first servicing mission samples was 45-percent of the elongation for unexposed material, whereas the materials exposed to soft x-rays elongated 20 to 40 percent of the elongation for unexposed material (ref. 2). Subsequent testing with molybdenum radiation (the source was operated at 9 keV, which is below the threshold for the  $K_{\alpha}$  characteristic radiation of molybdenum) provided evidence that continuous radiation can embrittle FEP.



*Tension-induced surface cracking of embrittled FEP Teflon. Left: FEP from first Hubble servicing mission. Right: FEP exposed to aluminum soft x-rays.*

Current work includes characterization of the x-ray intensity. Upon completion of facility characterization, proposed Hubble MLI replacement materials are to be exposed to soft x-rays to Hubble mission fluences as part of the failure review board test program. Plans also include a variety of soft x-ray exposure studies, such as variation in damage with energy, flux, and fluence. Also to be tested are the potential synergistic effects of soft x-ray exposure with thermal exposures, vacuum ultraviolet radiation, and atomic oxygen.

## References

1. Zubay, T.M.; de Groh, K.K.; and Smith, D.C.: Degradation of FEP Thermal Control Materials Returned From the Hubble Space Telescope. NASA TM-104627, 1995.
2. de Groh, K.K.; and Smith, D.A.: Investigation of Teflon FEP Embrittlement on Spacecraft in Low Earth Orbit. NASA TM-113153, 1997.

## Lewis contact:

Kim K. de Groh, (216) 433-2297,  
Kim.K.DeGroh@lerc.nasa.gov

**Author:** Kim K. de Groh

**Headquarters program office:** OSS

**Programs/Projects:** HST

# Evaluation of Low-Earth-Orbit Environmental Effects on International Space Station Thermal Control Materials

Many spacecraft thermal control coatings in low Earth orbit (LEO) can be affected by solar ultraviolet radiation and atomic oxygen. Ultraviolet radiation can darken some polymers and oxides commonly used in thermal control materials. Atomic oxygen can erode polymer materials, but it may reverse the ultraviolet-darkening effect on oxides. Maintaining the desired solar absorptance for thermal control coatings is important to assure the proper operating temperature of the spacecraft.

Thermal control coatings to be used on the International Space Station (ISS) were evaluated for their performance after exposure in the NASA Lewis Research Center's Atomic Oxygen-Vacuum Ultraviolet Exposure (AO-VUV) facility. This facility simulated the LEO environments of solar vacuum ultraviolet (VUV) radiation (wavelength range, 115 to 200 nanometers (nm)) and VUV combined with atomic oxygen. Solar absorptance was measured *in vacuo* to eliminate the "bleaching" effects of ambient oxygen on VUV-induced degradation. The objective of these experiments was to determine solar absorptance increases of various thermal control materials due to exposure to simulated LEO conditions similar to those expected for ISS. Work was done in support of ISS efforts at the requests of Boeing Space and Defense Systems and Lockheed Martin Vought Systems.

In one test, samples consisted of the white paint thermal control coating Z-93-P (zinc oxide pigment in potassium silicate binder formulated by the Illinois Institute of Technology Research Institute) applied to 0.9375-in.-diameter aluminum substrates. These samples were coated with approximately 1000 angstroms of products of Tefzel (DuPont) fluoropolymer degradation to simulate the on-orbit contamination that may occur from the degradation of power cable insulation. Samples thus coated in Boeing facilities were then exposed to VUV radiation of up to 2400 equivalent sun hours (ESH) in the Lewis facility, the equivalent of over 7 years in LEO for ISS radiator surfaces. These samples experienced a greater increase in solar absorptance than an uncoated control sample of the same Z-93-P coating. The implications of these results are that Z-93-P surfaces on ISS may

degrade at a faster rate when they are in an environment where they can be contaminated by the degradation of fluoropolymer power cable insulation. This test represented a worst-case scenario for Z-93-P solar absorptance degradation because atomic oxygen, which may remove some of the fluoropolymer contaminants and may reverse the darkening due to vacuum ultraviolet radiation, was not present during testing.

In two additional tests, samples of 0.9375-in.-diameter samples of silvered FEP Teflon (FEP/silver/inconel/acrylic adhesive/aluminum substrate), SiO<sub>2</sub>-coated silvered FEP Teflon (SiO<sub>2</sub>/FEP/silver/inconel/acrylic adhesive/aluminum substrate), and white paint Z-93-P coatings (Z-93-P/aluminum substrate) were exposed to the combined environments of VUV radiation and atomic oxygen. These samples experienced negligible changes in solar absorptance upon exposure to up to approximately 1300 ESH of VUV radiation combined with a fluence of  $4 \times 10^{21}$  oxygen atoms/cm<sup>2</sup>. Samples were thus exposed to

a LEO equivalent of approximately 4 years of atomic oxygen and 2.5 to 4 years of VUV radiation. This test verified the solar absorptance durability of thermal control materials selected for use on ISS in the absence of contaminants. Although these tests were specifically designed to simulate ISS conditions, the results are applicable to many missions that use these common thermal control coatings.

Results from the three tests are shown in the table. Error for the solar absorptance values is expected to be  $\pm 0.007$ .

SOLAR ABSORPTANCE CHANGES IN COATINGS EXPOSED TO SIMULATED LEO CONDITIONS

Sample	VUV exposure, ESH VUV atoms/cm <sup>2</sup>	Solar absorptance		
		Prior to exposure	After exposure	Increase
Test 1 (no atomic oxygen exposure)				
Tefzel-contaminated Z-93-P, #1	1700	0.154	0.208	0.054
Tefzel-contaminated Z-93-P, #2	2200	.156	.207	.051
Tefzel-contaminated Z-93-P, #3	2400	.168	.236	.068
Pristine Z-93-P	2200	.133	.159	.026
Test 2 (atomic oxygen exposure, 4.40×10 <sup>21</sup> atoms/cm <sup>2</sup> )				
SiO <sub>2</sub> /FEP Teflon/Ag..., <sup>a</sup> #1	850	0.072	0.07	-0.002
SiO <sub>2</sub> /FEP Teflon/Ag..., #2	1100	.072	.074	.002
SiO <sub>2</sub> /FEP Teflon/Ag..., #3	1000	.069	.062	-.007
Pristine Z-93-P	1300	.132	.125	-.007
Test 3 (atomic oxygen exposure, 4.20×10 <sup>21</sup> atoms/cm <sup>2</sup> )				
FEP Teflon/Ag..., <sup>b</sup> #1	1100	0.064	0.06	-0.004
FEP Teflon/Ag..., #2	850	.065	.06	-.005
FEP Teflon/Ag..., #3	980	.064	.061	-.003
Pristine Z-93-P	1300	.117	.11	-.007

<sup>a</sup>SiO<sub>2</sub>/FEP/silver/Inconel/acrylic adhesive/aluminum substrate.

<sup>b</sup>FEP/silver/Inconel/acrylic adhesive/aluminum substrate.

**Lewis contact:** Joyce A. Dever, (216) 433-6294, Joyce.A.Dever@lerc.nasa.gov

**Author:** Joyce A. Dever

**Headquarters program office:** OSATT

**Programs/Projects:** ISS

# Integrated Solar Upper Stage Technical Support

NASA Lewis Research Center is participating in the Integrated Solar Upper Stage (ISUS) program. This program is a ground-based demonstration of an upper stage concept that will be used to generate both solar propulsion and solar power. Solar energy collected by a primary concentrator is directed into the aperture of a secondary concentrator and further concentrated into the aperture of a heat receiver. The energy stored in the receiver-absorber-converter is used to heat hydrogen gas to provide propulsion during the orbital transfer portion of the mission. During the balance of the mission, electric power is generated by thermionic diodes.

Several materials issues were addressed as part of the technical support portion of the ISUS program, including (1) evaluation of primary concentrator coupons, (2) evaluation of secondary concentrator coupons, (3) evaluation of receiver-absorber-converter coupons, and (4) evaluation of in-test witness coupons. Two different types of primary concentrator coupons were evaluated from two different contractors—replicated coupons made from graphite-epoxy composite and coupons made from microsheet glass. Specular reflectivity measurements identified the replicated graphite-epoxy composite coupons as the primary concentrator material of choice. Several different secondary concentrator materials were evaluated, including a variety of silver and rhodium reflectors. The specular reflectivity of these materials was evaluated under vacuum at temperatures up to 800 °C. The optical properties of several coupons of rhenium on graphite were evaluated to predict the thermal performance of the receiver-absorber-converter. Finally, during the ground test demonstration, witness coupons placed in strategic locations throughout the thermal vacuum facility were evaluated for contaminants.

All testing for the ISUS program was completed successfully in 1997. Investigations related to materials issues have proven helpful in understanding the operation of the test article, leading to a potential ISUS flight test in 2002.

**Lewis contact:** Dr. Donald A. Jaworske, (216) 433-2312,  
Donald.A.Jaworske@lerc.nasa.gov

**Author:** Dr. Donald A. Jaworske

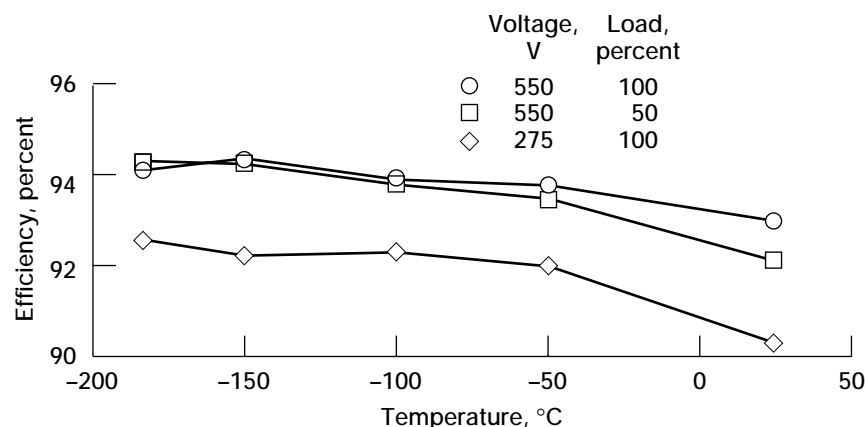
**Headquarters program office:** OSS

**Programs/Projects:** ISUS

# High-Voltage 1-kW dc/dc Converter Developed for Low-Temperature Operation

In the past, the NASA Lewis Research Center developed numerous types of direct-current to direct-current (dc/dc) converters with modest outputs (up to 100 watts (W) at 50 volts (V)) for operation over a wide range of temperatures from room temperature to  $-196^{\circ}\text{C}$  (the temperature of liquid nitrogen). For spacecraft that will operate in the cold temperatures of deep space, converters that can operate at low temperatures will require little or no heating (or the associated heating equipment). Consequently, they enable greater design versatility and lower cost. In addition, dc/dc converters can be operated more efficiently at low temperatures than at room temperature.

Recently, Lewis developed and demonstrated a high-voltage, 1-kW dc/dc converter that operates from room temperature to  $-184^{\circ}\text{C}$ . A power supply designed for use in a NASA ion beam propulsion system was utilized as a starting point for the design of a low- (wide-) temperature dc/dc converter. For safety, we decided to halve the output voltage and power level, so the converter was designed for an 80-Vdc input and a 550-Vdc output at 1 kW.



*System efficiency increases as operating temperature decreases for a high-voltage 1-kW dc/dc converter.*

The components used in the circuit design were selected from component classes that had been screened and tested for low-temperature operation. Certain N-channel MOSFETs<sup>1</sup> were chosen as switches because they function well at low temperatures and, when they are turned on at  $-196^{\circ}\text{C}$ , have only one-third to one-fourth of their room temperature losses. This graph for the new dc/dc converter shows (for three different operating conditions) that system efficiency increases gradually as temperature decreases from room temperature to  $-184^{\circ}\text{C}$ .

<sup>1</sup>Metal-oxide silicon field effect transistors.

The Low Temperature Electronics Program is an ongoing program at Lewis in support of missions and development programs at NASA's Jet Propulsion Laboratory and Goddard Space Flight Center, in aerospace industry, and in medical electronics.

**To find out more, visit us on the World Wide Web:**

<http://www.lerc.nasa.gov/WWW/epbranch/lowtmpel.htm>

**Lewis contact:**

Richard L. Patterson, (216) 433-8166,  
Richard.L.Patterson@lerc.nasa.gov

**Author:** Richard L. Patterson

**Headquarters program office:** OSS

**Programs/Projects:** ASTM, X2000 (JPL), Next Generation Space Telescope (Goddard), Low Temperature Electronics



# Atomic Oxygen Cleaning Shown to Remove Organic Contaminants at Atmospheric Pressure

Organic contaminants and coatings can be difficult to remove from delicate surfaces. Using harsh solvents or physical contact to clean such surfaces can result in damage. Testing the effects of the low-Earth-orbit environment on spacecraft surfaces has shown that the atomic oxygen present in space very readily reacts with most organic materials. The reaction converts the organic materials present on surfaces into gaseous components of mostly carbon monoxide, carbon dioxide, and water vapor. Because the reaction is limited to the surface, and there is no physical contact with the surface required other than a gentle flow of gas, atomic oxygen offers an attractive method to remove organic coatings and contaminants.

One of the drawbacks of using atomic oxygen is the rate at which it recombines to form molecular oxygen. This has required that any object to be cleaned be placed inside a vacuum chamber where the density of atomic oxygen can be kept low enough so that it reacts with the surface before recombining. Vacuum chambers, however, are not very portable and most are not large enough to accommodate many surfaces that need to be cleaned.

unit that can be portable enough to use for cleaning sections of large objects in place. This process has many broad applications in both nonterrestrial and terrestrial areas. Some examples of these applications are the removal of hydrocarbon contaminants from optical surfaces for spacecraft, decontamination of aircraft components, and removal of soot from artwork damaged during a fire.

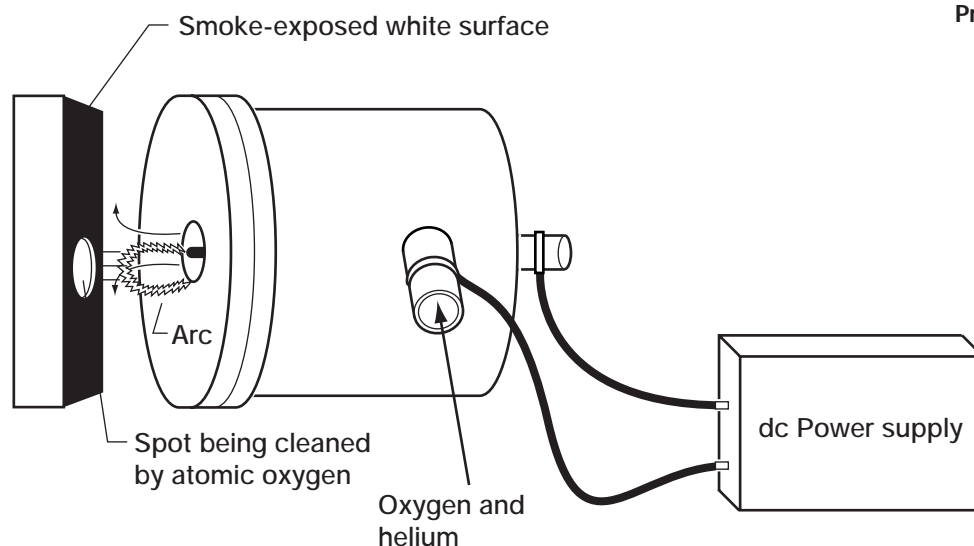
## Lewis contacts:

Sharon K. Rutledge, (216) 433-2219, Sharon.K.Rutledge@lerc.nasa.gov, and Bruce A. Banks, (216) 433-2308, Bruce.A.Banks@lerc.nasa.gov

**Author:** Sharon K. Rutledge

**Headquarters program office:** OASTT

**Programs/Projects:** HST, ISS, EOS



*Atmospheric atomic oxygen cleaning system.*

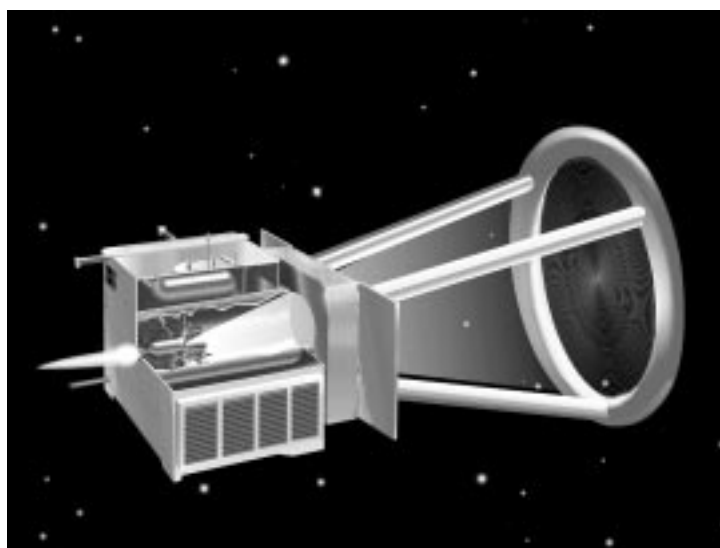
The NASA Lewis Research Center has developed and filed for a patent on a method to produce atomic oxygen at atmospheric pressure by using a direct current arc in a gas flow mixture of oxygen and helium. A prototype device has been tested for its ability to remove various soot residues from surfaces exposed to fire, and various varnishes such as acrylic and egg white. A typical soot deposit can be removed in an area about 0.5 cm in diameter in less than 2 minutes with optical restoration of the surface to very near its original condition. The device can be made into a hand-held

## Refractive Secondary Solar Concentrator Being Designed and Developed

As the need for achieving super high temperatures (2000 K and above) in solar heat receivers has developed so has the need for secondary concentrators. These concentrators refocus the already highly concentrated solar energy provided by a primary solar collector, thereby significantly reducing the light entrance aperture of the heat receiver and the resulting infrared radiation heat loss from the receiver cavity. Although a significant amount of research and development has been done on nonimaging hollow reflective concentrators, there has been no other research or development to date on solid, single-crystal, refractive concentrators that can operate at temperatures above 2000 K.

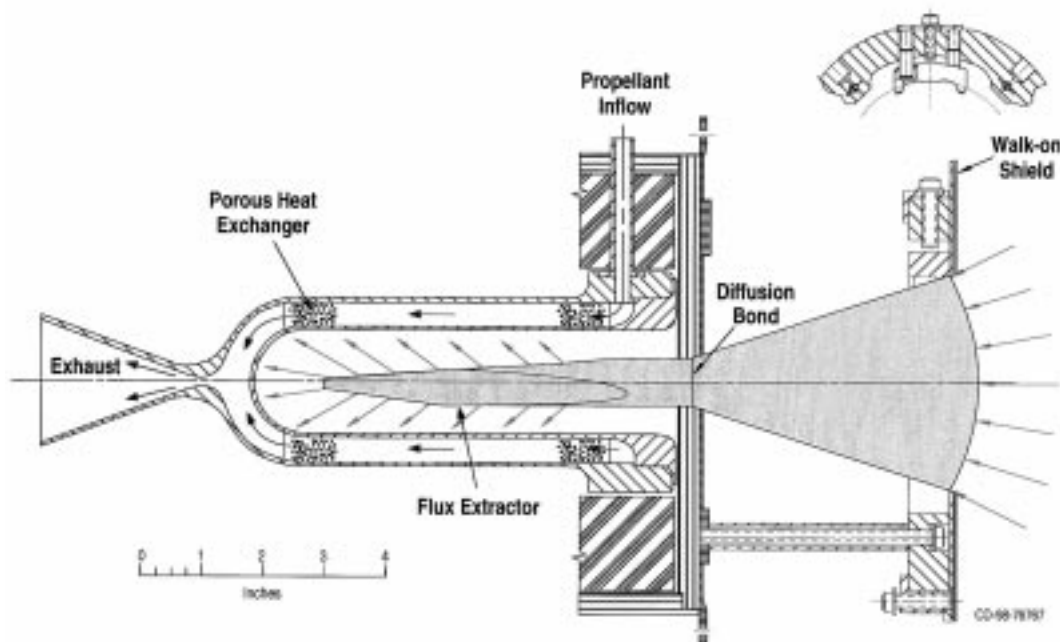
The NASA Lewis Research Center recently initiated the development of single-crystal, optically clear, refractive secondary concentrators that, combined with a flux extractor, offer a number of significant advantages over the more conventional, hollow, reflective concentrators at elevated temperatures. Such concentrators could potentially provide higher throughput (efficiency), require no special cooling device, block heat receiver material boiloff from the receiver cavity, provide for flux tailoring in the cavity via the extractor, and potentially reduce infrared heat loss via an infrared block coating.

The many technical challenges of designing and fabricating high-temperature refractive secondary concentrators and flux extractors

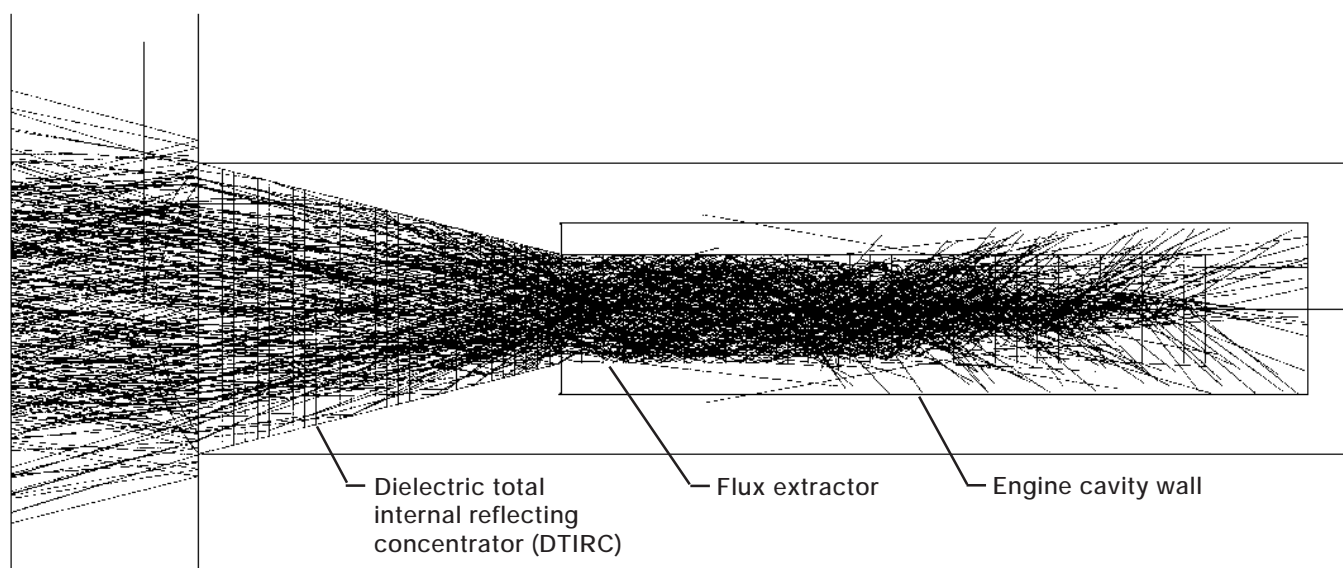


*Solar thermal propulsion system for Shooting Star Experiment.*

include identifying optical materials that can survive the environment (high-temperature, vacuum and/or hydrogen atmosphere), developing coatings for enhanced optical and thermal performance, and developing crystal joining techniques and hardware that can survive launch loads.



*Solar thermal engine for Shooting Star Experiment with refractive secondary concentrator.*



*Beam trace through refractive secondary concentrator. A color image of a beam trace is shown in the online version of this article (<http://www.lerc.nasa.gov/WWW/RT1997/5000/5490donovan.htm>).*

As a result of development work begun by NASA Lewis and Analex Corporation personnel in May 1996, a refractive secondary concentrator was baselined by the NASA Marshall Space Flight Center for their Shooting Star Experiment (SSE), which is to be placed in orbit by the shuttle in early 2000. This experiment will demonstrate all the technologies associated with a solar thermal propulsion system. The artist's rendering of the SSE (see the top figure on the preceding page) shows the primary sun collector lens deployed from NASA Goddard Space Flight Center's Spartan "free flyer" space platform. The solar thermal propulsion engine and secondary concentrator are located inside the Spartan platform.

The schematic on the preceding page shows a conceptual design of the engine and secondary concentrator. The secondary concentrator will be constructed of single-crystal zirconia, sapphire, or yttrium-aluminum-garnet (YAG), with the selection being made after extensive testing of all three materials. The engine, which will be constructed of rhenium, is designed for use with hydrogen propellant at temperatures approaching 2500 K but will use nitrogen propellant on the SSE. The propellant will enter the engine, flow through a rhenium-foam-filled annulus around the receiver cavity, be heated to temperatures approaching 2000 K, and expand through the nozzle, increasing the specific impulse over that of the cold gas. The figure above graphically demonstrates how a beam of light refracts and reflects in the concentrator and then enters the extractor where it is broken up into many rays of light that ultimately exit the extractor in a predicted distribution pattern.

Lewis' Secondary Concentrator Design Team developed the analytical tools needed for the optical design of a refractive secondary concentrator. A zirconia secondary concentrator and flux extractor were successfully fabricated for testing in 1998. Lewis is continuing to investigate materials and coatings that could extend the capabilities of these concentrators for various NASA and Air Force missions.

## Bibliography

Soules, J.A., et al.: Design and Fabrication of a Dielectric Total Internal Reflecting Solar Concentrator and Associated Flux Extractor for Extreme High Temperature (2500K) Applications. NASA CR-204145, 1997. Available online: <http://letrs.lerc.nasa.gov/cgi-bin/LeTRS/browse.pl?1997/CR-204145.html>

## Lewis contacts:

Richard M. Donovan, (216) 433-5355, [Richard.M.Donovan@lerc.nasa.gov](mailto:Richard.M.Donovan@lerc.nasa.gov), and Robert P. Macosko, (216) 433-6161, [Robert.P.Macosko@lerc.nasa.gov](mailto:Robert.P.Macosko@lerc.nasa.gov)

**Authors:** Robert P. Macosko and Richard M. Donovan

**Headquarters program office:** OASTT

**Programs/Projects:** ISS, space shuttles, SSE, space transportation, high-temperature solar applications (e.g., solar thermoelectric, solar thermionics, solar dynamics, and solar ovens)

**Special recognition:** A paper describing this research was nominated as one of the two most significant papers presented at the 1997 SPIE International Nonimaging Symposium.

# Aerospace Power Systems Design and Analysis (APSDA) Tool

The conceptual design of space and/or planetary electrical power systems has required considerable effort. Traditionally, in the early stages of the design cycle (conceptual design), the researchers have had to thoroughly study and analyze tradeoffs between system components, hardware architectures, and operating parameters (such as frequencies) to optimize system mass, efficiency, reliability, and cost. This process could take anywhere from several months to several years (as for the former Space Station Freedom), depending on the scale of the system.

Although there are many sophisticated commercial software design tools for personal computers (PC's), none of them can support or provide total system design. To meet this need, researchers at the NASA Lewis Research Center cooperated with Professor George Kusic from the University of Pittsburgh to develop a new tool to help project managers and design engineers choose the best system parameters as quickly as possible in the early design stages (in days instead of months). It is called the Aerospace Power Systems Design and Analysis (APSDA) Tool.

By using this tool, users can obtain desirable system design and operating parameters such as system weight, electrical distribution efficiency, bus power, and electrical load schedule. With APSDA, a large-scale specific power system (see the figure) was designed in a matter of days. It is an excellent tool to help designers make tradeoffs between system components, hardware architectures, and operation parameters in the early stages of the design cycle.

The APSDA tool is user friendly, with menu-driven, online help and a custom graphical user interface. It operates on any PC running the MS-DOS (Microsoft Corp.) operating system, version 5.0 or later. A color monitor (EGA or VGA) and two-button mouse are required.

The APSDA tool was presented at the 30th Intersociety Energy Conversion Engineering Conference (IECEC) and is being beta tested at several NASA centers. Beta test packages are available for evaluation by contacting the author.

**Lewis contact:**

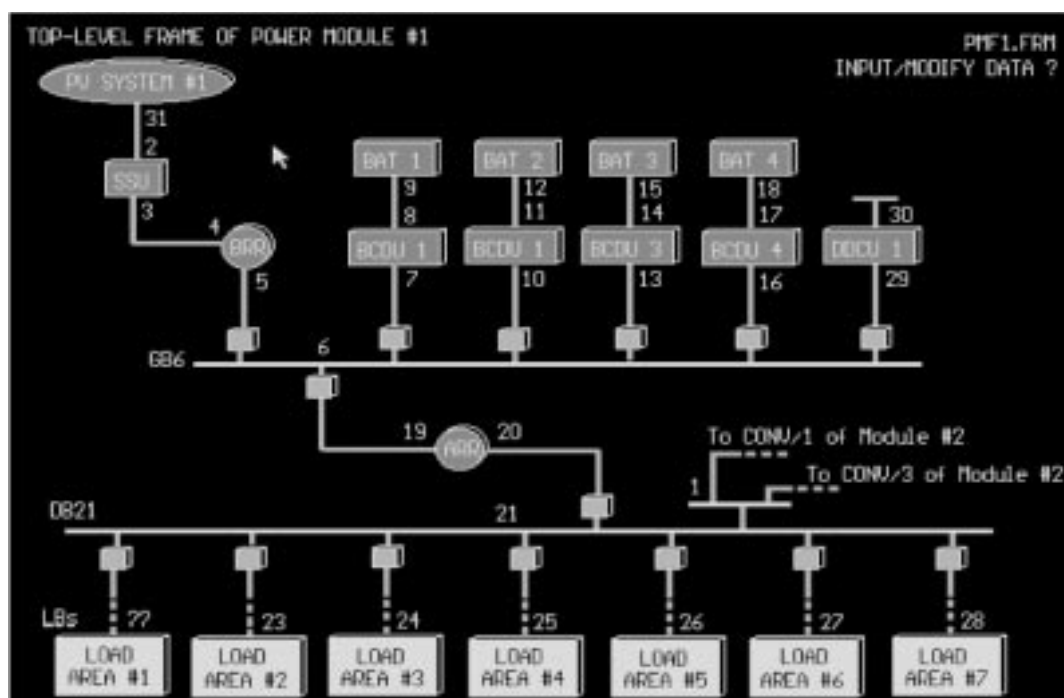
Long V. Truong, (216) 433-6153,  
Long.V.Truong@lerc.nasa.gov

**Author:** Long V. Truong

**Headquarters program office:** Office of the Administrator, Chief Engineer

**Programs/Projects:** Systems Engineering of Shared Resources

**Special recognition:** Special Act Award



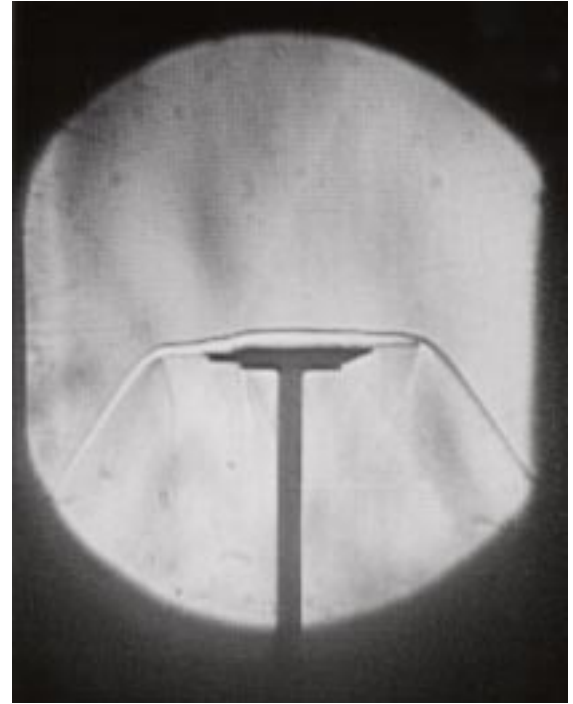
Screen sample of a top-level configuration of a typical space and/or planetary electrical power system from the APSDA graphics utility tool.

# Instrumentation and Controls

## Drag Force Anemometer Used in Supersonic Flow

To measure the drag on a flat cantilever beam exposed transversely to a flow field, the drag force anemometer (beam probe) uses strain gauges attached on opposite sides of the base of the beam (ref. 1). This is in contrast to the hot wire anemometer, which depends for its operation on the variation of the convective heat transfer coefficient with velocity. The beam probe retains the high-frequency response (up to 100 kHz) of the hot wire anemometer, but it is more rugged, uses simpler electronics, is relatively easy to calibrate, is inherently temperature compensated, and can be used in supersonic flow. The output of the probe is proportional to the velocity head of the flow,  $\frac{1}{2} \rho u^2$  (where  $\rho$  is the fluid density and  $u$  is the fluid velocity). By adding a static pressure tap and a thermocouple to measure total temperature, one can determine the Mach number, static temperature, density, and velocity of the flow.

The use of the beam probe has heretofore been limited to subsonic flow applications. However, as can be seen from the photo, it is possible to design the probe to produce a normal shock in supersonic flow. Thus, using the equations for conservation of mass, energy, and momentum across a normal shock, researchers at the NASA Lewis Research Center related the parameters of the flow upstream of the shock front produced by the probe to those measured by the probe, downstream of the shock. In particular,  $\rho_1 u_1^2 = [(\gamma - 1)/(\gamma + 1)] \rho_2 u_2^2 + [2\gamma/(\gamma + 1)] \rho_2$  (where  $\gamma$  is the ratio of specific heats, subscript 1 indicates a location upstream of the shock, and subscript 2 indicates a location downstream of the shock) relates the upstream and downstream velocity heads and, as shown in the graph, can be used to extend a subsonic calibration



*Normal shock produced by beam probe.*

to supersonic flow (ref. 2). This year Lewis researchers used the drag force anemometer in the flow field behind a supersonic flow-through fan at Mach numbers to 2.7.

### References

1. Krause, L.N.; and Fralick, G.C.: Miniature Drag Force Anemometers. NASA TM X-3507, 1977.
2. Richard, J.C.; and Fralick, G.C.: Use of Drag Probe in Supersonic Flow. AIAA J., vol. 34, no. 1, 1996, pp. 201-203.

### Lewis contact:

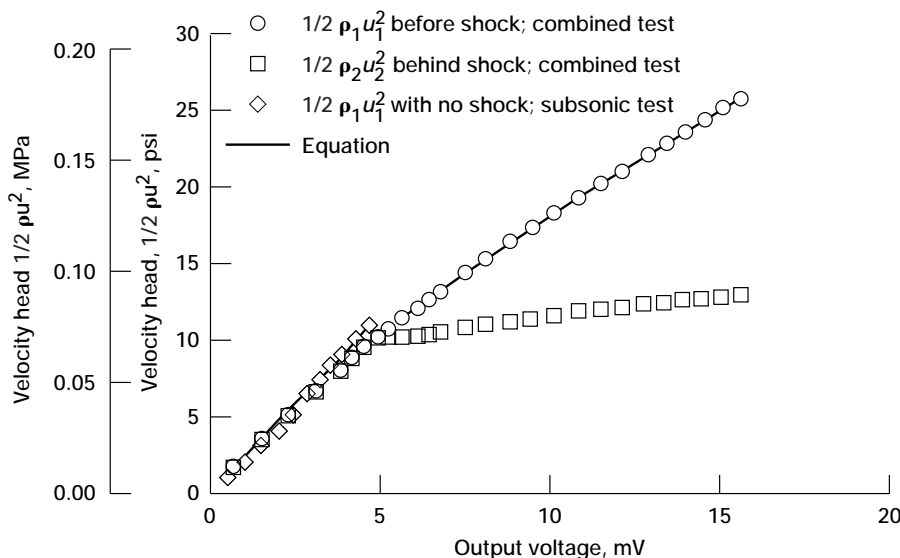
Gustave C. Fralick, (216) 433-3645,  
Gustave.C.Fralick@lerc.nasa.gov

### Argonne National Lab contact:

Jacques Richard, (630) 252-1050

**Author:** Gustave C. Fralick

**Headquarters program office:** OASTT  
**Programs/Projects:** AST



*Velocity head calibration curve.*



## Attachment of Free Filament Thermocouples for Temperature Measurements on Ceramic Matrix Composites

Measuring the temperatures of advanced materials, such as ceramic matrix composites (CMC's), in a hostile environment has been a difficult task because of the poor adhesion of the measurement systems. Commonly used wire thermocouples (TC) cannot be attached to such ceramic-based materials via conventional spot-welding techniques, and commercially available ceramic cements fail to provide sufficient adhesion at high temperatures. Although advanced thin-film TC's provide minimally intrusive surface temperature measurement and adhere well on CMC's, their fabrication requires sophisticated, expensive facilities and is time consuming. In addition, the durability of lead wire attachments to both thin-film TC's and substrate materials requires further improvement.

At the NASA Lewis Research Center, a new installation technique utilizing convoluted wire thermocouples (TC's) was developed and proven to produce very good adhesion on CMC's, even in a burner rig environment. Because of their unique convoluted design, such TC's of various types and sizes adhere to flat or curved CMC specimens with no sign of delamination, open circuits, or interactions—even after testing in a Mach 0.3 burner rig to 1200 °C (2200 °F) for several thermal cycles and at several hours at high temperatures. Large differences in thermal expansion between metal thermocouples and low-expansion materials, such as CMC's, normally generate large stresses in the wires. These stresses cause straight wires to detach, but convoluted wires that are bonded with strips of coating allow bending in the unbonded portion to relieve these expansion stresses.

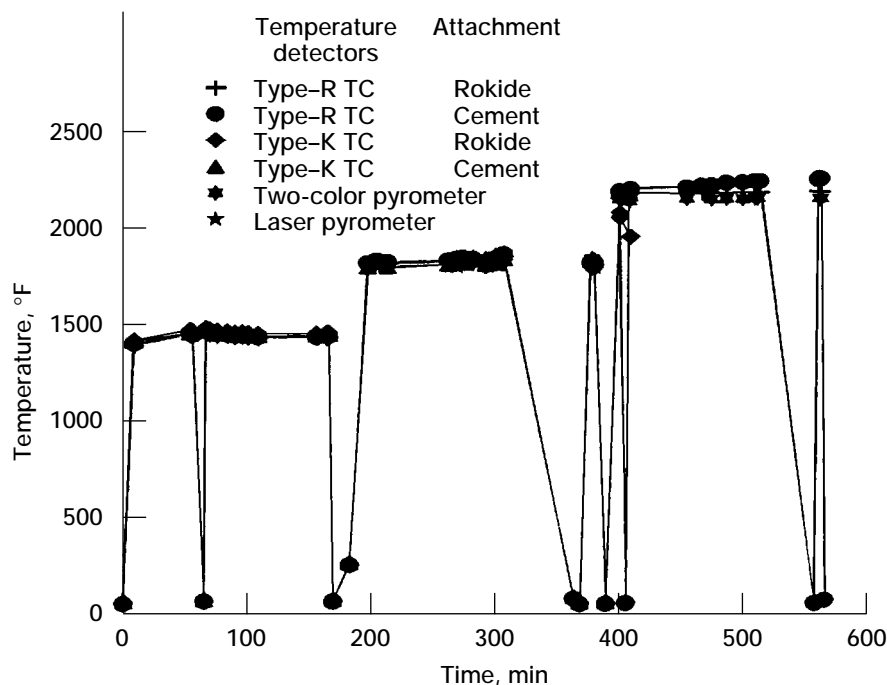
During testing, the temperature data taken from convoluted wire TC's were compared with those from Lewis' Mach 0.3 burner rig pyrometers. The SiC/SiC CMC temperature data measured by these TC's matched those of the facility's pyrometers to within 2 percent up to 1200 °C (2200 °F). However, the two-color facility pyrometer did not work with the transparent alumina/alumina CMC specimen, and the laser pyrometer, which has a signal wavelength of 0.865  $\mu\text{m}$ , only worked to 1100 °C (2010 °F). No data were obtained from the type-K TC's when the CMC specimen temperature reached 1200 °C (2200 °F). This was due to the wire breaking, as revealed during the posttest examination. The type-R TC's, however, were still intact after all the testing.

This newly developed contact TC provides a way to measure temperatures when minimally intrusive measurement is not required. Convoluted wire TC's are much cheaper and faster to fabricate than less intrusive thin-film TC's. In addition, unlike thin-film TC's, these TC's require no preoxidation, no post annealing, and no surface treatment of the CMC substrate materials. They can, therefore, reduce the time and cost for sensor fabrication and installation. The same installation technique used for convoluted wire TC's can be applied to attach lead wires for thin-film sensors when minimally intrusive measurements are required. This technique should work for any low thermal expansion materials, such as ceramics (alumina, sapphire, zirconia, and silicon nitride), and other composite materials, such as carbon/carbon composites.



*An array of thermocouples applied to a CMC under test in a Mach 0.3 burner rig. The array was over 1800 °F when the photo was taken.*





Surface temperature of a SiC/SiC CMC measured by two type-R thermocouples, two type-K thermocouples, and two types of pyrometers.

Find out more about these sensors on the World Wide Web:  
<http://www.lerc.nasa.gov/WWW/sensors/SENSORS.HTM>

**Lewis contact:**

Dr. Jih-Fen Lei, (216) 433-3922,  
 Jih-Fen.Lei@lerc.nasa.gov

**Authors:** Dr. Jih-Fen Lei, Michael D. Cuy, and Stephen P. Wnuk

**Headquarters program office:** OASTT  
**Programs/Projects:** EPM, HSR

**Special recognition:** This work was featured on the June 1997 cover of Sensor Magazine, which is published by the Journal of Applied Sensing Technology.

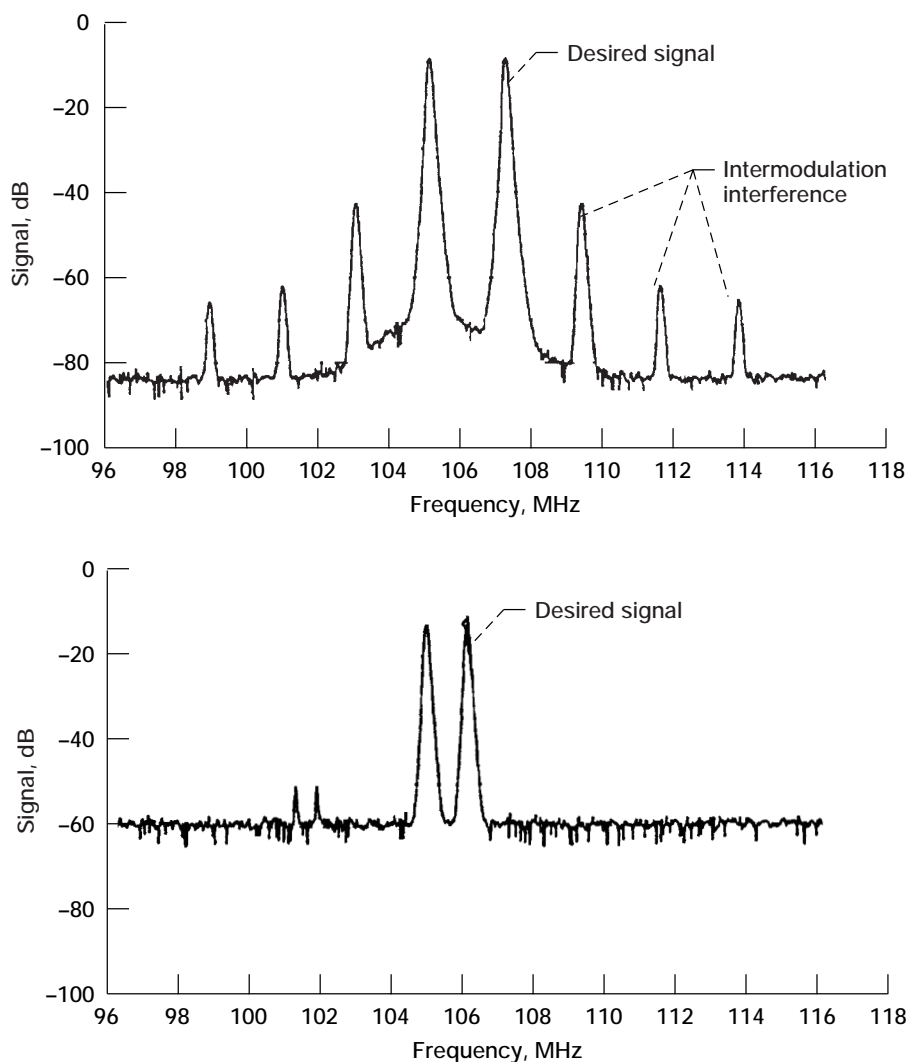
## Silicon Carbide Mixers Demonstrated to Improve the Interference Immunity of Radio-Based Aircraft Avionics

Concern over the interference of stray radiofrequency (RF) emissions with key aircraft avionics is evident during takeoff and landing of every commercial flight when the flight attendant requests that all portable electronics be switched off. The operation of key radio-based avionics (such as glide-slope and localizer approach instruments) depends on the ability of front-end RF receivers to detect and amplify desired information signals while rejecting interference from undesired RF sources both inside and outside the aircraft. Incidents where key navigation and approach avionics malfunction because of RF interference clearly represent an increasing threat to flight safety as the radio spectrum becomes more crowded.

In an initial feasibility experiment, the U.S. Army Research Laboratory and the NASA Lewis Research Center recently demonstrated the strategic use of silicon carbide (SiC) semiconductor components to significantly reduce the susceptibility of an RF receiver circuit to undesired RF interference. A pair of silicon carbide mixer diodes successfully reduced RF interference (intermodulation distortion) in a prototype receiver circuit by a factor of 10 (20 dB) in comparison to a pair of commercial silicon-based mixer diodes.

This can be seen by comparing the received signal spectrums from a conventional silicon-diode mixer test circuit (top figure) with the received

signal spectrum of an SiC-diode mixer circuit (bottom figure). The two largest peaks in the middle of both spectrums are the desired radio signals, which normally would contain avionics-related information. The peaks to either side of the desired signal in the top figure represent undesired intermodulation distortion signals, which can interfere with the proper detection and decoding of desired radio signals. The SiC-diode mixer circuit reduces these interference peaks to the point where they cannot be observed in the spectrum of the bottom figure. This circuit should enable aircraft avionics receivers to much more successfully extract weak desired information signals, even in the



*Received signal spectrum. (Attenuation 10 dB; RL 0 dBm.) Top: Conventional silicon-diode mixer circuit. Bottom: SiC-diode mixer circuit—note the absence of intermodulation interference peaks.*

presence of strong undesired RF interference. Such circuits would clearly improve the reliability of flight-critical radio-based instrumentation, even if passengers continued to operate portable electronics during takeoffs and landings. Furthermore, aviation-related RF transmitters and receivers could be located closer to each other (both in the air and on the ground) without severe interference penalties.

Manufactured in volume, these simple-to-produce SiC mixers should cost around \$10 to \$20 each, well below the \$1000 it presently costs to achieve the same degree of RF interference immunity from complex, series-matched mixer hybrid circuits.

**For more information about Lewis' SiC circuit research, visit us on the World Wide Web:**

<http://www.lerc.nasa.gov/WWW/SiC/SiC.html>

**Lewis contact:**

Dr. Philip G. Neudeck, (216) 433-8902,  
Philip.G.Neudeck@lerc.nasa.gov

**Author:** Dr. Philip G. Neudeck

**Headquarters program office:** OASTT

**Programs/Projects:**

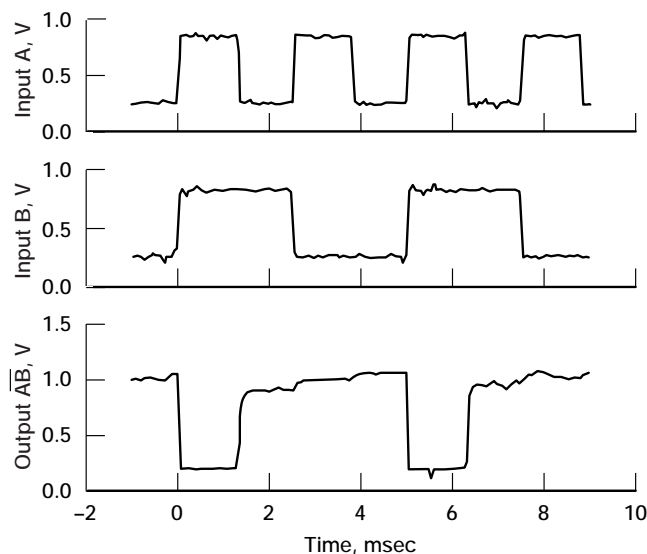
Propulsion Systems R&T, SGE, HITEMP

**Special recognition:** A paper about this research was selected by conference organizers as one of the highlights of the 1997 International Conference on Silicon Carbide, III-Nitrides and Related Materials.

# Silicon Carbide Junction Field Effect Transistor Digital Logic Gates Demonstrated at 600 °C

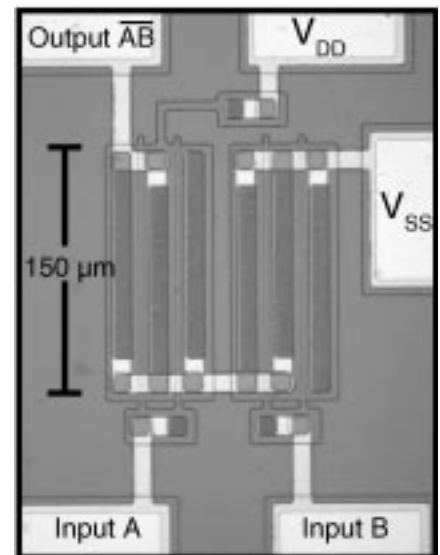
Complex electronics and sensors are increasingly being relied on to enhance the capabilities and efficiency of modern jet aircraft. Many of these electronics and sensors monitor and control vital engine components and aerosurfaces that operate at high temperatures. However, since today's silicon-based electronics technology cannot function at high temperatures, these electronics must reside in environmentally controlled areas. This necessitates either the use of long wire runs between sheltered electronics and hot-area sensors and controls, or the fuel cooling of electronics and sensors located in high-temperature areas. Both of these low-temperature-electronics approaches suffer from serious drawbacks in terms of increased weight, decreased fuel efficiency, and reduction of aircraft reliability. A family of high-temperature electronics and sensors that could function in hot areas would enable substantial aircraft performance gains. Especially since, in the future, some turbine-engine electronics may need to function at temperatures as high as 600 °C.

The High Temperature Integrated Electronics and Sensors (HTIES) Program at the NASA Lewis Research Center is currently developing silicon carbide (SiC) for use in harsh conditions where silicon, the semiconductor used in nearly all of today's electronics, cannot function. The HTIES team recently fabricated and demonstrated the first semiconductor digital logic gates ever to function at 600 °C. The photomicrograph shows a NAND (not A and not B) logic gate, consisting of two junction field effect transistors (JFET's) and a resistor fabricated in epitaxially grown SiC. The graph shows operational waveforms of the SiC NAND gate collected on a probing station when the sample was heated to a glowing, red-hot 600 °C. The input voltage waveforms are shown across the top, and the logic gate output voltage is shown on the bottom. On all the waveforms, a binary logic zero is represented by a voltage of 0.25 V or less, whereas a voltage of 0.85 V or higher corresponds to a binary logic one. Whenever one of the inputs is a logic zero (0.25 V), the output of the logic gate is greater than



Operational waveforms demonstrating the 600 °C functionality of the SiC NAND gate.

0.9 V (a logic one); only when two logic ones are input does the logic gate output drop to 0.2 V (a logic zero), consistent with the NAND binary logic function. In addition to the NAND gates, NOT (not A) and NOR (not A or not B) gates on the same SiC wafer demonstrated successful 600 °C operation.



600 °C NAND gate, consisting of two SiC JFET's and a resistor. Signal input and output pads are labeled, along with the  $V_{DD}$  and  $V_{SS}$  bonding pads that supply power to the circuit.

Demonstration of simple logic functions at 600 °C represents a measurable step forward. Nevertheless, many further advancements are necessary before SiC electronics will be ready for reliable long-term operation at extreme temperatures. These necessary advancements include increased circuit complexity, demonstration of long-term operation, and development of high-temperature electronics packaging and connectors.

For more information about SiC circuit research, visit us on the World Wide Web: <http://www.lerc.nasa.gov/WWW/SiC/SiC.html>

#### Lewis contact:

Dr. Philip G. Neudeck, (216) 433-8902, [Philip.G.Neudeck@lerc.nasa.gov](mailto:Philip.G.Neudeck@lerc.nasa.gov)

**Author:** Dr. Philip G. Neudeck

**Headquarters program office:** OASTT

**Programs/Projects:**

Propulsion Systems R&T, SGE, HITEMP

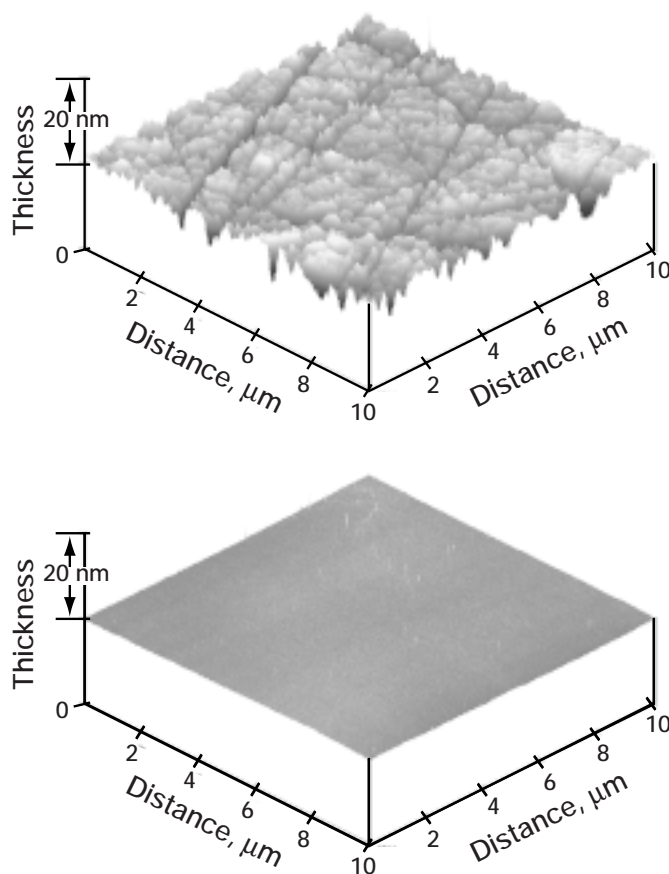
# Chemical Mechanical Polishing of Silicon Carbide

The High Temperature Integrated Electronics and Sensors (HTIES) team at the NASA Lewis Research Center is developing silicon carbide (SiC) as an enabling electronic technology for many aerospace applications. The ability of SiC to function under high-temperature, high-power, and/or high-radiation conditions allows it to be used in applications where silicon, the semiconductor used in nearly all of today's electronics, is not practical. In jet engines, SiC power electronics could be used with electric actuators to replace pneumatic and hydraulic actuators, resulting in greatly enhanced performance and reliability. Also, SiC gas sensors could monitor high-temperature jet engine exhaust, leading to cleaner and more efficient operation. Other nonaerospace applications include improved high-voltage switching for energy savings in public electric power distribution and in electric cars.

The Lewis team is focusing on the chemical vapor deposition of the thin, single-crystal SiC films from which devices are fabricated. These films, which are deposited (i.e., epitaxially "grown") on commercial wafers, must consist of a single crystal with very few structural defects so that the derived devices perform satisfactorily and reliably. Using optical microscopy and atomic force microscopy in conjunction with transmission electron microscopy, we determined that subsurface damage in the wafers was a significant factor in many of the morphological features observed in the

crystal films. Such subsurface damage can be caused by the cutting and polishing of wafers from the bulk crystals (boules), which are grown by a vendor.

Working in collaboration (NASA grant) with Professor Pirouz of Case Western Reserve University, we developed a chemical-mechanical polishing (CMP) technique for removing the subsurface polishing damage prior to epitaxial growth of the single-crystal SiC films. This technique uses a polishing procedure with an alkaline (pH >10) slurry of colloidal silica at elevated temperatures (about 55 °C) to achieve SiC surfaces that are free of subsurface damage (as verified by high-resolution transmission electron microscopy). This development was somewhat of a surprise because SiC was believed to be impervious to chemical attack at such low temperatures. Surfaces of SiC wafers prepared with and without CMP are shown in the figure. Epitaxial films grown on SiC wafers prepared using CMP had significantly fewer morphological defects than films prepared on conventionally polished wafers. The CMP technique is still in an early state of development, and much work remains before a commercially viable process can be produced.



Atomic Force Microscope images of SiC wafers. Top: As-received wafer. Bottom: Wafer after CMP.

## Bibliography

Zhou, L., et al.: Chemomechanical Polishing of Silicon Carbide. *J. Electrochem. Soc.*, vol. 144, no. 6, June 1997, pp. L161–L163.

## Lewis contact:

J. Anthony Powell, (216) 433–3652, J.A.Powell@lerc.nasa.gov

**Author:** J. Anthony Powell

**Headquarters program office:** OASTT

**Programs/Projects:**

Information Systems R&T

# Model-Trained Neural Networks and Electronic Holography Demonstrated to Detect Damage in Blades

Electronic holography can show damaged regions in fan blades at 30 frames/sec. The electronic holograms are transformed by finite-element-model-trained artificial neural networks to visualize the damage. The trained neural networks are linked with video and graphics to visualize the bending-induced strain distribution, which is very sensitive to damage. By contrast, it is very difficult to detect damage by viewing the raw, speckled, characteristic fringe patterns. For neural-network visualization of damage, 2 frames or 2 fields are used, rather than the 12 frames normally used to compute the displacement distribution from electronic holograms.

At the NASA Lewis Research Center, finite element models are used to compute displacement and strain distributions for the vibration modes of undamaged and cracked blades. A model of electronic time-averaged holography is used to transform the displacement distributions into finite-element-resolution characteristic fringe patterns. Then, a feed-forward neural network is trained with the fringe-pattern/strain-pattern pairs, and the neural network, electronic holography, and video are implemented on a workstation. Now that the neural networks have been tested successfully at 30 frames/sec on undamaged and cracked cantilevers, the electronic holography and neural-network processing are being adapted for onsite damage inspection of twisted fan blades and rotor-mounted blades. Our conclusion is that model-trained neural nets are effective when they are trained with good models whose application is well understood. This

work supports the aeromechanical testing portion of the Advanced Subsonic Technology Project.

## Bibliography

Decker, A.J., et al.: Vibrational Analysis of Engine Components Using Neural-Net Processing and Electronic Holography. NASA TM-113124, 1997. Available online: <http://letrs.lerc.nasa.gov/LeTRS/browse.pl?1997/TM-113124.html>

## Lewis contact:

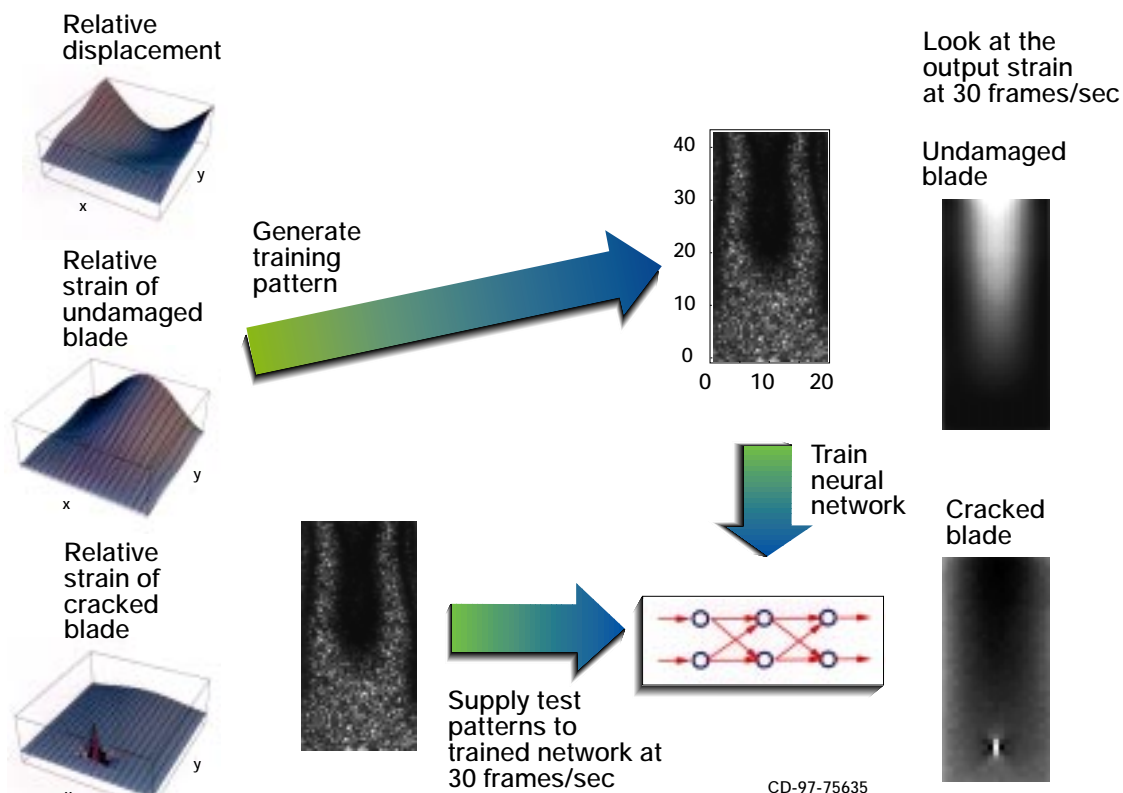
Dr. Arthur J. Decker, (216) 433-3639, [Arthur.J.Decker@lerc.nasa.gov](mailto:Arthur.J.Decker@lerc.nasa.gov)

**Authors:** Dr. Arthur J. Decker, E. Brian Fite, Oral Mehmed, and Scott A. Thorp

## Headquarters program office:

OASTT (funded by Lewis Director's Discretionary Fund)

**Programs/Projects:** AST



*Process for training and using neural networks for damage inspections.*



# Particle Imaging Velocimetry Used in a Transonic Compressor Facility

Particle Imaging Velocimetry (PIV) is an optical technique whereby a pulsed laser sheet is used to illuminate particles entrained in a fluid across an extended planar cross section of a flow field. Electronic recording of the particle positions at two closely timed laser pulses permits the computation of the flow velocity. PIV captures the instantaneous flow field, permitting the study of unsteady flow phenomena. Mean flow statistics can be computed by acquiring several hundred images and averaging the results.

The first-ever successful application of PIV to acquire measurements in a high-speed rotating turbomachinery blade row was completed in NASA Lewis Research Center's W-8 Single Stage Axial Compressor Facility. Measurements were acquired in a 20-in.-diameter transonic compressor rotor operating at 17,188 rpm. A custom-designed light-sheet-generating probe was used to insert the high-energy, pulsed light-sheet illumination required for recording the unblurred images of particles entrained in the fluid. Measurements of the shock wave formed within the rotor blade passage and of unsteady structures within the blade wakes were acquired. These measurements provide insight into unsteady spatial structures in the flow field which cannot be measured with the more conventional laser anemometry technique. The PIV technique provides both instantaneous and average velocity data in a transonic compressor in an order of magnitude less time than required for other conventional optical diagnostic techniques.

For more information about PIV, visit our site on the World Wide Web:

<http://www.lerc.nasa.gov/WWW/OptInstr/piv.html>

## Bibliography

Wernet, M.P.: Demonstration of PIV in a Transonic Compressor. NASA TM-113164, 1997. Available online: <http://letrs.lerc.nasa.gov/cgi-bin/LeTRS/browse.pl?1997/TM-113164.html>

## Lewis contact:

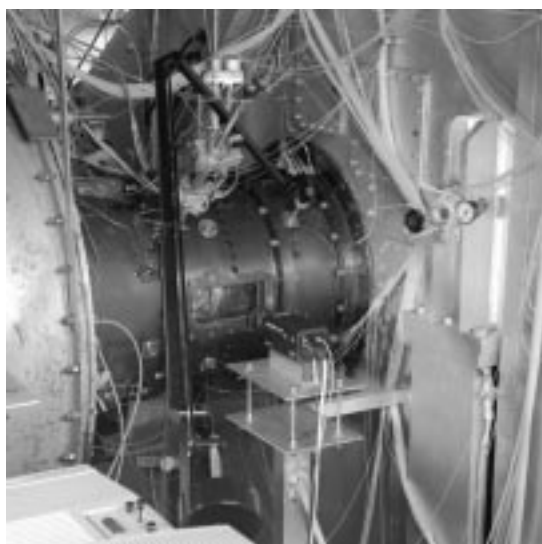
Dr. Mark P. Wernet, (216) 433-3752, [Mark.P.Wernet@lerc.nasa.gov](mailto:Mark.P.Wernet@lerc.nasa.gov)

**Author:** Dr. Mark P. Wernet

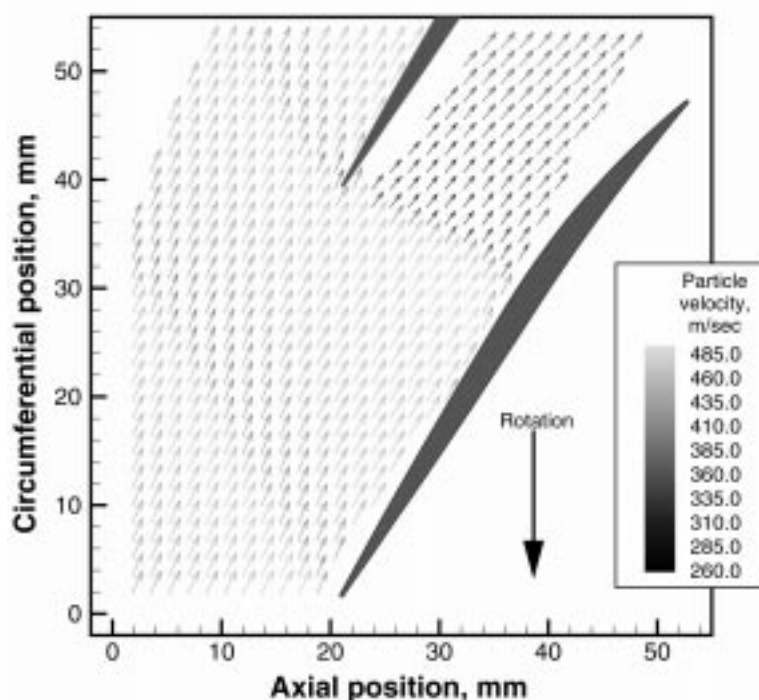
## Headquarters program office:

OASTT (funded by Lewis Director's Discretionary Fund)

**Programs/Projects:** Propulsion Systems R&T, SGE, P&PM Level II



PIV system installed in W-8 transonic compressor facility.



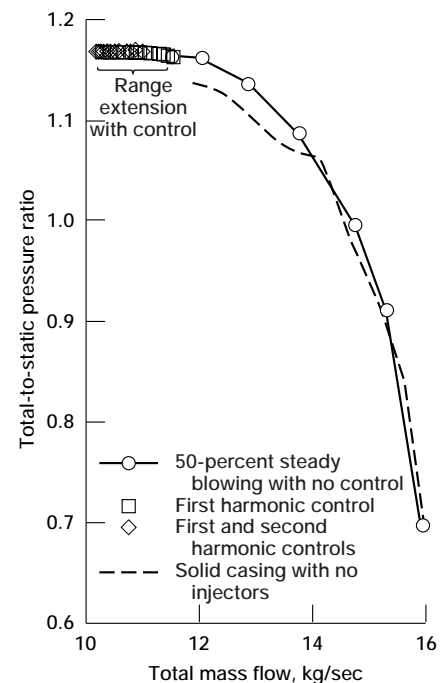
Average of 110 instantaneous PIV velocity vector maps. This figure is shown in color in the online version of this article (<http://www.lerc.nasa.gov/WWW/RT1997/5000/5520wernet.htm>).

# Jet Injection Used to Control Rotating Stall in a High-Speed Compressor

In a joint effort between the Massachusetts Institute of Technology (MIT) and the NASA Lewis Research Center, a new technology was demonstrated to identify and control rotating stall and surge in a single-stage, high-speed compressor. Through the use of high-velocity, high-frequency jet injectors, the instabilities of surge and stall were controlled in a high-speed compressor rig. Through the use of active stall control, modal instabilities that normally occur in the pressure measurements prior to stall were normalized and the range of the compressor was extended. Normally the events of rotating stall and surge instabilities limit the operation of the aeroengine compressor to a region below the surge line. To enhance the performance of the compressor, the Lewis/MIT team used active stall control methods to extend the normal operation of the compressor beyond the original stall point.

The single-stage transonic compressor facility at NASA Lewis was used in this demonstration. The compressor, NASA Stage 35, was run at tip Mach numbers of approximately 1.0 and 1.5. These operating conditions are similar to cruise and takeoff conditions in an aeroengine compressor. Through injection of high-velocity air through the compressor casing upstream of the rotor tip, the stalling mass flow of the compressor was reduced by 17 percent when operating at a tip speed of 1000 ft/sec. At a tip speed of 1475 ft/sec, the stalling mass flow was reduced by 4 percent beyond the normal stall point. This injected air was then oscillated to frequencies of nearly 450 Hz to cancel unsteady velocity perturbations forming in the compressor prior to rotating stall. This "active control" of the jet-injected air was used to further reduce the stalling mass flow by 8 percent over steady blowing at the 1000 ft/sec operating condition, and a 4-percent additional reduction was observed over steady blowing at the higher speed condition. These results were obtained by injecting less than 4 percent of the total compressor throughflow into the rotor tip region. The figure shows this marked increase in stall margin from the compressor maps. It shows the operation of the compressor under nominal operating conditions, with steady blowing, and with active control. These results mark the first successful demonstration of actively controlled air injection as a stall-control strategy for highly loaded compressors operating at speeds typical of an actual gas turbine engine.

To develop this capability for possible application on an engine, the Lewis/MIT team attempted active stall control of this high-speed compressor with both radial and circumferential inlet distortion screens present. In these distorted inflow cases, both steady blowing and active control of injected air provided increased stalling mass flow reductions from the aforementioned clean inlet case. These experimental results demonstrate a first-ever active control approach using jet injection to extend the stall margin in high-speed compressors. A near-term goal of this continuing research is to determine the combination of air-injection parameters and control strategies that are most effective in providing stall control for both clean and distorted inlet flow conditions. Mid-term research goals include demonstration of stall control in a multistage core compressor and development and application of either passive or active stall control strategies that will result in integral flight-worthy components of onboard engine hardware.



*Stabilized compressor characteristics at 70-percent speed with 1.5-percent injected mass flow rate.*

## Bibliography

Weigl, H.J. et al.: Active Stabilization of Rotating Stall and Surge in a Transonic Single Stage Axial Compressor. Accepted for publication in the J. Turbomachinery, ASME IGTI Conference, 1997.

Berndt, R.G., et al.: Experimental Techniques for Actuation, Sensing, and Measurement of Rotating Stall Dynamics in High-Speed Compressors. Proceedings of the SPIE Conference on Sensing, Actuation, and Control in Aeropropulsion, 1995, pp. 166–185.

## Lewis contacts:

Michelle M. Bright, (216) 433–2304, Michelle.M.Bright@lerc.nasa.gov, and Dr. Anthony J. Strazisar, (216) 433–5881, Anthony.J.Strazisar@lerc.nasa.gov

**Authors:** Michelle M. Bright, Dr. Anthony J. Strazisar, Harald J. Weigl, Zoltan Spakovszky, and James D. Paduano

**Headquarters program office:** OASTT

**Programs/Projects:**

Propulsion Systems R&T, SGE, PPM,

## Distortion Tolerant Control Demonstrated in Flight

Future aircraft turbine engines, both commercial and military, will have to be able to successfully accommodate expected increased levels of steady-state and dynamic engine-face distortion. Advanced tactical aircraft are likely to use thrust vectoring for enhanced aircraft maneuverability. As a result, the engines will see more extreme aircraft angle-of-attack  $\alpha$  and sideslip  $\beta$  levels than currently encountered with present-day aircraft. Also, the mixed-compression inlets needed for the High Speed Civil Transport (HSCT) will likely encounter disturbances similar to those seen by tactical aircraft, in addition to planar pulse, inlet buzz, and high distortion levels at low flight speed and off-design operation.

The current approach of incorporating sufficient component design stall margin to tolerate these expected levels of distortion would result in significant performance penalties. The objective of NASA's High Stability Engine Control (HISTEC) program is to design, develop, and flight demonstrate an advanced, high-stability, integrated engine control system that uses measurement-based real-time estimates of distortion to enhance engine stability. The resulting distortion tolerant control adjusts the stall margin requirement online in real-time. This reduces the design stall margin requirement, with a corresponding increase in performance and decrease in fuel burn.

The HISTEC approach includes two major systems: a Distortion Estimation System (DES) and Stability Management Control (SMC). The DES is an aircraft-mounted, high-speed processor that estimates the amount and type of distortion present and its effect on the engine. It uses high-response pressure measurements at the engine face to calculate indicators of the type and extent of distortion in real-time. From these indicators,

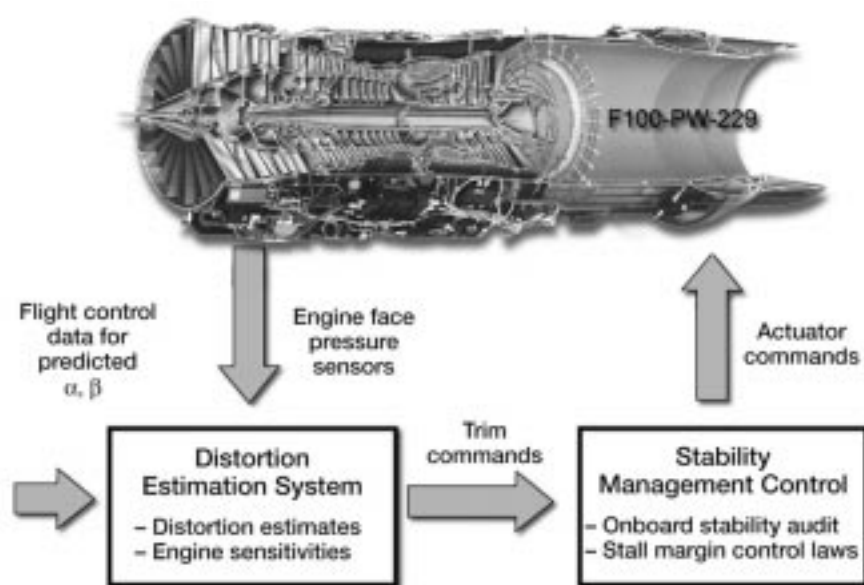
the DES determines the effects of the distortion on the propulsion system. In addition, the DES uses maneuver information from the flight control to anticipate high distortion conditions. The DES output consists of fan and compressor pressure ratio trim commands that are passed to the SMC. The SMC performs a stability audit online by using the trims from the DES and then accommodates the distortion through the production engine actuators.

This year, the HISTEC distortion tolerant control system was flight tested on the NASA F-15 ACTIVE aircraft at the NASA Dryden Flight Research Center in Edwards, California. The flight demonstration showed closed-loop control operation with the engine fan and compressor stall margins being adjusted on the basis of estimated distortion. Project pilots flew the F-15 ACTIVE aircraft through a variety of maneuvers—such as high angle of attack flight, windup turns, and takeoff—which create distorted airflow conditions at the inlet. Preliminary analysis of the data indicates that both the DES and SMC were performing as designed. The extensive flight test data is currently being analyzed in detail.

The NASA Lewis Research Center is conducting the HISTEC program in partnership with the NASA Dryden Flight Research Center, Pratt & Whitney, Boeing Phantom Works (formerly McDonnell Douglas), and the U.S. Air Force.

**Find out more about the High Stability Engine Control distortion tolerant control technologies on the World Wide Web:**

<http://www.lerc.nasa.gov/WWW/cdtb/projects/histec/>



*Distortion tolerant control. (Engine cutaway copyright Pratt & Whitney; used with permission.)*



F-15 ACTIVE aircraft.

## Bibliography

DeLaat, J.C.; Southwick, R.D.; and Gallops, G.W.: High Stability Engine Control (HISTEC). AIAA Paper 96-2586 (NASA TM-107272), 1996. Available online: <http://letrs.lerc.nasa.gov/cgi-bin/LeTRS/browse.pl?1996/TM-107272.html>

## Lewis contact:

John C. DeLaat, (216) 433-3744,  
John.C.DeLaat@lerc.nasa.gov

**Author:** John C. DeLaat

**Headquarters program office:** OASTT

**Program/Projects:**

Propulsion Systems R&T, PHSV, HISTEC

# Active Pattern Factor Control for Gas Turbine Engines

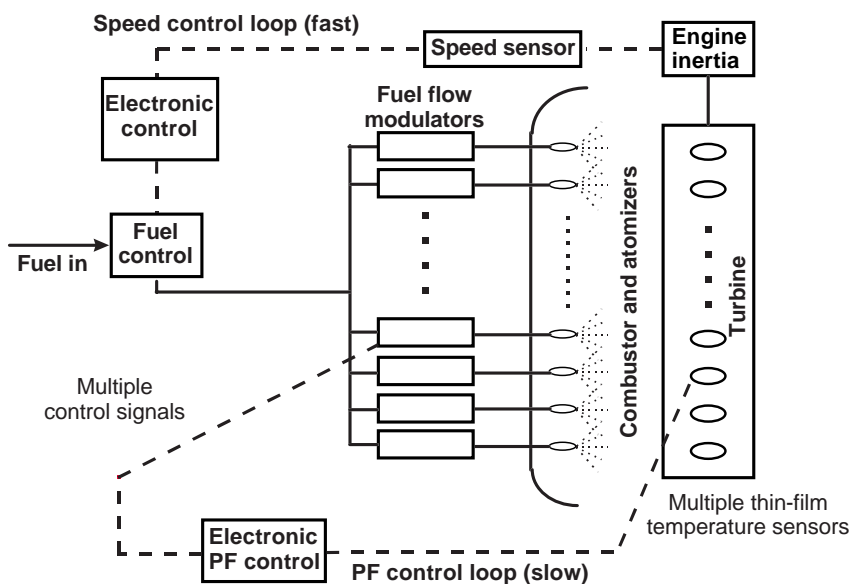
Small variations in fuel/air mixture ratios within gas turbine combustors can result in measurable, and potentially detrimental, exit thermal gradients. Thermal gradients can increase emissions, as well as shorten the design life of downstream turbomachinery, particularly stator vanes. Uniform temperature profiles are usually sought through careful design and manufacturing of related combustor components. However, small component-to-component variations as well as numerous aging effects degrade system performance. To compensate for degraded thermal performance, researchers are investigating active, closed-loop control schemes.

Most of this work is being done at AlliedSignal Engines under contract to the NASA Lewis Research Center (NASA Contract NAS3-27752).

Engine manufacturers assess thermal gradient performance by specifying and measuring a combustor's pattern factor (PF), which typically is defined as

$$PF = \frac{T_{4\text{peak}} - T_{4\text{avg}}}{T_{4\text{avg}}}$$

where  $T_4$  refers to the combustor exit temperature. The specific control objective, then, is to reduce PF and subsequently achieve and maintain a more uniform, two-dimensional temperature profile at the combustor exit plane. The control system configuration includes temperature sensing, digitally implemented control logic, and variable fuel flow modulators. A schematic diagram of the configuration is shown in the figure to the left. This diagram also highlights an implementation design



PF control system.



requirement. The PF control must be integrated with the existing fuel control design such that it does not affect the overall commanded power level of the engine.

The PF control system is composed of multiple temperature sensors and fuel modulators circumferentially placed around the combustor. Sensor and actuator counts, and their respective locations, have been determined from spatial resolution and controllability requirements. Several different state feedback control laws have been developed and analyzed. The schemes include optimal, (or performance-index-based) control, proportional-integral control, harmonic control, peak detection/switching control, spatial averaging control, and fuzzy logic control. Simulation studies have been completed to determine the relative merits of each approach.

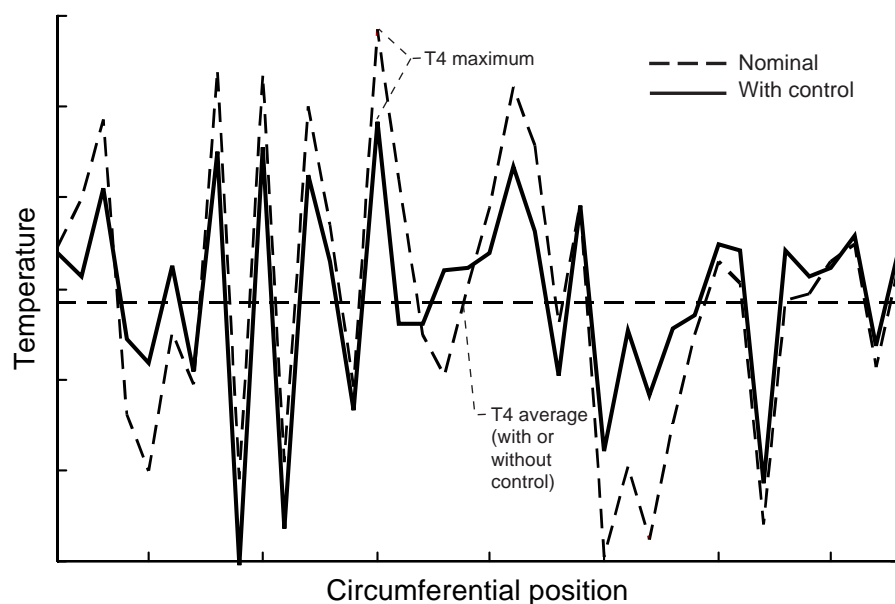
**Lewis contact:**

James E. May, (216) 433-3572,  
James.E.May@lerc.nasa.gov

**Author:** James E. May

**Headquarters program office:** OASTT

**Programs/Projects:** AST



*PF circumferential temperature profiles. Change in PF with control, -19 percent; change in rms with control, -34 percent.*

This graph is an example of the simulation output showing the analytical effects of PF control on a nominally perturbed temperature profile. The dashed trace is that of the circumferential, nonuniform temperature profile with the PF control switched off. The solid trace shows the resultant temperature profile after closed-loop control is switched on. Although the temperature excursions from  $T_{4\text{avg}}$  are not completely eliminated, peak temperatures are reduced. This equates to significant reduction in PF. Equally important, the average magnitude of the temperature excursions is notably reduced.

The next developmental step is to integrate the sensors, actuators, and control logic with actual combustor hardware to verify the analytical results. PF control is being developed by AlliedSignal Engines of Phoenix, Arizona, under NASA Lewis' Advanced Subsonic Technology (AST) Propulsion and Noise Reduction contract.

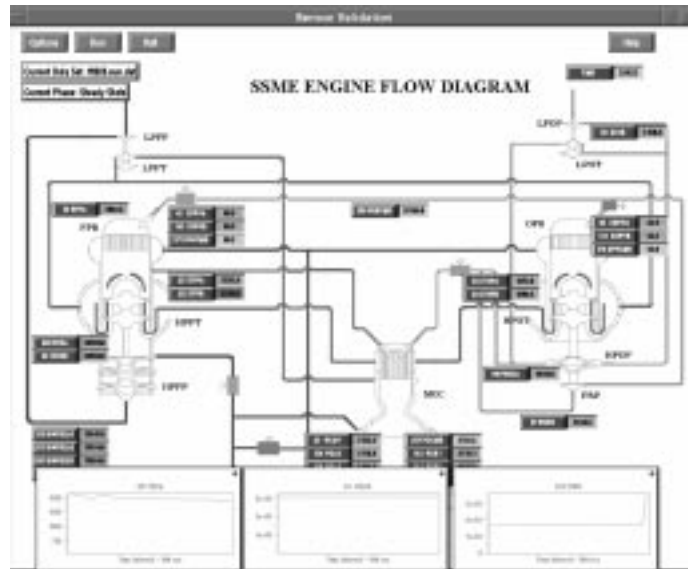


# Real-Time Sensor Validation System Developed

Real-time sensor validation improves process monitoring and control system dependability by ensuring data integrity through automated detection of sensor data failures. The NASA Lewis Research Center, Expert Microsystems, and Intelligent Software Associates have developed an innovative sensor validation system that can automatically detect automated sensor failures in real-time for all types of mission-critical systems. This system consists of a sensor validation network development system and a real-time kernel. The network development system provides tools that enable systems engineers to automatically generate software that can be embedded within an application. The sensor validation methodology captured by these tools can be scaled to validate any number of sensors, and permits users to specify system sensitivity. The resulting software reliably detects all types of sensor data failures.

A data failure is defined as any failure that corrupts the sensor signal and provides erroneous information to a process control or monitoring system. To identify these failures in real-time, we combined system design relationships, which are captured within individual models, and Bayesian probability theory. A set of sensor readings and the set of system models form a network of cross-checks that validate all the sensors within the network. The development system provides the workstation-based tools that define these analytically redundant models and the decision strategy used by the real-time kernel to detect the sensor failures.

The sensor validation system was applied to the Space Shuttle Main Engine, verifying that these sensor validation algorithms enable highly reliable data validation for critical sensors. Using these tools, we completed a prototype sensor validation network to validate the 22 Space Shuttle Main



User interface for the Space Shuttle Main Engine application of the sensor validation system was developed to view sensor failures in real-time.

Engine sensors. This network was embedded in two different controllers and successfully tested at the NASA Marshall Space Flight Center's simulation testbed. Current efforts are focused on extending and applying the tools to generate a larger sensor validation network for the Space Shuttle Main Engine.

## Bibliography

- Bickford, R.L.; Bickmore, T.W.; and Caluori, V.A.: Real-Time Sensor Validation for Autonomous Flight Control. AIAA Paper 97-2901, 1997.
- Bickford, R.L., et al.: Real-Time Flight Data Validation for Rocket Engines. AIAA Paper 96-2827, 1996.
- Bickmore, T.W.: A Probabilistic Approach to Sensor Data Validation. AIAA Paper 92-3163, 1992.

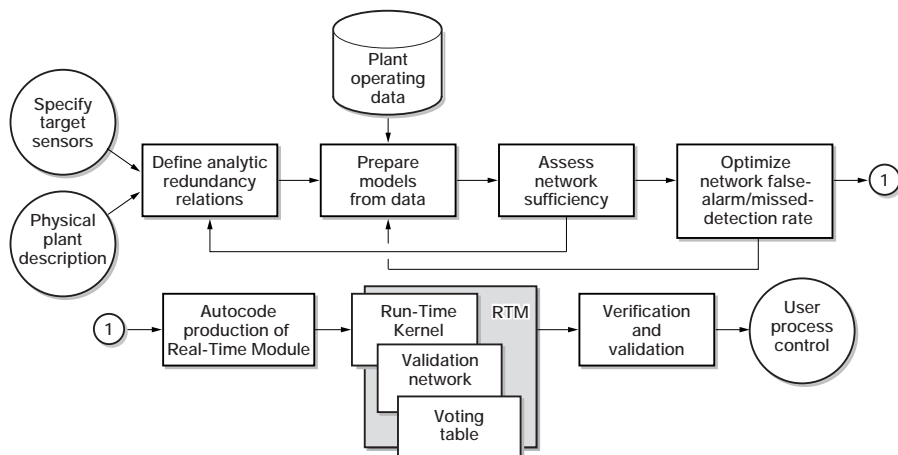
## Lewis contact:

June F. Zakrajsek, (216) 977-7470,  
June.F.Zakrajsek@lerc.nasa.gov

**Author:** June F. Zakrajsek

**Headquarters program office:** OSF

**Programs/Projects:** Broad-based technology, SSME, X-33/RLV, Aviation Safety, Information Systems



The sensor validation system automates the development and maintenance of an embeddable run-time sensor validation system.

# Communications Technology

## Asynchronous Transfer Mode Quality-of-Service Testing

In support of satellite-ATM interoperability, researchers at the NASA Lewis Research Center performed asynchronous transfer mode (ATM) quality-of-service experiments using MPEG-2 (ATM application layer 5, AAL5) over ATM over an emulated satellite link. The purpose of these experiments was to determine the free-space link quality necessary to use the ATM protocol to transmit high-quality multimedia information. The experimental results have been submitted to various International Telecommunications Union (ITU) study groups in order to improve and modify current standards and recommendations for the telecommunications industry.

Quality-of-service parameters for Class I, stringent class requirements for ITU-T I.356 are currently being debated. The experimental results presented will help to establish these quality-of-service thresholds. This material will also be useful in the development of the ITU-R WP-4B's Draft Preliminary New Recommendation on the Transmission of Asynchronous Transfer Mode Traffic via Satellite (Rec. S.atm). The results show that ITU-T Recommendation I.356 Class I, stringent ATM applications will require better link quality than currently specified—specifically, cell loss ratios of better than  $1.0 \times 10^{-8}$  and cell error ratios of better than  $1.0 \times 10^{-7}$ .

The diagram shows the setup for these tests. This testbed, which is extremely flexible, can be easily expanded to run over actual satellite and

terrestrial links since we have direct ATM connections to the high data rate terminal of NASA's Advanced Communication Technology Satellite (ACTS) and to the NASA Research and Education Network (NREN).

**More information about ATM and satellite communications research is available on the World Wide Web:**  
<http://sulu.lerc.nasa.gov/5610/qualityofservice.html>

**Lewis contact:**

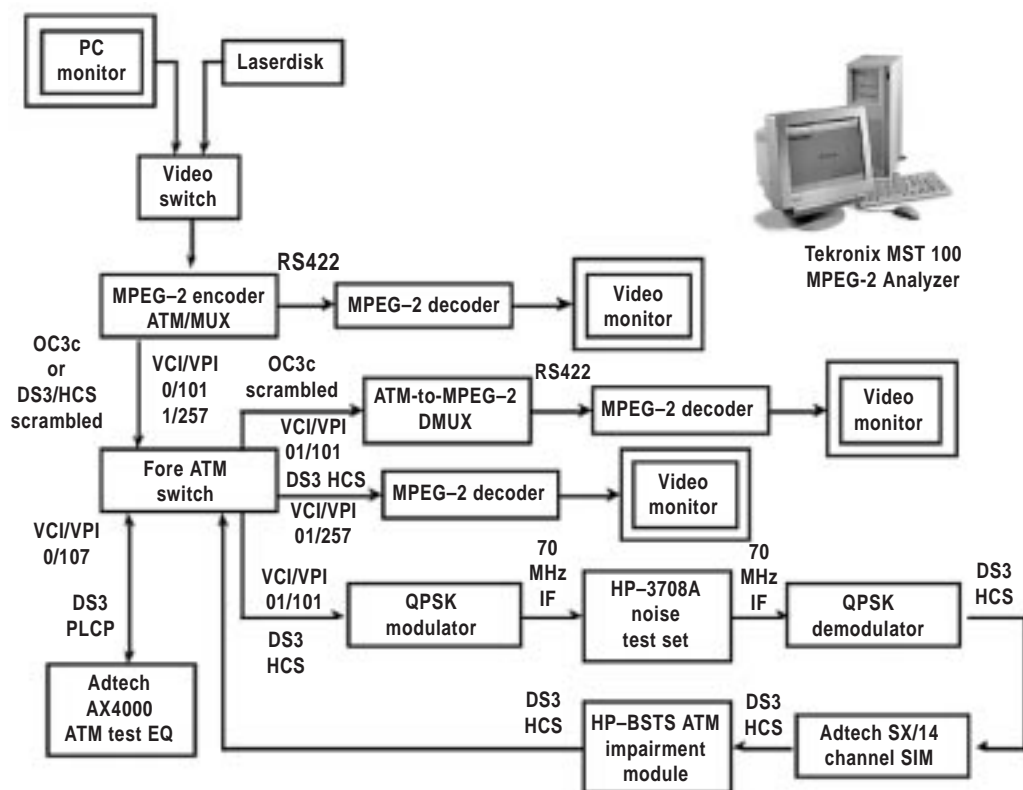
William D. Ivancic, (216) 433-3494,  
 William.D.Ivancic@lerc.nasa.gov

**Author:** William D. Ivancic

**Headquarters program office:** OSS

**Programs/Projects:**

ACTS, telecommunications



*Test setup for MPEG-2 over ATM (for further explanation, see <http://sulu.lerc.nasa.gov/5610/qualityofservice.html>).*

# Satellite-Terrestrial Network Interoperability

The developing national and global information infrastructures (NII/GII) are being built upon the asynchronous transfer mode (ATM) telecommunications protocol and associated protocol standards. These protocols are themselves under development through the telecommunications standards process defined by the International Telecommunications Union (ITU), which as a body is sanctioned by the United Nations. All telecommunications manufacturers use these standards to create products that can interoperate.

The ITU has recognized the ATM Forum as the instrument for the development of ATM protocols. This forum is a consortium of industry, academia, and government entities formed to quickly develop standards for the ATM infrastructure. However, because the participants represent a predominantly terrestrial network viewpoint, the use of satellites in the national and global information infrastructures could be severely compromised. Consequently, through an ongoing task order, the NASA Lewis Research Center asked Sterling Software, Inc., to communicate with the ATM Forum in support of the interoperability of satellite-terrestrial networks.

This year, Dr. Raj Jain of the Ohio State University, under contract to Sterling, authored or coauthored 32 explanatory documents delivered to the ATM Forum in the areas of Guaranteed Frame Rate for Transmission Control Protocol/Internet Protocol (TCP/IP), Available Bit Rate, performance testing, Variable Bit Rate voice over ATM, TCP over Unspecified Bit Rate+, Virtual Source/Virtual Destination, and network management. These contributions have had a significant impact on the content of the standards that the ATM Forum is developing. Some of the more significant accomplishments have been (1) the adoption by the ATM Forum of a new definition for Message-In, Message-Out latency and (2) improved text (clearer wording and newly defined terms) for measurement procedures, foreground and background traffic, and scalable configuration in the latency and throughput sections of the Performance Testing Baseline Text.

**More information about these contributions can be found on the World Wide Web:** <http://www.cis.ohio-state.edu/~jain/>

**Lewis contact:** Thomas C. von Deak, (216) 433-3277,  
[Thomas.C.Vondeak@lerc.nasa.gov](mailto:Thomas.C.Vondeak@lerc.nasa.gov)

**Author:** Thomas C. von Deak

**Headquarters program office:** OSS

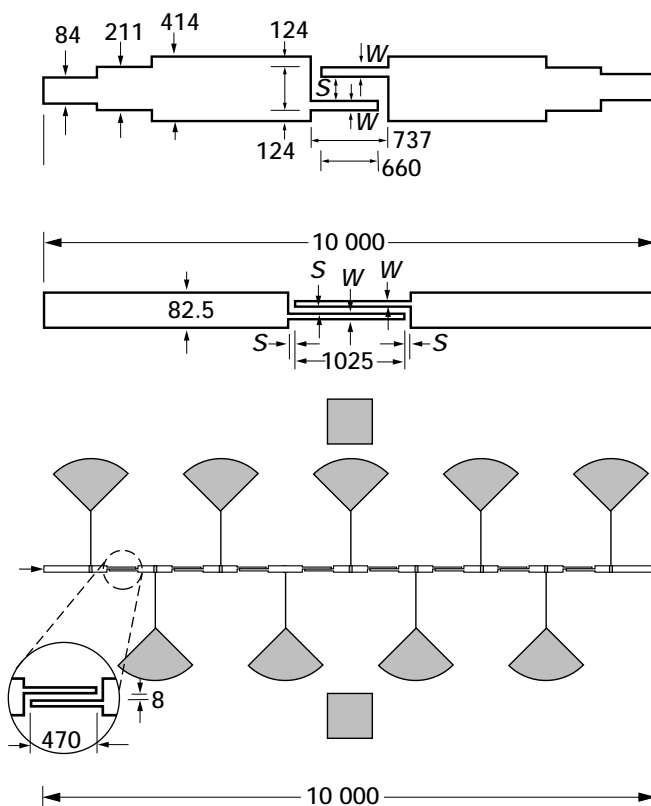
**Programs/Projects:** Space Communications, NII/GII, ATM, GIBN, NREN

# High-Temperature Superconducting/Ferroelectric, Tunable Thin-Film Microwave Components

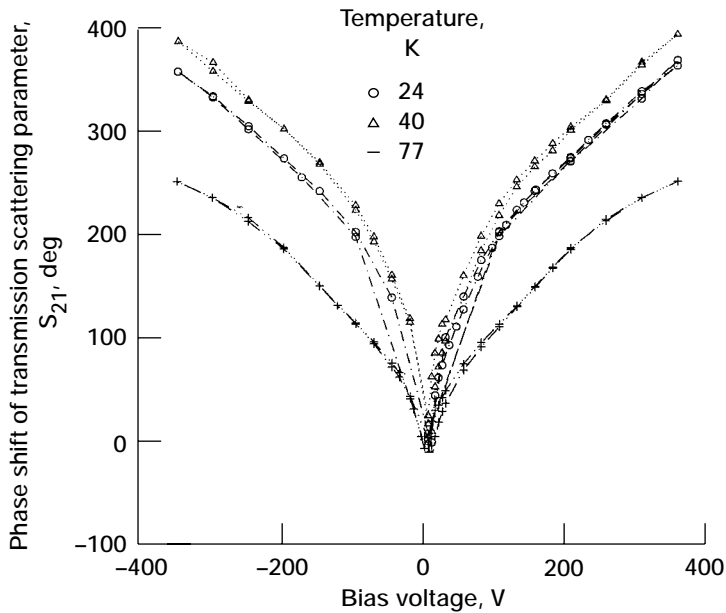
At the NASA Lewis Research Center, ferroelectric films such as  $\text{SrTiO}_3$  and  $\text{Ba}_x\text{Sr}_{1-x}\text{TiO}_3$ , are being used in conjunction with  $\text{YBa}_2\text{Cu}_3\text{O}_{7-\delta}$  high-temperature superconducting thin films to fabricate tunable microwave components such as filters, phase shifters, and local oscillators. These structures capitalize on the variation of the dielectric constant of the ferroelectric film upon the application of a direct-current electric field, as well as on the low microwave losses of high-temperature superconductors relative to their conventional conductor counterparts. For example, the surface resistance for a  $\text{YBa}_2\text{Cu}_3\text{O}_{7-\delta}$  thin film at 10 GHz and 77 K is more than two orders of magnitude lower than that of copper or gold at the same temperature and frequency.  $\text{SrTiO}_3$  and  $\text{Ba}_x\text{Sr}_{1-x}\text{TiO}_3$  films are used because their crystal structure and lattice parameters are similar to those of  $\text{YBa}_2\text{Cu}_3\text{O}_{7-\delta}$ , thus enabling the growth of highly textured  $\text{YBa}_2\text{Cu}_3\text{O}_{7-\delta}$  films with high critical current densities (i.e., greater than 1 MA/cm<sup>2</sup>) on the underlying ferroelectric film, or alternatively, of highly textured ferroelectric film on the underlying  $\text{YBa}_2\text{Cu}_3\text{O}_{7-\delta}$  film.

So far, our efforts have been concentrated on supporting industry and academia in determining the deposition parameters required for optimal ferroelectric thin-film growth (i.e., maximum tunability and lowest loss) and in investigating different varactor and microwave component configurations to determine which geometry is most advantageous in terms of tunability, losses, and required bias for a given communication application. For example, we have observed that for optimized  $\text{SrTiO}_3$  films in a parallel-plate capacitor configuration with  $\text{YBa}_2\text{Cu}_3\text{O}_{7-\delta}$  conducting plates, tunabilities of up to 47 percent and dissipation losses ( $\tan\delta$ ) of 0.05 are attainable at 1 MHz and 80 K, within a 0- to 5-Vdc range. In contrast, for interdigital configurations made of the same films, tunabilities of up to 70 percent and  $\tan\delta$  ranging from 0.015 to 0.001 (depending on the bias) have been observed at 1 MHz and 77 K within the 0- to 100-V bias range.

Efforts are underway to use these results in developing planar microstrip phase shifters for phased arrays, tunable filters for receiver front ends, and tunable local oscillators for Ku- and K-band communication systems. For example, we recently demonstrated an eight-element,  $\text{YBa}_2\text{Cu}_3\text{O}_{7-\delta}/\text{SrTiO}_3$  on  $\text{LaAlO}_3$  coupled microstripline phase shifter (CMPS) with a phase shift of 390° and an insertion loss of less than 10 dB at 16 GHz and 350 Vdc (see the figures). The effective coupling length for this device is 0.33 cm, and its total length is less than 1 cm. Similarly, we demonstrated tunable filters and multiconfiguration (e.g., contiguous, interdigital, and concentric) ring resonators at 19 GHz that



*( $\text{YBa}_2\text{Cu}_3\text{O}_{7-\delta}\text{Au}$ )/ $\text{SrTiO}_3/\text{LaAlO}_3$  coupled microstripline phase shifters. All dimensions are in micrometers. Top: 25- $\Omega$  phase shifter;  $S = 12.7\text{ }\mu\text{m}$ ,  $W = 76.2\text{ }\mu\text{m}$ . Middle: 50- $\Omega$  phase shifter;  $S = 7.5\text{ }\mu\text{m}$ ,  $W = 25\text{ }\mu\text{m}$ . Bottom: Eight-element, 50- $\Omega$  phase shifter;  $S = 7.5\text{ }\mu\text{m}$ ,  $W = 25\text{ }\mu\text{m}$ . Shaded areas represent bias pads and radial stubs for direct-current bias.*



*Insertion phase shift versus voltage for an eight-element, 50- $\Omega$   $\text{YBa}_2\text{Cu}_3\text{O}_{7-\delta}$  (350-nm-thick)/ $\text{SrTiO}_3$  (2.0- $\mu\text{m}$ -thick)/ $\text{LaAlO}_3$  (254- $\mu\text{m}$ -thick) coupled microstripline phase shifter. Data were taken at 16 GHz.*

exhibit frequency tunabilities of up to 1 GHz with respect to the center frequency without insertion loss and quality factor degradation. These components are the proof of concept of a hitherto unavailable technology to meet the stringent performance requirements of foreseeable satellite and wireless communication systems (e.g., contiguous, vibration-free steering antennas; bandpass filters with narrow bandwidth, small insertion losses, and steep out-of-band rejection; and low-noise figure and phase noise receivers) in a more advantageous fashion than with currently available technology (e.g., phase-shifting diodes, dielectric-filled cavities, and dielectric resonator oscillators). Optimization of the aforementioned components is underway at NASA Lewis.

### Bibliography

- Miranda, F.A., et al.: HTS/Ferroelectric Thin Films for Tunable Microwave Components. *IEEE Trans. Appl. Supercond.*, vol. 5, no. 2, 1995, pp. 3191–3194.
- Miranda, F.A., et al.: Electrical Response of Ferroelectric/Superconducting/Dielectric  $\text{Ba}_x\text{Sr}_{1-x}\text{TiO}_3/\text{YBa}_2\text{Cu}_3\text{O}_{7-\delta}/\text{LaAlO}_3$  Thin Film Multilayer Structures. *Supercond. Sci. Technol.*, vol. 8, 1995, pp. 755–763.
- Miranda, F.A., et al.: Effect of  $\text{SrTiO}_3$  Deposition Temperature on the Dielectric Properties of  $\text{SrTiO}_3/\text{YBa}_2\text{Cu}_3\text{O}_{7-\delta}/\text{LaAlO}_3$  Structures. *Integrated Ferroelectrics*, vol. 14, nos. 1–4, 1996, pp. 173–180.
- Miranda, F.A., et al.: Thin Film Multilayer Conductor/Ferroelectric Tunable Microwave Components for Communication Applications. *Integrated Ferroelectrics*, vol. 17, 1997, pp. 231–246.
- Van Keuls, F.W., et al.:  $(\text{YBa}_2\text{Cu}_3\text{O}_{7-\delta}, \text{Au})/\text{SrTiO}_3/\text{LaAlO}_3$  Thin Film Conductor/Ferroelectric Coupled Microstripline Phase Shifters and Their Potential for Phased Array Applications. *Appl. Phys. Lett.*, vol. 71, no. 21, 1997, pp. 3075–3077.

### Lewis contacts:

Dr. Félix A. Miranda, (216) 433–6589, [Felix.A.Miranda@lerc.nasa.gov](mailto:Felix.A.Miranda@lerc.nasa.gov), and  
Robert R. Romanofsky, (216) 433–3705, [Robert.R.Romanofsky@lerc.nasa.gov](mailto:Robert.R.Romanofsky@lerc.nasa.gov)

**Author:** Dr. Félix A. Miranda

**Headquarters program office:** OSS

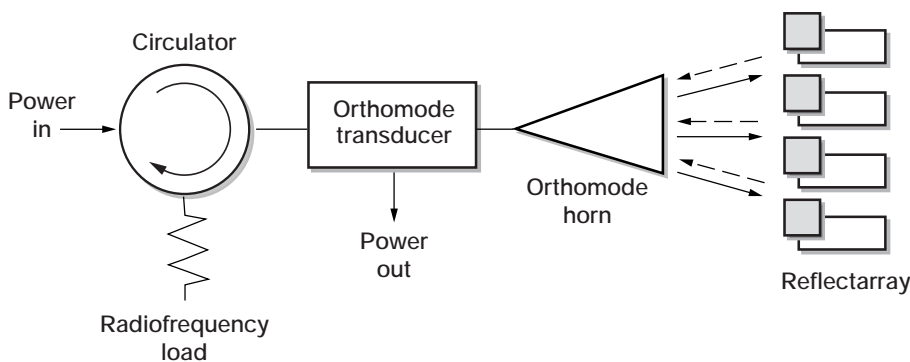
**Programs/Projects:**

Low-cost tracking ground terminals,  
low-phase noise receivers



# Reflectarray Demonstrated to Transform Spherical Waves Into Plane Waves

The development of low-cost, high-efficiency array antennas has been the research focus of NASA Lewis Research Center's Communications Technology Division for the past 15 years. One area of current interest is reflectarray development. Reflectarrays have generally been used to replace reflector antennas. In this capacity, different configurations (such as prime focus and offset) and various applications (such as dual frequency and scanning) have been demonstrated with great success. One potential application that has not been explored previously is the use of reflectarrays to compensate for phase errors in space-power-combining applications, such as a space-fed lens and power-combining amplifiers. Recently, we experimentally investigated the feasibility of using a reflectarray as an alternative to a dielectric lens for such applications. The experiment involved transforming the spherical waves from an orthomode horn to plane waves at the horn aperture. The reflectarray consists of square patches terminated in open stubs to provide the necessary phase compensation.

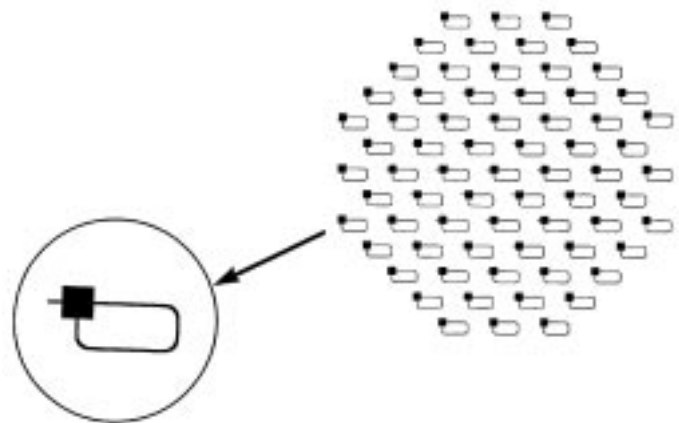


*Horn/planar array power-combining arrangement.*

The preceding diagram illustrates the conceptual layout of a horn/planar array power-combining arrangement. An orthomode horn was used to transmit vertically polarized fields to a planar array of patch radiating elements, each connected to a feedback loop of microstrip line as shown. The following figure shows the reflectarray and one of its patch elements. The phase-compensating devices were stubs or open-circuit transmission lines. The stub electrical length for a patch at the aperture center was adjusted in relation to the one displaced from the center such that it produced a phase delay that converted the spherical wave front to a planar wave front. The vertically polarized field received by the patches was phase delayed and then retransmitted to the horn in horizontal polarization. An orthomode transducer at the horn input isolated the two polarized waves.

For comparison, the absolute transmission scattering parameter  $S_{12}$  was measured at the horizontal port of the orthomode transducer for an identical array with-

out phase compensation and for the same array with a three-layer dielectric lens for phase compensation. The lens was placed inside the horn about 2 inches from the horn aperture. The array was mounted at the horn aperture against an aluminum plane that was securely bolted to the rim of the horn. For frequencies ranging from 16.0 to 17.5 GHz, the maximum reradiated horizontally polarized electric field from the array was on the average about -13 dB without phase compensation across the aperture; whereas the measured  $S_{12}$  when the phase was corrected by a reflectarray improved 4 dB on the average, and the measured  $S_{12}$  when the phase was corrected with a lens improved about 8 dB on the average. Although the difference between these two results indicates that more accurate phase information is needed to optimize the performance of the reflectarray for proper phase compensation, the feasibility of the reflectarray concept has been established as an alternative to using a dielectric lens in space power combining.



*Reflectarray and its radiating element.*

Although the reflectarray demonstrated for this space-power-combining application was passive, this concept is being extended to an active reflectarray where each antenna element is integrated with a solid state power amplifier. Some advantages of using an active reflectarray include smaller aperture sizes and a higher power-combining efficiency due to lower power combiner loss.

**Lewis contacts:** Dr. Afroz J. Zaman, (216) 433-3415, Afroz.J.Zaman@lerc.nasa.gov, and Dr. Richard Q. Lee, (216) 433-3489, Richard.Q.Lee@lerc.nasa.gov

**Author:** Dr. Afroz J. Zaman

**Headquarters program office:** OSS

**Programs/Projects:** Propulsion Systems R&T, Space-fed lens, Power-combining amplifiers

## Turbomachinery and Propulsion Systems

### Wave Rotor Research and Technology Development

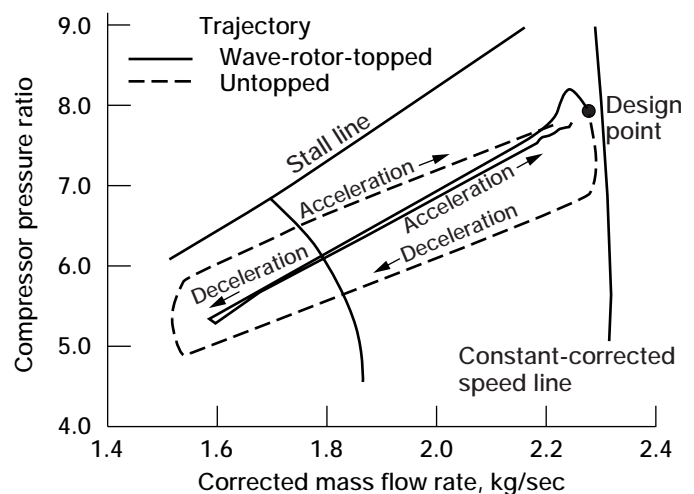
Wave rotor technology offers the potential to increase the performance of gas turbine engines significantly, within the constraints imposed by current material temperature limits. The wave rotor research at the NASA Lewis Research Center is a three-element effort: (1) development of design and analysis tools to accurately predict the performance of wave rotor components, (2) experiments to characterize component performance, and (3) system integration studies to evaluate the effect of wave rotor topping on the gas turbine engine system.

In the last year, significant progress was made in the dynamic simulation of wave rotors and gas turbine engines. The figure shows the response of wave-rotor-topped and baseline gas turbine engines to a step change in fuel flow: the wave-rotor-topped engine is more stable with respect to burner-induced surge (ref. 1).

Progress was also made in advanced component research: (1) rotor passage flow area variation was found to improve aerodynamic performance (ref. 2); (2) a new gas dynamic wave cycle was developed that greatly alleviates the thermal loading of the wave rotor and its ducting (ref. 3); (3) gas dynamic wave cycles and fuel/air premixing schemes were developed for wave rotors with combustion internal to the wave rotor (this approach conceptually eliminates the conventional burner of the gas turbine engine while still providing the engine-performance benefits afforded by wave rotor topping (ref. 4)); (4) a preliminary assessment of wave turbines (i.e., wave rotors that produce net shaft power) revealed that wave turbine topping potentially enhances engine specific power more than

the classical pressure-exchanger (i.e., zero-net-shaft-power wave rotor) topping does (ref. 5).

Progress has continued on the four-port pressure-exchanger experiment, which is designed to demonstrate startup, self-cooling effectiveness, and passive end-wall-leakage control, and to generate on- and off-design wave rotor



*Comparison of the dynamic responses of wave-rotor-topped and untopped gas turbine engines to step changes in fuel flow.*

performance data (i.e., a wave rotor map). The experiment uses an electric heater to add energy to the wave cycle in place of the burner component of the gas turbine engine. The experiment will operate at lower temperatures and pressures than would a wave rotor in an engine; however, all pressure and temperature ratios will be reproduced without the complications of variable gas properties (ref. 6).

A collaborative effort with the Allison Engine Company has yielded a preliminary design layout for a potential wave-rotor-enhanced demonstrator based on the Allison 250 turboshaft engine (ref. 7). Significant findings from this contracted effort include the following: (1) with existing Allison 250 engine turbomachinery hardware, wave rotor topping increases specific power by 20 percent and concomitantly decreases specific fuel consumption by 22 percent at full power; (2) improvements in specific power are maintained at part-power operation; (3) the surge margin of the topped engine is equivalent to that of the production engine; and (4) the wave rotor maintains high off-design performance.

## References

1. Greendyke, R.B.; Paxson, D.E.; and Schobeiri, M.T.: Dynamic Simulation of a Wave Rotor Topped Turboshaft Engine. AIAA Paper 97-3143 (NASA TM-107514), 1997. Available online: <http://letrs.lerc.nasa.gov/cgi-bin/LeTRS/browse.pl?1997/TM-107514.html>
2. Paxson, D.E.; and Lindau, J.W.: Numerical Assessment of Four-Port Through-Flow Wave Rotor Cycles With Passage Height Variation. AIAA Paper 97-3142 (NASA TM-107490), 1997. Available online: <http://letrs.lerc.nasa.gov/cgi-bin/LeTRS/browse.pl?1997/TM-107490.html>
3. Paxson, D.E.; and Nalim, M.R.: A Modified Through-Flow Wave Rotor Cycle With Combustor Bypass Ducts. AIAA Paper 97-3140, 1997.
4. Nalim, M.R.; and Paxson, D.E.: Numerical Study of Stratified Charge Combustion in Wave Rotors. AIAA Paper 97-3141 (NASA TM-107513), 1997. Available online: <http://letrs.lerc.nasa.gov/cgi-bin/LeTRS/browse.pl?1997/TM-107513.html>
5. Welch, G.E.: Wave Engine Topping Cycle Assessment. AIAA Paper 97-0707 (NASA TM-107371), 1997.
6. Wilson, J.: Design of NASA Lewis 4-Port Wave Rotor Experiment. AIAA Paper 97-3139 (NASA CR-202351), 1997. Available online: <http://letrs.lerc.nasa.gov/cgi-bin/LeTRS/browse.pl?1997/CR-202351.html>
7. Snyder, P.H.; and Fish, R.E.: Assessment of a Wave Rotor Topped Demonstrator Gas Turbine Engine Concept. ASME Paper 96-GT-41, 1996.

**Lewis contacts:** Dr. Gerard E. Welch, (216) 433-8003, Gerard.E.Welch@lerc.nasa.gov; Jack Wilson, (216) 977-1204, Jack.Wilson@lerc.nasa.gov; and Daniel E. Paxson, (216) 433-8334, Daniel.E.Paxson@lerc.nasa.gov

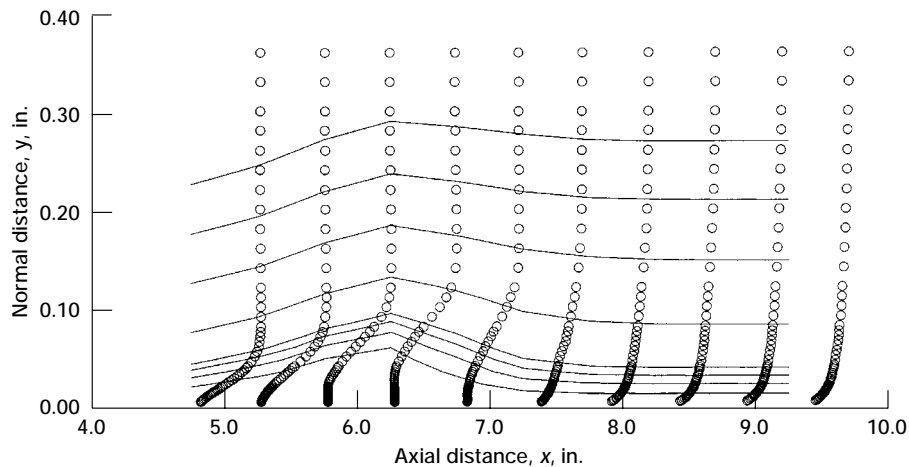
**Author:** Dr. Gerard E. Welch

**Headquarters program office:** OASTT

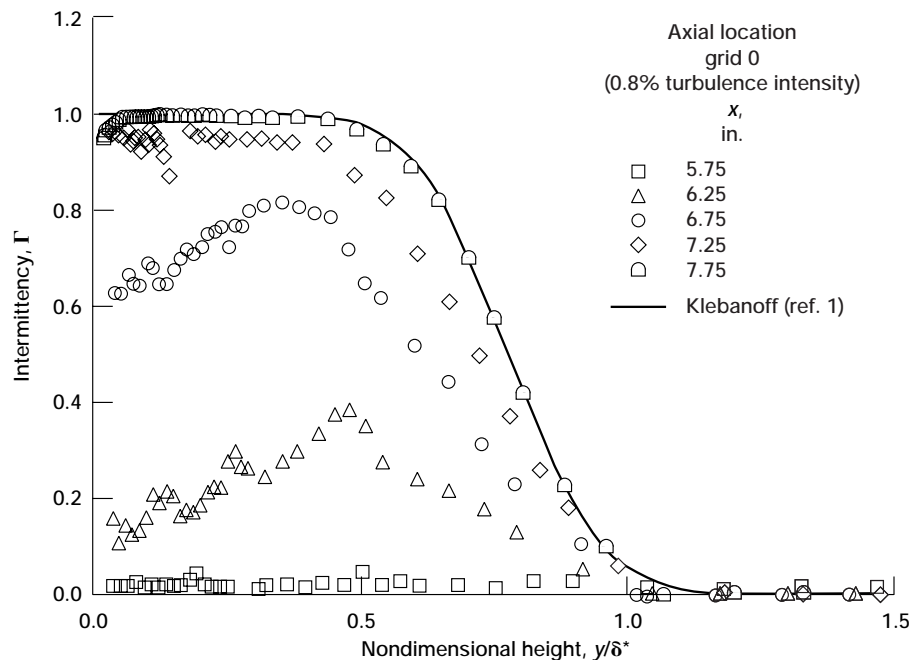
**Programs/Projects:** Propulsion Systems R&T, SGE, gas turbine engines

# Low-Pressure Turbine Flow Physics Program

This year, a simulated low-pressure turbine (LPT) was tested in NASA Lewis Research Center's CW-7 facility. This experimental test program is part of the collaborative NASA/industry/academia LPT Flow Physics program. The top figure is a carpet plot showing velocity and streamline profiles for a Reynolds number of approximately 100,000 and a free-stream turbulence intensity of 0.8 percent (grid 0). The top plot shows a separation bubble occurring at an axial location of 5.25 in. on the flat plate ( $x$  measured from the leading edge of the bottom test plate) of the simulated LPT test



*Carpet plot of velocity and streamline profiles for simulated LPT test section. Reynolds number, 100,000; free-stream turbulence intensity, 0.8 percent.*



*Intermittency profiles for simulated LPT test section. Reynolds number, 100,000; free-stream turbulence intensity, 0.8 percent.*

section. The flow reattaches turbulently at an axial location of approximately 6.75 in., and the reattachment is corroborated by the intermittency profiles shown in the bottom figure for the same test conditions.

This program is ongoing. Future tests are planned to focus on the behavior of the separation bubble as a function of the Reynolds number and free-stream turbulence intensity.

## Reference

1. Klebanoff, P.S.: Characteristics of Turbulence in a Boundary Layer With Zero Pressure Gradient. NACA TR-1247, 1955.

## Lewis contacts:

Rickey J. Shyne, (216) 433-3595, Rickey.J.Shyne@lerc.nasa.gov, and Dr. Ki-Hyeon Sohn, (216) 433-5949, Ki-Hyeon.Sohn@lerc.nasa.gov

## Authors:

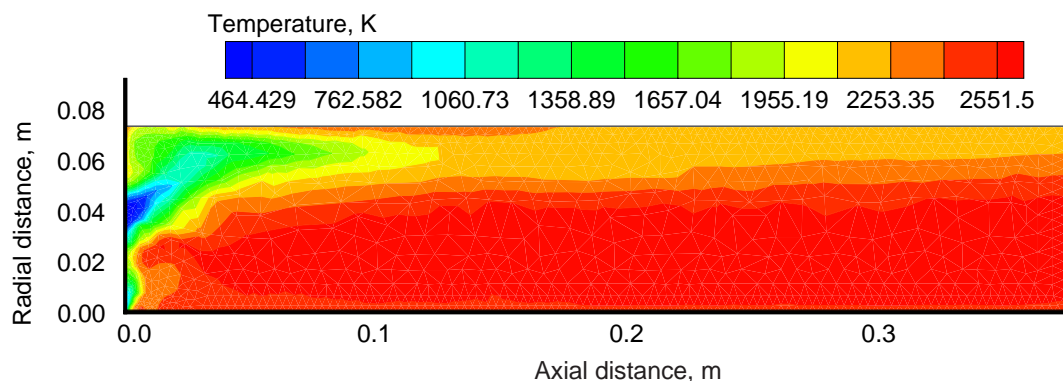
Rickey J. Shyne and Dr. Ki-Hyeon Sohn

Headquarters program office: OASTT

## Programs/Projects:

LPT Flow Physics, AST, ReCAT

# LSPRAY: Lagrangian Spray Solver for Applications With Parallel Computing and Unstructured Gas-Phase Flow Solvers



Temperature distribution in a confined, swirl-stabilized spray flame. Figure is shown in color in the online version of this article (<http://www.lerc.nasa.gov/WWW/RT1997/5000/5830gorland1.htm>).

Sprays occur in a wide variety of industrial and power applications and in the processing of materials. A liquid spray is a phase flow with a gas as the continuous phase and a liquid as the dispersed phase (in the form of droplets or ligaments). Interactions between the two phases, which are coupled through exchanges of mass, momentum, and energy, can occur in different ways at different times and locations involving various thermal, mass, and fluid dynamic factors. An understanding of the flow, combustion, and thermal properties of a rapidly vaporizing spray requires careful modeling of the rate-controlling processes associated with the spray's turbulent transport, mixing, chemical kinetics, evaporation, and spreading rates, as well as other phenomena.

In an attempt to advance the state-of-the-art in multidimensional numerical methods, we at the NASA Lewis Research Center extended our previous work on sprays to unstructured grids and parallel computing (refs. 1 to 3). LSPRAY, which was developed by M.S. Raju of Nyma, Inc., is designed to be massively parallel and could easily be coupled with any existing gas-phase flow and/or Monte Carlo probability density function (PDF) solver. The LSPRAY solver accommodates the use of an unstructured mesh with mixed triangular, quadrilateral, and/or tetrahedral elements in the gas-phase solvers. It is used specifically for fuel sprays within gas turbine combustors, but it has many other uses. The spray model used in LSPRAY provided favorable results when applied to stratified-charge rotary combustion (Wankel) engines and several other confined and unconfined spray flames (refs. 2 to 3). The source code will be available with the National Combustion Code (NCC) as a complete package.

## References

1. Raju M.S.; and Sirignano, W.A.: Multi-Component Spray Computations in a Modified Centerbody Combustor. J. Propul. P. (AIAA Paper 88-0638), vol. 6, Mar.-Apr. 1990.
2. Raju, M.S.: Heat Transfer and Performance Characteristics of a Dual-Ignition Wankel Engine. J. Engines, 1992 SAE Transactions, Sec. 3, pp. 466-509.
3. Raju, M.S.: Application of Scalar Monte Carlo Probability Density Function Method for Turbulent Spray Flames. Numer. Heat Transfer, Part A, vol. 30, no. 8, 1996, pp. 753-777.

## Lewis contacts:

Dr. Manthena S. Raju, (216) 977-1366, [toraju@lerc.nasa.gov](mailto:toraju@lerc.nasa.gov), and  
Dr. Nan-Suey Liu, (216) 433-8722, [Nan-Suey.Liu@lerc.nasa.gov](mailto:Nan-Suey.Liu@lerc.nasa.gov)

**Author:** Dr. Manthena S. Raju

**Headquarters program office:** OASTT

**Programs/Projects:**

Propulsion Systems R&T, NCC, SGE



# EUPDF: Eulerian Monte Carlo Probability Density Function Solver for Applications With Parallel Computing, Unstructured Grids, and Sprays

The success of any solution methodology used in the study of gas-turbine combustor flows depends a great deal on how well it can model the various complex and rate-controlling processes associated with the spray's turbulent transport, mixing, chemical kinetics, evaporation, and spreading rates, as well as convective and radiative heat transfer and other phenomena. The phenomena to be modeled, which are controlled by these processes, often strongly interact with each other at different times and locations. In particular, turbulence plays an important role in determining the rates of mass and heat transfer, chemical reactions, and evaporation in many practical combustion devices. The influence of turbulence in a diffusion flame manifests itself in several forms, ranging from the so-called wrinkled, or stretched, flamelets regime to the distributed combustion regime, depending upon how turbulence interacts with various flame scales. Conventional turbulence models have difficulty treating highly nonlinear reaction rates.

A solution procedure based on the composition joint probability density function (PDF) approach holds the promise of modeling various important combustion phenomena relevant to practical combustion devices (such as extinction, blowoff limits, and emissions predictions) because it can account for nonlinear chemical reaction rates without making approximations. In an attempt to advance the state-of-the-art in multidimensional numerical methods, we at the NASA Lewis Research Center extended our previous work on the PDF method to unstructured grids, parallel computing, and sprays (refs. 1 to 2). EUPDF, which was developed by M.S. Raju of Nyma, Inc., was designed to be massively parallel and could easily be coupled with any existing gas-phase and/or spray solvers. EUPDF can use an unstructured mesh with mixed triangular, quadrilateral, and/or tetrahedral elements. The application of the PDF method showed favorable results when applied to several supersonic-diffusion flames and spray flames (refs. 1 to 2). The EUPDF source code will be available with the National Combustion Code (NCC) as a complete package (see the figure in ref. 3).

## **Lewis contacts:**

Dr. Manthena S. Raju, (216) 977-1366,  
toraju@lerc.nasa.gov, and  
Dr. Nan-Suey Liu, (216) 433-8722,  
Nan-Suey.Liu@lerc.nasa.gov

**Author:** Dr. Manthena S. Raju

**Headquarters program office:** OASTT

**Programs/Projects:**

Propulsion Systems R&T, NCC, SGE

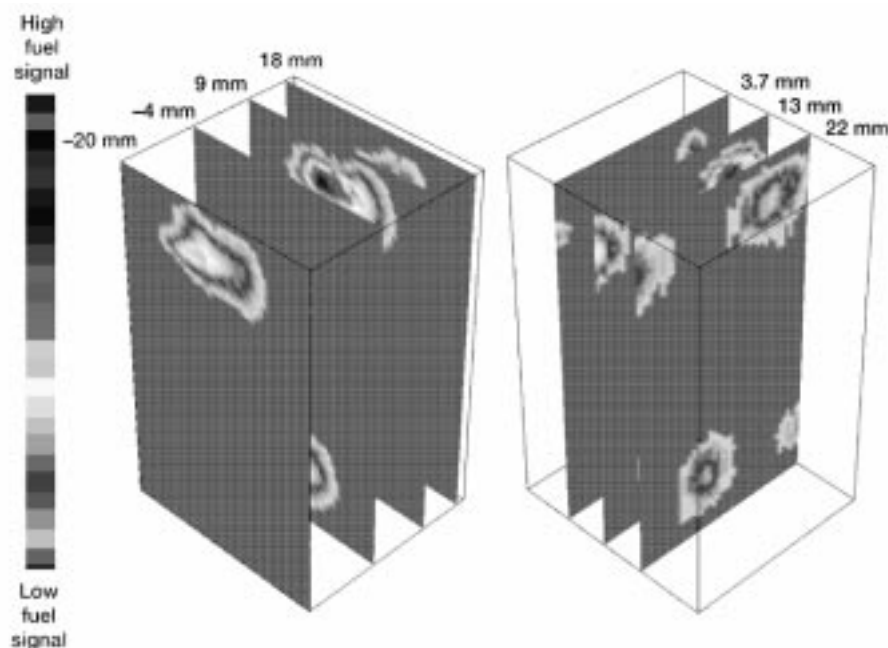
## **References**

1. Raju, M.S.: Application of Scalar Monte Carlo Probability Density Function Method for Turbulent Spray Flames. *Numer. Heat Trans., Part A*, vol. 30, no. 8, 1996, pp. 753-777.
2. Raju, M.S.: Combined Scalar-Monte-Carlo-PDF/CFD Computations of Spray Flames on Unstructured Grids With Parallel Computing. *AIAA Paper 97-2969*, 1997.
3. Raju, M.S.: LSPRAY: Lagrangian Spray Solver for Applications With Parallel Computing and Unstructured Gas-Phase Flow Solvers. *Research & Technology* 1997. NASA TM-206312, 1997, pp. 73. Available online: <http://www.lerc.nasa.gov/WWW/RT1997/5000/5830gorland1.htm>

## Three-Dimensional Measurements of Fuel Distribution in High-Pressure, High-Temperature, Next-Generation Aviation Gas Turbine Combustors

In our world-class, optically accessible combustion facility at the NASA Lewis Research Center, we have developed the unique capability of making three-dimensional fuel-distribution measurements of aviation gas turbine fuel injectors at actual operating conditions. These measurements are made in situ at the actual operating temperatures and pressures using the JP-grade fuels of candidate next-generation advanced aircraft engines for the High Speed Research (HSR) and Advanced Subsonics Technology (AST) programs.

The inlet temperature and pressure ranges used thus far are 300 to 1100° F and 80 to 250 psia. With these data, we can obtain the injector spray angles, the fuel mass distributions of liquid and vapor, the degree of fuel vaporization, and the degree to which fuel has been consumed. The data have been used to diagnose the performance of injectors designed both in-house and by major U.S. engine manufacturers and to design new fuel injectors with overall engine performance goals of increased efficiency and reduced environmental impact. Mie scattering is used to visualize the liquid fuel, and laser-induced fluorescence is used to visualize both liquid and fuel vapor.



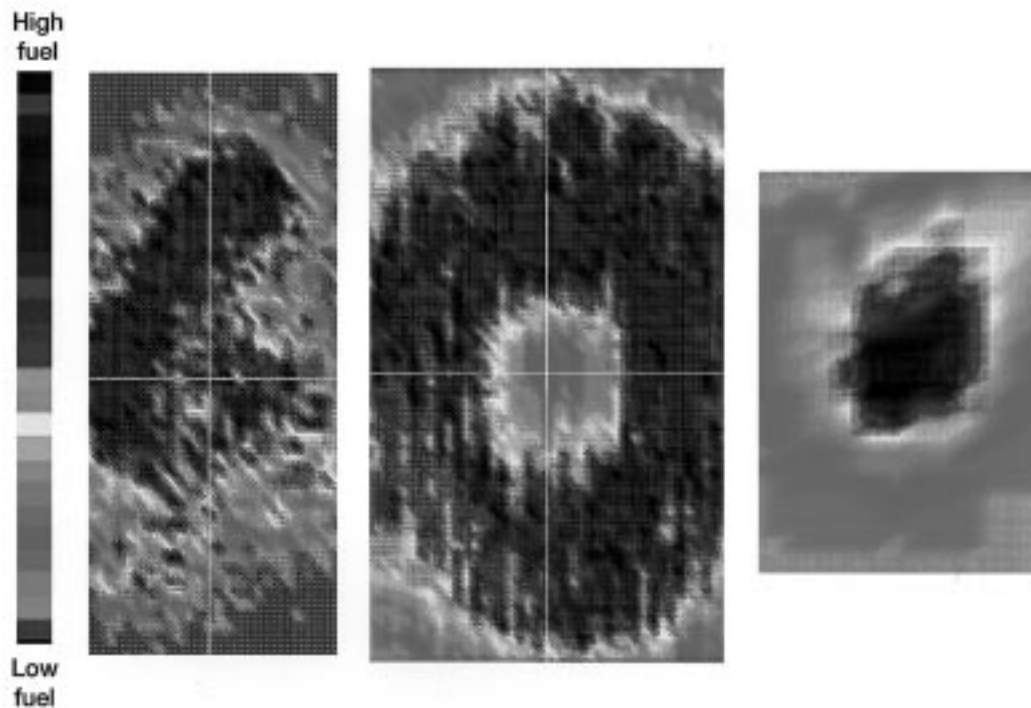
*Fuel distribution visualized via PLIF. Inlet temperature, 980 °F; inlet pressure, 212 psia; equivalence ratio, 0.42. Left: Raw fuel PLIF images in the z-y plane. Right: Composite PLIF fuel images in x-y plane.*

The preceding figure is an example of the process used to produce a three-dimensional flowfield. Measurements were made by taking a spatial sequence (typically with 1-mm spacing) of two-dimensional, planar, laser-induced fluorescence (PLIF) or Mie-scattering digital images. These raw images were taken in planes parallel to the flow axis, z. Then, they were

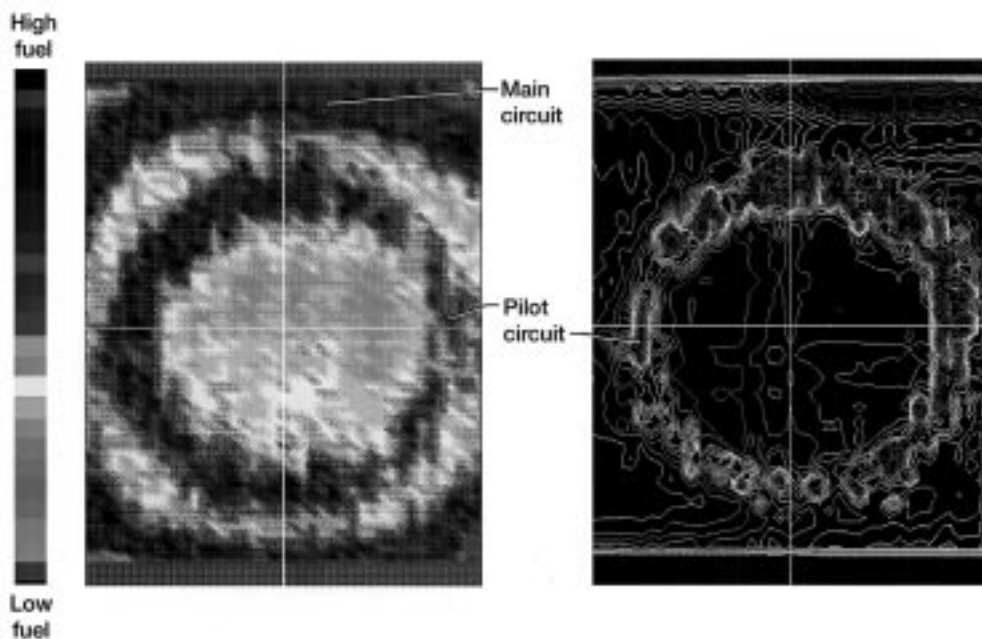
processed by placing them in a three-dimensional grid, as demonstrated by the PLIF image on the left. A three-dimensional composite image was generated by interpolating between the points within the grid. The resulting image can be viewed from any perspective. The image on the right shows selected composite PLIF cross-sectional (x-y plane) images. Each segment of the linear color bar (images are shown in color in the online version of this document—[http://www.lerc.nasa.gov/WWW/RT1997/5000/5830\\_hicks.htm](http://www.lerc.nasa.gov/WWW/RT1997/5000/5830_hicks.htm)) represents approximately 4 percent of the signal. The lowest signal is shown at the bottom of the scale.

Cross-sectional composites provide an important assessment of fuel injector patterns, which are used to assess the radial symmetry produced by an injector. The next figure uses PLIF to show the patterns of three fuel injectors approximately 10-mm downstream from their respective exit planes. Using these composite views makes it easier to determine if an injector is performing as designed.

The final figure compares the resultant PLIF (left) and planar Mie-scattering (right) patterns for a fuel injector at a downstream distance, z, of 14 mm. The injector has two fuel circuits, a pilot and a main, whose distributions are obvious from the fuel PLIF composite. The Mie-scattering image shows only the fuel distribution arising from the pilot circuit, thereby indicating that the fuel from the main circuit is in the vapor phase. The combination of the two measurement techniques allows us to assess the degree of fuel vaporization.



*Fuel patterns via fluorescence approximately 10-mm downstream from three concept fuel injectors at various temperatures, pressures, and equivalence ratios.*



*Comparison of Mie-scattering and fuel PLIF images shows that the main circuit produces vapor whereas the pilot circuit produces liquid. Inlet temperature, 768 °F; inlet pressure, 232 psia; equivalence ratio, 0.304; downstream distance,  $z$ , 14 mm. Left: Fuel PLIF image. Right: Mie-scattering image.*

**Lewis contacts:** Dr. Randy J. Locke, (216) 433-6110, [Randy.J.Locke@lerc.nasa.gov](mailto:Randy.J.Locke@lerc.nasa.gov), and Dr. Yolanda R. Hicks, (216) 433-3410, [Yolanda.R.Hicks@lerc.nasa.gov](mailto:Yolanda.R.Hicks@lerc.nasa.gov)

**Authors:** Dr. Yolanda R. Hicks, Dr. Randy J. Locke, Robert C. Anderson, and Michelle M. Zaller

**Headquarters program office:** OASTT

**Programs/Projects:** AST, HSR

# Mixing of Multiple Jets With a Confined Subsonic Crossflow

Results from a recently completed enhanced mixing program are summarized in the two technical papers in references 1 and 2. These studies were parts of a High Speed Research (HSR)-supported joint Government/industry/university program that involved, in addition to the NASA Lewis Research Center, researchers at United Technologies Research Center, Allison Engine Company, CFD Research Corporation, and the University of California, Irvine. The studies investigated the mixing of jets injected normal to a confined subsonic mainstream in both rectangular and cylindrical ducts. Experimental and computational studies were performed in both nonreacting and reacting flows. The orifice geometries and flow conditions were selected as typical of the complex three-dimensional flows in the combustion chambers in low-emission gas turbine engines.

The principal conclusion from both the experiments and modeling was that the momentum-flux ratio  $J$  and orifice spacing  $S/H$  were the most significant flow and geometry variables, respectively. Conserved scalar distributions were similar—independent of reaction, orifice diameter  $H/d$ , and shape—when the orifice spacing and the square root of the momentum-flux ratio were inversely proportional. Jet penetration was critical, and penetration decreased as either momentum-flux ratio or orifice spacing decreased. We found that planar averages must be considered in context with the distributions.

The mass-flow ratios and the orifices investigated were often very large. The jet-to-mainstream mass-flow ratio was varied from significantly less than 1 to greater than 1. The orifice-area to mainstream-cross-sectional-area was varied from  $\sim 0$  to 0.5, and the axial planes of interest were often just downstream of the orifice trailing edge. Three-dimensional flow was a key part of efficient mixing and was observed for all configurations. As an example of the results, the accompanying figure shows the effects of different rates of mass addition on the opposite walls of a rectangular duct.

## References

1. Holdeman, J.D., et al.: Mixing of Multiple Jets With a Confined Subsonic Crossflow: Part I—Cylindrical Duct. *J. Eng. Gas Turbines Power* (ASME Paper 96-GT-482 and NASA TM-107185), vol. 119, Oct. 1997.
2. Holdeman, J.D.; Liscinsky, D.S.; and Bain, D.B.: Mixing of Multiple Jets With a Confined Crossflow: Part II—Opposed Rows of Orifices in Rectangular Ducts. ASME Paper 97-GT-439 (NASA TM-107461), 1997. Available online: <http://letrs.lerc.nasa.gov/cgi-bin/LeTRS/browse.pl?1997/TM-107461.html>

## Lewis contact:

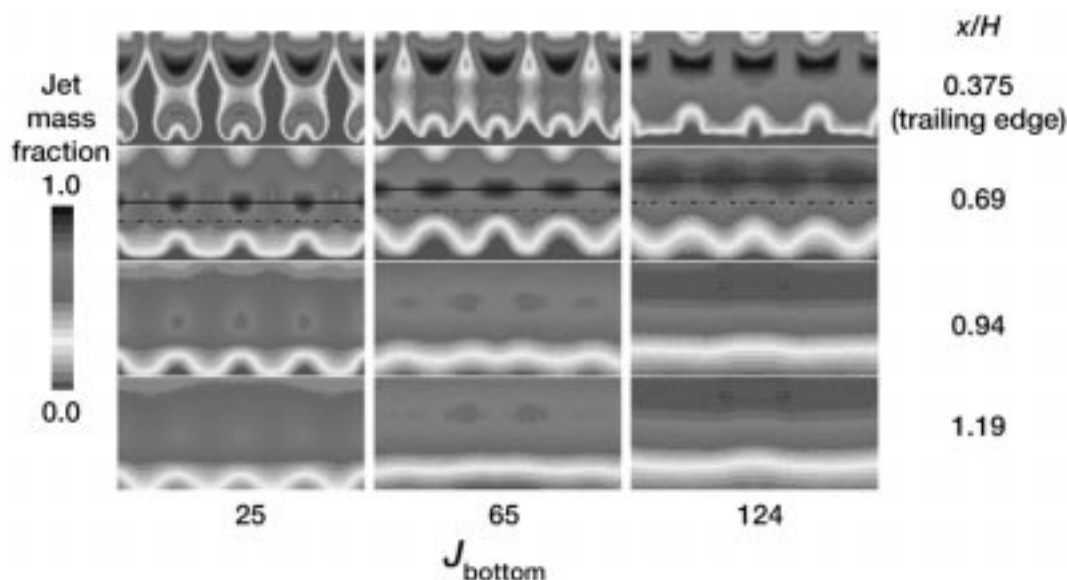
Dr. James D. Holdeman,  
(216) 433-5846,  
[James.D.Holdeman@lerc.nasa.gov](mailto:James.D.Holdeman@lerc.nasa.gov)

**Author:** Dr. James D. Holdeman

**Headquarters program office:** OASTT

**Programs/Projects:**

AST, Propulsion Systems R&T



Effect of nonsymmetric mass addition.  $J_{top} = 25$ ;  $H/d_{top} = 2.67$ ;  $H/d_{bottom} = 4.0$ ;  $S/H = 0.5$ .  
Figure is shown in color in the online version of this article (<http://www.lerc.nasa.gov/WWW/RT1997/5000/5830holdeman.htm>).

# Advanced Subsonic Combustion Rig

Researchers from the NASA Lewis Research Center have obtained the first combustion/emissions data under extreme future engine operating conditions. In Lewis' new world-class 60-atm combustor research facility—the Advanced Subsonic Combustion Rig (ASCR)—a flametube was used to conduct combustion experiments in environments as extreme as 900 psia and 3400 °F. The greatest challenge for combustion researchers is the uncertainty of the effects of pressure on the formation of nitrogen oxides ( $\text{NO}_x$ ). Consequently, U.S. engine manufacturers are using these data to guide their future combustor designs.

The flametube's metal housing has an inside diameter of 12 in. and a length of 10.5 in. The flametube can be used with a variety of different flow paths. Each flow path is lined with a high-temperature, castable refractory material (alumina) to minimize heat loss. Upstream of the flametube is the injector section, which has an inside diameter of 13 in. and a length of 0.5-in. It was designed to provide for quick changeovers.

This flametube is being used to provide all U.S. engine manufacturers early assessments of advanced combustion concepts at full power conditions prior to engine production. To date, seven concepts from engine manufacturers have been evaluated and improved. This collaborated development can potentially give U.S. engine manufacturers the competitive advantage of being first in the market with advanced low-emission technologies.

**Lewis contact:**

Dr. Chi-Ming Lee, (216) 433-3413,  
Chi-Ming.Lee@lerc.nasa.gov

**Author:** Dr. Chi-Ming Lee

**Headquarters program office:** OASTT

**Programs/Projects:**

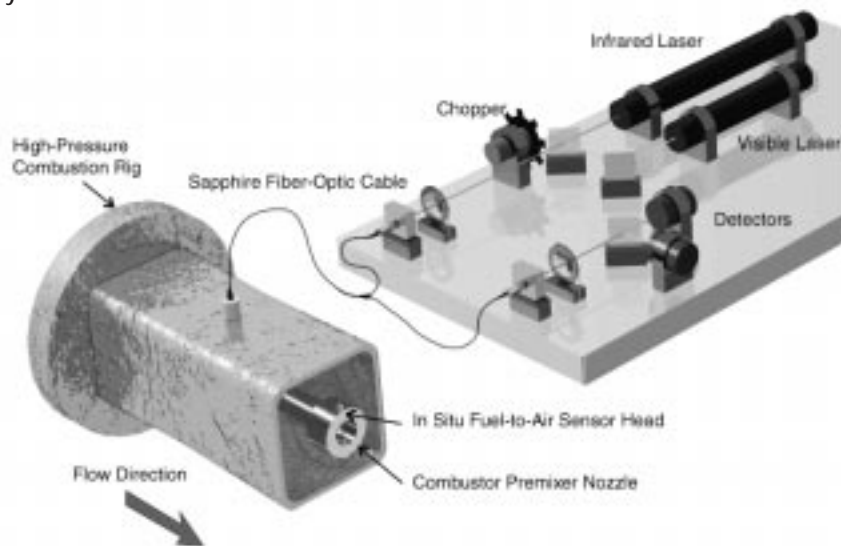
Propulsion Systems R&T, AST



## Time-Resolved Optical Measurements of Fuel-Air Mixedness in *Windowless* High Speed Research Combustors

Fuel distribution measurements in gas turbine combustors are needed from both pollution and fuel-efficiency standpoints. In addition to providing valuable data for performance testing and engine development, measurements of fuel distributions uniquely complement predictive numerical simulations. Although equally important as spatial distribution, the temporal distribution of the fuel is an often overlooked aspect of combustor design and development. This is due partly to the difficulties in applying time-resolved diagnostic techniques to the high-pressure, high-temperature environments inside gas turbine engines. Time-resolved measurements of the fuel-to-air ratio (F/A) can give researchers critical insights into combustor dynamics and acoustics.

Beginning in early 1998, a *windowless* technique that uses fiber-optic, line-of-sight, infrared laser light absorption to measure the time-resolved fluctuations of the F/A (refs. 1 and 2) will be used within the pre-mixer section of a lean-premixed, prevaporized (LPP) combustor in NASA Lewis Research Center's CE-5 facility. The fiber-optic F/A sensor will permit optical access while eliminating the need for film-cooled windows, which perturb the flow. More importantly, the real-time data from the fiber-optic F/A sensor will provide unique information for the active feedback control of combustor dynamics. This will be a prototype for an airborne sensor control system.



*Fiber-optic F/A sensor apparatus. The optics are mounted on a 4- by 2-ft optical breadboard. An electron beam brazing technique developed at Lewis was used to hermetically seal the sapphire fiber inside a small stainless steel tube. The chopper is used for calibration purposes only; without the chopper, the bandwidth of the instrument is 1 MHz.*

The illustration shows a schematic of the fiber-optic F/A sensor apparatus under development for NASA's High Speed Research (HSR) program. Infrared and visible light (3.39  $\mu\text{m}$  and 633 nm) from two helium/neon lasers are combined using a beam splitter. The light then enters a sapphire

optical fiber that guides it to the inside of the high-pressure combustor rig. (Sapphire transmits infrared light and can withstand temperatures up to 1800 °C.) A small parabolic mirror collimates and directs the light across the pre-mixer nozzle, where fuel vapor will attenuate only the infrared wavelength but fuel droplets or particulates will attenuate both wavelengths. The ratio of the transmitted infrared light to the visible light intensities provides time-resolved and quantitative measurements of the fuel vapor and droplet number densities. After traversing the pre-mixer nozzle, the light is then refocused into a return fiber, whereupon it is spectrally separated and directed to both infrared and visible light detectors. The signals from the detectors are processed in real time for online control. Future versions will use compact diode lasers, providing a more robust instrument for flight use.

In addition, the AST program will be using a high-speed fuel vapor sensor based on this technique to detect the presence of fuel leaks in the new Advanced Subsonic Combustor Rig (ASCR) windowed sector rig. The sensor will initiate an emergency shutdown if enough fuel vapor accumulates to create an explosion hazard (1300 °F and 900 psia). Conventional fuel leak detection, which requires an extractive sample line connected to a remote hydrocarbon gas analyzer, would have a response time on the order of tens of seconds. The fiber-optic fuel-air sensor, which responds in real time, will serve as a mission critical component of the ASCR test rig.

In the Fast Quiet Engine Program (High Speed Research), the fiber-optic F/A sensor will provide time-resolved F/A information in conjunction with acoustic instability information from microphones for the active-feedback dynamics control of future gas turbine combustors.

**Find out more about this research on the World Wide Web:**

<http://www.lerc.nasa.gov/WWW/HSR/CPCCComb.html>

<http://chartres.lerc.nasa.gov:1220/FQE/fy98.html>

**References**

1. Mongia, R., et al.: Proceedings from the 26th International Symposium on Combustion. The Combustion Institute, Pittsburgh, PA, 1996.

2. Dibble, R.W.; Mongia, R.; and Nguyen, Q.V.: U.S. Patent Application Serial No. 696,296, 1997.

**Lewis contact:**

Dr. Quang-Viet Nguyen,  
(216) 433-3574,  
[Quang-Viet.Nguyen@lerc.nasa.gov](mailto:Quang-Viet.Nguyen@lerc.nasa.gov)

**Author:** Dr. Quang-Viet Nguyen

**Headquarters program office:** OASTT

**Programs/Projects:** HSR, AST, ASCR, FQE, other applications requiring remote detection of fuel or hydrocarbon vapor

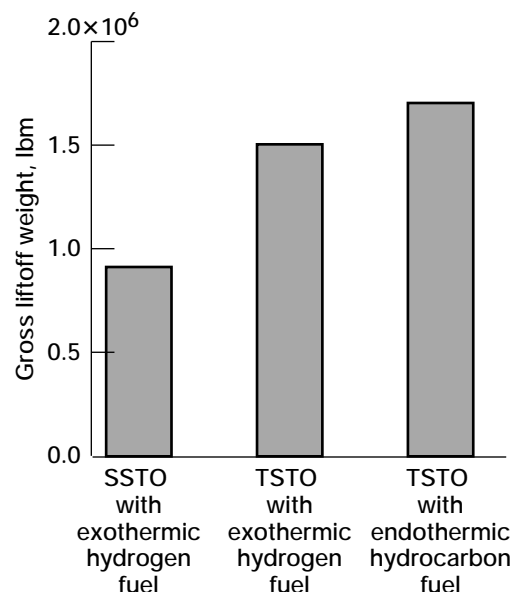
## Advanced Fuels Can Reduce the Cost of Getting Into Space

Rocket propellant and propulsion technology improvements can reduce the development time and operational costs of new space vehicle programs, and advanced propellant technologies can make space vehicles safer and easier to operate, and can improve their performance. Five major areas have been identified for fruitful research: monopropellants, alternative hydrocarbons, gelled hydrogen, metallized gelled propellants, and high-energy-density propellants (ref. 1).

During the development of the NASA Advanced Space Transportation Plan, these technologies were identified as those most likely to be effective for new NASA vehicles. Several NASA research programs had fostered work in fuels under the topic *Fuels and Space Propellants for Reusable Launch Vehicles* (ref. 2) in 1996 to 1997. One component of this topic was to promote the development and commercialization of monopropellant rocket fuels, hypersonic fuels, and high-energy-density propellants. This research resulted in the teaming of small business with large industries, universities, and Government laboratories. This work is ongoing with seven contractors. The commercial products from these contracts will bolster advanced propellant research.

Work also is continuing under other programs, which were recently realigned under the "Three Pillars" of NASA: Global Civil Aviation, Revolutionary Technology Leaps, and Access to Space (ref. 3). One of the five areas is described below, and its applications and effect on future missions is discussed. This work is being conducted at the NASA Lewis Research Center with the assistance of the NASA Marshall Space Flight Center.

The regenerative cooling of spacecraft engines and other components can improve overall vehicle performance. Endothermic fuels can absorb energy from an engine nozzle and chamber and help to vaporize high-density fuel before it enters the combustion chamber (refs. 4 and 5). For supersonic and hypersonic aircraft, endothermic fuels can absorb the high heat fluxes created on the wing leading edges and other aerodynamically heated components. Dual-fuel options are also possible, where endothermic



*Endothermic fuels increase gross liftoff weight but simplify operations for both single-stage-to-orbit (SSTO) and two-stage-to-orbit (TSTO) vehicles.*

hydrocarbon fuels are used for the lower speed portions of flight below Mach 8, and hydrogen fuel is used for the final acceleration to the upper stage separation velocity.

This bar graph shows the gross liftoff weight for several airbreathing space vehicles (ref. 1). The baseline case is a hydrogen-fueled single-stage-to-orbit vehicle, whose gross liftoff weight is less than

1 million lb. The gross liftoff weights of the two-stage-to-orbit vehicles are 1.5 and 1.7 million lb, respectively. Endothermic hydrocarbon fuels, because they absorb more heat, require an increased gross liftoff weight over hydrogen-fueled two-stage-to-orbit vehicles. However this increase in gross liftoff weight is relatively small at 0.2 million lb, and it eliminates the need for hydrogen for the first stage. Several types of related hydrocarbons can increase fuel density and reduce the overall mass of the vehicle structure, tankage, and related thermal protection systems.



*Airbreathing orbital vehicle lifts off. This vehicle can use endothermic hydrocarbon fuel for part of its ascent to orbit.*

**Find out more at the Fuels and Space Propellants Web site of Lewis' Small Business Innovation Research program:**

<http://www.lerc.nasa.gov/WWW/TU/launch/foctopsb.htm>

## References

1. Palaszewski, B.; Ianovski, L.S.; and Carrick, P.: . Propellant Technologies: A Persuasive Wave of Future Propulsion Benefits. Primary, Upper-Stage, and On-Board Propulsion for Space Transportation, Proceedings of the Third International Symposium on Space Propulsion, V. Yang, et al., eds. The Chinese Society of Astronautics, Beijing, China, 1997, pp. 1.10-1 to 1.10-14.
2. NASA Strategic Plan—1998. NASA Headquarters, Washington, DC, Oct. 30, 1997. Available online: <http://www.hq.nasa.gov/office/nsp/>
3. SBIR Focused Topic Web Site: On-Line Briefings to SBIR Convocation, April 1996, and propellant technology white papers. Available online: <http://www.lerc.nasa.gov/WWW/TU/launch/foctopsb.htm>
4. Ianovski, L.S.; and Moses, C.: Endothermic Fuels for Hypersonic Aviation. Fuels and Combustion Technology for Advanced Aircraft Engines, AGARD CP-536, 1993.
5. Petley, D.H.; and Jones, S.C.: Thermal Management for a Mach 5 Cruise Aircraft Using Endothermic Fuel. AIAA Paper 90-3284, 1990.

## Lewis contact:

Bryan A. Palaszewski, (216) 977-7493,  
[Bryan.A.Palaszewski@lerc.nasa.gov](mailto:Bryan.A.Palaszewski@lerc.nasa.gov)

**Author:** Bryan A. Palaszewski

**Headquarters program office:** OASTT

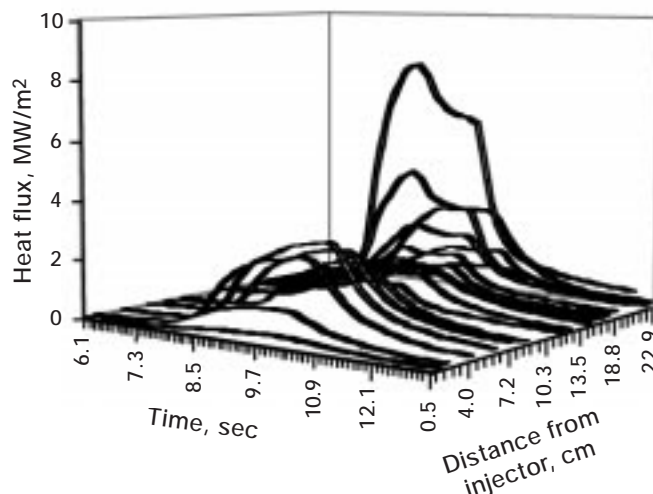
**Programs/Projects:** Global Civil Aviation, Revolutionary Technology Leaps, Access to Space, HEDS, MTPE, other programs involving propulsion

# Metallized Gelled Propellants: Heat Transfer of a Rocket Engine Fueled by Oxygen/RP-1/Aluminum Was Measured by a Calorimeter

A set of analyses was conducted to determine the heat transfer characteristics of metallized gelled liquid propellants in a rocket engine. These analyses used data from experiments conducted with a small 30- to 40-lbf thrust engine composed of a modular injector, igniter, chamber, and nozzle (refs. 1 and 2). The fuels used were traditional liquid RP-1 and gelled RP-1 with 0-, 5-, and 55-wt % loadings of aluminum (Al) with gaseous oxygen as the oxidizer. Heat transfer measurements were made with a calorimeter chamber and nozzle setup that had a total of 31 cooling channels (refs. 1 and 2).

A gelled fuel coating, composed of unburned gelled fuel and partially combusted RP-1, formed in the 0-, 5- and 55-wt % engines. For the 0- and 5-wt % RP-1/Al, the coating caused a large decrease in calorimeter engine heat flux in the last half of the chamber. This heat flux reduction was analyzed by comparing engine firings and the changes in the heat flux during a firing at NASA Lewis Research Center's Rocket Laboratories. This work is part of an ongoing series of analyses of metallized gelled propellants.

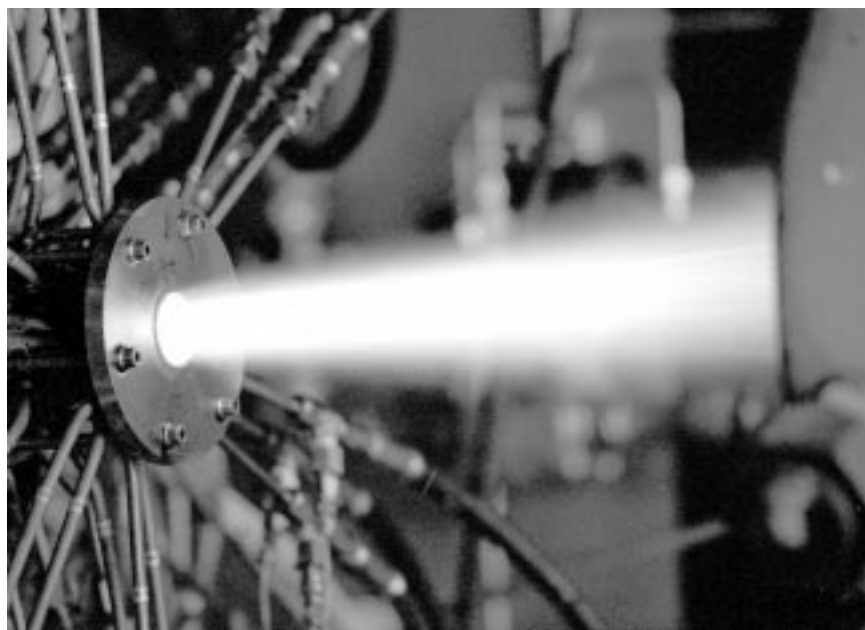
A three-dimensional roller-coaster plot for the 5-wt % RP-1/Al is provided in the preceding graph. This plot shows the engine heat flux as it varies with time and location along the axis of the engine. There are three distinct sections to the plot: the first half of the chamber (0 to 7.6 cm), the second half (7.6 to 15.2 cm), and the nozzle (15.2 cm to the end). The initial heat



*Three-dimensional roller-coaster plot of metallized gelled propellant heat flux: 5-wt % RP-1/Al.*

flux peak was created by the igniter firing; the lower steady-state value (or flat part of the curve) represents the main propellant combustion. The peak nozzle flux reached a value of 6.5 MW/m<sup>2</sup>. In the first half of the chamber, the flux reached a peak value, but not a steady-state value; and in the second half, the heat flux quickly reached a steady-state value that was significantly lower than the peak value in the first half of the chamber. This heat flux difference was caused by the formation of a gelled layer.

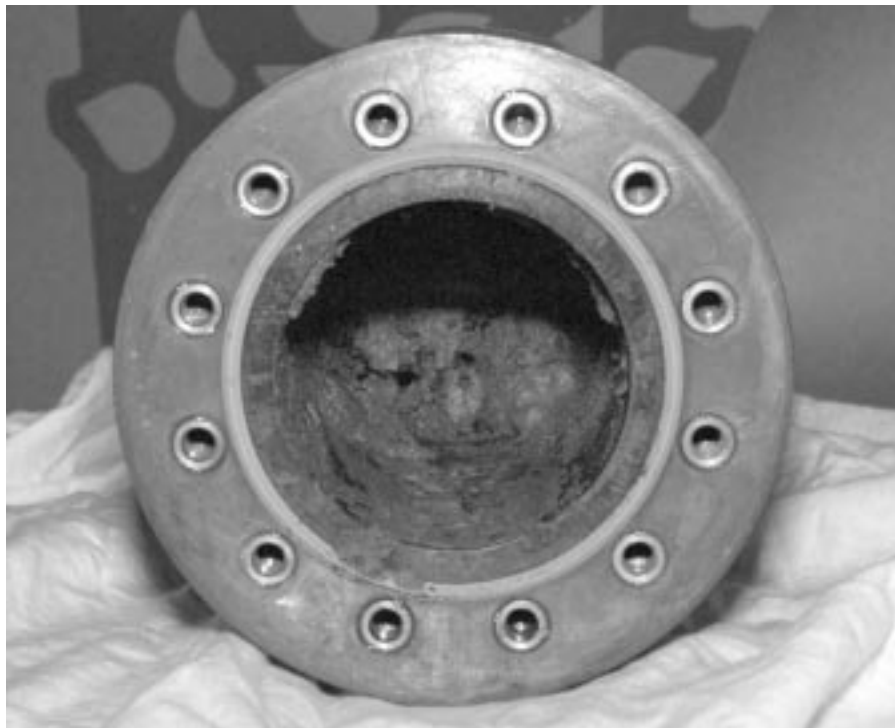
The gelled layer formed in several steps. As the gelled fuel was injected into the chamber, the O<sub>2</sub> gas streams impinging on the gelled fuel stream caused a ligand structure to form (ref. 3). Some of the propellant, rather than undergoing combustion, deposited on the chamber walls. An intense combustion environment was present in the chamber, but the gelled fuel was not completely atomized and,



*5-wt % RP-1/Al rocket engine firing.*



therefore, not consumed. Additional shear stress, which could be delivered by improved injector designs, would be needed to completely atomize the propellants. After the gel deposited on the walls, some of this propellant vaporized and contributed further to the combustion process, but some of it remained on the walls.



*Gelled propellant layer formed in the chamber after many firings.*

**Find out more; visit the Fuels and Space Propellants Web site of Lewis' Small Business Innovation Research:**  
<http://www.lerc.nasa.gov/WWW/TU/launch/foctopsb.htm>

#### References

1. Palaszewski, B.: Metallized Gelled Propellants: Oxygen/RP-1/Aluminum Rocket Engine Calorimeter Heat Transfer Measurements and Analysis. AIAA Paper 97-2974 (NASA TM-107495), 1997.
2. Palaszewski, B.; and Zakany, J.S.: Metallized Gelled Propellants: Oxygen/RP-1/Aluminum Rocket Heat Transfer and Combustion Experiments. AIAA Paper 96-2622 (NASA TM-107309), 1996.
3. Green, J.; Rapp, D.; and Roncace, J.: Flow Visualization of a Rocket Injector Spray Using Gelled Propellant Simulants. AIAA Paper 91-2198, 1991.

#### Lewis contact:

Bryan A. Palaszewski, (216) 977-7493,  
[Bryan.A.Palaszewski@lerc.nasa.gov](mailto:Bryan.A.Palaszewski@lerc.nasa.gov)

**Author:** Bryan A. Palaszewski

**Headquarters program office:** OASTT

**Programs/Projects:** Advanced Space Transportation, HEDS, Access to Space



# F100 Engine Emissions Tested in NASA Lewis' Propulsion Systems Laboratory



*F100 engine test at NASA Lewis' Propulsion Systems Laboratory altitude chamber.*

Recent advances in atmospheric sciences have shown that the chemical composition of the entire atmosphere of the planet (gases and airborne particles) has been changed due to human activity and that these changes have changed the heat balance of the planet. National Research Council findings indicate that anthropogenic aerosols<sup>1</sup> reduce the amount of solar radiation reaching the Earth's surface. Atmospheric global models suggest that sulfate aerosols change the energy balance of the Northern Hemisphere as much as anthropogenic greenhouse gases have. In response to these findings, NASA initiated the Atmospheric Effects of Aviation Project (AEAP) to advance the research needed to define present and future aircraft emissions and their effects on the Earth's atmosphere.

Although the importance of aerosols and their precursors is now well recognized, the characterization of current subsonic engines for these emissions is far from complete. Furthermore, since the relationship of engine operating parameters to aerosol emissions is not known, extrapolation to untested and unbuilt engines necessarily remains highly uncertain. Tests in 1997—an engine test at the NASA Lewis Research Center and the corresponding flight measurement test at the NASA Langley Research Center—attempted to address both issues by measuring emissions when fuels containing different levels of sulfur were burned. Measurement systems from four research groups were involved in the Lewis engine test: (1) a Lewis gas analyzer suite to measure the concentration of gaseous species

including NO, NO<sub>x</sub>, CO, CO<sub>2</sub>, O<sub>2</sub>, THC, and SO<sub>2</sub> as well as the smoke number; (2) a University of Missouri-Rolla Mobile Aerosol Sampling System to measure aerosol and particulate properties including the total concentration, size distribution, volatility, and hydration property; (3) an Air Force Research Laboratory Chemical Ionization Mass Spectrometer to measure the concentration of SO<sub>2</sub> and SO<sub>3</sub>/H<sub>2</sub>SO<sub>4</sub>; and (4) an Aerodyne Research Inc. Tunable Diode Laser System to measure the concentrations of SO<sub>2</sub>, SO<sub>3</sub>, NO, NO<sub>2</sub>, CO<sub>2</sub>, and H<sub>2</sub>O.

By September 1997, an F100 engine operating at several power levels at sea level and up to six simulated altitudes had been tested with commercial jet fuels with three levels of sulfur content and one military jet fuel. The data are being vigorously analyzed. A complete report is anticipated for the 1998 Atmospheric Effects of Aviation Project Annual Conference.

**Lewis contact:**

Dr. Chowen C. Wey, (216) 433-8357,  
Chowen.C.Wey@lerc.nasa.gov

**Author:** Dr. Chowen C. Wey

**Headquarters program office:** OASTT

**Programs/Projects:** AEAP, HSR, AST

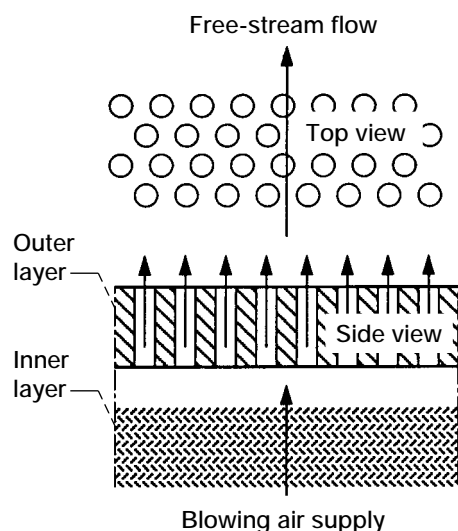
---

<sup>1</sup>An aerosol is a suspension of solid or liquid particles in a gas. An anthropogenic aerosol is one created by humans that influences nature.

# Microblowing Technique Demonstrated to Reduce Skin Friction

One of the most challenging areas of research in aerodynamics is the reduction of skin friction, especially for turbulent flow. Reduced skin friction means less drag. For aircraft, less drag can lead to less fuel burned or to a greater flight range for a fixed amount of fuel. Many techniques and methods have been tried; however, none of them has significantly reduced skin friction in the flight environment.

An innovative skin-friction reduction technique, the Microblowing Technique (MBT), was invented in 1993. This is a unique concept in which an extremely small amount of air is blown vertically at a surface through very small holes. It can be used for aircraft or marine vehicles, such as submarines (where water is blown through the holes instead of air). As shown in the figure, the outer layer, which controls vertical flow, is a plate with high-porosity (high open area), laser-drilled vertical holes. The inner layer, which produces evenly distributed flow, is a low-permeability porous plate. Microblowing reduces the surface roughness and changes the flow velocity profile on the surface, thereby reducing skin friction.



*Microblowing Technique skin.*

In 1995, a Phase-I proof-of-concept experiment was conducted in NASA Lewis Research Center's Advanced Nozzle and Engine Components Test Facility. Of seven porous plates tested, three were identified as MBT skins. An MBT skin is one that has an unblown skin friction (i.e., the skin friction of a porous plate without blowing) not more than 20 percent above the skin friction of a solid flat plate. For these MBT skins, microblowing flow rates less than 0.5 percent of the free-stream flow rate reduced the skin friction below that of a solid flat plate by up to 60 percent.

In 1996, a Phase-II experiment to evaluate the increased pressure drag penalty associated with this technique was conducted in the same facility. The results showed the increase in pressure drag caused by MBT skins, especially for high Reynolds number flow (i.e., conditions such as those in which commercial airplanes fly). Considering these results, we predicted that a skin friction reduction of up to 30 percent below that of a solid flat plate is possible under certain conditions.

In September 1997, a joint program of NASA Lewis, United Technologies Research Center, Northrop Grumman Corporation, and Pratt & Whitney was completed. A 30-in. engine nacelle with an MBT skin was tested in the United Technologies' wind tunnel. Results of the experiment indicate that

skin friction reductions of 50 to 70 percent are possible over portions of the nacelle, with the addition of only small amounts of blowing air. Tests applying MBT to supersonic flow (i.e., flow conditions greater than the speed of sound) and the search for an optimal MBT skin are continuing.

## Bibliography

Hwang, D.P.: A Proof of Concept Experiment for Reducing Skin Friction by Using a Micro-Blowing Technique. AIAA Paper 97-0546 (NASA TM-107315), 1997. Available online: <http://letrs.lerc.nasa.gov/cgi-bin/browse.pl?1997/TM-107315.html>

Hwang, D.P.; and Biesiadny, T.J.: Experimental Evaluation of Penalty Associated With Micro-Blowing for Reducing Skin Friction. AIAA Paper 98-0677, 1998.

Tillman, T.G.: Drag Reduction on a Large-Scale Nacelle Using Micro-Porous Blowing. UTRC Report R97-4.910.0001, 1997.

## Lewis contact:

Dr. Danny P. Hwang, (216) 433-2187, [Danny.P.Hwang@lerc.nasa.gov](mailto:Danny.P.Hwang@lerc.nasa.gov)

**Authors:** Dr. Danny P. Hwang and Tom J. Biesiadny

**Headquarters program office:** OASTT

**Programs/Projects:**

Propulsion Systems R&T, FQE

**Special recognition:** Superior Accomplishment Award, Space Act Award, and Space Act Board Award (NASA Inventions and Contributions Board)

# Effect of Installation of Mixer/Ejector Nozzles on the Core Flow Exhaust of High-Bypass-Ratio Turbofan Engines

The aerospace industry is currently investigating the effect of installing mixer/ejector nozzles on the core flow exhaust of high-bypass-ratio turbofan engines. This effort includes both full-scale engine tests at sea level conditions and subscale tests in static test facilities. Subscale model tests are to be conducted prior to full-scale testing. With this approach, model results can be analyzed and compared with analytical predications. Problem areas can then be identified and design changes made and verified in subscale prior to committing to any final design configurations for engine ground tests.

One of the subscale model test programs for the integrated mixer/ejector development was a joint test conducted by the NASA Lewis Research Center and Pratt & Whitney Aircraft. This test was conducted to study various mixer/ejector nozzle configurations installed on the core flow exhaust of advanced, high-bypass-ratio turbofan engines for subsonic, commercial applications. The mixer/ejector concept involves the introduction of large-scale, low-loss, streamwise vortices that entrain large amounts of secondary air and rapidly mix it with the primary stream. This results in increased ejector pumping relative to conventional ejectors and in more complete mixing within the ejector shroud. The latter improves thrust performance through the efficient energy exchange between the primary and secondary streams.

This experimental program was completed in April 1997 in Lewis' CE-22 static test facility. Variables tested included the nozzle area ratio ( $A_9/A_8$ ), which ranged from 1.6 to 3.0. This ratio was varied by increasing or decreasing the nozzle throat area,  $A_8$ . Primary nozzles tested included both lobed mixers and conical primaries. These configurations were tested with and without an outer shroud, and the shroud position was varied by inserting spacers in it. In addition, data were acquired with and without secondary flow.

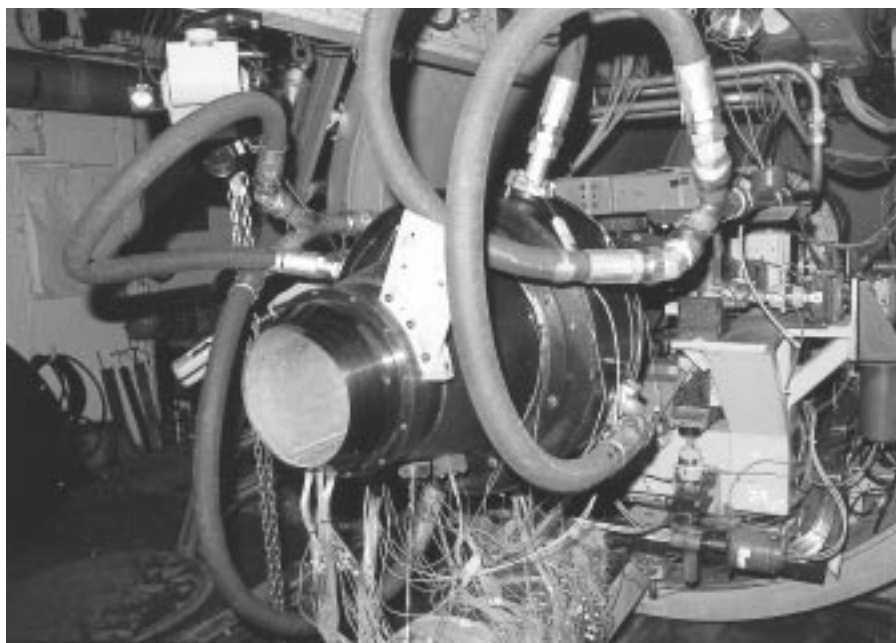
**Lewis contact:**

Douglas E. Harrington,  
(216) 433-3591,  
Douglas.E.Harrington@lerc.nasa.gov

**Author:** Douglas E. Harrington

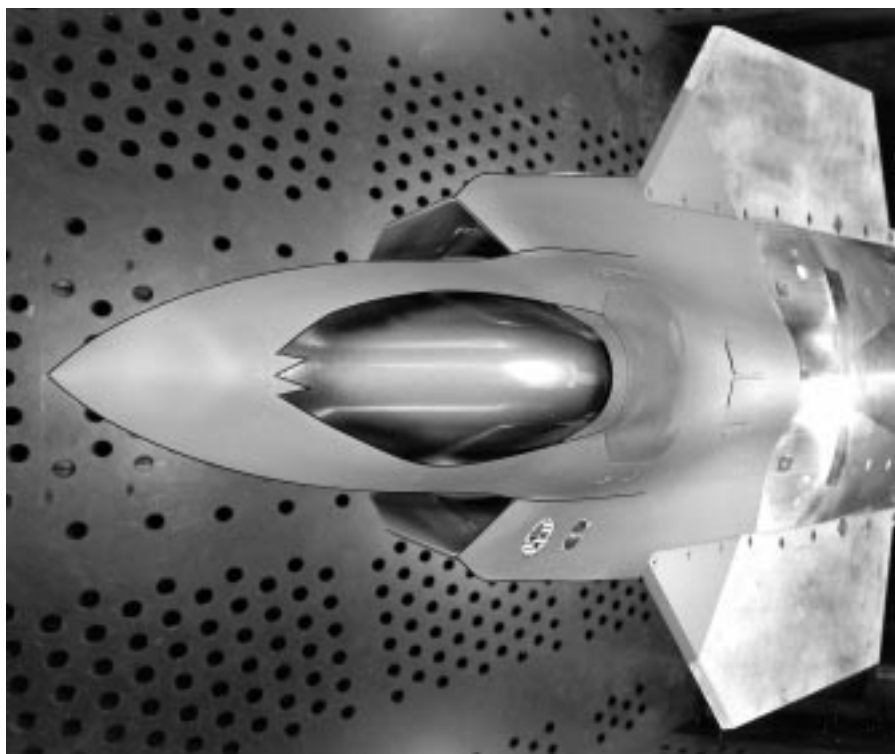
**Headquarters program office:** OASTT

**Programs/Projects:** HSCT, HSR



*Typical test model installed in Lewis' CE-22 facility.*

## Forebody/Inlet of the Joint Strike Fighter Tested at Low Speeds



*Joint Strike Fighter model installed in Lewis' 8- by 6-Foot Supersonic Wind Tunnel.*

As part of a national cooperative effort to develop a multinational fighter aircraft (ref. 1), a model of a Joint Strike Fighter concept was tested in several NASA Lewis Research Center wind tunnels at low speeds over a range of headwind velocities and model attitudes. This Joint Strike Fighter concept, which is scheduled to go into production in 2005, will greatly improve the range, capability, maneuverability, and survivability of fighter aircraft, and (as indicated in ref. 2) the production program could ultimately be worth \$100 billion.

The photo shows the forebody/inlet model installed in Lewis' 8- by 6-Foot Supersonic Wind Tunnel. The model was tested at low speeds ( $0 \leq M_0 \leq 0.45$ ) in Lewis' 8- by 6-Foot wind tunnel and in Lewis' 9- by 15-Foot Low-Speed Wind Tunnel.

The test program was a team effort between Lewis and Lockheed Martin Tactical Aircraft Systems. Testing was completed in September 1997, several weeks ahead of schedule, allowing Lockheed additional time to review the results and analysis data before the next test and resulting in significant cost savings for Lockheed.

Several major milestones related to dynamic and steady-state data acquisition and overall model performance were reached during this model test. Results from this program will contribute to both the concept demonstration phase and the production aircraft, and will greatly increase and improve both NASA's and Lockheed's technical databases. The program is ongoing and will continue to define the performance and operating characteristics of the concept. Recent modifications to the dynamic data acquisition system led to a substantial reduction in Lockheed's personnel support requirement at Lewis, which translated into a substantial cost savings for Lockheed. The program also has had a visible positive effect on NASA Lewis.

### References

1. Australia to Join JSF Program Soon. *Aviat. Week Space Technol.*, vol. 147, no. 8, Aug. 25, 1997, p. 52.
2. Morrocco, J.D. : BAE Joins Lockheed Martin in Joint Strike Fighter Bid. *Aviat. Week Space Technol.*, vol. 146, no. 26, 1997, pp. 22–23.

### Lewis contact:

Albert L. Johns, (216) 433–3972,  
Albert.L.Johns@lerc.nasa.gov

**Author:** Albert L. Johns

**Headquarters program office:** OASTT

**Programs/Projects:** JSF



## Lift Fan Nozzle for Joint Strike Fighter Tested in NASA Lewis' Powered Lift Rig

Under a nonreimbursable space act agreement between the NASA Lewis Research Center and the Allison Advanced Development Company, Allison tested a lift fan nozzle in Lewis' Powered Lift Rig. This test was in support of the Joint Strike Fighter program (formerly the Joint Advanced Strike Technology) sponsored by the Department of Defense, which will develop and field an affordable, multirole, next-generation, strike fighter aircraft for the Navy, Air Force, Marine Corps, and foreign allies. Allison, along with Pratt & Whitney Company, is part of the Lockheed Martin Corporation team that is scheduled to build a concept demonstrator aircraft by fiscal year 2001.

The test was initiated in April and successfully completed in mid-July of 1997. Allison supplied a one-third-scale model of the lift fan nozzle, and Lewis provided the facility and the necessary support team. Various configurations, including pitching vectored angles ranging from 15° forward to 60° backward, were tested over a range of nozzle pressure ratios. Nozzle flow rates, thrust, and static pressures were measured for each of the configurations.

Results from the test met the design requirements for the Joint Strike Fighter program and were in agreement with Allison's internal computational fluid dynamics (CFD) analyses. Data obtained from this test will also be used in the full-scale design of the lift fan system.

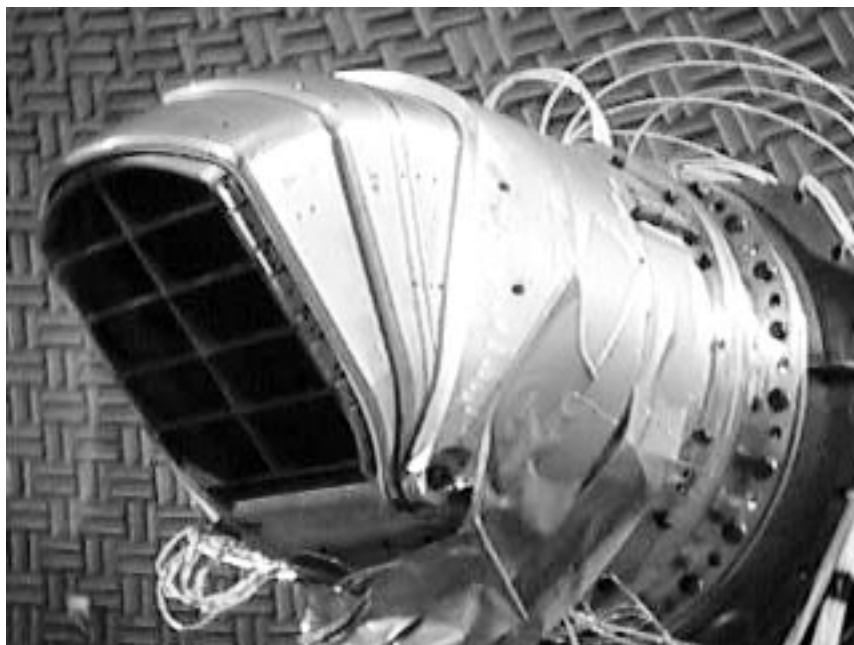
**Lewis contact:**

David W. Lam, (216) 433-8875,  
David.W.Lam@lerc.nasa.gov

**Author:** David W. Lam

**Headquarters program office:** OASTT

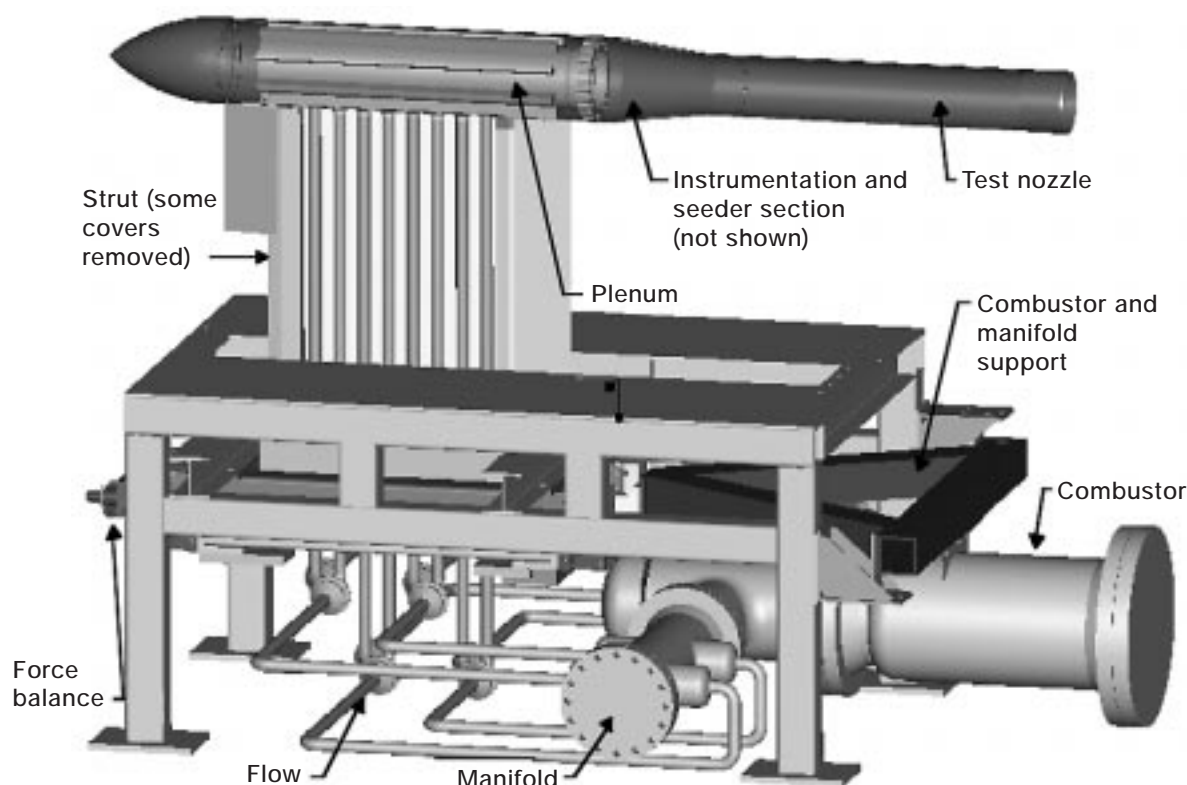
**Programs/Projects:** JSF



*Model installed at Lewis' Powered Lift Rig inside the Aero-Acoustic Propulsion Laboratory.*



## New Nozzle Test Rig Developed



*High-Flow Jet Exit Rig.*

Renewed interest in reducing aircraft noise has spurred the development of a new testing facility. One of the major sources of jet aircraft noise is the engine nozzle exhaust, so wind tunnel and freejet testing have been used to evaluate nozzle concepts for thrust and noise reduction. In the past, the NASA Lewis Research Center used its Jet Exit Rig to supply hot, high-pressure air to the nozzle to simulate engine exhaust, but the flow capacity of this rig was not large enough to supply larger nozzles, which are needed for more accurate noise assessment. Therefore, Lewis developed a new testing tool for this effort, the High-Flow Jet Exit Rig.

The High-Flow Jet Exit Rig is a single-stream, strut-mounted sting that can accommodate up to 33 lb/sec of ambient temperature air at nozzle pressure ratios up to 4.5, or accommodate up to 20 lb/sec of heated air at up to 2000 °R at nozzle pressure ratios up to 4.5. This range of flow is suitable for nozzles with throat areas up to 22 in.<sup>2</sup> Air is heated by a combustor unit based on a J-58 combustor, and forces are measured with a single-component, loadcell-based force balance. The rig can be mounted in either the Nozzle Aeroacoustic Test Rig (NATR) freejet or the 8- by 6-Foot Supersonic Wind Tunnel at Lewis.

Lewis' Engineering Design and Analysis Division designed the rig in-house, and fabrication was done at West Tool and Die, Inc. Checkout testing was performed in Lewis' Propulsion System Laboratory, including static-force balance calibration and cold- and hot-flow testing with a standard nozzle.

### Find out more on the World Wide Web:

#### NATR freejet:

<http://www.lerc.nasa.gov/WWW/AFED/facilities/aapl.html>

#### 8- by 6-Foot Supersonic Wind Tunnel:

<http://www.lerc.nasa.gov/WWW/AFED/facilities/8x6.html>

#### Propulsion System Laboratory:

<http://www.lerc.nasa.gov/WWW/AFED/facilities/psl.html>

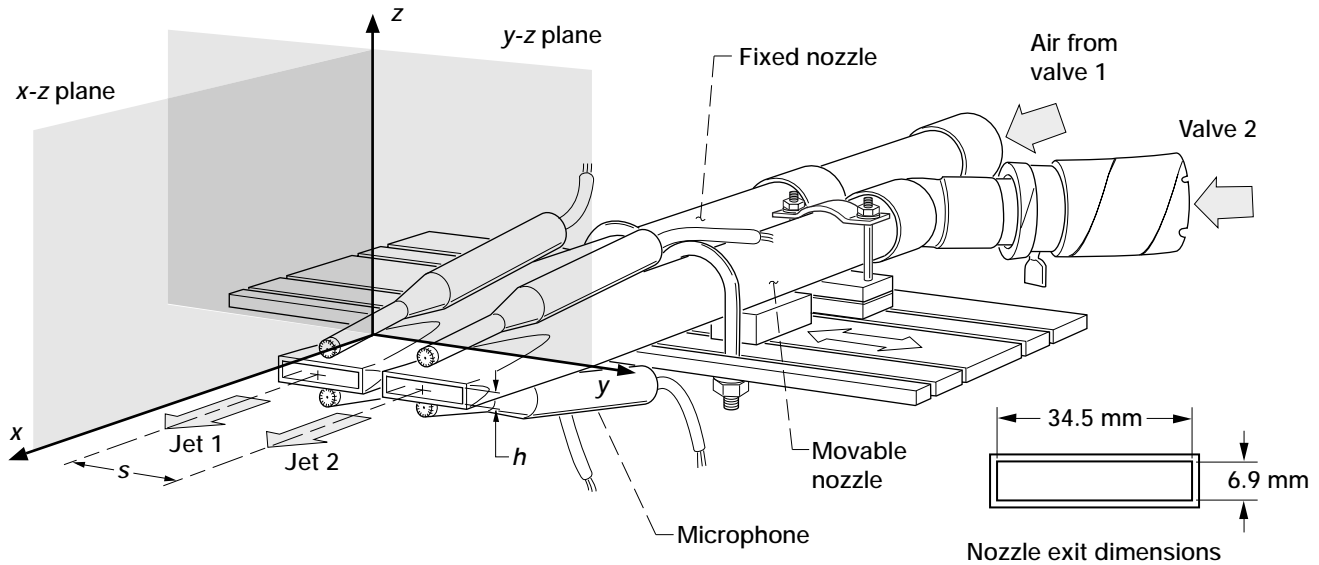
#### Lewis contact:

John D. Wolter, (216) 433-3941,  
John.D.Wolter@lerc.nasa.gov

**Authors:** John D. Wolter and  
Raymond S. Castner

**Headquarters program office:** OASTT  
**Programs/Projects:** HSR

# Resonance of Twin Jet Plumes Studied



*Twin supersonic rectangular nozzle setup.*

Twin jet plumes on aircraft can couple, producing higher dynamic pressures in the internozzle region, which in turn can cause sonic fatigue of the external nozzle flaps. Thus, there is significant value in performing laboratory studies on twin supersonic jets that couple and screech at a discrete frequency. The coupling of rectangular jets is of particular interest because of the use of these jets in military aircraft, especially in situations requiring vectored thrust, stealth, or tailless flight. Considerable work was done in the late 1980's on twin jets at the NASA Langley Research Center and by the U.S. Air Force to alleviate problems with the B1-B and F15-E aircraft. However, the mechanism of twin jet coupling has remained far from being clearly understood.

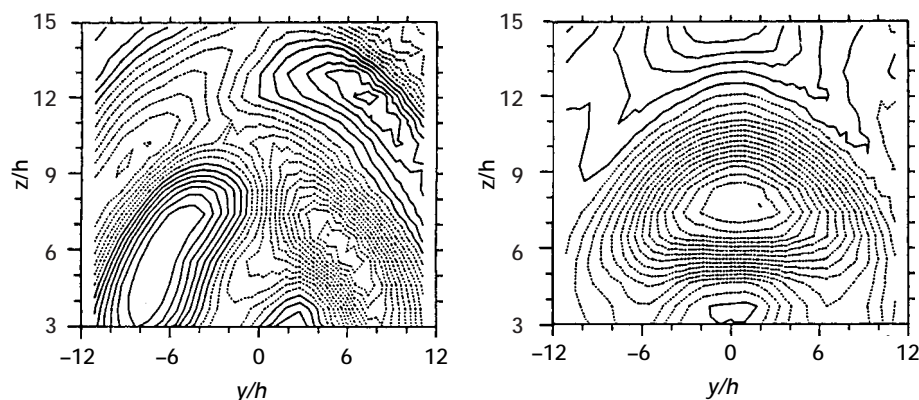
Research being conducted by NASA Lewis Research Center's Nozzle Branch is focusing on fundamental mechanisms by assessing the steady and unsteady aspects of twin jet coupling. As shown in the preceding sketch, two rectangular nozzles are placed side by side, with their narrow dimensions parallel and their long dimensions in the same plane. A positioning apparatus keeps one of the nozzles fixed and moves the second one to achieve various internozzle spacings. Microphones mounted on the nozzles monitor the characteristics of the acoustic field, and a movable microphone measures the acoustic phase and amplitude distribution on the  $x$ - $z$  and  $y$ - $z$  planes. The sound pressure amplitude distributions on the  $y$ - $z$  plane are shown in the following figure for two slightly different jet Mach numbers. The slight difference in operating condition caused completely different modes of jet coupling—antisymmetric and symmetric pressure waves.

While documenting the parametric range of nozzle spacing and Mach numbers over which the jets couple, we have been addressing the following questions:

- (1) What causes the jets to couple in one mode or the other, or not at all?

- (2) Why do the jets switch from one mode to another?
- (3) Are the two modes mutually exclusive, or do they overlap at the transition point?

So far, our results have revealed the following. The coupling occurs through the near acoustic field surrounding the jets. Particularly important is the "null" phase region surrounding the jets, where the phase of an acoustic wavefront (arriving from downstream) does not vary over a small radial distance. When the null regions of the two jets overlap, symmetric coupling occurs; when they do not overlap, the jets couple antisymmetrically. We use a parameter  $\alpha$  as a simple test to determine the mode of coupling. Apparently, coupling switches from the antisymmetric to the symmetric mode because of an abrupt shift in the effective screech source from the third to the fourth shock, which in turn causes the null phase region surrounding the jets to grow abruptly and overlap. These results are summarized in reference 1.



Phase-averaged sound pressure level contours. Left: Antisymmetric jet coupling. Right: Symmetric jet coupling.

## Reference

1. Raman, G.; and Taghavi, R.: Coupling of Twin Rectangular Supersonic Jets. AIAA Paper 97-1624, 1997.

## Lewis contact:

Dr. Khairul Zaman, (216) 433-5888, Khairul.B.Zaman@lerc.nasa.gov

**Authors:** Dr. Ganesh Raman and Dr. Ray Taghavi

**Headquarters program office:** OASTT

**Programs/Projects:**

Propulsion Systems R&T, FQE, ASCOT

# Design Concepts Studied for the Hydrogen On-Orbit Storage and Supply Experiment

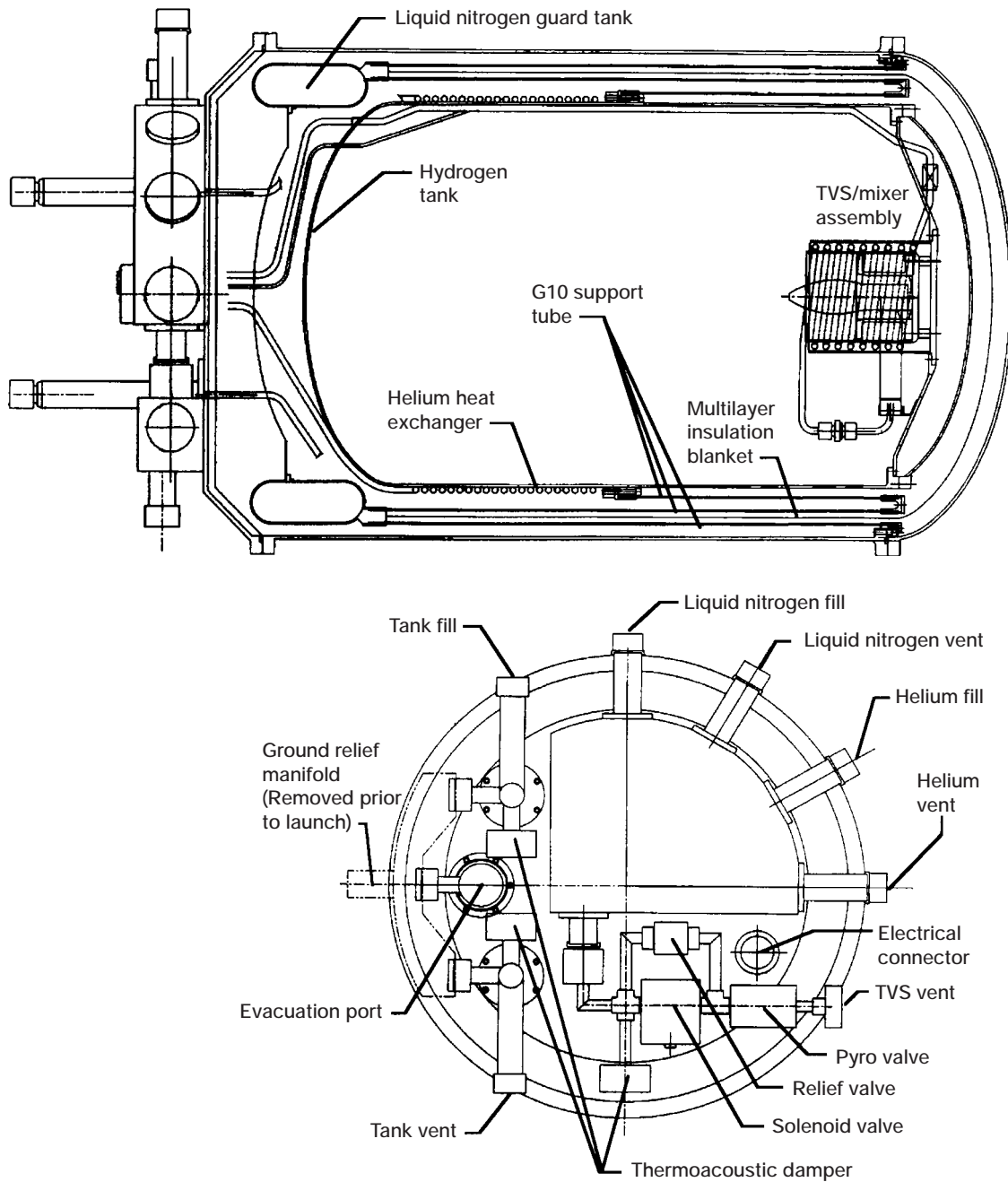
The NASA Lewis Research Center, in conjunction with the Utah State University Space Dynamics Laboratory, studied concepts for the Hydrogen On-Orbit Storage and Supply Experiment (HOSS). HOSS is a space flight experiment whose objectives are (1) to show stable gas supply for solar-thermal thruster designs by using both storage and direct-gain approaches and (2) to evaluate and compare the low-gravity performance of active and passive pressure control via a thermodynamic vent system (TVS) suitable for solar-thermal upper stages. This study showed that the necessary experimental equipment for HOSS can be accommodated in a small hydrogen Dewar (36 to 80 liter). Thermal designs can be achieved that meet the on-orbit storage requirements for these Dewars. Furthermore, ground hold insulation concepts are easily achieved that can store liquid hydrogen in these small Dewars for more than 144 hr without venting.

The drawing shows an 80-liter Dewar design that holds 5.6 kg of hydrogen. The valve panel layout was detailed using off-the-shelf valves like those used on previous flight programs. The dry weight of this Dewar layout, including valves and plumbing, is estimated at 91.6 kg. The vacuum space is filled with 80 layers of multilayer insulation. Three nested G10 fiberglass<sup>1</sup> tubes greatly increase the length of the tank support, thereby reducing conduction heat transfer. A toroidal liquid nitrogen tank is attached to one end of the tubes. This tank will be filled on the ground to intercept heat and allow the tank to remain filled with hydrogen for long periods of time without venting. A coil of tubing attached to the inner tank allows the liquid hydrogen to be subcooled by liquid helium flowing through these coils. This again extends the ground hold capabilities of the tank and provides a means of quickly reducing tank pressure without venting.

After the 80-liter design was completed, a 36-liter design was made that incorporated the design features of the 80-liter design. The 36-liter Dewar will hold 2.52 kg of hydrogen and weigh 58.6 kg, only 35-percent less than the 80-liter Dewar. One reason that the weights are close is that the valving is identical but the smaller space on the 36-liter Dewar necessitates the use of a stepped lid to achieve the required mounting space. Valve sizes were dictated by commercially available sizes since such valves are difficult to customize.

Now that the HOSS Dewar has been designed, other areas can be detailed. Design studies underway include the selection of suitable low-cost launch vehicles and integration of the Dewar design into a satellite bus. These efforts are bringing the flight of the HOSS experiment inexorably closer.

<sup>1</sup>Fiberglass prepared according to the G10 military standard.



*HOSS experiment Dewar layout. Top: Side view. Bottom: Top view.*

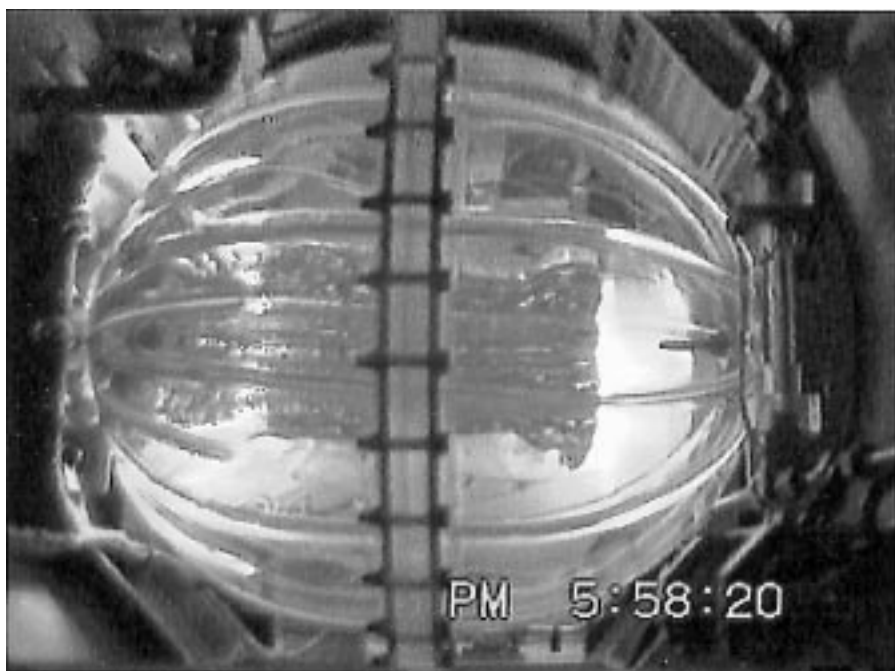
**Lewis contact:** David J. Chato, (216) 977-7488, David.J.Chato@lerc.nasa.gov

**Author:** David J. Chato

**Headquarters program office:** OASTT

**Programs/Projects:** HOSS, Mars exploration, RLV

## Vented Tank Resupply Experiment Demonstrated Vane Propellant Management Device for Fluid Transfer



*Vented Tank Resupply Experiment test tank during fill; vanes turn back liquid inflow.*

Find out more about this research on the World Wide Web:

<http://zeta.lerc.nasa.gov/expr2/vtre.htm>

**Lewis contact:** David J. Chato,  
(216) 977-7488,  
[David.J.Chato@lerc.nasa.gov](mailto:David.J.Chato@lerc.nasa.gov)

**Author:** David J. Chato

**Headquarters program office:** OASTT

**Programs/Projects:** VTRE, HEDS, RLV,  
unmanned planetary exploration

**Special recognition:** Lewis Team  
Achievement Award (given to Vented  
Tank Resupply Experiment Project  
Team); Astronaut Corps' Silver Snoopy  
Award (given to Principal Investigator  
David Chato)

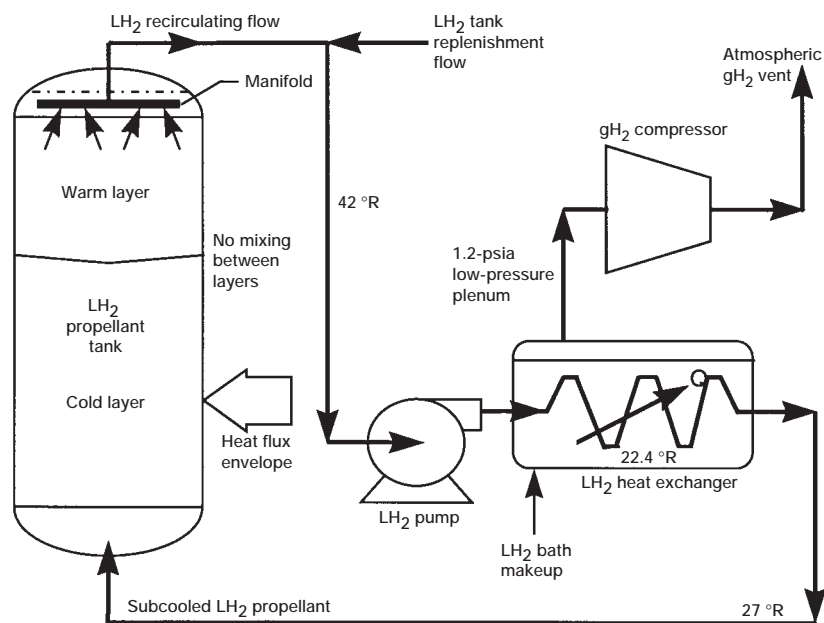
The Vented Tank Resupply Experiment (VTRE) flown on STS-77 confirmed the design approaches presently used in the development of vane-type propellant management devices (PMD) for use in resupply and tank-venting situations, and it provided the first practical demonstration of an autonomous fluid transfer system. All the objectives were achieved. Transfers were more stable than drop tower testing indicated. Liquid was retained successfully at the highest flow rate tested (2.73 gal/min), demonstrating that rapid fills could be achieved. Liquid-free vents were achieved for two different tanks, although the flow rate was higher for the spherical tank (0.1591 ft<sup>3</sup>/min) than for the tank with a short barrel section (0.0400 ft<sup>3</sup>/min). Recovery from a thruster firing, which moved the liquid to the opposite end of the tank from the PMD, was achieved in 30 sec, showing that liquid rewicked more quickly into the PMD after thruster firing than pretest projections had predicted. In addition, researchers obtained great insights into the PMD behavior from the video footage provided, and discovered new considerations for future PMD designs that would not have been seen without this flight test.



# Recent Advancements in Propellant Densification

Next-generation launch vehicles demand several technological improvements to achieve lower cost and more reliable access to space. One technology area whose performance gains may far exceed others is densified propellants. The ideal rocket engine propellant is characterized by high specific impulse, high density, and low vapor pressure. A propellant combination of liquid hydrogen and liquid oxygen (LH<sub>2</sub>/LOX) is one of the highest performance propellants, but LH<sub>2</sub> stored at standard conditions has a relatively low density and high vapor pressure. Propellant densification can significantly improve this propellant's properties relative to vehicle design and engine performance. Vehicle performance calculations based on an average of existing launch vehicles indicate that densified propellants may allow an increase in payload mass of up to 5 percent.

Since the NASA Lewis Research Center became involved with the National Aerospace Plane program in the 1980's, it has been leading the way in making densified propellants a viable fuel for next-generation launch vehicles. Lewis researchers have been working to provide a method and critical data for continuous production of densified hydrogen and oxygen.



*Integrated reusable launch vehicle propellant tank and liquid hydrogen propellant densification unit based on thermodynamic vent principle.*

The LH<sub>2</sub> production process is shown in the simplified schematic. This process uses a high-efficiency, subatmospheric boiling bath heat exchanger to cool the working fluid. A near triple-point hydrogen boiling bath is used to condition hydrogen, and a nitrogen boiling bath is used for oxygen. In December 1996, Lewis engineers demonstrated successful operation of an LH<sub>2</sub> propellant densification unit that can subcool LH<sub>2</sub> to near triple-point conditions with this continuous process.

In October 1996, Lewis engineers demonstrated the successful ignition of an existing RL10B-2 rocket engine with densified hydrogen. The fuel pump

inlet temperature for the densified hydrogen ignition demonstration test was 27 °R in comparison to 39 °R for the nominal test. The only difference in the ignition sequence between the tests was the time of ignitor activation. For the densified ignition demonstration, the ignitor was activated earlier (T+0.082 sec in comparison to T+0.27 sec for the nominal test). This was done to account for the slight increase in oxygen-to-hydrogen ratio resulting from hydrogen densification. Ignition for the nominal test occurred at 281 msec, whereas ignition for the densified test occurred at 244 msec.

This work has provided the critical steps to bring densified propellants to a technology readiness level of six. As a result, densified propellants will be flown as a flight experiment on the last two flights of the X-33 and are baselined as the fuel for next-generation reusable launch vehicles.

## Bibliography

McNelis, N.B.; and Habersbusch, M.S.: Hot Fire Ignition Test With Densified Liquid Hydrogen Using a RL10B-2 Cryogenic H<sub>2</sub>/O<sub>2</sub> Rocket Engine. AIAA Paper 97-2688 (NASA TM-107470), 1997. Available online: <http://letrs.lerc.nasa.gov/cgi-bin/LeTRS/browse.pl?1997/TM-107470.html>

Tomsik, T.M.: Performance of a Liquid Hydrogen Propellant Densification Ground System for the X33/RLV. AIAA Paper 97-2976 (NASA TM-107469), 1997.

## Lewis contacts:

Nancy B. McNelis, (216) 977-7474, Nancy.B.McNelis@lerc.nasa.gov, and Thomas M. Tomsik, (216) 977-7519, Thomas.M.Tomsik@lerc.nasa.gov

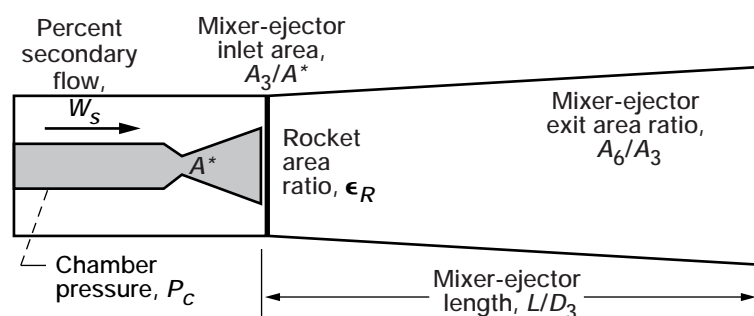
**Authors:** Nancy B. McNelis and Thomas M. Tomsik

**Headquarters program office:** OASTT  
**Programs/Projects:** NASP, RLV, X-33

# Parametric Study Conducted of Rocket-Based, Combined-Cycle Nozzles

Having reached the end of the 20th century, our society is quite familiar with the many benefits of recycling and reusing the products of civilization. The high-technology world of aerospace vehicle design is no exception. Because of the many potential economic benefits of reusable launch vehicles, NASA is aggressively pursuing this technology on several fronts. One of the most promising technologies receiving renewed attention is Rocket-Based, Combined-Cycle (RBCC) propulsion. This propulsion method combines many of the efficiencies of high-performance jet aircraft with the power and high-altitude capability of rocket engines. The goal of the present work at the NASA Lewis Research Center is to further understand the complex fluid physics within RBCC engines that govern system performance. This work is being performed in support of NASA's Advanced Reusable Technologies program.

A robust RBCC engine design optimization demands further investigation of the subsystem performance of the engine's complex propulsion cycles. The RBCC propulsion system under consideration at Lewis is defined by four modes of operation in a single-stage-to-orbit configuration. In the first mode, the engine functions as a rocket-driven ejector. When the rocket engine is switched off, subsonic combustion (mode 2) is present in the ramjet mode. As the vehicle continues to accelerate, supersonic combustion (mode 3) occurs in the ramjet mode. Finally, as the edge of the atmosphere is approached and the engine inlet is closed off, the rocket is reignited and the final ascent to orbit is undertaken in an all-rocket mode (mode 4). The performance of this fourth and final mode is the subject of this present study. Performance is being monitored in terms of the amount of thrust generated from a given amount of propellant.

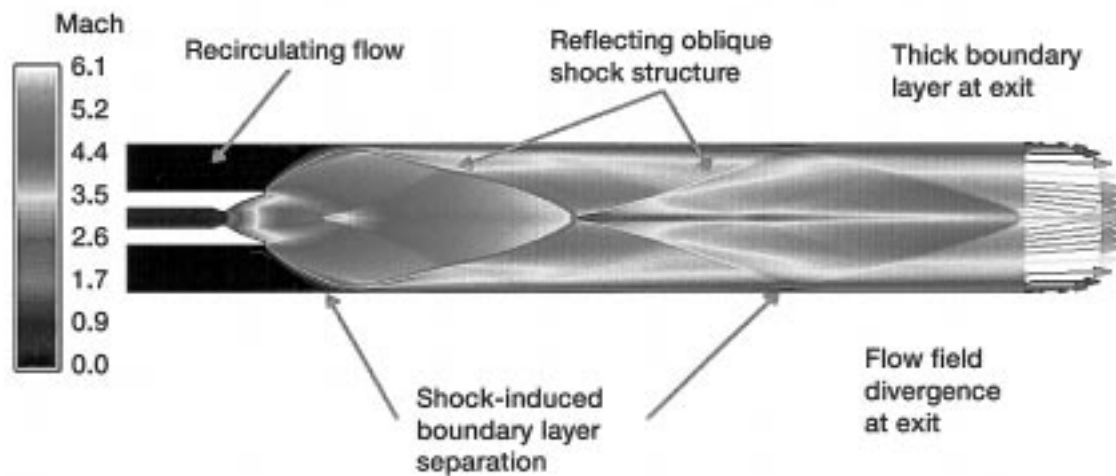


Description of RBCC nozzle geometry.

A statistical approach to experimental design was used to study the performance of the RBCC all-rocket mode. Six independent variables were considered at three values each: low, medium, and high (see the preceding schematic). The full design matrix of 729 cases was efficiently pared down to 36 cases by utilizing a D-optimal response surface design. This approach has enabled us to model the linear, curvilinear, and two-way interaction effects efficiently by running a minimum number of cases distributed throughout the six-dimensional design space. The details of this approach to experiment design are given in references 1 and 2.

The analysis of a given nozzle's performance was based on an involved computer simulation, commonly referred to as computational fluid dynamics (CFD). NPARC v. 3.0 software was used for these simulations to solve the axisymmetric, steady-state Navier-Stokes equations on multiblock meshes with the assumption of a perfect gas equation of state. For turbulent flow, closure was provided via the Spalart-Allmaras or Chien models. Simulations were executed on a variety of NASA computers, including Unix workstations and supercomputers. Specific impulse data were calculated by integrating the streamwise momentum flux and massflow across the exit plane of the RBCC nozzle. These values were then compared with the theoretical maximum that could be achieved by a thermodynamically similar isentropic engine. This comparison was reported as specific impulse efficiency. The results thus far have exhibited efficiencies as low as 78 percent and as high as 95 percent. The complex flow field evident in the following figure reveals some of the loss mechanisms involved in reducing thrust.

The numerical simulations are complete, and the final analysis is underway. The results have revealed that several factors can have a significant effect on the mode-4 performance of RBCC systems. Overall length, mixer/ejector inlet area ratio, exit area ratio, primary rocket exit area ratio, and secondary flow are all capable of affecting the efficiency. More work is necessary to understand these effects for RBCC configurations outside of this particular design. Details of the computational fluid dynamics experiments and flow



*RBCC nozzle flow field showing Mach number contours. Figure is shown in color in the online version of this article (<http://www.lerc.nasa.gov/WWW/RT1997/5000/5880steffen.htm>).*

field analysis are included in reference 1. The details of the experimental design, statistical results, and implications for RBCC system design are discussed in reference 2. The results of this effort will be of use to other related efforts underway within NASA's Advanced Reusable Technologies program.

## References

1. Steffen, C.J., Jr., et al.: Rocket Based Combined-Cycle Nozzle Analysis Using NPARC. AIAA Paper 98-0954, 1998.
2. Smith, T.D., et al.: Analysis of Rocket Based Combined Cycle Engine During Rocket Only Operation. AIAA Paper 98-1612, 1998.

**Lewis contacts:** Christopher J. Steffen, Jr., (216) 433-8508, Christopher.J.Steffen@lerc.nasa.gov; Timothy D. Smith, (216) 977-7546, Timothy.D.Smith@lerc.nasa.gov; and Dr. Shaye Yungster, (216) 433-6120, Shaye.Yungster@lerc.nasa.gov

**Authors:** Christopher J. Steffen, Jr., and Timothy D. Smith

**Headquarters program office:** OASTT

**Programs/Projects:** ART, RLV

# Structures and Acoustics

## Design Process for High Speed Civil Transport Aircraft Improved by Neural Network and Regression Methods

A key challenge in designing the new High Speed Civil Transport (HSCT) aircraft is determining a good match between the airframe and engine. Multidisciplinary design optimization can be used to solve the problem by adjusting parameters of both the engine and the airframe. Earlier (ref. 1), an example problem was presented of an HSCT aircraft with four mixed-flow turbofan engines and a baseline mission to carry 305 passengers 5000 nautical miles at a cruise speed of Mach 2.4. The problem was solved by coupling NASA Lewis Research Center's design optimization testbed (COMETBOARDS) with NASA Langley Research Center's Flight Optimization System (FLOPS). The computing time expended in solving the problem was substantial, and the instability of the FLOPS analyzer at certain design points caused difficulties.

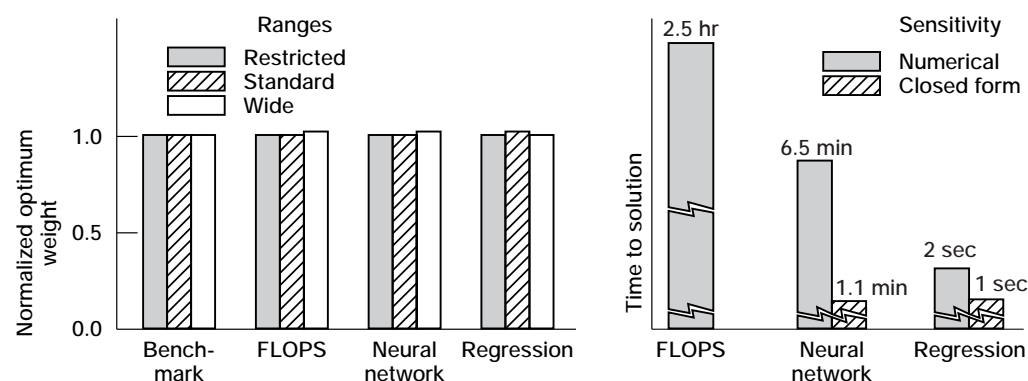
In an attempt to alleviate both of these limitations, we explored the use of two approximation concepts in the design optimization process. The two concepts, which are based on neural network and linear regression approximation (ref. 2), provide the reanalysis capability and design sensitivity analysis information required for the optimization process. The HSCT aircraft optimization problem was solved by using three alternate approaches; that is, the original FLOPS analyzer and two approximate (derived) analyzers. The approximate analyzers were calibrated and used in three different ranges of the design variables; narrow (interpolated), standard, and wide (extrapolated).

Performance of the regression and neural network approximation methods for both the analysis and design of the HSCT aircraft could be considered satisfactory. For example, in the restricted range, 1-percent deviation was observed in the optimum gross takeoff weight of the aircraft. In the standard and wide ranges, the deviation increased to 2 percent. The approximation concepts significantly reduced the computing time expended during the optimization process. For the FLOPS-based optimization process, computing time was measured in hours, whereas for both approximation-

based optimization processes, it was measured in minutes. Furthermore, difficulties associated with the instability of the FLOPS analyzer were eliminated with the approximation methods. However, calibrating the approximate (derived) analyzers required substantial computational time for both neural network and regression methods. For the HSCT aircraft problem, it was preferable to calibrate the approximate analyzers over a wider (standard) range and then use them to optimize over a narrower (restricted) range. Overall, neural network and regression approximation concepts were found to be satisfactory for the analysis and design optimization of the HSCT aircraft problem.

### References

1. Patnaik, S.N., et al.: Cascade Optimization Strategy for Aircraft and AirBreathing Propulsion System Concepts. *J. Aircraft*, vol. 34, no. 1, pp. 136–139, 1997.
2. Patnaik, S.N., et al.: Neural Network and Regression Approximations in High Speed Civil Transport Aircraft Design Optimization. NASA TM–206316, 1998.



Optimum solutions for HSCT aircraft. Left: Normalized optimum weight of aircraft. Right: Central processing unit (CPU) time to solution.

### Lewis contact:

Dale A. Hopkins,  
(216) 433–3260,  
Dale.A.Hopkins@lerc.nasa.gov

### Ohio Aerospace Institute contact:

Dr. Surya N. Patnaik,  
(216) 433–5916,  
Surya.N.Patnaik@lerc.nasa.gov

**Author:** Dale A. Hopkins

**Headquarters program office:** OASTT

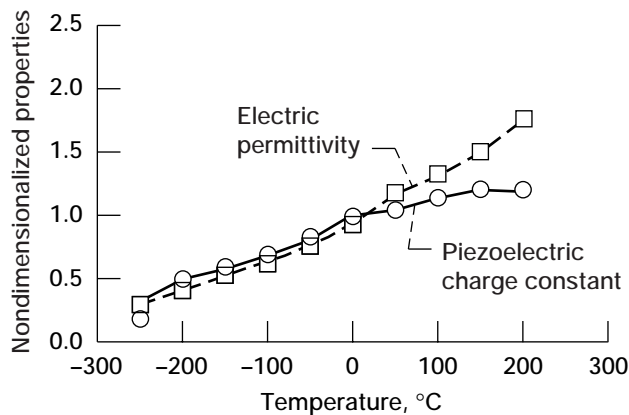
### Programs/Projects:

Propulsion Systems R&T,  
P&PM, HSCT

# Thermal Effects Modeling Developed for Smart Structures

Applying smart materials in aeropropulsion systems may improve the performance of aircraft engines through a variety of vibration, noise, and shape-control applications. To facilitate the experimental characterization of these smart structures, researchers have been focusing on developing analytical models to account for the coupled mechanical, electrical, and thermal response of these materials.

One focus of current research efforts has been directed toward incorporating a comprehensive thermal analysis modeling capability. Typically, temperature affects the behavior of smart materials by three distinct mechanisms: (1) induction of thermal strains because of coefficient of thermal expansion mismatch, (2) pyroelectric effects on the piezoelectric elements, and (3) temperature-dependent changes in material properties. Previous analytical models only investigated the first two thermal effects mechanisms. However, since the material properties of piezoelectric materials generally vary greatly with temperature (see the graph), incorporating temperature-dependent material properties will significantly affect the structural deflections, sensory voltages, and stresses.



*Temperature dependence of piezoelectric material properties.*

Thus, the current analytical model captures thermal effects arising from all three mechanisms through thermopiezoelectric constitutive equations. These constitutive equations were incorporated into a layerwise laminate theory with the inherent capability to model both the active and sensory response of smart structures in thermal environments. Corresponding finite element equations were formulated and implemented for both the beam and plate elements to provide a comprehensive thermal effects modeling capability.

## Bibliography

Lee, H.-J.; and Saravanos, D.A.: The Effect of Temperature Induced Material Property Variations on Piezoelectric Composite Plates. AIAA Paper 97-1355, 1997.

Lee, H.-J.; and Saravanos, D.A.: A Review of Smart Structures Modeling Activities. HITEMP Review 1997. NASA CP-10192, 1997, paper 37, pp. 1-10. (Permission to cite this material was granted by Carol A. Ginty, February 19, 1998.)

Lee, H.-J.; and Saravanos, D.A.: Thermal Shape Control of Active and Sensory Piezoelectric Composite Plates. Analysis and Design Issues for Modern Aerospace Vehicles 1997. ASME AD-Vol. 55, 1997.

## Lewis contacts:

Ho-Jun Lee, (216) 433-3316, Ho-Jun.Lee@lerc.nasa.gov, and Dale A. Hopkins, (216) 433-3260, Dale.A.Hopkins@lerc.nasa.gov

## Ohio Aerospace Institute contact:

Dimitrios A. Saravanos, Dimitrios.A.Saravanos@lerc.nasa.gov

**Author:** Ho-Jun Lee

**Headquarters program office:** OASTT

**Programs/Projects:**

Propulsion Systems R&T, HITEMP



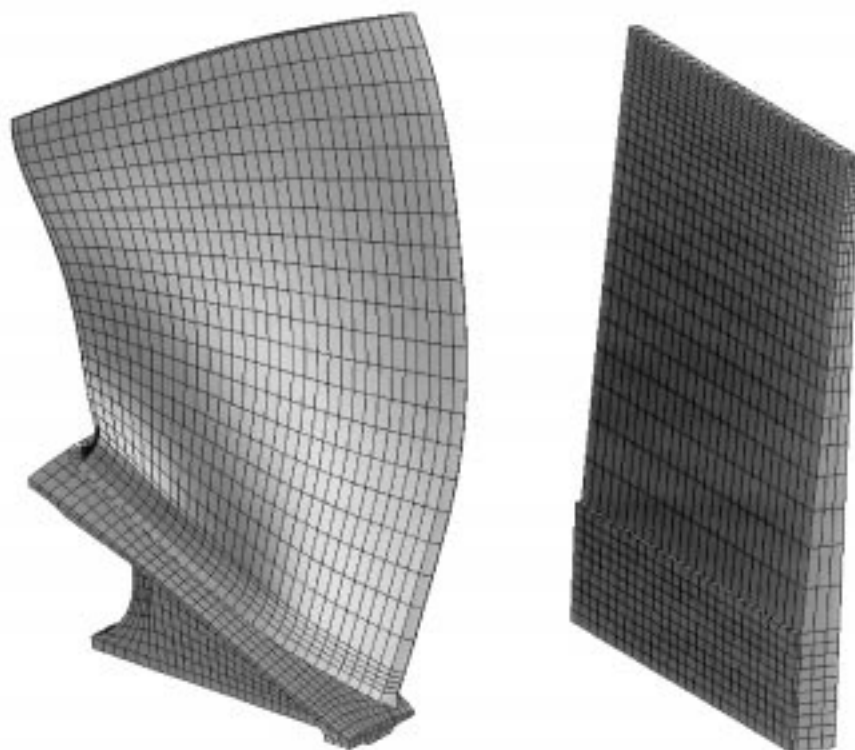
## Procedure Developed for Ballistic Impact Testing of Composite Fan Containment Concepts

The fan-containment system in a jet engine is designed to prevent a fan blade from penetrating the engine case in the event that the blade or a portion of the blade separates from the rotor during operation. Usually, these systems consist of a thick metal case that is strong enough to survive such an impact. Other systems consist of a dry aramid fabric wrapped around a relatively thin metal case. In large turbofan engines, metal-containment systems can weigh well over 300 kg, and there is a strong impetus to reduce their weight. As a result, the NASA Lewis Research Center is involved in an effort to develop polymer matrix composite (PMC) fan-containment systems to reduce the weight and cost while maintaining the high levels of safety associated with current systems. Under a Space Act Agreement with AlliedSignal Aircraft Engines, a new ballistic impact test procedure has been developed to quantitatively evaluate the performance of polymer matrix composite systems.

The test procedure uses a curved (half-ring) specimen with an inside diameter of 38 cm (15 in.) and a width of 20.3 cm (8 in.). A metal specimen with this geometry is shown in the photo; however, typical polymer matrix composite test specimens are considerably thicker. During testing, the specimen is supported along both ends and on one edge.



*Metal test specimen.*



*Finite element models. Left: Scaled fan blade. Right: Blade-simulating projectile.*

The projectile used in this test is designed to simulate the most important features of a full-scale fan blade at a low cost (see the figure to the left). It features a relatively thick shank section to simulate the blade attachment region, and the stiffness induced by the geometry of a twisted fan blade is approximated by tapering the thickness of the projectile from tip to shank. The projectile material has a mass of 330 g, and the projectile material is Ti-6Al-4V. In the test, the projectile is accelerated toward the specimen by NASA Lewis' 20.3-cm-diameter gas gun, which can achieve speeds of over 350 m/sec.

Transient finite element analyses showed that the blade simulating projectile performs in a manner similar to that of a scaled fan blade. In a typical test, the projectile was oriented at a 45° angle from the vertical, so that the tip of the projectile would impact the specimen

first. The blade then began to bend and rotate about the tip region, resulting in a secondary impact between the heavy shank section and the specimen. Analyses predicted that this secondary impact would produce more damage than the initial impact at the tip. This is consistent with experimental results.

The test procedure has been used to evaluate a number of different fan containment concepts, including two metallic systems and two composite systems. Preparations are under way for tests of more composite and hybrid metal/composite systems.

### **Bibliography**

Pereira, J.M., et al.: Fan Containment Impact Testing and Analysis at NASA Lewis Research Center. HITEMP Review 1997. NASA CP-10192, 1997, paper 13, pp. 1–12. (Permission to cite this material was granted by Carol A. Ginty, February 19, 1998.)

### **Lewis contacts:**

Dr. J. Michael Pereira, (216) 433–6738, J.M.Pereira@lerc.nasa.gov; Matthew E. Melis, (216) 433–3322, Matthew.E.Melis@lerc.nasa.gov; Duane M. Revilock, (216) 433–3186, Duane.M.Revilock@lerc.nasa.gov; and Dr. Gary D. Roberts, (216) 433–3244, Gary.D.Roberts@lerc.nasa.gov

**Authors:** Dr. J. Michael Pereira and Matthew E. Melis

**Headquarters program office:** OASTT

**Programs/Projects:** HSR, EPM, Propulsion Systems R&T, HITEMP

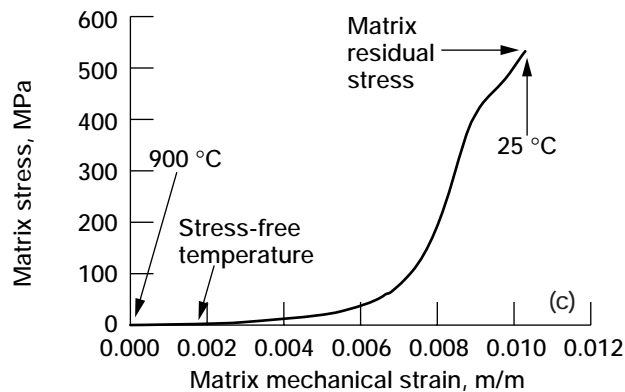
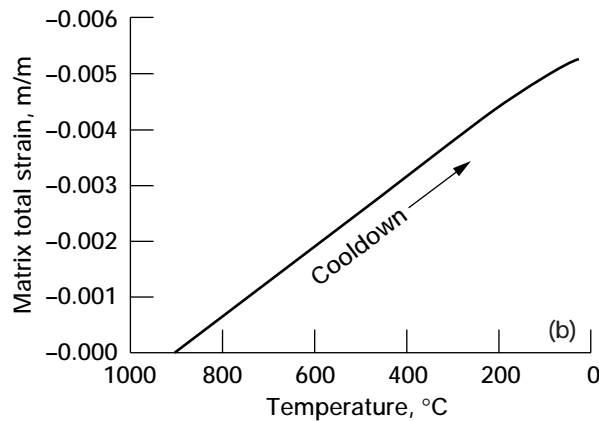
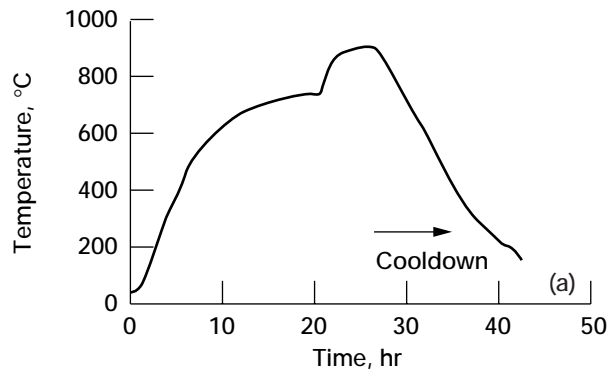
## **Mechanical Characterization of Thermomechanical Matrix Residual Stresses Incurred During MMC Processing**

In recent years, much effort has been spent examining the residual stress-strain states of advanced composites. Such examinations are motivated by a number of significant concerns that affect composite development, processing, and analysis. The room-temperature residual stress states incurred in many advanced composite systems are often quite large and can introduce damage even prior to the first external mechanical loading of the material. These stresses, which are induced during the cooldown following high-temperature consolidation, result from the coefficient of thermal expansion mismatch between the fiber and matrix.

Experimental techniques commonly used to evaluate composite internal residual stress states are nonmechanical in nature and generally include forms of x-ray and neutron diffraction. Such approaches are usually complex, involving a number of assumptions and limitations associated with a wide range of issues, including the depth of penetration, the volume of material being assessed, and erroneous effects associated with oriented grains. Furthermore, and more important to the present research, these techniques can assess only “single time” stress in the composite. That is, little, if any, information is obtained that addresses the time-dependent point at which internal stresses begin to accumulate, the manner in which the accumulation occurs, and the presiding relationships between thermoelastic, thermoplastic, and thermoviscous behaviors. To address these critical issues, researchers at the NASA Lewis Research Center developed and implemented an innovative mechanical test technique to examine in real time, the time-dependent thermomechanical stress behavior of a matrix alloy as it went through a consolidation cycle.

In general, a standalone matrix material is subjected to the strain-temperature history experienced by the in situ matrix material during a uniaxially simulated hot isostatic pressing (HIP), or hot press cycle. First,

the identical temperature time history experienced during the HIP cycle is imposed on the composite coupon while the composite cooldown thermal strain response is measured in a load-controlled environment. Employing the concept of fiber/matrix strain compatibility, we assume that the measured macroscopic strain history is identical to that experienced by the individual constituents. With this information, the measured composite cooldown thermal strain response is “enforced” on the standalone matrix material during an identical cooldown cycle in a strain-controlled environment. This allows the thermomechanical matrix stress response to be explicitly measured in real time without presupposing a given material behavior. From this technique, several critical measurements can be made, including (1) the time-dependent, stress-free temperature, (2) the degree of thermoelastic, thermoplastic, and thermoviscous behavior, (3) the real-time points within the HIP



*Thermomechanical test technique to simulate in situ metal matrix composite HIP cycle conditions on a standalone matrix. (a) Step 1—Measure composite cooldown strain. (b) Step 2—Enforce composite strain on matrix. (c) Step 3—Measure thermomechanical matrix response in terms of stress-free temperature; thermoelastic, thermoplastic, and thermoviscous behavior; and residual stress.*

cycle where the respective behaviors occur, and (4) the residual stress locked into the matrix subsequent to the HIP cycle cooldown. Such results have been generated for several SiC-reinforced titanium matrix composites.

#### Bibliography

Castelli, M.G.: Mechanical Characterization of the Thermomechanical Matrix Residual Stresses Incurred During MMC Processing. HITEMP Review 1997. NASA CP-10192, 1997, paper 29, pp, 1-12. (Permission to cite this material was granted by Carol A. Ginty, February 19, 1998.)

#### Lewis contact:

Michael G. Castelli, (216) 433-8464, Michael.G.Castelli@lerc.nasa.gov

**Author:** Michael G. Castelli

**Headquarters program office:** OASTT

**Programs/Projects:**

Propulsion Systems R&T, HITEMP

# Test Standard Developed for Determining the Slow Crack Growth of Advanced Ceramics at Ambient Temperature

The service life of structural ceramic components is often limited by the process of slow crack growth. Therefore, it is important to develop an appropriate testing methodology for accurately determining the slow crack growth design parameters necessary for component life prediction. In addition, an appropriate test methodology can be used to determine the influences of component processing variables and composition on the slow crack growth and strength behavior of newly developed materials, thus allowing the component process to be tailored and optimized to specific needs.

At the NASA Lewis Research Center, work to develop a standard test method to determine the slow crack growth parameters of advanced ceramics was initiated by the authors in early 1994 in the C 28 (Advanced Ceramics) committee of the American Society for Testing and Materials (ASTM). After about 2 years of required balloting, the draft written by the authors was approved and established as a new ASTM test standard: ASTM C 1368-97, *Standard Test Method for Determination of Slow Crack Growth Parameters of Advanced Ceramics by Constant Stress-Rate Flexural Testing at Ambient Temperature*.

Briefly, the test method uses constant stress-rate testing to determine strengths as a function of stress rate at ambient temperature. Strengths are measured in a routine manner at four or more stress rates by applying constant displacement or loading rates. The slow crack growth parameters required for design are then estimated from a relationship between strength and stress rate. This new standard will be published in the Annual Book of ASTM Standards, Vol. 15.01, in 1998. Currently, a companion draft ASTM standard for determination of the slow crack growth parameters of advanced ceramics at elevated temperatures is being prepared by the authors and will be presented to the committee by the middle of 1998.

Consequently, Lewis will maintain an active leadership role in advanced ceramics standardization within ASTM. In addition, the authors have been and are involved with several international standardization organizations including the Versailles Project on Advanced Materials and Standards (VAMAS), the International Energy Agency (IEA), and the International Organization for Standardization (ISO). The associated standardization activities involve fracture toughness, strength, elastic modulus, and the machining of advanced ceramics.

**Lewis contacts:** Dr. Sung R. Choi, (216) 433-8366, Sung.R.Choi@lerc.nasa.gov, and Jonathan A. Salem, (216) 433-3313, Jonathan.A.Salem@lerc.nasa.gov

**Authors:** Dr. Sung R. Choi and Jonathan A. Salem

**Headquarters program office:** OASTT

**Programs/Projects:** CARES/*Life*, Propulsion systems R&T, P&PM

# Accelerated Testing Methodology Developed for Determining the Slow Crack Growth of Advanced Ceramics

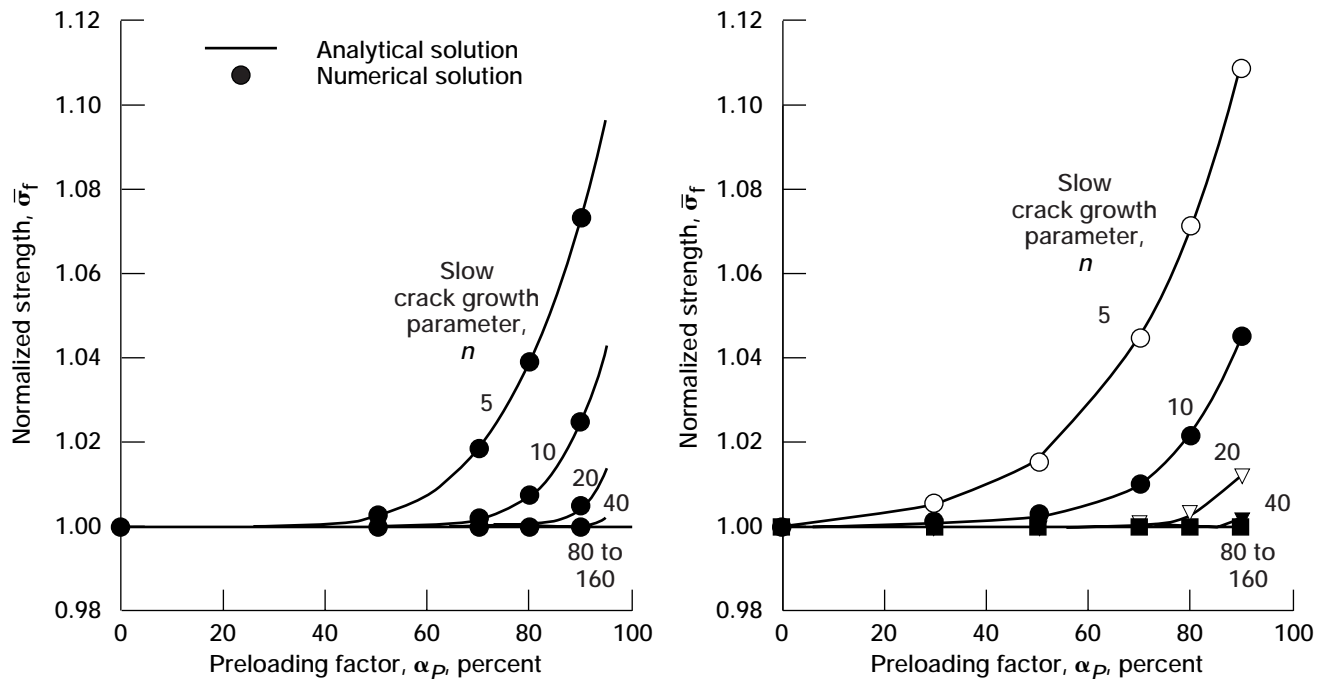
Constant stress-rate ("dynamic fatigue") testing has been used for several decades to characterize the slow crack growth behavior of glass and structural ceramics at both ambient and elevated temperatures. The advantage of such testing over other methods lies in its simplicity: strengths are measured in a routine manner at four or more stress rates by applying a constant displacement or loading rate. The slow crack growth parameters required for component design can be estimated from a relationship between strength and stress rate.

With the proper use of preloading in constant stress-rate testing, test time can be reduced appreciably. If a preload corresponding to 50 percent of the strength is applied to the specimen prior to testing, 50 percent of the test time can be saved as long as the applied preload does not change the strength. In fact, it has been a common, empirical practice in the strength testing of ceramics or optical fibers to apply some preloading (<40 percent). The purpose of this work at the NASA Lewis Research Center is to study the effect of preloading on measured strength in order to add a theoretical foundation to the empirical practice.

An analytical and numerical solution of strength as a function of preloading has been developed, as shown in the graph. In this solution,  $\bar{\sigma}_f$  is the normalized strength, in which the strength with preloading is normalized with respect to the strength with zero preloading; and  $\alpha_p$  is the preloading fraction ( $1 \leq \alpha_p < 1$ ), where the preloading stress is normalized with respect to the strength with zero preloading. Finally,  $n$  is the slow crack

growth parameter used in the expression of slow crack growth rate,  $v = da/dt = A(K_I/K_{IC})^n$ , where  $v$ ,  $a$ ,  $t$ ,  $A$ ,  $K_I$ , and  $K_{IC}$  are the crack velocity, crack size, time, slow crack growth parameter, stress intensity factor, and fracture toughness, respectively. The solution has been verified with experimental results obtained from constant stress-rate testing of glass and alumina at room temperature and of alumina, silicon nitride, and silicon carbide at elevated temperatures.

The most direct and powerful effect of preloading is the reduction of test time, which greatly affects test efficiency. For example, if it takes about 9 hr to perform constant stress-rate testing on one ceramic specimen and if a minimum of 20 specimens are required to obtain reliable statistical data, the total testing time at that stress-rate



Normalized strength,  $\bar{\sigma}_f$ , as a function of preloading factor,  $\alpha_p$ . Left: Natural flaw system. Right: Indentation-induced flaw system with residual stress field.



would be 180 hr. However, if a preloading of 80 percent was applied, the total testing time would be reduced to 36 hr, saving 80 percent of the total test time. For a preload of 70 percent, 70 percent of the time would be saved, and so on. The use of preloading has been adopted in a recently established American Society for Testing and Materials standard (C1368) on slow crack growth testing of advanced ceramics.

### Bibliography

Choi, S.R.; and Salem, J.A.: Effect of Preloading on Fatigue Strength in Dynamic Fatigue Testing of Ceramic Materials at Elevated Temperatures. *Ceram. Eng. Sci. Proc.*, vol. 16, no. 4, 1995, pp. 87–94.

Choi, S.R.; and Gyekenyesi, J.P.: Fatigue Strength as a Function of Preloading in Dynamic Fatigue Testing of Glass and Ceramics. *J. Eng. Gas Turbines Power*, vol. 119, no. 3, 1997, pp. 493–499.

Choi, S.R.; and Salem, J.A.: Preloading Technique in Dynamic Fatigue Testing of Glass and Ceramics With an Indentation Flaw System. *J. Am. Ceram. Soc.*, vol. 79, no. 5, 1996, pp. 1228–1232.

Choi, S.R.; and Salem, J.A.: Preloading Technique in Dynamic Fatigue Testing of Ceramics: Effect of Preloading on Strength Variation. *J. Mater. Sci. Lett.*, vol. 15, 1996, pp. 1963–1965.

### Lewis contacts:

Dr. Sung R. Choi, (216) 433–8366, Sung.R.Choi@lerc.nasa.gov, and Dr. John P. Gyekenyesi, (216) 433–3210, John.P.Gyekenyesi@lerc.nasa.gov

**Authors:** Dr. Sung R. Choi and Dr. John P. Gyekenyesi

**Headquarters program office:** OASTT

**Programs/Projects:** CARES/*Life*, Propulsion Systems R&T, P&PM

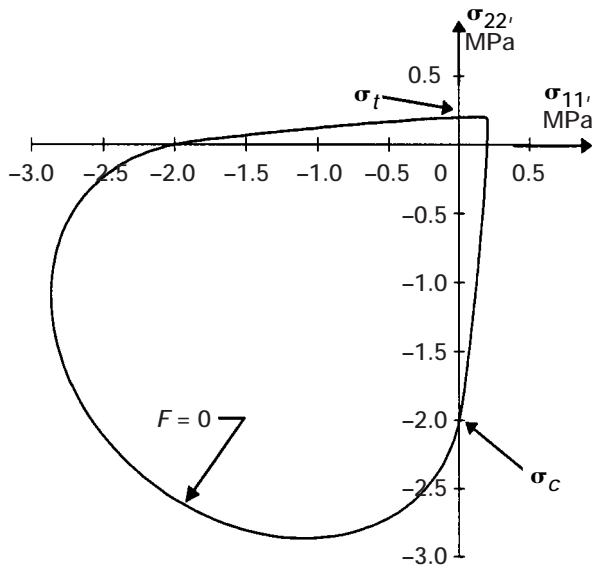
## Constitutive Theory Developed for Monolithic Ceramic Materials

With the increasing use of advanced ceramic materials in high-temperature structural applications such as advanced heat engine components, the need arises to accurately predict thermomechanical behavior that is inherently time-dependent and that is hereditary in the sense that the current behavior depends not only on current conditions but also on the material's thermomechanical history. Most current analytical life prediction methods for both subcritical crack growth and creep models use elastic stress fields to predict the time-dependent reliability response of components subjected to elevated service temperatures. Inelastic response at high temperatures has been well documented in the materials science literature for these material systems, but this issue has been ignored by the engineering design community. From a design engineer's perspective, it is imperative to emphasize that accurate predictions of time-dependent reliability demand accurate stress field information.

Ceramic materials exhibit different time-dependent behavior in tension and compression. Thus, inelastic deformation models for ceramics must be constructed in a fashion that admits both sensitivity to hydrostatic stress and differing behavior in tension and compression. A number of constitutive theories for materials that exhibit sensitivity to the hydrostatic component of stress have been proposed that characterize deformation using time-independent classical plasticity as a foundation. However, none of these theories allow different behavior in tension and compression. In addition, these theories are somewhat lacking in that they are unable to capture the creep, relaxation, and rate-sensitive phenomena exhibited by ceramic materials at high temperatures.

The objective of this effort at the NASA Lewis Research Center has been to formulate a macroscopic continuum theory that captures these time-

dependent phenomena. Specifically, the effort has focused on inelastic deformation behavior associated with these service conditions by developing a multiaxial viscoplastic constitutive model that accounts for time-dependent hereditary material deformation (such as creep and stress relaxation) in monolithic structural ceramics. Using continuum principles of engineering mechanics, we derived the complete viscoplastic theory from a scalar dissipative potential function. Constitutive equations for the flow law (strain rate) and evolutionary law were formulated on the basis of a threshold function, identified here as  $F$  (see the figure), that is sensitive to hydrostatic stress and allows different behavior in tension and compression. For illustration, a set of threshold flow stress values has been adopted that roughly corresponds to values anticipated for isotropic monolithic ceramics. Specifically, the compressive uniaxial threshold stress value  $\sigma_c$  is



Threshold function projected onto the  $\sigma_{11}$ - $\sigma_{22}$  stress plane.

2.00 MPa, and the tensile uniaxial threshold stress value  $\sigma_t$  is 0.20 MPa. Furthermore, inelastic deformation is treated as inherently time dependent. A rate of inelastic strain is associated with every state of stress. As a result, creep, stress relaxation, and rate sensitivity are phenomena resulting from applied boundary conditions and are not treated separately in an ad hoc fashion.

Complete details of the model and its attending geometrical implications have been developed, but a quantitative assessment has yet to be conducted since the material constants have not been suitably characterized for a specific

material. Incorporating this model into a nonlinear finite element code would provide industry a means to numerically simulate the inherently time-dependent and hereditary phenomena exhibited by these materials in service. Utilization of this approach has the potential to improve the accuracy of life prediction results for structural ceramics in high-temperature power and propulsion applications.

#### Bibliography

Janosik, L.A.; and Duffy, Stephen F.: A Viscoplastic Constitutive Theory for Monolithic Ceramics—I. ASME Paper 96-GT-368, 1996.

#### Lewis contact:

Lesley A. Janosik, (216) 433-5160, Lesley.A.Janosik@lerc.nasa.gov

**Author:** Lesley A. Janosik

**Headquarters program office:** OASTT

**Programs/Projects:**

Propulsion Systems R&T, P&PM

## Noncontact Determination of Antisymmetric Plate Wave Velocity in Ceramic Matrix Composites

High-temperature materials are of increasing importance in the development of more efficient engines and components for the aeronautics industry. In particular, ceramic matrix composite (CMC) and metal matrix composite (MMC) structures are under active development for these applications.

The acousto-ultrasonic (AU) method has been shown to be useful for assessing mechanical properties in composite structures. In particular, plate wave analysis can characterize composites in terms of their stiffness moduli. It is desirable to monitor changes in mechanical properties that occur during thermomechanical testing and to monitor the health of components whose geometry or position make them hard to reach with conventional ultrasonic probes. In such applications, it would be useful to apply AU without coupling directly to the test surface.

For a number of years, lasers have been under investigation as remote ultrasonic input sources and ultrasound detectors. The use of an ultrasonic transducer coupled through an air gap has also been under study. So far at the NASA Lewis Research Center, we have been more successful in using lasers as ultrasonic sources than as output devices. On the other hand, we

have been more successful in using an air-coupled piezoelectric transducer as an output device than as an input device. For this reason, we studied the laser in/air-coupled-transducer out combination—using a pulsed NdYAG laser as the ultrasonic source and an air-coupled-transducer as the detector.

The present work is focused on one of the AU parameters of interest, the ultrasonic velocity of the antisymmetric plate-wave mode. This easily identified antisymmetric pulse can be used to determine shear and flexure modulus. It was chosen for this initial work because the pulse arrival times are likely to be the most precise. The following

schematic illustrates our experimental arrangement for using laser in/air-transducer out on SiC/SiC composite tensile specimens. The NdYAG pulse was directed downward by a 90° infrared prism to the top of the specimen, but at the edge of one end. An energy sensor measured a single pulse at 13 millijoules (mJ) before it passed through the prism, which attenuated 15 percent of its energy. It also provided an output trigger for the waveform time-delay synthesizer.

A broadband, air-coupled, piezoelectric transducer was centered nominally at 0.5 MHz and coupled to the air through a buffer that was shaped to focus the ultrasound 5.08 cm beyond its surface. We have shown that, for ceramic matrix composite specimens of the present geometry, this frequency range is very much dominated by the lowest antisymmetric plate mode.

Six specimens each of three layups, 0°/90°, ±45°, and [0°/+45°/90°/-45°]<sub>s</sub>, of approximately 20-percent porous SiC/SiC were studied. For each layup, eight-ply panels were cut into 1.27- by 15.24-cm rectangular bars with thicknesses of 0.25 to 0.29 cm. Then, the bars, which had a 40-percent fiber fraction, were treated with a seal coating.

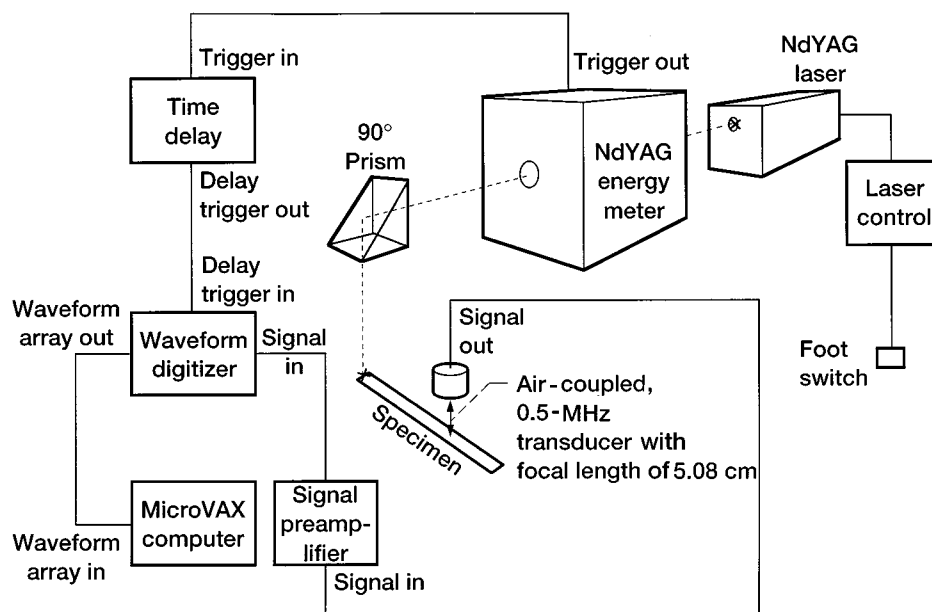
In the figure on the next page, the noncontact average plate-wave velocities are plotted against the contact average values. The standard deviation of the 18 sets of velocities was determined. For the noncontact data, the average was 2.8 percent, and for the contact data, it was 2.3 percent, indi-

cating very similar reproducibility. Standard deviation bars are not plotted in the figure so that the correlation between the contact and noncontact velocity can be seen more readily. The laser in/air-coupled-transducer out system can provide data as accurate as that from contact-coupled transducers for determining the velocity associated with the lowest antisymmetric plate mode for SiC/SiC ceramic matrix composites.

### Bibliography

HITEMP Review 1988, 1989, 1990, 1991, and 1992. NASA CP-10025, CP-10039, CP-10051, CP-10082, and CP-10104, 1988-1992. (Permission to cite this material was granted by Carol A. Ginty, February 19, 1998.)

Tang, B.; and Henneke II, E.G.: Long Wavelength Approximation for Lamb Wave Characterization of Composite Laminates. Res. Nondestr. Eval., vol. 1, no. 1, 1989, pp. 51-64.



*Experimental laser input/air-coupled-transducer output arrangement for collecting waveforms.*

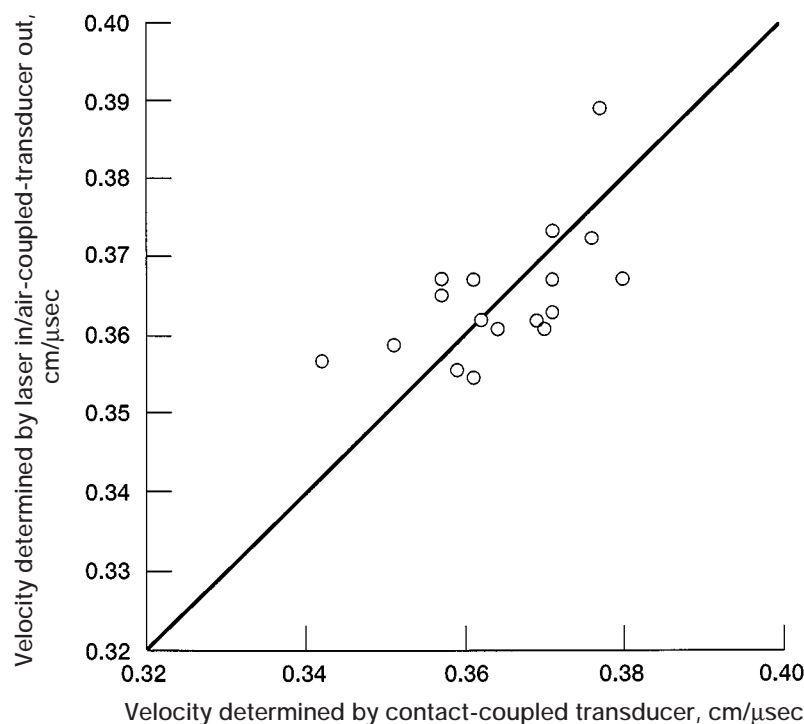


*Plate-wave velocities from laser input/air-coupled-transducer output compared with those from contact-plate transducers.*

Kautz, H.E.: Detecting Lamb Waves With Broadband Acousto-Ultrasonic Signals in Composite Structures. *Res. Nondestr. Eval.*, vol. 4, no. 3, 1992, pp. 151–164.

Huber, R.D.; and Green, R.E.: *Acousto-Ultrasonic Nondestructive Evaluation of Materials Using Laser Beam Generation and Detection*. NASA CR-186694, 1994.

Scrubby, C.B.; and Drain, L.E.: *Laser Ultrasonics*. Adam Hilger, New York, 1990.

Monchalin, J.P.: Optical Detection of Ultrasound. *IEEE Trans. UFFC*, vol. 33, no. 5, Sept. 1986, pp. 485–499.

Safaeinili, A.; Lobkis, O.I.; and Chimenti, D.E.: Air-Coupled Ultrasonic Characterization of Composite Plates. *Materials Eval.*, vol. 53, 1995, pp. 1186–1190.

Kautz, H.E.: Non-Contact Determination of Antisymmetric Plate Wave Velocity in Ceramic Matrix Composites. NASA TM-107125, 1996.

**Lewis contact:**

Harold E. Kautz, (216) 433-6015, Harold.E.Kautz@lerc.nasa.gov

**Author:** Harold E. Kautz

**Headquarters program office:** OASTT

**Programs/Projects:** Propulsion Systems R&T, HITEMP, EPM

# Experimental Techniques Verified for Determining Yield and Flow Surfaces

Structural components in aircraft engines are subjected to multiaxial loads when in service. For such components, life prediction methodologies are dependent on the accuracy of the constitutive models that determine the elastic and inelastic portions of a loading cycle. A threshold surface (such as a yield surface) is customarily used to differentiate between reversible and irreversible flow. For elastoplastic materials, a yield surface can be used to delimit the elastic region in a given stress space. The concept of a yield surface is central to the mathematical formulation of a classical plasticity theory, but at elevated temperatures, material response can be highly time dependent. Thus, viscoplastic theories have been developed to account for this time dependency.

Since the key to many of these theories is experimental validation, the objective of this work (refs. 1 and 2) at the NASA Lewis Research Center was to verify that current laboratory techniques and equipment are sufficient to determine flow surfaces at elevated temperatures. By probing many times in the axial-torsional stress space, we could define the yield and flow surfaces. A small offset definition of yield ( $10 \mu\epsilon$ ) was used to delineate the boundary between reversible and irreversible behavior so that the material state remained essentially unchanged and multiple probes could be done on the same specimen. The strain was measured with an off-the-shelf multiaxial extensometer that could measure the axial and torsional strains over a wide range of temperatures. The accuracy and resolution of this extensometer was verified by comparing its data with

strain gauge data at room temperature. The extensometer was found to have sufficient resolution for these experiments. In addition, the amount of crosstalk (i.e., the accumulation of apparent strain in one direction when strain in the other direction is applied) was found to be negligible.

Tubular specimens were induction heated to determine the flow surfaces at elevated temperatures. The heating system induced a large amount of noise in the data. By reducing thermal fluctuations and using appropriate data averaging schemes, we could render the noise inconsequential. Thus, accurate and reproducible flow surfaces (see the figure) could be obtained.

With the experimental equipment verified, it is now possible to validate multiaxial, viscoplastic theories. Future work is planned to examine multiaxial effects in composites and superalloys commonly used in advanced aircraft engines.

## References

1. Lissenden, C.J., et al.: Verification of Experimental Techniques for Flow Surface Determination. NASA TM-107053, 1996.
2. Lissenden, C.J., et al.: Experimental Determination of Yield and Flow Surfaces Under Axial-Torsional Loading. S. Kalluri and P.J. Bonacuse, eds., Am. Soc. Test. Mater. Spec. Tech. Publ. 1280, 1997, pp. 92-112.

## Lewis contacts:

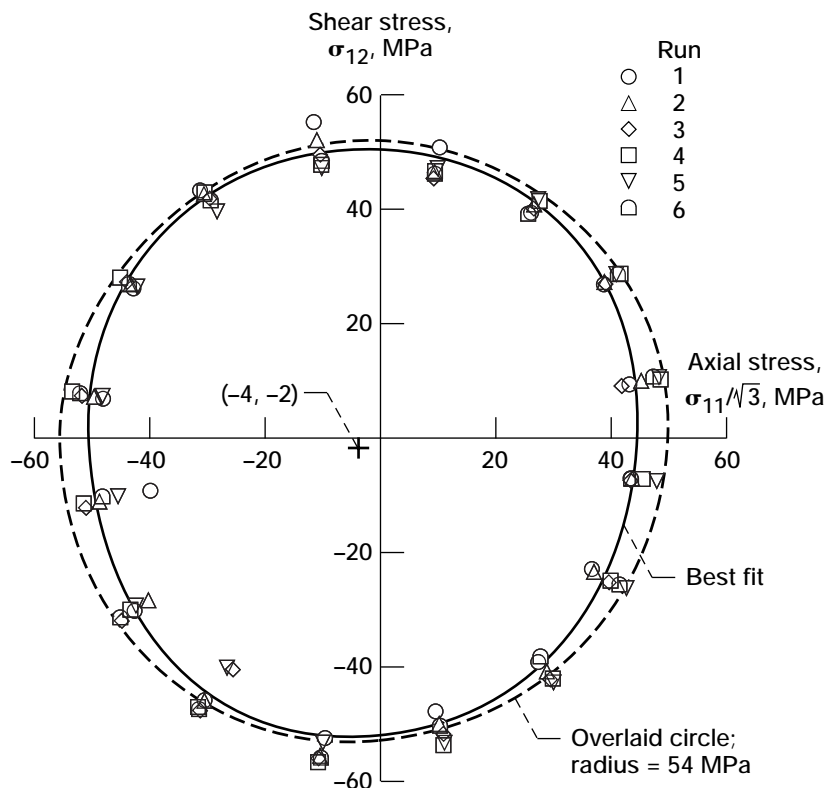
Brad A. Lerch, (216) 433-5522,  
Bradley.A.Lerch@lerc.nasa.gov, and  
Rod Ellis, (216) 433-3340,  
John.R.Ellis@lerc.nasa.gov

**Authors:** Brad A. Lerch, Rod Ellis, and  
Cliff J. Lissenden

**Headquarters program office:** OASTT

**Programs/Projects:**

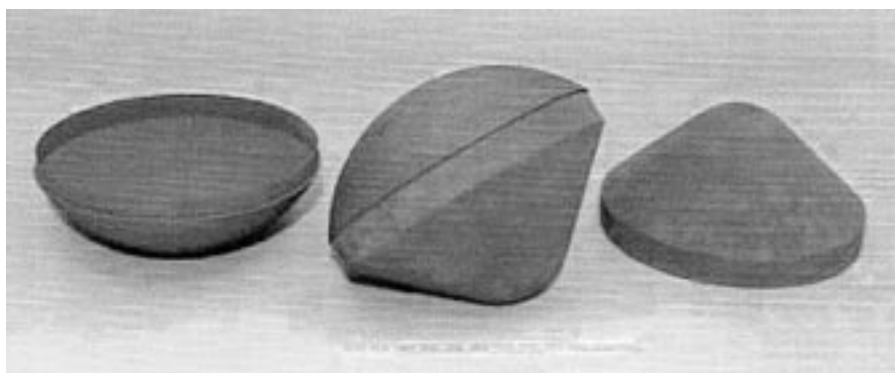
Propulsion Systems R&T, HITEMP



*Flow surfaces for 316 stainless steel at 650 ° C.*



# CARES/*Life* Ceramics Durability Evaluation Software Used for Mars Microprobe Aeroshell



*Mars Microprobe Aeroshell made of heat-resistant silicon carbide material. (Copyright Jet Propulsion Laboratory; used with permission.)*

The CARES/*Life* computer program, which was developed at the NASA Lewis Research Center, predicts the probability of a monolithic ceramic component's failure as a function of time in service. The program has many features and options for materials evaluation and component design. It couples commercial finite element programs—which resolve a component's temperature and stress distribution—to reliability evaluation and fracture mechanics routines for modeling strength-limiting defects. These routines are based on calculations of the probabilistic nature of the brittle material's strength. The capability, flexibility, and uniqueness of CARES/*Life* has attracted many users representing a broad range of interests and has resulted in numerous awards for technological achievements and technology transfer.

One noteworthy highlight was the use of CARES/*Life* to assess the survivability of the Mars Microprobe Aeroshell from launch-induced stresses. When the two Mars Microprobes piggyback aboard the Mars Surveyor '98 Lander (scheduled for launch in January 1999), they will be encased in basketball-sized, protective aeroshells made of silicon carbide. These aeroshells will free fall through the Martian atmosphere and crash into the polar surface. Shattering upon impact, the shells will release a miniature science probe designed to determine the presence of water ice. Although the shells are designed to shatter on Mars, they must, nonetheless, survive the high stresses associated with the launch. Analysis with CARES/*Life* indicated a high likelihood that the shells will remain intact after launch.

A key to maintaining interest in CARES/*Life* has been to actively maintain and promote the program as well as to enhance the program's ease of use. Toward this end, ANSCARES 2.0 was created. This computer program couples CARES/*Life* to the ANSYS finite element analysis program. Most noteworthy is that ANSCARES 2.0 contains an automatic surface recognition feature that frees CARES/*Life* users from manually modeling component surfaces. The majority of CARES/*Life* customers are also ANSYS users, so upgrading the links between the two codes was an imperative goal.

For more information, visit NASA Lewis' Life Prediction Branch:

<http://www.lerc.nasa.gov/WWW/LifePred>

Or go directly to CARES:

<http://www.lerc.nasa.gov/WWW/LifePred/BrittleStructures/CARES/>

## Bibliography

Nemeth, N.N., et al.: Designing Ceramic Components for Durability. Advanced Ceramic Matrix Composites—Design Approaches, Testing and Life Prediction Methods, E.R. Generazio, ed., Technomic Publishing Company, Lancaster, PA, 1996, pp. 3–16.

Nemeth, N.N., et al.: Durability Evaluation of Ceramic Components Using CARES/*LIFE*. J. Eng. Gas Turbines Power, vol. 118, Jan. 1996, pp. 150–158.

## Lewis contacts:

Noel N. Nemeth, (216) 433–3215, [Noel.N.Nemeth@lerc.nasa.gov](mailto:Noel.N.Nemeth@lerc.nasa.gov);  
Lynn M. Powers, (216) 433–8374, [Lynn.M.Powers@lerc.nasa.gov](mailto:Lynn.M.Powers@lerc.nasa.gov); and  
Lesley A. Janosik, (216) 433–5160, [Lesley.A.Janosik@lerc.nasa.gov](mailto:Lesley.A.Janosik@lerc.nasa.gov)

**Author:** Noel N. Nemeth

**Headquarters program office:** OASTT

**Programs/Projects:** CARES/*Life*,  
Propulsion Systems R&T, P&PM

**Special recognition:** American Ceramic Society's 1997 Corporate Technical Achievement Award was given jointly to NASA Lewis and Philips Display Components Company for the development and commercialization of new design, durable, lightweight, and environmentally friendly television picture tubes.

# Continuum Damage Mechanics Used to Predict the Creep Life of Monolithic Ceramics

Significant improvements in propulsion and power generation for the next century will require revolutionary advances in high-temperature materials and structural design. Advanced ceramics are candidate materials for these elevated temperature applications. High-temperature and long-duration applications of monolithic ceramics can place their failure mode in the creep rupture regime.

An analytical methodology in the form of the integrated design program—Ceramics Analysis and Reliability Evaluation of Structures/*Creep* (CARES/*Creep*) has been developed by the NASA Lewis Research Center to predict the life of ceramic structural components subjected to creep rupture conditions. This program utilizes commercially available finite element packages and takes into account the transient state of stress and creep strain distributions (stress relaxation as well as the asymmetric response to tension and compression). The creep life of a component is discretized into short time steps, during which the stress distribution is assumed constant. Then, the damage is calculated for each time step on the basis of a modified Monkman-Grant (MMG) creep rupture criterion. The cumulative damage is subsequently calculated as time elapses in a manner similar to Miner's rule for cyclic fatigue loading. Failure is assumed to occur when the normalized cumulative damage at any point in the component reaches unity. The corresponding time is the creep rupture life for that component.

To account for the deteriorating state of the material due to creep damage (cavitation) as time elapses as well as the effects of tertiary creep, we implemented a creep life prediction methodology based on a modified form of the Kachanov-Rabotnov Continuum Damage Mechanics (CDM) theory. In this theory, the uniaxial creep rate is described in terms of stress, temperature, time, and the current state of material damage. This scalar damage state parameter is basically an abstract measure of the current state of creep in the material. The damage rate is assumed to vary with stress, temperature, time, and the current state of damage itself. Multiaxial creep and creep rupture formulations of the CDM approach have been characterized.

The CARES/*Creep* code predicts the deterministic life of a ceramic component. Future work involves the role of probabilistic models in this design process. The complete package will predict the life of monolithic ceramic components, using simple, uniaxial creep laws to account for multiaxial creep loading. The combination of the CARES/*Creep* and CARES/*Life* codes gives design engineers the tools necessary to predict component life for the two dominant delayed failure mechanisms, creep and slow crack growth.

## More information is available on the World Wide Web:

<http://www.lerc.nasa.gov/WWW/LifePred/BrittleStructures/CARES/creep/>

## Bibliography

Powers, L.M.; Jadaan, O.M.; and Gyekenyesi, J.P.: Creep Life of Ceramic Components Using a Finite Element Based Integrated Design Program (CARES/*CREEP*). ASME Paper 96-GT-369, 1996.

Jadaan, O.M.; Powers, L.M.; and Gyekenyesi, J.P.: Creep Life Prediction of Ceramic Components Subjected to Transient Tensile and Compressive Stress States. ASME Paper 97-GT-319, 1997.

## Lewis contacts:

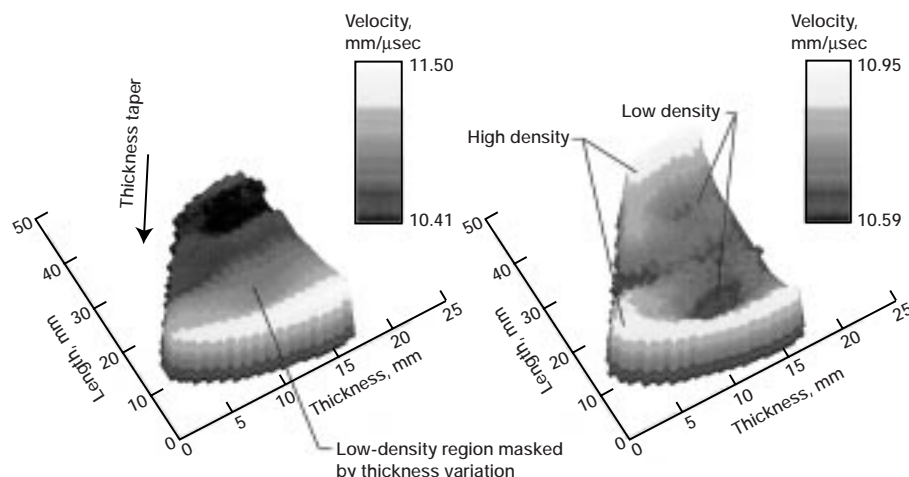
Lynn M. Powers, (216) 433-8374, [Lynn.M.Powers@lerc.nasa.gov](mailto:Lynn.M.Powers@lerc.nasa.gov), and Lesley A. Janosik, (216) 433-5160, [Lesley.A.Janosik@lerc.nasa.gov](mailto:Lesley.A.Janosik@lerc.nasa.gov)

**Authors:** Lynn M. Powers and Osama M. Jadaan

**Headquarters program office:** OASTT

**Programs/Projects:** CARES/*Creep*, Propulsion Systems R&T, P&PM

# Single-Transducer, Ultrasonic Imaging Method for High-Temperature Structural Materials Eliminates the Effect of Thickness Variation in the Image



*Conventional ultrasonic imaging versus thickness-independent ultrasonic imaging for silicon nitride monolithic ceramic with pore fraction variations and 10-percent thickness variation. Left: Conventional ultrasonic image. Thickness effect not eliminated; defects not revealed. Right: New thickness-independent ultrasonic imaging. Thickness eliminated; defects revealed. Images are shown in color in the online version of this article (<http://www.lerc.nasa.gov/WWW/RT1997/5000/5920roth.htm>).*

NASA Lewis Research Center's Life Prediction Branch, in partnership with Sonix, Inc., and Cleveland State University, recently advanced the development of, refined, and commercialized an advanced nondestructive evaluation (NDE) inspection method entitled the *Single Transducer Thickness-Independent Ultrasonic Imaging Method* (refs. 1 to 4). Selected by *R&D Magazine* as one of the 100 most technologically significant new products of 1996, the method uses a single transducer to eliminate the superimposing effects of thickness variation in the ultrasonic images of materials. As a result, any variation seen in the image is due solely to microstructural variation. This nondestructive method precisely and accurately characterizes material gradients (pore fraction, density, or chemical) that affect the uniformity of a material's physical performance (mechanical, thermal, or electrical). Advantages of the method over conventional ultrasonic imaging include (1) elimination of machining costs (for precision thickness control) during the quality control stages of material processing and development and (2) elimination of labor costs and subjectivity involved in further image processing and image interpretation.

At NASA Lewis, the method has been used primarily for accurate inspections of high-temperature structural materials including monolithic ceramics, metal matrix composites, and polymer matrix composites. Data were published this year for platelike samples, and current research is focusing on applying the method to tubular components.

The initial publicity regarding the development of the method generated 150 requests for further information from a wide variety of institutions and

individuals including the Federal Bureau of Investigation (FBI), Lockheed Martin Corporation, Rockwell International, Hewlett Packard Company, and Procter & Gamble Company. In addition, NASA has been solicited by the 3M Company and Allison Abrasives to use this method to inspect composite materials that are manufactured by these companies.

## References

1. Roth, D.J.: Single Transducer Ultrasonic Imaging Method That Eliminates the Effect of Plate Thickness Variation in the Image. NASA TM-107184, 1996.
2. Roth, D. J., et al.: Commercial Implementation of Ultrasonic Velocity Imaging Methods via Cooperative Agreement Between NASA Lewis Research Center and Sonix, Inc. NASA TM-107138, 1996.
3. Roth, D.J., et al.: Commercial Implementation of NASA-Developed Ultrasonic Imaging Methods via Technology Transfer. Mater. Eval., vol. 54, no. 11, 1996, pp. 1305-1309.
4. Roth, D.J.: Using a Single Transducer Ultrasonic Imaging Method to Eliminate the Effect of Thickness Variation in the Images of Ceramic and Composite Plates. J. Nondestruct. Eval., vol. 16, no. 2, June 1997.

## Lewis contact:

Dr. Don J. Roth, (216) 433-6017,  
Don.J.Roth@lerc.nasa.gov

**Author:** Dr. Don J. Roth

**Headquarters program office:** OASTT

**Programs/Projects:** HITEMP, Propulsion Systems R&T, P&PM

## Special recognition:

1996 R&D 100 Award

# Neural Network Control of a Magnetically Suspended Rotor System

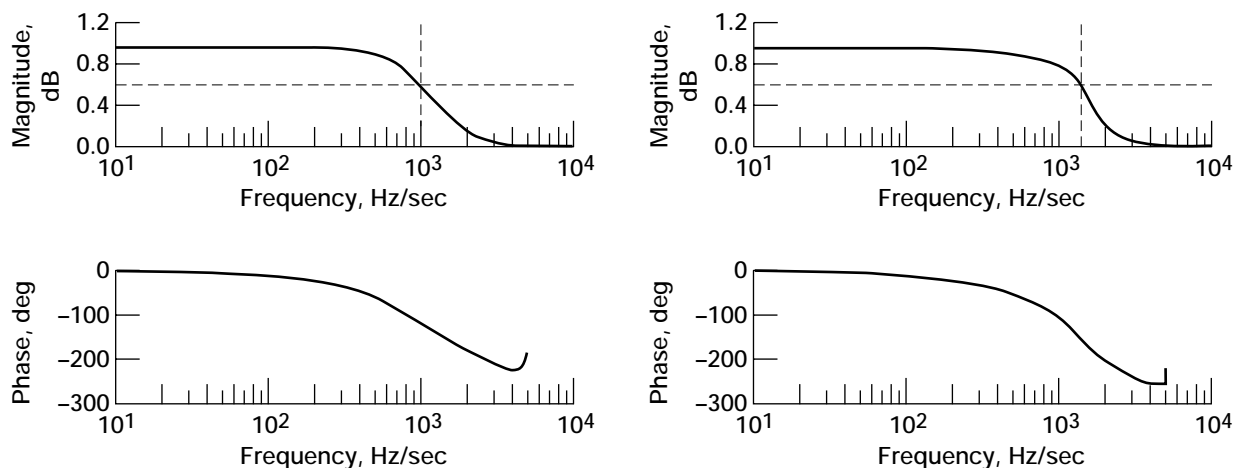
Magnetic bearings offer significant advantages because they do not come into contact with other parts during operation, which can reduce maintenance. Higher speeds, no friction, no lubrication, weight reduction, precise position control, and active damping make them far superior to conventional contact bearings. However, there are technical barriers that limit the application of this technology in industry. One of them is the need for a nonlinear controller that can overcome the system nonlinearity and uncertainty inherent in magnetic bearings. At the NASA Lewis Research Center, a neural network was selected as a nonlinear controller because it generates a neural model without any detailed information regarding the internal working of the magnetic bearing system. It can be used even for systems that are too complex for an accurate system model to be derived. A feed-forward architecture with a back-propagation learning algorithm was selected because of its proven performance, accuracy, and relatively easy implementation.

The neural net plant emulator was first trained to emulate a theoretical model of the nonlinear plant. A discrete theoretical model of the plant dynamics in state-space notation was used to choose the present states of the plant (rotor displacement and velocity) and the plant input (control current) as the input to the emulator. The next states, the rotor displacement and velocity after one sample time, were chosen as the output. During the learning procedure, we minimized the errors between the actual network output and the desired values by upgrading the weights. After training, the neural emulator perfectly predicted the next states (delayed by one sample time) of the magnetic bearing system for the current states and control force, which were not in the training sample data.

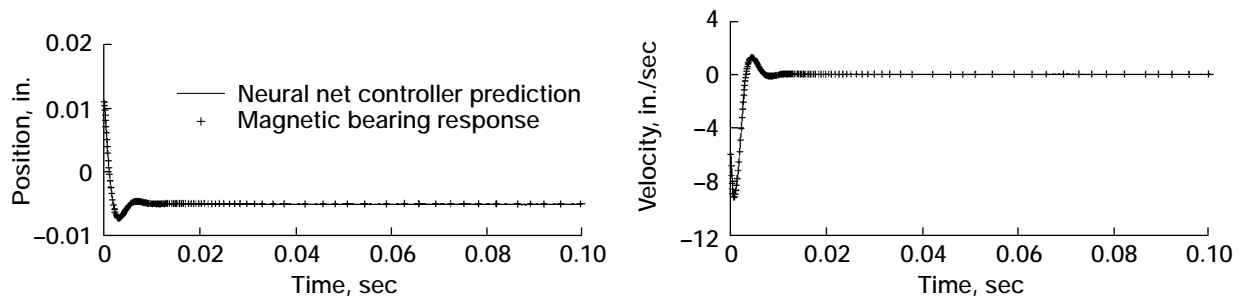
Our second step was to use the trained neural emulator to train a neural net controller to make the whole system meet conventional performance specifications on such parameters as the bandwidth, settling time, and overshoot. We wanted the controller to take the current magnetic bearing

states  $\bar{x}(t)$  and the demand  $r$  as input parameters, and to output a control force  $u(t)$  to the magnetic bearing system. These current state values should make the magnetic bearing's next state vector  $\bar{x}(t + 1)$  be identical to that defined by the desired linear reference system, satisfying performance specifications in either the frequency or time domain.

The left side of the following figure is the Bode plot of a simple second-order linear reference model derived from frequency domain specifications; the right side shows the closed-loop magnetic bearing system after training. They are almost identical even after 200 training epochs. Another neural controller based on time domain specifications was trained and tested by simulating its response for the initial condition and comparing the results to the actual magnetic bearing response (see the figure on the next page). The neural net controller was so accurate that it perfectly overlapped the magnetic bearing response (+ markers).



*Bode plots of desired and neural network models in frequency domain, showing averaged transfer function. Left: Simple second-order linear reference model for a frequency domain of peak magnitude,  $m_p$ , 1.1, and cutoff frequency,  $w_c$ , 1000 Hz. Right: Trained closed-loop system.*



*Desired and actual response in time domain. Left: Simple second-order linear reference model response for percent of overshoot,  $P_0$ , 4.3 percent, and settling time,  $T_s$ , 0.0001 sec. Right: Trained closed-loop system response for initial position,  $x_0$ , 0.0011 in.; initial velocity,  $\dot{x}_0$ , -6 in./sec; and reference position,  $r_f$ , -0.005 in.*

In summary, a neural network controller that circumvents the magnetic bearing's nonlinearity was developed and successfully demonstrated on a small Bentley-Nevada magnetic bearing rig. The neural plant emulator and neural controller were so accurate that the neural network controller did a near perfect job of making the nonlinear magnetic bearing system act like the linear reference model. This novel approach demonstrated the feasibility of using it for advanced turbomachinery systems with large-scaled magnetic bearings with unknown dynamics.

**Lewis contacts:** Dr. Benjamin B. Choi, (216) 433-6040, Benjamin.B.Choi@lerc.nasa.gov; Dr. Gerald V. Brown, (216) 433-6047, Gerald.V.Brown@lerc.nasa.gov; and Dr. Dexter Johnson, (216) 433-6046, Dexter.Johnson@lerc.nasa.gov

**Author:** Dr. Benjamin B. Choi

**Headquarters program office:** OASTT

**Programs/Projects:** Propulsion Systems R&T, P&PM



# Feasibility of Using Neural Network Models to Accelerate the Testing of Mechanical Systems

Verification testing is an important aspect of the design process for mechanical mechanisms, and full-scale, full-length life testing is typically used to qualify any new component for use in space. However, as the required life specification is increased, full-length life tests become more costly and lengthen the development time. In addition, this type of testing becomes prohibitive as the mission life exceeds 5 years, primarily because of the high cost and the slow turnaround time for new technology. As a result, accelerated testing techniques are needed to reduce the time required for testing mechanical components.

Current accelerated testing methods typically consist of increasing speeds, loads, or temperatures to simulate a high cycle life in a short period of time. However, two significant drawbacks exist with this technique. The first is that it is often not clear what the accelerated factor is when the operating conditions are modified. Second, if the conditions are changed by a large degree (an order of magnitude or more), the mechanism is forced to operate out of its design regime. Operation in this condition often exceeds material and mechanical system parameters and renders the test meaningless.

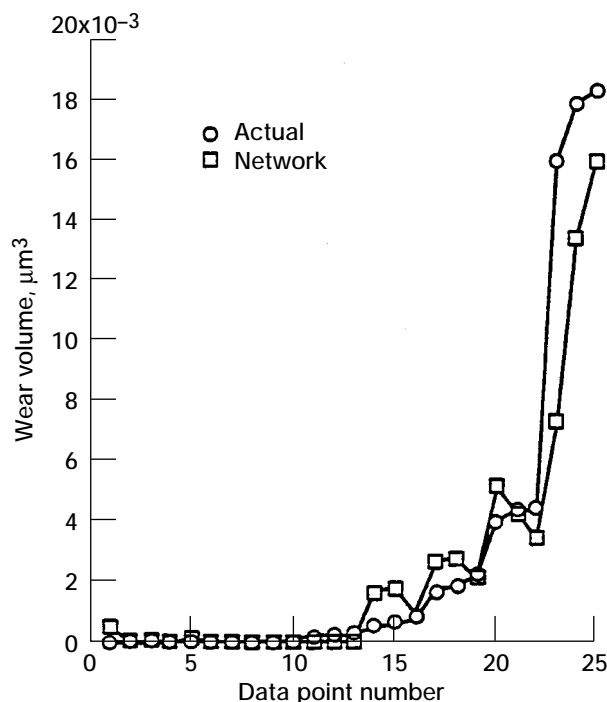
At the NASA Lewis Research Center, we theorized that neural network systems may be able to model the operation of a mechanical device. If so, the resulting neural network models could simulate long-term mechanical testing with data from a short-term test. This combination of computer

modeling and short-term mechanical testing could then be used to verify the reliability of mechanical systems, thereby eliminating the costs associated with long-term testing. Neural network models could also enable designers to predict the performance of mechanisms at the conceptual design stage by entering the critical parameters as input and running the model to predict performance.

The purpose of this study was to assess the potential of using neural networks to predict the performance and life of mechanical systems. To do this, we generated a neural network system to model wear obtained from three accelerated testing devices: (1) a pin-on-disk tribometer, (2) a line-contact rub-shoe tribometer, and (3) a four-ball tribometer. Critical parameters such as load, speed, oil viscosity, temperature, sliding distance, friction coefficient, wear, and material properties were used to produce models for each tribometer.

The study showed that neural networks were able to model these simple tribological systems, illustrating the feasibility of using neural networks to perform accelerated life testing on more complicated mechanical systems (e.g., bearings). The graph to the left compares actual wear data generated on a rub-shoe tribometer with data that were generated from a neural network. As the graph illustrates, the correlation is very good.

Neural networks can also be used to predict input variables for conditions that have not been run experimentally. The following figure is a neural-network-generated, three-dimensional plot of wear rate



*Comparison of previously unknown rub-shoe wear volumes (actual data) to those of a neural network model approximation.*

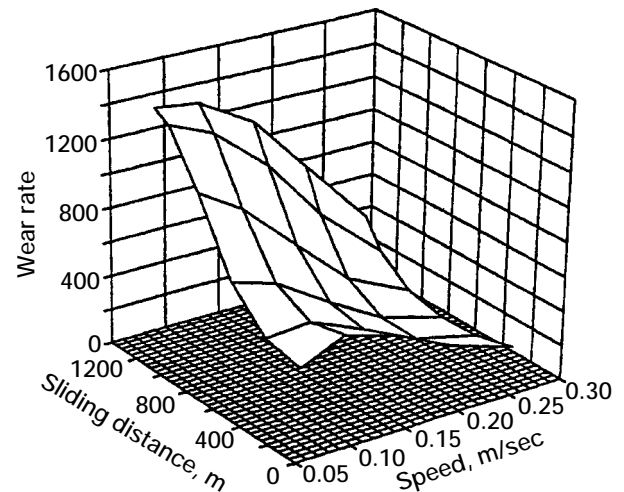
(for the pin-on-disk tribometer) as a function of sliding distance and sliding speed. This figure depicts wear rate values that would be obtained for different distances and speeds.

**Lewis contact:** Robert L. Fusaro, (216) 433-6080,  
Robert.L.Fusaro@lerc.nasa.gov

**Author:** Robert L. Fusaro

**Headquarters program office:** OSMA

**Programs/Projects:** Safety & Mission Assurance



*Three-dimensional plots generated from a neural network model illustrating the relationship between speed, load, and pin-on-disk wear rate.*

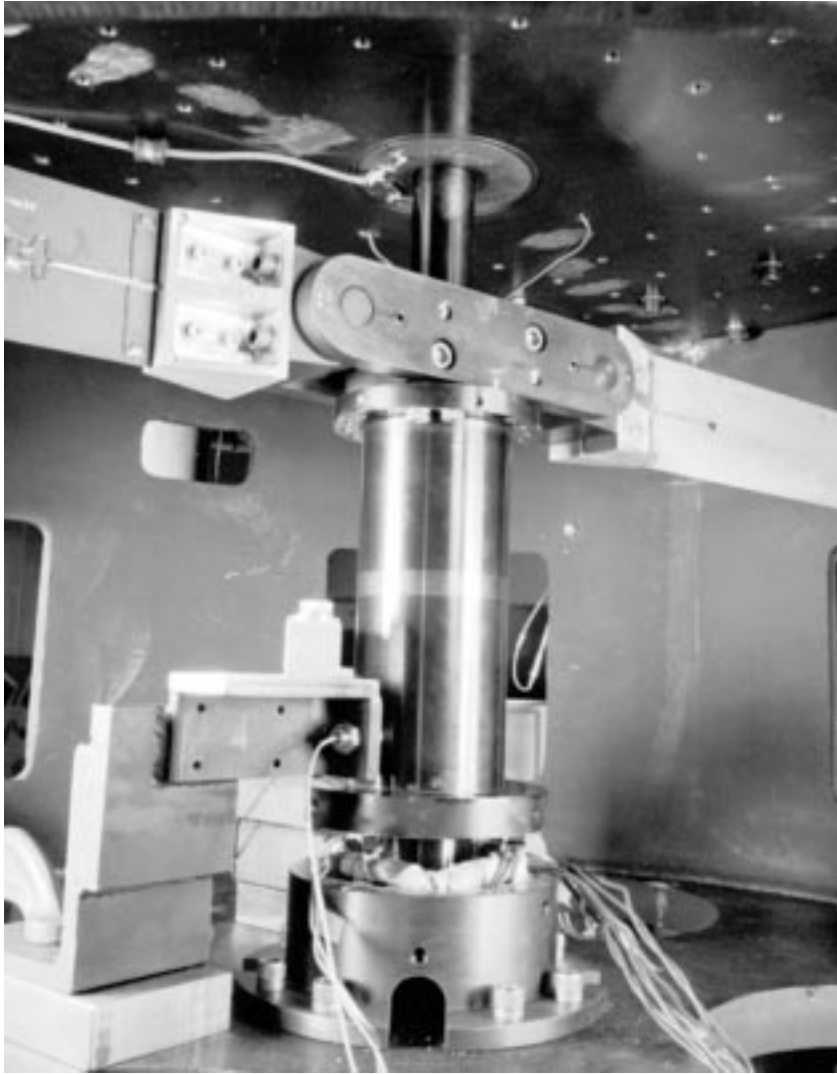
## Magnetic Suspension for Dynamic Spin Rig



*NASA Lewis' Dynamic Spin Rig.*

NASA Lewis Research Center's Dynamic Spin Rig, located in Building 5, Test Cell CW-18 (see the photo to the left), is used to test turbomachinery blades and components by rotating them in a vacuum chamber. A team from Lewis' Machine Dynamics Branch successfully integrated a magnetic bearing and control system into the Dynamic Spin Rig (see the photo on the next page). The magnetic bearing worked very well both to support and shake the shaft. It was demonstrated that the magnetic bearing can transmit more vibrational energy into the shaft and excite some blade modes to larger amplitudes than the existing electromagnetic shakers can.

Experiments were successfully conducted with the University of California, San Diego, on the damping of composite plates. These experiments demonstrated the system's robustness for long-term testing. Also, our team



*Radial magnetic bearing in NASA Lewis' Dynamic Spin Rig showing viscoelastic damped composite plates attached to the rotor.*

discovered that the bearing can use feedback from the blade's strain gauges to provide blade damping. This is an additional benefit since insufficient blade damping is a critical problem in advanced turbomachinery blades.

The success of the initial work led to the development and design of a full magnetic suspension system (using three magnetic bearings) for the Dynamic Spin Rig. The upgraded facility provides either a mechanical or magnetic support system for rotors. The magnetic support will enable longer run times for rotating blades at higher speeds and larger vibration amplitudes.

**Lewis contacts:**

Dr. Dexter Johnson, (216) 433-6046, [Dexter.Johnson@lerc.nasa.gov](mailto:Dexter.Johnson@lerc.nasa.gov);  
Oral Mehmed, (216) 433-6036, [Oral.Mehmed@lerc.nasa.gov](mailto:Oral.Mehmed@lerc.nasa.gov); and  
Dr. Gerald V. Brown, (216) 433-6047, [Gerald.V.Brown@lerc.nasa.gov](mailto:Gerald.V.Brown@lerc.nasa.gov)

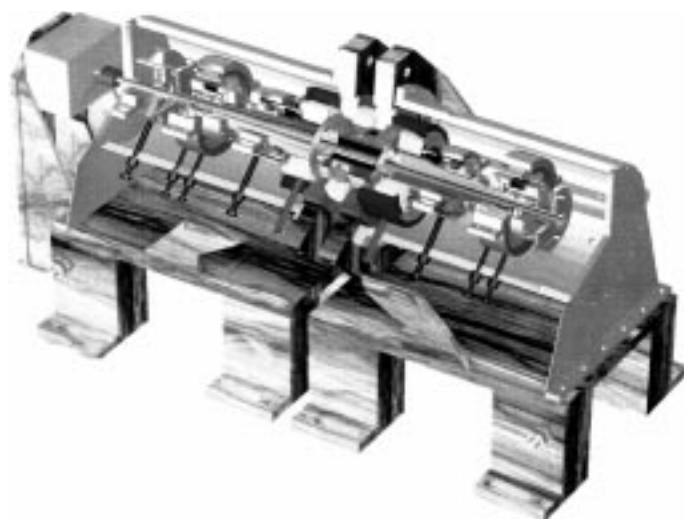
**Author:** Dr. Dexter Johnson

**Headquarters program office:** OASTT

**Programs/Projects:**

Propulsion systems R&T, P&PM, SGE

# High-Temperature Magnetic Bearings Being Developed for Gas Turbine Engines



*NASA Lewis' 1000 °F Magnetic Bearing Test Rig.*

Magnetic bearings are the subject of a new NASA Lewis Research Center and U.S. Army thrust with significant industry participation, and cooperation with other Government agencies. The NASA/Army emphasis is on high-temperature applications for future gas turbine engines. Magnetic bearings could increase the reliability and reduce the weight of these engines by eliminating the lubrication system. They could also increase the DN (diameter of bearing times the rpm) limit on engine speed and allow active vibration cancellation systems to be used, resulting in a more efficient, "more electric" engine. Finally, the Integrated High Performance Turbine Engine Technology (IHPTET) program, a joint Department of Defense/industry program, identified a need for a high-temperature (1200 °F) magnetic bearing that could be demonstrated in their Phase III engine.

This magnetic bearing is similar to an electric motor. It has a laminated rotor and stator made of cobalt steel. Wound around the stator's circumference are a series of electrical wire coils which form a series of electric magnets that exert a force on the rotor. A probe senses the position of the rotor, and a feedback controller keeps it centered in the cavity. The engine rotor, bearings, and casing form a flexible structure with many modes. The bearing feedback controller, which could cause some of these modes to become unstable, could be adapted to varying flight conditions to minimize seal clearances and monitor the health of the system.

Cobalt steel has a curie point greater than 1700 °F, and copper wire has a melting point beyond that. However, practical limitations associated with the maximum magnetic field strength in the cobalt steel and the stress in the rotating components limit the temperature of the magnetic bearing to about 1200 °F. The objective of this effort is to determine the temperature and speed limits of a magnetic bearing operating in an engine. Our approach was to use Lewis' in-house experience in magnets, mechanical components, high-temperature materials, and surface lubrication to build and test a magnetic bearing in both a rig and an engine. Testing was to be done at Lewis or through cooperative programs in industrial facilities.

During the last year, we made significant progress. We have a cooperative program with Allison Engine Company to work on a high-temperature magnetic thrust bearing. During this program, we uncovered a problem with the conventional design of the magnetic thrust bearing. Because the thrust bearing is not laminated, it causes eddy currents that severely reduce the bandwidth. Also, we worked at Allison to bring their high-temperature magnetic bearing rig to full speed. We predicted both in-house and Allison magnetic bearing stability limits, and we tested a high-temperature displacement probe. Our flexible casing rig is being converted to a high-temperature magnetic bearing rig (see the illustration). Testing should start in the third quarter of 1997.

Our plan is to develop a high-temperature compact wire insulation, and to fiber reinforce the core lamination to operate at higher temperature and DN values. We also plan to modify our stability analysis and controller theory by including a nonlinear magnetic bearing model. We are developing an expert system that adapts to changing flight conditions and that diagnoses the health of the system. Then, we will demonstrate the bearing on our rotor dynamics rig and, finally, in an engine.

#### **Lewis contacts:**

Albert F. Kascak, (216) 433-6024,  
Albert.F.Kascak@lerc.nasa.gov, and  
Dr. Gerald V. Brown, (216) 433-6047,  
Gerald.V.Brown@lerc.nasa.gov

**Author:** Albert F. Kascak

**Headquarters program office:** OASTT

**Programs/Projects:** Propulsion  
Systems R&T, P&PM, IHPTET



# Integrated Fiber-Optic Light Probe: Measurement of Static Deflections in Rotating Turbomachinery

At the NASA Lewis Research Center, in cooperation with Integrated Fiber Optic Systems, Inc., an integrated fiber-optic light probe system was designed, fabricated, and tested for monitoring blade tip deflections, vibrations, and to some extent, changes in the blade tip clearances of a turbomachinery fan or a compressor rotor. The system comprises a set of integrated fiber-optic light probes that are positioned to detect the passing blade tip at the leading and trailing edges. In this configuration, measurements of both nonsynchronous blade vibrations and steady-state blade deflections can be made from the timing information provided by each light probe—consisting of an integrated fiber-optic transmitting channel and numerical aperture receiving fibers, all mounted in the same cylindrical housing. With integrated fiber-optic technology, a spatial resolution of 50  $\mu\text{m}$  is possible while the outer diameter is kept below 2.5 mm. To

evaluate these probes, we took measurements in a single-stage compressor facility and an advanced fan rig in Lewis' 9- by 15-Foot Low-Speed Wind Tunnel.

**Lewis contact:**

Dr. Anatole P. Kurkov, (216) 433-5695,  
Anatole.P.Kurkov@lerc.nasa.gov

**Author:** Dr. Anatole P. Kurkov

**Headquarters program office:** OASTT

**Programs/Projects:** AST

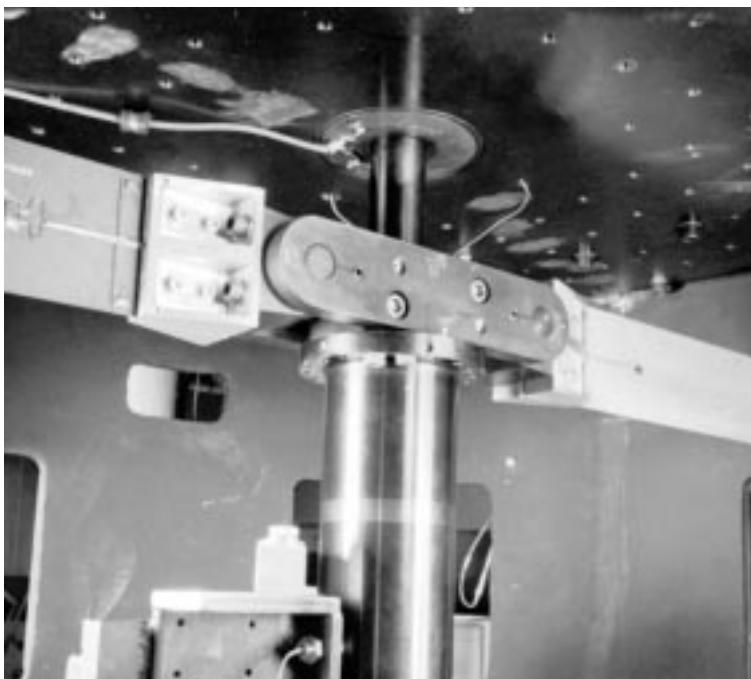
## Damping Experiment of Spinning Composite Plates With Embedded Viscoelastic Material

One way to increase gas turbine engine blade reliability and durability is to reduce blade vibration. It is well known that vibration can be reduced by adding damping to metal and composite blade-disk systems. As part of a joint research effort of the NASA Lewis Research Center and the University of California, San Diego, the use of integral viscoelastic damping treatment

to reduce the vibration of rotating composite fan blades was investigated. The objectives of this experiment were to verify the structural integrity of composite plates with viscoelastic material patches embedded between composite layers while under large steady forces from spinning, and to measure the damping and natural frequency variation with rotational speed.

Data were obtained from in-vacuum vibration spin experiments of flat and twisted graphite composite plates damped with 3M ISD 113 viscoelastic material patches embedded between composite layers. The photograph shows the rotor installation in the spin rig. The rotor has a tip diameter of 792 mm, and the plates have an aspect ratio of 3 and a chord of 76 mm.

Damping was calculated from measured transfer functions of blade base acceleration to blade



*Viscoelastic damped composite plates in NASA Lewis' Dynamic Spin Rig.*



strain. Damping was repeatable, and there were no failures or delaminations of the plates. This is significant since 3M ISD 113 has a low creep modulus at room temperature, and the plates had a centrifugal load of up to 28,000g at the tip. Centrifugal stiffening was large for the plates and caused a significant drop in the damping ratios, but the viscoelastic material damping remained about constant. Even though the damping ratios decreased, they were always greater than 2 times the damping ratios of undamped control plates. Real fan blades have smaller increases in natural frequencies with rotational speed, and therefore, the decrease in fan blade damping ratio should be smaller than measured in this experiment.

From the results, we concluded that the presence of centrifugal forces, which are well-known to increase blade bending stiffness and corresponding natural frequencies, decreased damping ratios. This phenomenon occurred because as the blade stiffened the percent of modal strain energy in the damping material decreased, thus decreasing the modal damping ratios. To further improve damping, designers will need to consider how to

increase the strain energy level in the viscoelastic material, such as using a stiffer viscoelastic damping material than used here. This study reveals not only the potential of integral viscoelastic material damping in composite fan blades, but also illustrates that there are technical challenges that still must be overcome before it can be effectively used as a design option.

**Lewis contact:**

Oral Mehmed, (216) 433-6036,  
Oral.Mehmed@lerc.nasa.gov

**Author:** Oral Mehmed

**Headquarters program office:** OASTT

**Programs/Projects:**

Propulsion systems R&T, SGE

## Lewis-Developed Seal Is a Key Technology for High-Performance Engines

Ultrahot, pressurized combustion gases within the National Aerospace Plane (NASP) engine needed to be sealed to prevent them from leaking past the movable engine panels to rear engine cavities and causing the engine or entire aircraft to fail. The need to seal the hot gases and distortion of the engine's sidewalls required the development of a device nearly as flexible as a rubber O-ring yet able to operate at over 2000 °F. The advanced, High-Temperature, Flexible Fiber Preform Seal is one very important step in that direction.

This seal is braided of emerging high-temperature ceramic fibers or super-alloy wires into a flexible, flow-resistant seal. It has been used for numerous NASA applications since it was patented in 1992. The patented technology was used by GE in the joint NASA/Department of Defense/GE Integrated High Performance Turbine Engine Technology (IHPTET) program. This hybrid rope seal successfully sealed the perimeter of advanced nickel-aluminide turbine vane airfoils, allowing the vanes to grow relative to the supporting structure, thus overcoming the thermal shock failure experienced with the conventional sealing approach. In a successful full-scale Joint Turbine Advanced Gas Generator (JTAGG) engine test, the high-temperature turbine vane/seals, in combination with several other advanced technologies, contributed to meeting the program goals of reducing specific fuel consumption by 20 percent and increasing the engine power-to-weight ratio by 40 percent.

The invention is being evaluated by Pratt & Whitney as a potential replacement for sealing interfaces between large nozzle turning vanes and flow-path fairing elements (see the figure) for the F119 engine that will be used in the F22 fighter, the country's next-generation premier fighter. Pratt &

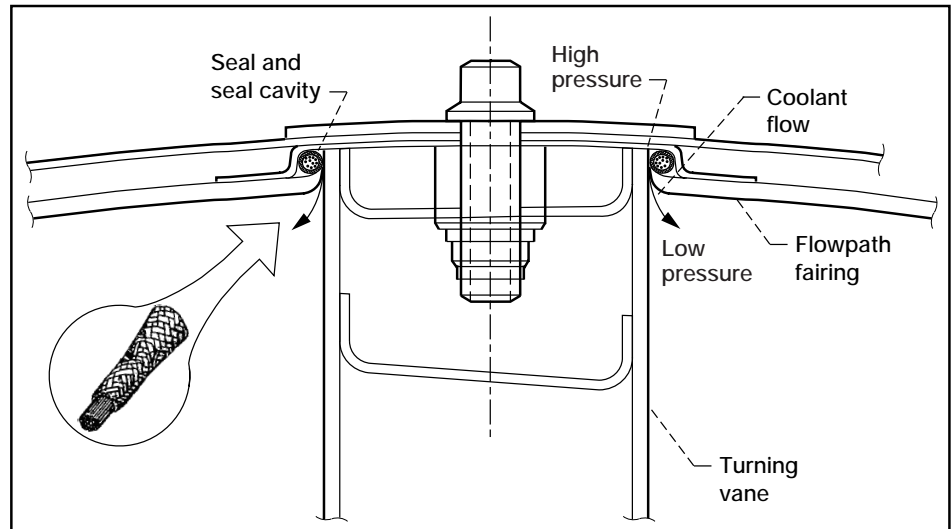
Whitney tested the seal in a full-scale engine (Fall 1997), and after 24 hr of testing the seals showed no signs of degradation.

In addition, Williams International is evaluating the seal for an advanced turbine engine, and AlliedSignal Inc. is considering using the seal as part of an industrial gas turbine generator for auxiliary electric power. Lewis researchers helped qualify the seals for subsequent engine and industrial system tests.

NASA is developing a future replacement for the space shuttle and will be testing many of the technologies on an experimental vehicle, the X-33. The X-33 contractor team is exploring possible use of the NASA rope seals for sealing the joints between the aerospike engine nozzles and the joints between the vehicle's heat-resistant thermal tiles.

### Seal Requirements

- Operate hot—  
Seal/metal temperature, 1200 °F  
Gas stream temperature, last stage vane
- Exhibit low leakage; minimize cooling requirements
- Permit relative vane-to-shroud thermal growths
- Seal complex turbine airfoil geometries
- Resist abrasion in high acoustic environment
- Maintain structural integrity



*Pratt & Whitney turbine vane seal for the F22 fighter engine.*

Although the seal was developed for aerospace uses, it is being evaluated for industrial applications as well. Under a reimbursable Space Act Agreement, NASA Lewis is working with Praxair, a major U.S. producer of industrial gases, to adapt the seal technology for use in the company's high-temperature, proprietary industrial gas systems. Other potential future applications include sealing furnace doors, heat exchangers, and continuous-casting and glass-processing equipment.

The seal is able to bend around sharp radii (about equal to the seal's diameter) conforming to and sealing complex components. In addition, the seal exhibits low leakage, retains resilience after high-temperature cycling, and can support structural loads.

**For more information, be sure to check our web site:**

[http://www.lerc.nasa.gov/WWW/TU/InventYr/1996Inv\\_Yr.htm](http://www.lerc.nasa.gov/WWW/TU/InventYr/1996Inv_Yr.htm)

**Lewis contact:** Dr. Bruce M. Steinetz, (216) 433-3302,  
[Bruce.M.Steinetz@lerc.nasa.gov](mailto:Bruce.M.Steinetz@lerc.nasa.gov)

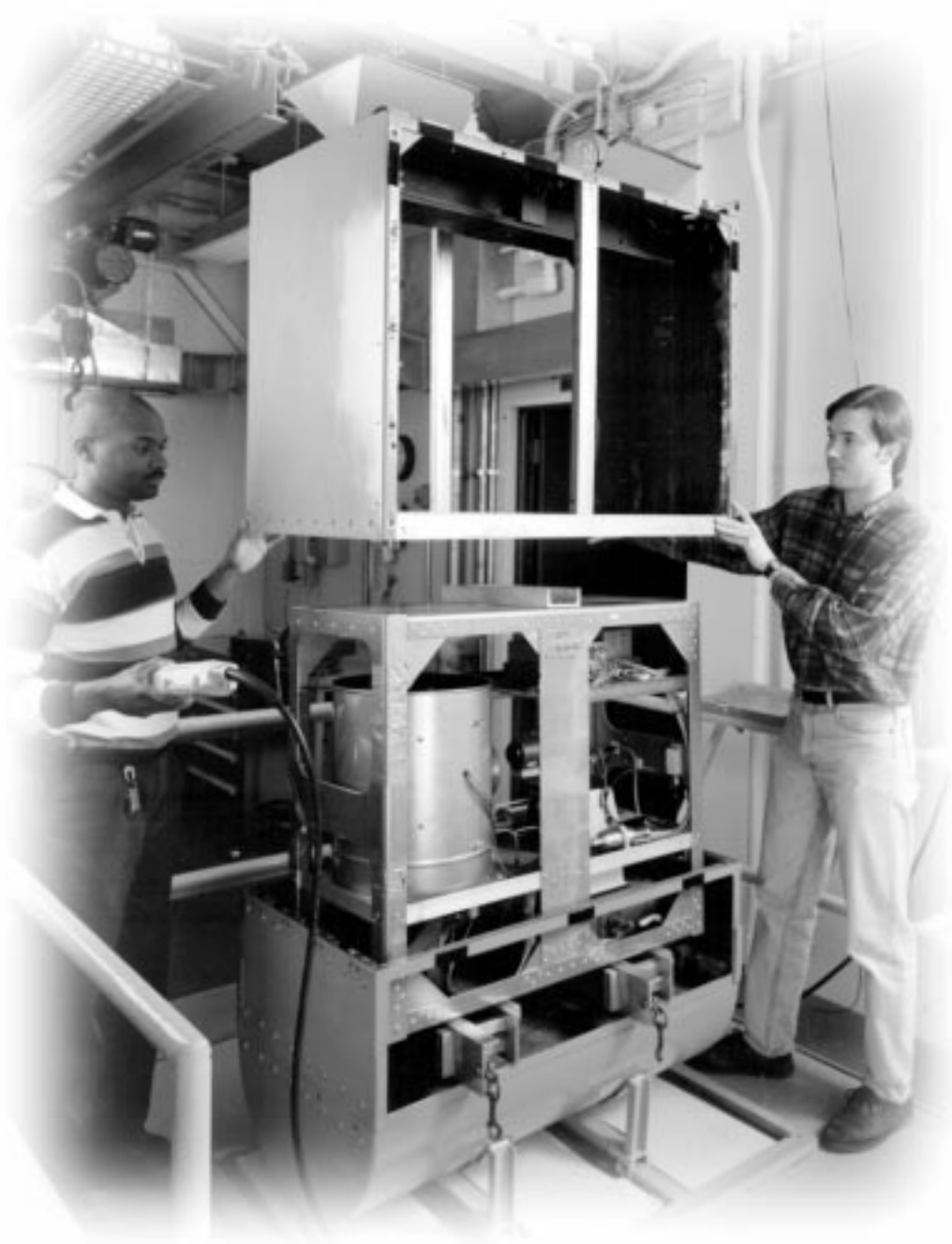
**Author:** Dr. Bruce M. Steinetz

**Headquarters program office:** OASTT

**Programs/Projects:** Propulsion Systems R&T, HITEMP

**Special recognition:** The 1996 Government Invention of the Year was awarded to Dr. Bruce Steinetz and Mr. Paul Sirocky (retired) for co-developing the advanced, High-Temperature, Flexible Fiber Preform Seal. This is the first time Lewis has won this NASA-wide competition since 1988 when Harold Sliney won the award for his high-temperature solid-film lubricants.

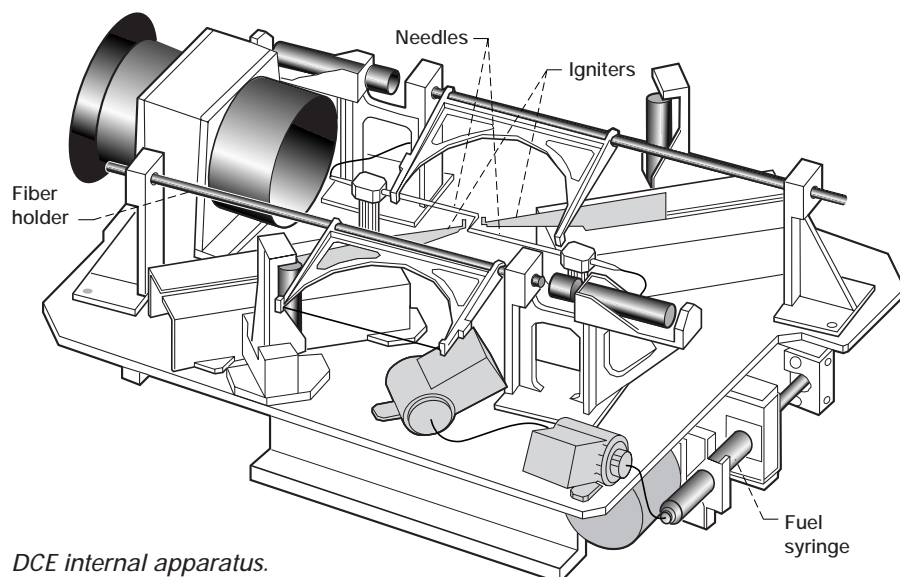
# Space



# Microgravity Science

## Droplet Combustion Experiment

Liquid fuel combustion provides a major portion of the world's energy supply. In most practical combustion devices, liquid burns after being separated into a droplet spray. Essential to the design of efficient combustion systems is a knowledge of droplet combustion behavior. The microgravity environment aboard spacecraft provides an opportunity to investigate the complex interactions between the physical and chemical combustion processes involved in droplet combustion without the complications of natural buoyancy.



*DCE internal apparatus.*

Launched on STS-83 and STS-94 (April 4 and July 1, 1997), the Droplet Combustion Experiment (DCE) investigated the fundamentals of droplet combustion under a range of pressures (0.25 to 1 atm), oxygen mole fractions ( $<0.5$ ), and droplet sizes (1.5 to 5 mm). Principal DCE flight hardware features were a chamber to supply selected test environments, the use of crew-inserted bottles, and a vent system to remove unwanted gaseous combustion products. The illustration above shows the internal apparatus located inside the test chamber. The internal apparatus contained the droplet deployment and ignition mechanisms to burn single, freely deployed droplets in microgravity. Diagnostics systems included a 35-mm high-speed motion picture camera (see the sequence of photos on the opposite page) with a backlight to photograph burning droplets and a camcorder to monitor experiment operations. Additional diagnostics included an ultraviolet-light-sensitive CCD (charge couple discharge) camera to obtain flame radiation from hydroxyl radicals (see the bottom figure on the opposite page) and a 35-mm SLR (single-lens-reflex) camera to obtain color still photographs of the flames.

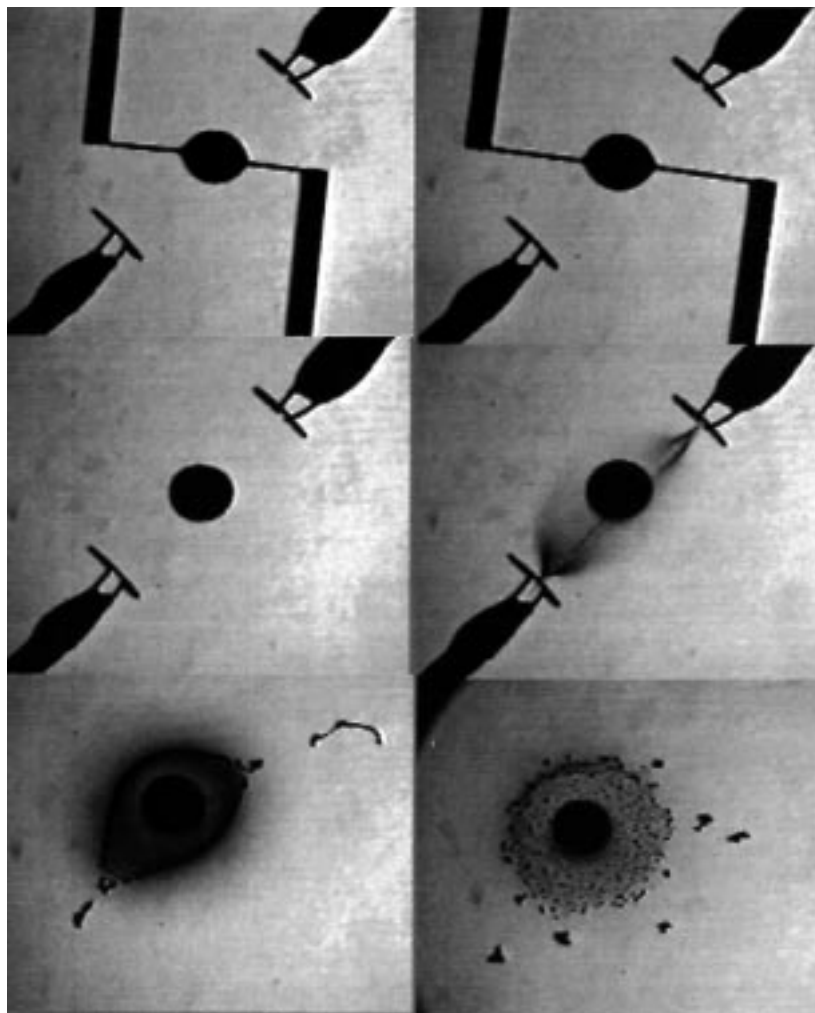
The DCE experiments, which were carried out during the Microgravity Science Laboratory (MSL-1) mission in Spacelab, burned n-heptane droplets in helium-oxygen test gases and identified three regimes of droplet combustion. Droplets burned for as long as 20 seconds, much too long a

time to be studied in Earth-bound facilities. The first regime was the quasi-steady regime, a fairly well documented regime in which the droplets and flames decrease linearly with time until extinction. The extinction size can be related to the chemical kinetics of combustion. A much less well documented regime (flame radiation) occurred when sufficiently large droplets and low oxygen levels were used.

Extinction occurred soon after ignition because of the large radiation heat losses from the flames. Finally, another less well documented regime (droplet disappearance) occurred when oxygen levels were sufficiently high. A flame would persist for a short time after the droplet had completely vaporized and would extinguish at a nonzero flame radius. This regime leaves behind a small vapor cloud that might be responsible for combustion inefficiencies in practical combustion systems.

Professor Forman A. Williams of the University of California, San Diego, and Professor Frederick L. Dryer of Princeton University served as the principal investigator and coinvestigator, respectively, for the DCE experiments. The DCE hardware was designed and built at the NASA Lewis Research Center.

The experiment results will aid in reducing air pollution, conserving fuel energy sources, and improving fire safety. Extinction and soot-generation phenomena will help researchers to determine the best way to build fire protection systems as well as help designers to design efficient combustion systems for space that are low in unwanted combustion product pollutants.



*Droplet growth, deployment, and burning sequence from a 35-mm high-speed camera.*

**Lewis contacts:**

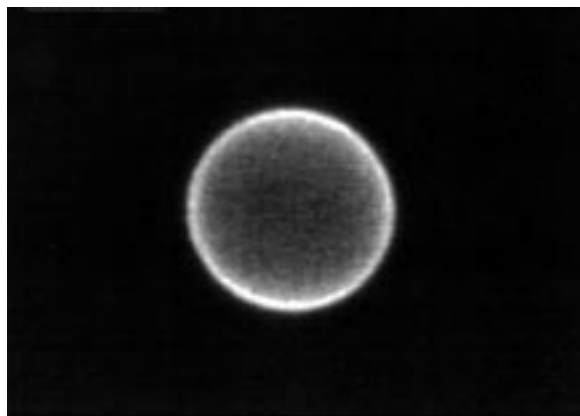
Dr. Vedha Nayagam (Project Scientist)  
(216) 433-8702,  
Vedha.Nayagam@lerc.nasa.gov, and  
John Haggard (Project Manager),  
(216) 433-2832,  
John.B.Haggard@lerc.nasa.gov

**Author:** Dr. Vedha Nayagam

**Headquarters program office:** OLMSA

**Programs/Projects:**

HEDS, Microgravity Science, STS-83,  
STS-94, MSL-1, MSL-1R



*Hydroxyl radical chemiluminescence obtained from an ultraviolet camera for an n-heptane droplet burning in a 30 oxygen – 70 helium (mole fraction) environment at 1-atm pressure.*



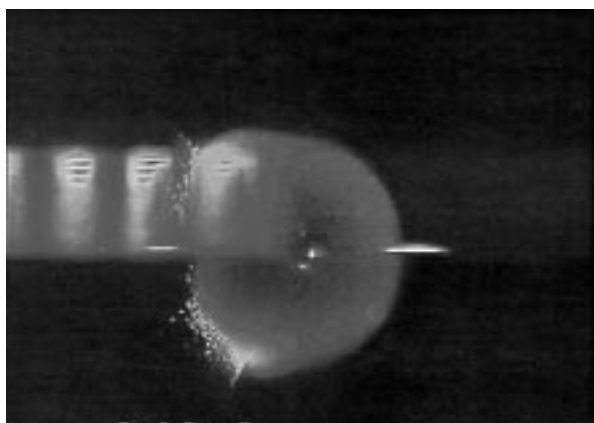
## Fiber-Supported Droplet Combustion Experiment–2

A major portion of the energy produced in the world today comes from the burning of liquid hydrocarbon fuels in the form of droplets. Understanding the fundamental physical processes involved in droplet combustion is not only important in energy production but also in propulsion, in the mitigation of combustion-generated pollution, and in the control of the fire hazards associated with handling liquid combustibles. Microgravity makes spherically symmetric combustion possible, allowing investigators to easily validate their droplet models without the complicating effects of gravity. The Fiber-Supported Droplet Combustion (FSDC–2) investigation was conducted in the Microgravity Glovebox facility of the shuttles' Spacelab during the reflight of the Microgravity Science Laboratory (MSL–1R) on STS–94 in July 1997. FSDC–2 studied fundamental phenomena related to liquid fuel droplet combustion in air. Pure fuels and mixtures of fuels were burned as isolated single and duo droplets with and without forced air convection. FSDC–2 is sponsored by the NASA Lewis Research Center, whose researchers are working in cooperation with several investigators from industry and academia.

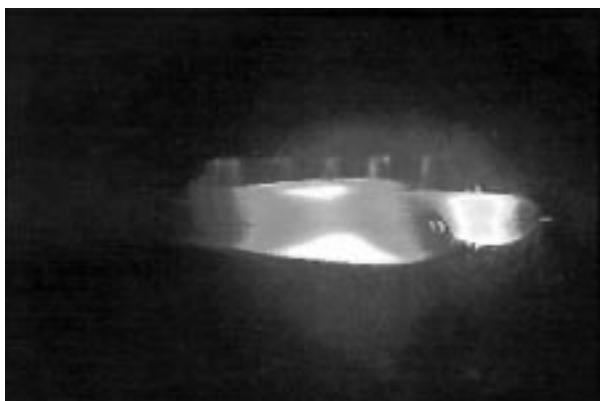
The rate at which a droplet burns is important in many commercial applications. The classical theory of droplet burning assumes that, for an isolated, spherically symmetric, single-fuel droplet, the gas-phase combustion processes are much faster than the droplet surface regression rate and that the liquid phase is at a uniform temperature equal to the boiling point. Recent, more advanced models predict that both the liquid and gas phases are unsteady during a substantial portion of the droplet's burning history, thus affecting the instantaneous and average burning rates, and that flame radiation is a dominant mechanism that can extinguish flames in a microgravity environment. FSDC–2 has provided well-defined, symmetric droplet burning data including radiative emissions to validate these theoretical models for heptane, decane, ethanol, and methanol fuels. Since most commercial combustion systems burn droplets in a convective environment, data were obtained without and with convective flow over the burning droplet (see the following photos).

Multicomponent droplet burning studies are motivated by the need to understand the burning characteristics of blended fuels and liquid hazardous wastes. Depending on the relative concentrations and volatilities of the components and their miscibility, multicomponent fuels can exhibit peculiar, unsteady burning characteristics such as the formation of vapor bubbles in the droplet if the droplet internal temperature exceeds the bubble nucleation temperature of a fuel component.

The importance of liquid species diffusion in multicomponent droplet burning has also been recognized. In normal-gravity experiments, buoyancy can destroy the spherical symmetry by inducing convective mixing in the gas and liquid phases; therefore, microgravity experiments help to clarify the phenomena occurring during multicomponent droplet burning. Also, product dissolution can change an initially pure fuel into a multicomponent fuel, a behavior observed in alcohol fuels when combustion-generated water is absorbed by the fuel, leading to nonlinear burning. FSDC–2 has



*Heptane droplet. Left: Without flow. Right: With flow.*



*Double decane droplets with flow.*

provided data on the burning of methanol/water, ethanol/water, and heptane/hexadecane fuel mixtures.

Most combustion systems involve the burning of many droplets. On FSDC-2, droplet interactions were investigated with decane fuel with and without convective flow (see the preceding photo). Two droplets were

placed side by side. The data obtained from the burning of a single stationary droplet and double droplets is helping researchers understand and solve physical processes in more complex combustion systems.

**Lewis contact:**

Dr. Vedha Nayagam, (216) 433-8702,  
Vedha.Nayagam@lerc.nasa.gov

**Author:** Dr. Renato O. Colantonio

**Headquarters program office:** OLMSA

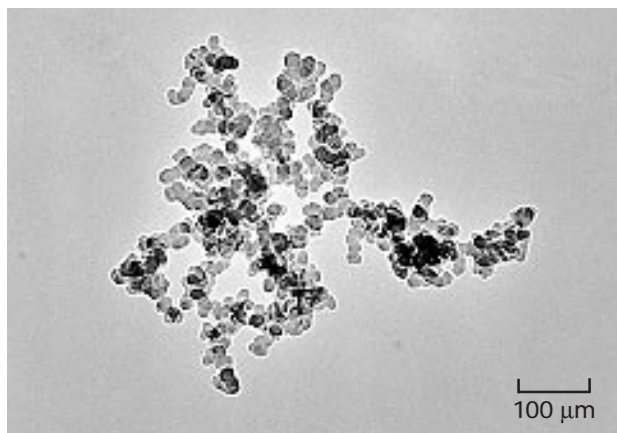
**Programs/Projects:** HEDS, Microgravity Science, STS-94, MSL-1R, FSDC-2

## Laminar Soot Processes Experiment Is Shedding Light on Flame Radiation

The Laminar Soot Processes (LSP) experiment investigated soot processes in nonturbulent, round gas jet diffusion flames in still air. The soot processes within these flames are relevant to practical combustion in aircraft propulsion systems, diesel engines, and furnaces. However, for the LSP experiment, the flames were slowed and spread out to allow measurements that are not tractable for practical, Earth-bound flames.

It is a remarkable paradox of nature that flames, which are widely recognized to consume solid fuels and create gaseous combustion products, also create new solid materials—soot—in their highest-temperature regions

(as shown in the photomicrograph). The mechanisms that produce soot in flames are among the most important unknowns of combustion science because soot affects contemporary life in many ways. Even though the production of soot as carbon black is important for numerous ordinary industrial products, soot contributes to many serious problems: pollution, undesirable radiative heat loads to combustion chambers, and the spread of unwanted fires via radiant emission. The peer-reviewed LSP experiment was developed to enhance our understanding of this critical combustion product. It was conceived at the University of Michigan by Professor Gerard M. Faeth and developed by the NASA Lewis Research Center in collaboration with Analex Corporation and Aerospace Design & Fabrication (ADF).



*Transmission electron micrograph of soot from STS-83.*

LSP flew as scheduled on April 4, 1997, on the STS-83 space shuttle mission. Because STS-83 had to be shortened, LSP flew again on STS-94. LSP is a complex experiment; nevertheless, it functioned flawlessly on both flights and yielded new results well beyond expectations. In fact, with the cooperation of the crew, we successfully completed 2 tests on STS-83 and 19 on STS-94, which is 7 more than originally planned. Major findings are summarized in the following paragraphs.

The new measurements demonstrated for the first time that the propensity of nonbuoyant flames to contain large concentrations of soot is not related to their propensity to emit soot. This finding is relevant to both practical nonbuoyant flames and spacecraft fire safety. It also is important in the selection of test conditions for future testing of nonbuoyant, soot-containing flames. This result had not been demonstrated previously because of the limited test times available in ground-based low-gravity facilities.

Most importantly, our initial analysis of the new measurements suggests that universal relationships exist between the soot processes and the degree of mixing within nonbuoyant flames. These relationships are known as the soot paradigm, a controversial hypothesis based on indirect observations of practical nonbuoyant flames. If the paradigm proves to be

true—after further analysis of this unique data set of “steady,” soot-containing, nonbuoyant flames with and without soot emissions—it offers simple ways to control and model soot processes in practical flames.

The mechanism of flame extinction caused by radiative heat loss, in this case from soot, was quantified for the first time by direct measurements of soot temperatures. This mechanism is unusual because a microgravity flame quenches near its tip, unlike a buoyant flame on Earth, which quenches near its base. The new measurements also yielded the first observations of the simultaneous emission of soot and unburned hydrocarbons from steady nonbuoyant flames and the first-ever observation of a smoke point (minimum flame height for soot emission) from steady, nonbuoyant flames.

Finally, the nonbuoyant flames are larger and emit soot at lower flame heights than flames observed in ground-based microgravity facilities because testing during orbit allows truly steady flames to be observed. These flames were 100-percent larger than weakly buoyant flames on Earth and were 50-percent larger than flames observed in transient tests in Lewis’ ground-based microgravity facilities. The following figure shows soot in a steady microgravity flame.

**More information about this research is available on the World Wide Web:**  
<http://einstein.lerc.nasa.gov/dlurban/lsp/lspbrouchure.html> (All l’s in this URL are lowercase L’s.)

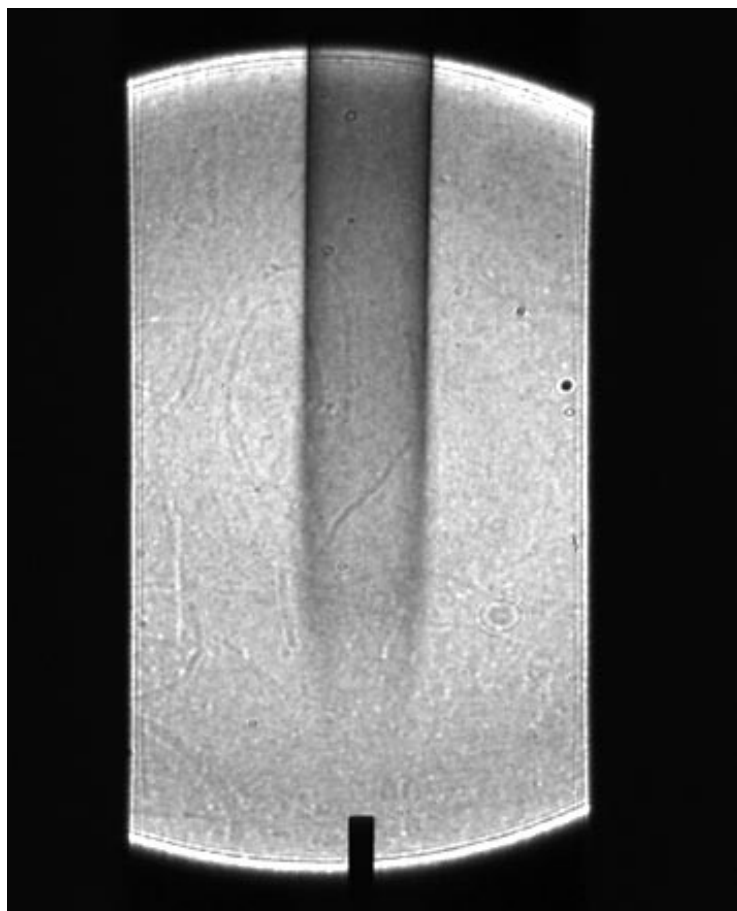
**Lewis contact:**

Dr. David L. Urban, (216) 433-2835,  
[David.L.Urban@lerc.nasa.gov](mailto:David.L.Urban@lerc.nasa.gov)

**Author:** Dr. David L. Urban

**Headquarters program office:** OLMSA

**Programs/Projects:** HEDS, Microgravity Science, STS-83, STS-94, MSL-1



*Shadow image of soot in a microgravity ethylene flame on STS-83. The bright area is illuminated by the laser, the “notch” at the bottom is the shadow of the nozzle, and the soot shadow is above the “notch.”*

## Structure of Flame Balls at Low Lewis-Number

The Structure of Flame Balls at Low Lewis-Number (SOFBALL) experiment explored the behavior of a newly discovered flame phenomena called "flame balls." These spherical, stable, stationary flame structures, observed only in microgravity, provide a unique opportunity to study the interactions of the two most important processes necessary for combustion (chemical reaction and heat and mass transport) in the simplest possible configuration. The previously unobtainable experimental data provided a comparison with models of flame stability and flame propagation limits that are crucial both in assessing fire safety and in designing efficient, clean-burning combustion engines.

The SOFBALL experiment was conceived by Professor Paul Ronney of the University of Southern California and designed and developed by the NASA Lewis Research Center. It was conducted in the Combustion Module-1 (CM-1) of the Microgravity Science Laboratory payload during Space Shuttle Columbia missions STS-83 and STS-94. Mixtures of hydrogen, oxygen, and a third inert component of either nitrogen, carbon dioxide, or sulfur hexafluoride were burned. Video images, radiant fluxes, chamber pressure, temperature, and gas concentrations were measured to characterize flame ball properties and behavior.

Instead of the 15 tests planned, a total of 19 experiment runs were completed on the two missions, and 18 of the mixtures ignited. These mixtures produced from one to nine flame balls, with the mixtures that had more fuel producing multiple flame balls. Most of the tests burned for 500 sec until the experiment timeout extinguished the flames by turning on a fan. Eleven of the initial burns were ignited by spark a second time, and eight of them burned for an additional 500 sec until experiment timeout. A total of 60 flame balls were produced.



*Flame balls from a mixture of 4 vol % hydrogen in air, 30 sec after ignition. The flame ball diameters ranged from 5 to 15 mm.*

From the preliminary data obtained during the test runs, we have made the following conclusions:

- (1) Steady, nearly stationary flame balls exist in an extended-duration microgravity environment.
- (2) The extended length of the burns verifies the theoretical predictions that these flames evolve on a very slow time scale, on the order of hundreds of seconds.
- (3) The flame balls are sensitive to orbiter thrust firings above 50  $\mu\text{g}$ -sec. During free-drift periods, the flame balls were nearly motionless for many minutes, whereas the flame ball moved slightly after vernier thruster firings or water dumps.
- (4) All the burns, regardless of the inert component of the flame ball, the number of flame balls, or the pressure, produced between 1 and 1.8 W of radiant power, in disagreement with pre-mission predictions.

The SOFBALL experiment accomplished a number of scientific firsts:

- (1) it was the first premixed gas combustion experiment in space,
- (2) it produced the weakest flames ever burned, either on the ground or in space,
- (3) it measured flame ball powers as low as 1 W, and
- (4) it produced the longest-lived gas flames ever burned in space.

The SOFBALL experiment also accomplished a number of combustion program firsts: (1) multiple combustion investigations were conducted in a single facility, (2) a pressure vessel was breached and recertified on-orbit to handle hazardous gases, (3) spark ignition



was used for combustion in space, (4) gases were mixed on-orbit to create new test mixtures, and (5) hazardous postcombustion products were cleaned up on-orbit before they were vented into space.

**More information is available on the World Wide Web:**

<http://cpl.usc.edu/sofball/>

<http://zeta.lerc.nasa.gov/cm1/webbed.htm>

**Lewis contact:** Dr. Karen J. Weiland, (216) 433-3623,  
[Karen.J.Weiland@lerc.nasa.gov](mailto:Karen.J.Weiland@lerc.nasa.gov)

**Authors:** Dr. Karen J. Weiland and Prof. Paul Ronney

**Headquarters program office:** OLMSA

**Programs/Projects:**

HEDS, Microgravity Science, STS-83, STS-94, MSL-1, MSL-1R, CM-1

**Special recognition:** The SOFBALL experiment was mentioned in several publications during and after the STS-94 mission: USA Today and the Associated Press, Science News, and Chemical and Engineering News.

## Physics of Hard Spheres Experiment (PhaSE) or "Making Jello in Space"

The Physics of Hard Spheres Experiment (PhaSE) is a highly successful experiment that flew aboard two shuttle missions to study the transitions involved in the formation of jellolike colloidal crystals in a microgravity environment. A colloidal suspension, or colloid, consists of fine particles, often having complex interactions, suspended in a liquid. Paint, ink, and milk are examples of colloids found in everyday life. In low Earth orbit, the effective force of gravity is thousands of times less than at the Earth's surface. This provides researchers a way to conduct experiments that cannot be adequately performed in an Earth-gravity environment. In microgravity, colloidal particles freely interact without the complications of settling that occur in normal gravity on Earth. If the particle interactions within these colloidal suspensions could be predicted and accurately modeled, they

could provide the key to understanding fundamental problems in condensed matter physics and could help make possible the development of wonderful new "designer" materials. Industries that make semiconductors, electro-optics, ceramics, and composites are just a few that may benefit from this knowledge.



*Interior view of PhaSE test section.*

Atomic interactions determine the physical properties (e.g., weight, color, and hardness) of ordinary matter. PhaSE uses colloidal suspensions of microscopic solid plastic spheres to model the behavior of atomic interactions. When uniformly sized hard spheres suspended in a fluid reach a certain concentration (volume fraction), the particle-fluid mixture changes from a disordered fluid state, in which the spheres are randomly organized, to an ordered "crystalline" state, in which they are structured periodically. The thermal energy of the spheres causes them to form ordered arrays, analogous to crystals. Seven of the eight PhaSE samples ranged in volume fraction from 0.483 to 0.624 to cover the range of interest, while one sample, having a concentration of 0.019, was included for instrument calibration.

The hardware that housed the experiment included a complex state-of-the-art optics system, the experiment samples, cameras, fiber optics, temperature sensors, and



the motor drives necessary to control the experiment. The preceding photo shows an interior view of the test section, including the carousel of eight sample cells, a Bragg imaging screen, cell mixing and positioning motors, and lights for photography. Not visible are the dynamic and static light-scattering systems, the color CCD (charge couple discharge) camera for digital imaging, and the avionics.

PHaSE flew in an EXPRESS rack (EXpedite the PROcessing of Experiments to Space Station) on the first Microgravity Science Laboratory (MSL-1), onboard Columbia during shuttle missions STS-83 and STS-94. The experiment was conceived by Professors Paul M. Chaikin and William B. Russel with Research Scientist Dr. Jixiang Zhu, all of Princeton University. The hardware and software were designed, built, and tested by NYMA, Inc., and Aerospace Design & Fabrication (ADF) at the NASA Lewis Research Center in Cleveland, Ohio.

Several novel light-scattering techniques were used to gather data from experiment samples. The investigative team compared these data with measurements performed under normal gravity to discern the equilibrium behavior from the effects due to gravity, as well as to determine the structure of the crystalline phase, the dynamics of crystal growth, the viscosity of the disordered phase, the elasticity of the ordered phase, and the nature and appearance of the glass transition. The following illustration shows a chronological series of digital images of a sample in various stages of

crystallization both on Earth in normal gravity and in microgravity. In normal gravity, the dominant crystal structure appears to have a face-centered cubic orientation with irregularities in successive layers. In microgravity, however, the dominant structure appears to have a random hexagonal-close-packed orientation with very little face-centered cubic orientation present. Preliminary data also suggest that the crystallization process is accelerated in microgravity at lower sample concentrations. Because of the quantity of data obtained during this very successful experiment, postflight data analysis will continue during the next year.

**More information about this research is available on the World Wide Web:**

**PHaSE science home page:**

<http://zeta.lerc.nasa.gov/6712/ling/chaikin/science.htm>

**PHaSE official home page:** <http://sven.lerc.nasa.gov/projects/Phase/>

**Lewis contacts:**

Jerri S. Ling (Project Scientist),  
(216) 433-2841,  
[Jerri.S.Ling@lerc.nasa.gov](mailto:Jerri.S.Ling@lerc.nasa.gov), and  
Michael P. Doherty (Project Manager),  
(216) 433-6641,  
[Michael.P.Doherty@lerc.nasa.gov](mailto:Michael.P.Doherty@lerc.nasa.gov)

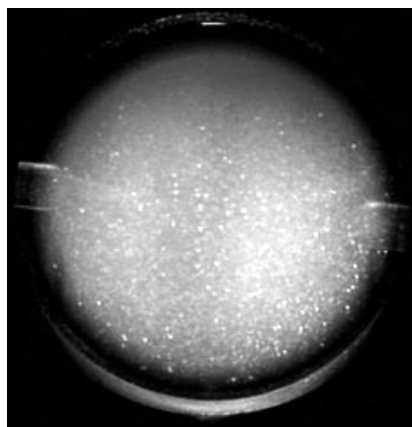
**Authors:** Jerri S. Ling and  
Michael P. Doherty

**Headquarters program office:** OLMSA

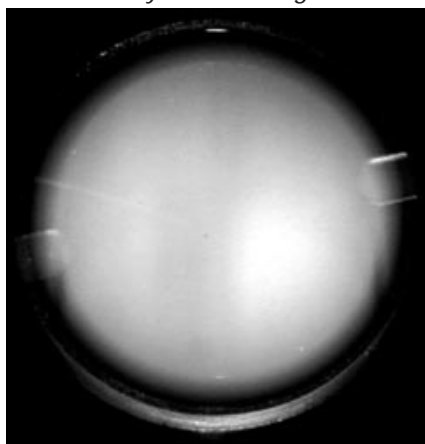
**Programs/Projects:** HEDS, Microgravity  
Science, STS-83, STS-94, MSL-1



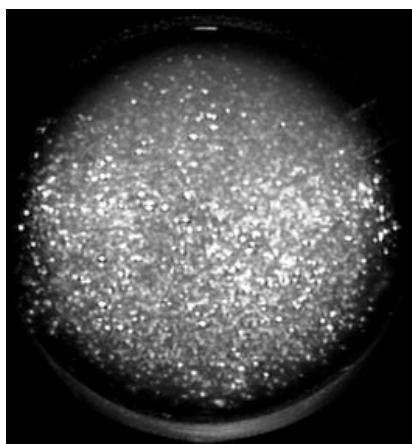
*Crystallized at 1g*



*Nucleation on-orbit*



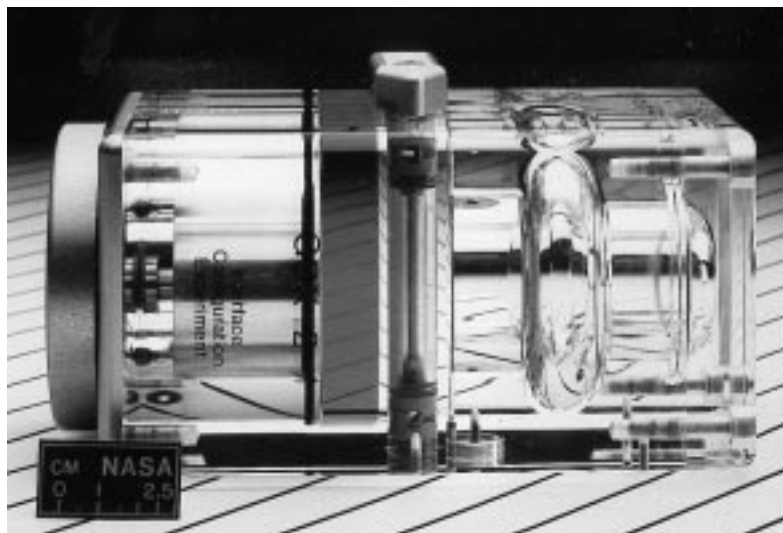
*Mixed on-orbit*



*Crystallized on-orbit*

*Digital images of an STS-94 PHaSE sample with a volume fraction of 0.528.*

# Liquid-Vapor Interface Configurations Investigated in Low Gravity



*ICE vessel used on Mir.*

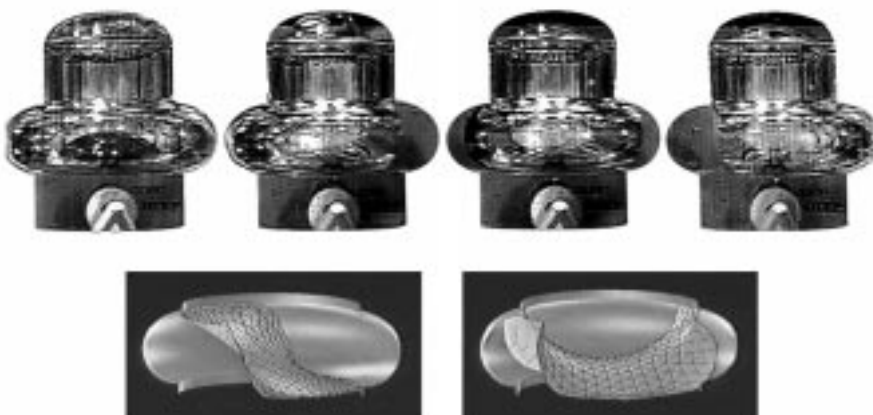
The Interface Configuration Experiment (ICE) is part of a multifaceted study that is exploring the often striking behavior of liquid-vapor interfaces in low-gravity environments. Although the experiment was posed largely as a test of current mathematical theory, applications of the results should be manifold.

In space almost every fluid system is affected, if not dominated, by capillarity (the effects of surface tension). As a result, knowledge of fluid interface behavior, in particular an equilibrium interface shape from which any analysis must begin, is fundamental—from the control of liquid fuels and oxygen in storage tanks to the design and development of in-space thermal systems, such as heat pipes and capillary pumped loops. ICE has increased, and should continue to increase, such knowledge as it probes the specific peculiarities of current theory upon which our present understanding rests.

Several versions of ICE have been conducted in the drop towers at the NASA Lewis Research Center, on the space shuttles during the first and second United States Microgravity Laboratory missions (USML-1 and USML-2), and most recently aboard the Russian Mir space station. These studies focused on interfacial problems concerning the existence, uniqueness, configuration, stability, and flow characteristics of liquid-vapor interfaces. Results to date have clearly demonstrated the value of the present theory and the extent

to which it can predict the behavior of capillary systems.

For example, on Mir the experiments conducted by crew member Shannon Lucid revealed that multiple, locally stable interface shapes are indeed possible in a single rotationally symmetric container. What is striking about these capillary surface configurations is that some of them are not rotationally symmetric. Though such configurations have been predicted mathematically and numerically, the concept of asymmetric surfaces in symmetric containers is startling, particularly when such surfaces can possess differing characteristics, such as natural frequency, damping, and stability. At present there is no method to predict how many locally stable interfaces a given container might yield, even for the relatively simple geometry of ICE aboard Mir. Nonetheless, such results communicate clearly that designers of in-space fluids systems should be aware of, if not account for or exploit, such possibilities in fluids management processes.



*Interfaces observed during Mir space station ICE experiments and numerical predictions. Top, left to right: observed symmetric, spoon right, potato chip, and spoon left configurations. Bottom, left to right: computed spoon left and potato chip configurations.*

These experiments were conceived and developed by Paul Concus of the Lawrence Berkeley Laboratory and the University of California at Berkeley, Robert Finn of Stanford University, and Mark Weislogel of the NASA Lewis Research Center. The experiment hardware was designed and built at Lewis.

**Find out more on the World Wide Web:**

<http://zeta.lerc.nasa.gov/expr2/ice-mir.htm>  
<http://zeta.lerc.nasa.gov/expr2/ice.htm>

**Lewis contact:** Mark M. Weislogel, (216) 433-2877,  
 Mark.M.Weislogel@lerc.nasa.gov

**Authors:** Paul Concus, Robert Finn, and Mark M. Weislogel

**Headquarters program office:** OLMSA

**Programs/Projects:** HEDS, Microgravity Science, USML-1, USML-2, Mir

## NASA Lewis' Telescience Support Center Supports Orbiting Microgravity Experiments



*Mission operations area of the Telescience Support Center.*

The Telescience Support Center (TSC) at the NASA Lewis Research Center was developed to enable Lewis-based science teams and principal investigators to monitor and control experimental and operational payloads onboard the International Space Station. The TSC is a remote operations hub that can interface with other remote facilities, such as universities and industrial laboratories. As a pathfinder for International Space Station telescience operations, the TSC has incrementally developed an operational capability by supporting space shuttle missions. The TSC has evolved into an environment where experimenters and scientists can control and monitor the health and status of their experiments in near real time. Remote operations (or telescience) allow local scientists and their experiment teams to minimize their travel and maintain a local complement of expertise for hardware and software troubleshooting and data analysis.

The TSC was designed, developed, and is operated by Lewis' Engineering and Technical Services Directorate and its support contractors, Analex Corporation and White's Information System, Inc. It is managed by Lewis' Microgravity Science Division.

The TSC provides operational support in conjunction with the NASA Marshall Space Flight Center and NASA Johnson Space Center. It enables its customers to command, receive, and view telemetry; monitor the science video from their on-orbit experiments; and communicate over mission-support voice loops. Data can be received and routed to experimenter-supplied ground support equipment and/or to the TSC data system for display. Video teleconferencing capability and other video sources, such as NASA TV, are also available. The TSC has a full complement of standard services to aid experimenters in telemetry operations.

In fiscal year 1997, the TSC supported three missions and their associated simulations. In the past

year, there have been many Lewis-sponsored microgravity experiments onboard the shuttles: The mission provided support for the Solid Surface Combustion Experiment (SSCE) on STS-85, and for the Space Acceleration Measurement System (SAMS), PI Microgravity Management Services team, Droplet Combustion Experiment (DCE), Combustion Module-1 (CM-1), Glovebox, Large Isothermal Furnace (LIF), Physics of Hard Spheres Experiment (PHaSE), and Orbital Acceleration Research Experiment (OARE) experiments on the STS-83/MSL-1 mission. STS-94 was a reflight of STS-83 and supported all of the experiments listed for STS-83. The STS-87/USMP-4 mission, which is scheduled for November 1997, includes support for SAMS, the PI Microgravity Management Services team, and the Isothermal Dendritic Growth Experiment (IDGE).

After STS-87/USMP-4 in November of 1997, the TSC will redirect all resources toward the upcoming International Space Station era. At that time, TSC equipment will undergo a major systems upgrade in preparation for incremental Space Station Utilization Flight 1 (UF-1) support. The TSC will support fluids, combustion, and microgravity environment experiments from NASA Lewis during the International Space Station era.

**Find out more about the TSC on the World Wide Web:**

[http://einstein.lerc.nasa.gov/tsc/html's/TSC\\_Main\\_blk.html](http://einstein.lerc.nasa.gov/tsc/html's/TSC_Main_blk.html)

**Lewis contacts:**

Karen L. Carlisle, (216) 433-5297,  
Karen.L.Carlisle-Morgan@lerc.nasa.gov,  
and Bob W. Hawersaat,  
(216) 433-8157,  
Robert.W.Hawersaat@lerc.nasa.gov

**Author:** Bob W. Hawersaat

**Headquarters program office:** OLMSA

**Programs/Projects:** HEDS, Microgravity Science, STS-83, STS-85, STS-87, STS-94, MSL-1, USMP-4, CM-1, ISS

## Capillary-Driven Heat Transfer Experiment: Keeping It Cool in Space

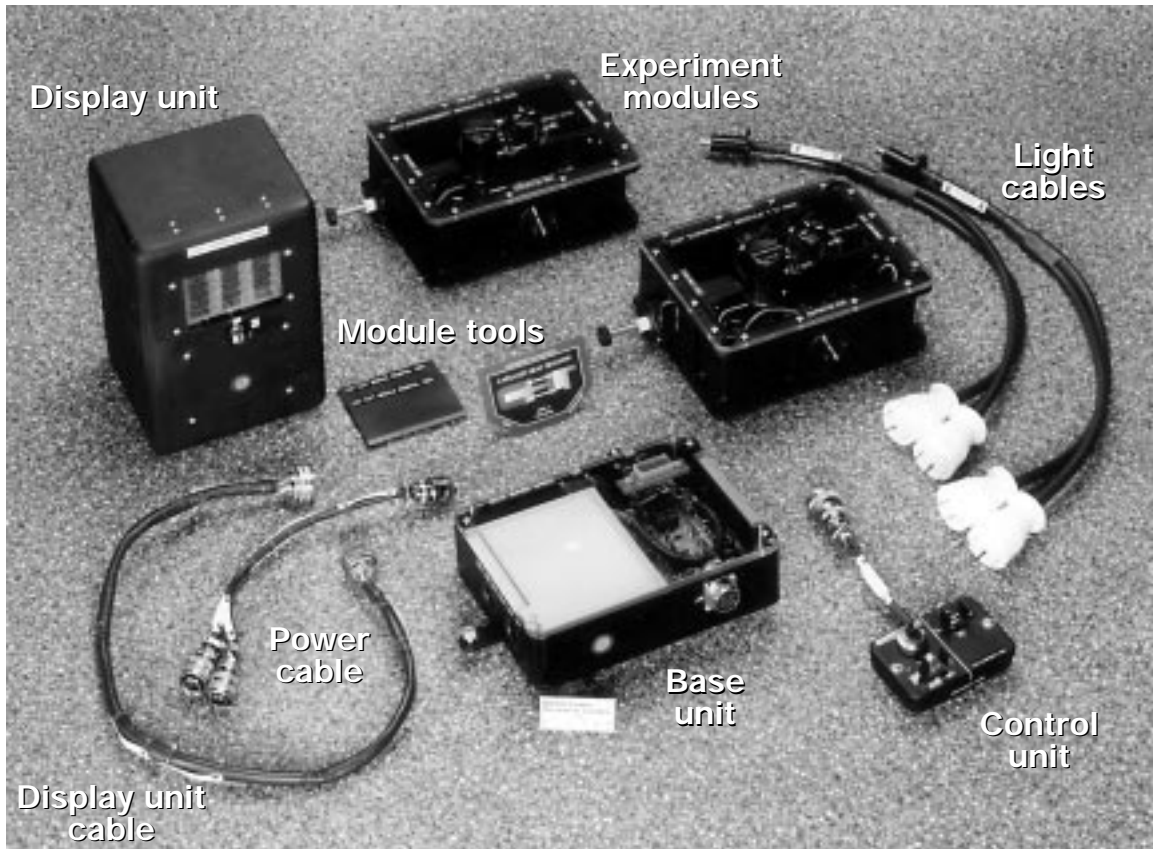
Capillary-pumped loops (CPL's) are devices that are used to transport heat from one location to another—specifically to transfer heat away from something. In low-gravity applications, such as satellites (and possibly the International Space Station), CPL's are used to transfer heat from electrical devices to space radiators. This is accomplished by evaporating one liquid surface on the hot side of the CPL and condensing the vapor produced onto another liquid surface on the cold side. Capillary action, the phenomenon that causes paper towels to absorb spilled liquids, is used to “pump” the liquid back to the evaporating liquid surface (hot side) to complete the “loop.”

CPL's require no power to operate and can transfer heat over distances as large as 30 ft or more. Their reliance upon evaporation and condensation to transfer heat makes them much more economical in terms of weight than conventional heat transfer systems. Unfortunately, they have proven to be unreliable in space operations, and the explanation for this unreliability has been elusive.

The Capillary-Driven Heat Transfer (CHT) experiment is investigating the fundamental fluid physics phenomena thought to be responsible for the failure of CPL's in low-gravity operations. If the failure mechanism can be identified, then appropriate design modifications can be developed to make capillary phase-change heat-transport devices a more viable option in space applications. CHT was conducted onboard the Space Shuttle Columbia during the first Microgravity Science Laboratory (MSL-1) mission, STS-94, which flew from July 1 to 17, 1997.

The CHT glovebox investigation, which was conceived by Dr. Kevin Hallinan and Jeffrey Allen of the University of Dayton, focused on studying the dynamics associated with the heating and cooling at the evaporating meniscus within a capillary phase-change device in a low-gravity environment. The CHT experimental hardware was designed by a small team of engineers from Aerospace Design & Fabrication, (ADF), the NASA Lewis Research Center, and the University of Dayton. The hardware consisted of two experiment modules that each contained an instrumented test loop (idealized capillary-pumped loop), a base unit for power conversion and backlighting, a display unit with 15 LED's (light-emitting diodes) to display temperatures, pressure, heater power, and time, a control unit to select heaters and heater settings, a cooling fan, and associated cables.





*Flight hardware components of the Capillary-Driven Heat Transfer (CHT) experiment. The experiment modules contain the instrumented capillary-pumped loops.*

Several different CHT experiments were performed by the astronaut crew during the course of the MSL-1 mission. Although there is still a large volume of flight data to analyze, preliminary results indicate the following. First, instabilities of the evaporator meniscus can be violent enough to cause system failure. Also liquid slugs were found to develop in the vapor leg of the loop. These slugs blocked the vapor flow to the condenser, thus rendering another failure mode. This situation was not appreciated prior to on-orbit operations. Since all the CPL designs have a significant number of bends in the vapor leg, it is very probable that previous low-gravity capillary-pumped-loop experiments exhibited poor performance because liquid slugs were formed in the vapor line.

**For more information about this research, visit us on the World Wide Web:**  
<http://zeta.lerc.nasa.gov/expr3/cht.htm>

**Lewis contacts:** Jack F. Lekan, (216) 433-3459, [John.F.Lekan@lerc.nasa.gov](mailto:John.F.Lekan@lerc.nasa.gov), and Jeffrey S. Allen, (216) 433-3087, [Jeffrey.S.Allen@lerc.nasa.gov](mailto:Jeffrey.S.Allen@lerc.nasa.gov)

**Authors:** Jack F. Lekan and Jeffrey S. Allen

**Headquarters program office:** OLMSA

**Programs/Projects:** HEDS, Microgravity Science, ISS, STS-94, MSL-1, Space Technology: Heat Transfer Mechanisms



# Ground-Based Reduced-Gravity Facilities

For the past 30 years, NASA Lewis Research Center's ground-based reduced-gravity facilities have supported numerous investigations for several research disciplines. Lewis' two drop towers and its DC-9 aircraft have provided a low-gravity environment (gravitational levels that range from 1 percent of Earth's gravitational acceleration to one-millionth of that measured at the Earth's surface) for brief periods of time. "Zero gravity," the weightless condition also known as microgravity, can be produced in these facilities by creating a free-fall or semi-free-fall condition where the force of gravity on an experiment is offset by its linear acceleration during a "fall" (a drop in a tower or a parabolic maneuver by an aircraft). The low-gravity environment obtained "on the ground" in NASA facilities is the same as that of a spacecraft in orbit around the Earth.

Even though ground-based facilities offer relatively short experiment times (a few seconds to 20 seconds), they have advanced our scientific understanding of many phenomena. In addition, many experiments scheduled to fly on sounding rockets, NASA's fleet of space shuttles, the Mir space station, and the International Space Station have been tested and validated in these ground facilities prior to testing in space. Experimental studies in low-gravity environments can provide new discoveries and advance our fundamental understanding of science. Many tests performed in NASA's facilities, particularly in the disciplines of combustion science and fluid physics, have resulted in exciting findings.



*Astronaut crew training performed onboard Lewis' DC-9 aircraft in preparation for the Microgravity Science Laboratory missions flown on the Space Shuttle Columbia in April and July of 1997.*

NASA Lewis' facilities host scientists and engineers, both domestic and foreign, from universities and Government agencies. In a typical year, well over 100 microgravity experiments are supported by these unique national resources. The following paragraphs highlight the accomplishments of these facilities for just the past year.

Lewis' DC-9 aircraft, our largest reduced-gravity platform, can accommodate several experiments during a flight. Pilots can obtain low-gravity conditions of approximately 20 seconds by flying a parabolic trajectory that includes a rapid climb at about 55° to 60°, a slow pushover at the top of the climb, and descent of about 30° to 40°. During the course of this maneuver, an altitude change of approximately 6000 ft is experienced. Over 50 of these maneuvers can be performed on a single flight.

Lewis' DC-9 continued to play a key role in microgravity research in 1997, with 73 flights that totaled 180 flight hours and 3313 trajectories while supporting 38 investigations, many of which involved multiple flights. Astronaut crews trained for several experiments that flew on STS-83 and STS-94, and the president of the Canadian Space Agency, William Evans, and the Canadian Minister of Industry, John Manly, participated in research flights that included experiments sponsored by the Canadian Space Agency. These milestones were all reached before the DC-9 was eliminated from the microgravity program on July 21. Future reduced-gravity aircraft flights will be performed on NASA Johnson Space Center's KC-135 aircraft. Six to twelve KC-135 flight campaigns will be conducted out of Lewis every year with this aircraft.

Lewis' 2.2-Second Drop Tower obviously offers a shorter test time than the DC-9, but because of its simple mode of operation and its ability to perform several tests per day, it is an attractive and highly utilized test facility, particularly for performing evaluation and feasibility tests. Over 16,000 tests have been performed in this drop tower to date. During fiscal year 1997, as in the past several years, drop tests averaged about 100 per month.

In the 2.2-Second Drop Tower, reduced-gravity conditions are created by dropping an experiment in an enclosure known as a drag shield to isolate the test hardware from aerodynamic drag during a 24-m free fall in the open environment. Over 30 experiments were supported during the 1200 drops performed in fiscal year 1997. As in the past, several of these experiments were preliminary tests of space shuttle experiments. The steady utilization of this drop tower is envisioned to continue since many new experiments are in the design and fabrication phases of development for the coming years.

The Zero Gravity Research Facility, a registered U.S. National landmark, provides a very clean low-gravity environment for 5.18 sec as experiments are dropped 132 m in a vacuum chamber. The aerodynamic drag on the free-falling experiment is nearly eliminated by dropping it in a vacuum. This procedure restricts drop tests in this facility to two per day. However, the relatively long test time and excellent low-gravity conditions more than compensate for the lower test throughput rate. Because of these operating conditions, this facility usually supports fewer projects than Lewis' other facilities. In fiscal year 1997, seven major projects were supported as 130 test drops were executed.

**To find out more, visit us on the World Wide Web:**

<http://zeta.lerc.nasa.gov/new/facility.htm>

**Lewis contacts:** Jack F. Lekan (2.2 Second Drop Tower), (216) 433-3459, [John.F.Lekan@lerc.nasa.gov](mailto:John.F.Lekan@lerc.nasa.gov); Dennis M. Thompson (Zero-Gravity Research Facility), (216) 433-5485, [Dennis.M.Thompson@lerc.nasa.gov](mailto:Dennis.M.Thompson@lerc.nasa.gov); and Eric S. Neumann (Reduced Gravity Aircraft Operations), (216) 433-2608, [Eric.S.Neumann@lerc.nasa.gov](mailto:Eric.S.Neumann@lerc.nasa.gov)

**Authors:** Jack F. Lekan, Eric S. Neumann, and Dennis M. Thompson

**Headquarters program office:** OLMSA

**Programs/Projects:** HEDS, Microgravity Science, STS, Mir, ISS



*The top of the drag shield is lowered into position over a combustion experiment from the University of Michigan prior to a test in Lewis' 2.2-Second Drop Tower.*

# Power and Propulsion

## Pulsed Plasma Thruster Technology Development and Flight Demonstration Program

Because of anticipated near- and far-term mission needs for innovative new electric propulsion technologies, the NASA On-Board Propulsion program is sponsoring NASA Lewis Research Centers' Pulsed Plasma Thruster (PPT) technology development program to rapidly advance PPT technology. This is a joint effort of Lewis' On-Board Propulsion Branch and Space Flight Project Branch. Building on state-of-the-art technology developed and flown in the 1970's and 1980's for Department of Defense missions, newly developed PPT program designs are realizing significant gains in system mass reduction, thrust to mass ratio, total impulse to mass ratio, and variability of impulse bit.

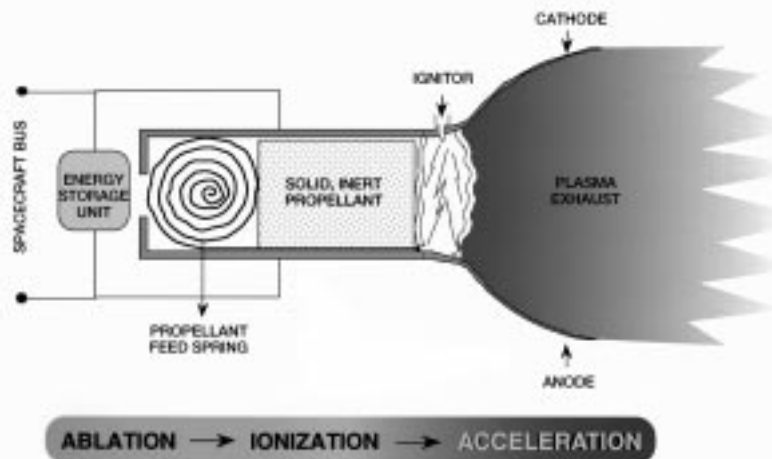
At the beginning of the PPT development program, and well before the inception of any flight programs, the effort was truly characterized by the term "technology push." After the fundamental feasibility, initial technology evaluations, multiple mission applications, and potential benefits of a new generation of PPT's were established in-house at Lewis, a contracted effort with the PRIMEX Aerospace Company was initiated, and more exhaustive market and technology assessments were conducted. From these combined efforts, a baseline system for near-term technology development

was established. At the same time, a PPT technology development roadmap was developed to focus PPT efforts on both near- and far-term mission performance requirements.

The PPT system is composed of power and control electronics, a high-energy capacitor, electrodes, and chlorofluorocarbon-based fuel bars. The use of solid, nontoxic propellant bars eliminates fluid propellant systems (valves, piping, fuel tanks, and heaters) and the complex ground handling systems used in traditional propulsion systems. The fuel is ablated, ionized, and accelerated electromagnetically from the PPT during a high-voltage capacitor discharge across the face of the fuel bar (see the figure).

The PPT system offers a simple, lightweight, microthrust propulsion capability with minimal spacecraft interface requirements (power, control and data, and mechanical requirements only) for spacecraft attitude control, orbit-raising and translation, and precision positioning. To assess various component and system technologies, PRIMEX designed and assembled a breadboard PPT unit early in the contracted effort (see the photo). This device allows easy assembly and disassembly to facilitate rapid hardware modification and testing. The breadboard PPT has undergone extensive testing at PRIMEX and is currently being tested at Lewis to assess system-level performance and environmental characteristics. Results from these breadboard PPT system and ongoing component tests are being applied to

PPT CHARACTERISTICS AND CANDIDATE MISSIONS	
Characteristics	
Variable operating range, W. ....	1 to 200
Specific impulse, $I_{sp}$ , sec. ....	<300, >2000
Propellant .....	Solid, inert
Candidate missions	
Insertion and deorbit	
Propulsive attitude control system	
Precision station keeping	
Drag makeup	



*PPT operating principle.*

near-term flight demonstration PPT designs. In addition, fundamental supporting research is being performed by the Ohio State University, Worcester Polytechnic Institute, the University of Illinois (Urbana), and Auburn University.

The first PPT flight is planned to use a single PPT system to demonstrate propulsive attitude control (pitch-axis only) for NASA's Earth Observer-1 spacecraft (EO-1). EO-1, which is scheduled to fly in mid-1999, will be the first Earth-orbiting mission under NASA's New Millennium Program. The NASA Goddard Space Flight Center has responsibility for EO-1, and Lewis engineers are working closely with Goddard personnel to assure that the EO-1 PPT system meets performance, life, and spacecraft integration requirements.

Beyond EO-1, the program is targeting technology for precision formation flying for applications such as long baseline interferometry using distributed spacecraft (such as the New Millennium Program's Deep Space 3 mission). Multiple PPT units with three-axis fuel bars are currently envisioned for this application to provide translation and precision positioning of two to three formation-flying spacecraft.

**Find out more about this research on the World Wide Web:**

<http://www.lerc.nasa.gov/WWW/onboard/onboard.html>

**Bibliography**

Curran, F.M.; et al.: Pulsed Plasma Thruster Technology Direction. AIAA Paper 97-2926, 1997.

**Lewis contacts:** Dr. Frank M. Curran, (216) 977-7424, Francis.M.Curran@lerc.nasa.gov, and Todd T. Peterson, (216) 433-5350, Todd.T.Peterson@lerc.nasa.gov

**Authors:** Todd T. Peterson and Dr. Frank M. Curran

**Headquarters program offices:** OSS, OMTPE

**Programs/Projects:** MTPE, ATMS, New Millennium Program, EO-1, Deep Space 3, MightySat II (USAF), OBP, PPT



*NASA Lewis/PRIMEX breadboard PPT.*

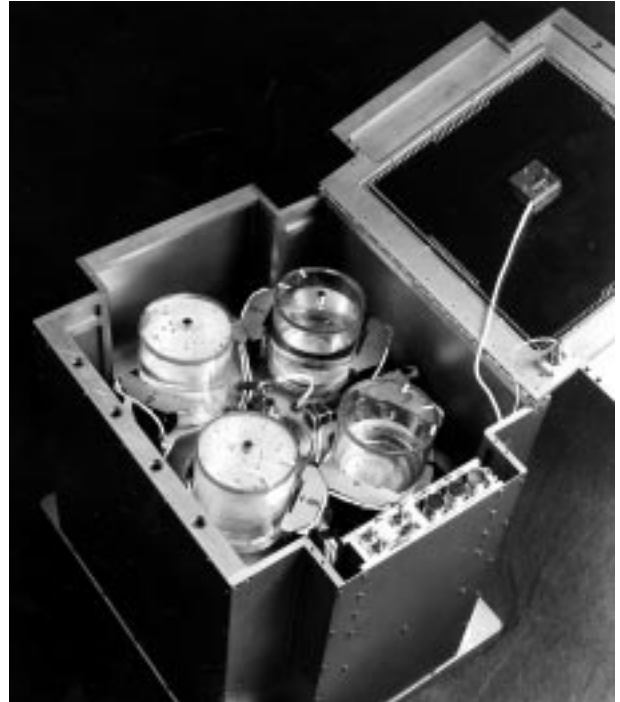


## Liquid Motion Experiment Flown on STS-84

During some part or all of each mission, about half of all scientific and commercial spacecraft will spin. For example, commercial spacecraft are made to spin during the transfer maneuver from low Earth orbit to the mission orbit to obtain gyroscopic stiffness. Many spacecraft spin continuously in orbit for the same reason. Other reasons for spinning include controlling the location of liquid propellants within their tanks and distributing solar heat loads.

Although spinning has many benefits, it also creates problems because of the unavoidable wobble motion that accompanies spinning. Wobbling makes the spacecraft's flexible components oscillate. The energy dissipated by the internal friction of these components causes the wobbling amplitude to increase continually until, at some point, the attitude control thrusters must be fired to bring the spacecraft's amplitude back to an acceptable level.

For modern spacecraft, by far the most massive flexible component and the largest source of energy dissipation is a mobile liquid propellant in a partially filled spinning tank. The liquid's energy dissipation cannot, however, be quantified adequately by any ground test, and current analytical models are also inadequate. Consequently, spacecraft attitude control systems are designed and operated very conservatively. Nonetheless, spacecraft often perform poorly in orbit and some have even been lost by a rapid and unanticipated increase of the wobbling amplitude.



*Interior view of LME prior to installation in the Space Shuttle Atlantis.*

NASA Lewis Research Center's Liquid Motion Experiment (LME) was designed to study these energy dissipation effects for liquids in rotating tanks. Data generated on LME will be used to validate and provide guidance for improved analytical models of liquid motions in the tanks of spinning spacecraft. Such improved models will lead to less conservative attitude control system designs, which will reduce the mass and increase the life of spacecraft.

LME was successfully integrated into the SpaceHab and launched as a secondary payload on the STS-84 Phase I Mir flight in May 1997. Astronauts Carlos Noriega and Dr. Ed Lu operated the LME following undocking with Mir. The experiment performed nominally throughout the flight, generating both energy dissipation data and video of the actual liquid motions inside the tanks.



*Astronaut Carlos Noriega videotapes LME in operation.*



Data analysis is ongoing. Current plans call for a final data review, a meeting of an industry-led users' panel for data dissemination, and publication of the results. Lewis is pursuing the possibility of a reflight of LME, primarily to investigate the use of various proprietary propellant management devices within the tanks.

LME was built under contract to Lewis by the Southwest Research Institute of San Antonio, Texas. Their principal LME investigator is Dr. Franklin Dodge, and their LME project manager is Danny Deffenbaugh. From NASA Lewis, the LME project manager is Penni Dalton and the project scientist is David Chato.

**For more information, visit LME on the World Wide Web:**  
<http://godzilla.lerc.nasa.gov/ppo/lme/lme.html>

**Lewis contact:**

Penni J. Dalton, (216) 433-5223,  
 Penni.J.Dalton@lerc.nasa.gov

**Author:** Penni J. Dalton

**Headquarters program office:** OSS

**Programs/Projects:** ATMS, HEDS, Microgravity Science, In-STEP

## Closed Cycle Engine Program Used in Solar Dynamic Power Testing Effort

NASA Lewis Research Center is testing the world's first integrated solar dynamic power system in a simulated space environment. This system converts solar thermal energy into electrical energy by using a closed-cycle gas turbine and alternator. A NASA-developed analysis code called the Closed Cycle Engine Program (CCEP) has been used for both pretest predictions and posttest analysis of system performance.

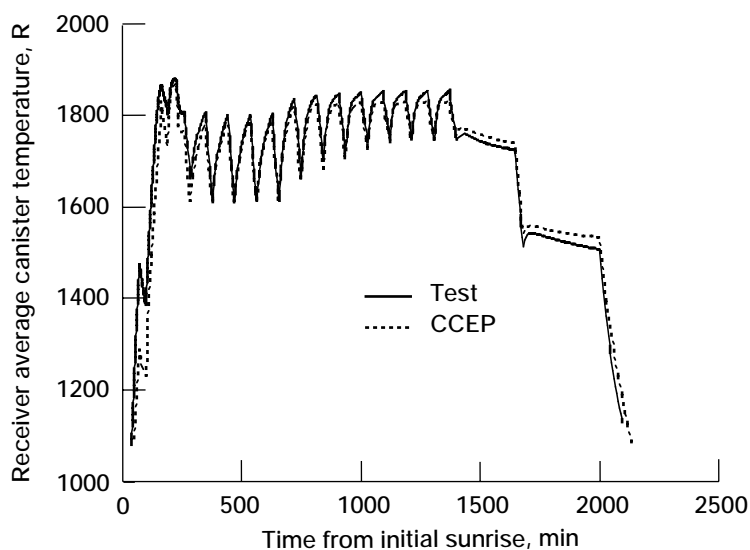
The solar dynamic power system has a reflective concentrator that focuses solar thermal energy into a cavity receiver. The receiver is a heat exchanger that transfers the thermal power to a working fluid, an inert gas mixture of helium and xenon. The receiver also uses a phase-change material to store the thermal energy so that the system can continue producing power when there is no solar input power, such as when an Earth-orbiting satellite is in eclipse.

The system uses a recuperated closed Brayton cycle to convert thermal power to mechanical power. Heated gas from the receiver expands through a turbine that turns an alternator and a compressor. The system also includes a gas cooler and a radiator, which reject waste cycle heat, and a recuperator, a gas-to-gas heat exchanger that improves cycle efficiency by recovering thermal energy.

CCEP was adapted more than 15 years ago from the Navy/NASA Engine Program, a computer program written to design and analyze open-cycle aircraft engines and auxiliary systems. Modifications have included provision for closed-cycle analysis and addition of solar dynamic system components such as concentrators, receivers, and space radiators. More recently, CCEP's Fortran code has been

updated and plotting capabilities have been added.

This program allows users to model all the components of a solar dynamic power system by using input data sets. Some components, such as turbomachinery, can be modeled with performance maps. Heat exchanger and radiator performance is based on input geometry and material property



*Test data and CCEP simulation of receiver canister temperatures for startup, orbital operation, and steady-state operation. Receiver canisters contain a phase-change material for thermal energy storage.*

data. The code can be used to design new systems and analyze existing ones.

CCEP has been used in designing tests of the solar dynamic power system in Lewis' Tank 6, which provides a space thermal vacuum environment. Testing typically includes a heatup period followed by simulated orbital operations with sun/shade cycles. Predictions of cycle temperatures and output powers for an entire test run can be made on the basis of given test parameters, such as input solar power, engine speed, and coolant temperatures. During posttest analysis, key measured parameters are used to compare predicted performance with actual performance. Deviations from expected performance and sensitivities to testing conditions and component performance can be explored by varying appropriate CCEP input data.

Future testing of the solar dynamic system in Lewis' Tank 6 is planned to include the automatic system thermal management, where engine speed control is used to maintain receiver temperatures at acceptable levels. CCEP will be used in test design and posttest analysis.

**Find out more on the World Wide Web:** <http://godzilla.lerc.nasa.gov/ppo/sdreplan.html>

**Lewis contacts:**

Clint B. Ensworth III, (216) 433-6297, [Clinton.B.Ensworth@lerc.nasa.gov](mailto:Clinton.B.Ensworth@lerc.nasa.gov), and David B. McKissock, (216) 433-6304, [David.B.McKissock@lerc.nasa.gov](mailto:David.B.McKissock@lerc.nasa.gov)

**Authors:** Clint B. Ensworth III and David B. McKissock

**Headquarters program office:** OSF

**Programs/Projects:**  
Solar Dynamic Power System

## Dark Forward Electrical Test Techniques Developed for Large-Area Photovoltaic Arrays

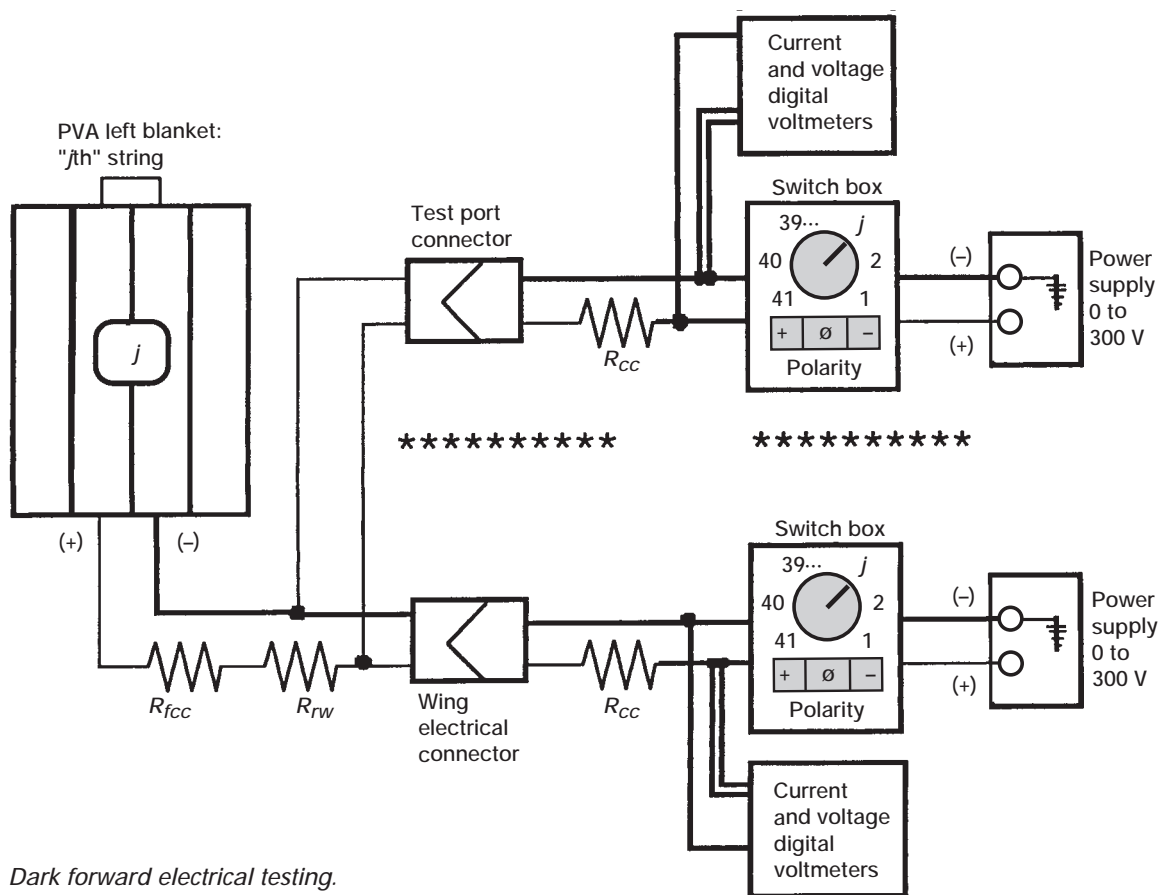
Spacecraft photovoltaic arrays (PVA's) must be carefully handled during ground integration processing and transportation to the launch site. Care is exercised to avoid damage that could degrade on-orbit electrical performance. Because of this damage risk, however, PVA's are typically deployed and illuminated with a light source so performance characteristics can be measured prior to launch. For large-area arrays, such as the Mir Cooperative Solar Array (2.7 by 18 m) and the International Space Station PVA blankets (4.6 by 31.7 m) this integrity check becomes resource intensive. Large test support structures are needed to offload the array during deployment in 1g, and large-aperture illumination equipment is required to uniformly illuminate array panels. Significant program time, funds, and manpower must be allocated for this kind of test program. Alternatively, launch site electrical performance tests can be bypassed with an attendant increase in risk.

Another alternative is dark forward electrical testing. This testing is performed while the array stowed, obviating the need for deployment and illumination test support equipment. Dark test support equipment is inexpensive, it is easily portable to launch site facilities, and testing can be accomplished with only one or two test engineers. The dark test equipment consists of a direct-current power supply, a switching unit, a personal computer (PC), and instrumentation (several digital voltmeters) as shown in the schematic diagram. During dark testing, individual array strings are forward-biased to a preset voltage level through the use of the power supply. With forward biasing, the polarity of the array during normal illuminated operation is matched. The resulting direct current is then measured. Several different current-voltage (IV) data points are obtained to generate

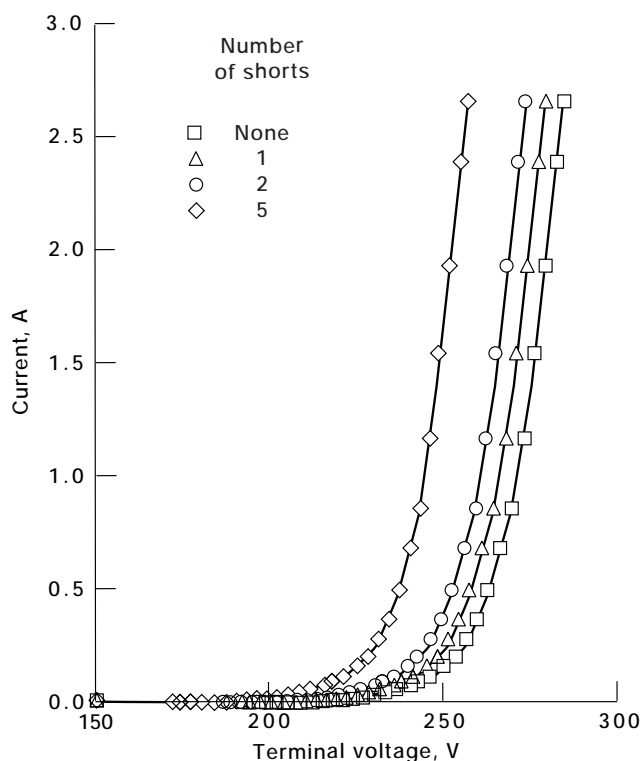
the array's characteristic diode IV curve. The PC controls the power supply and collects and stores the data.

After testing, the data can be manipulated to obtain the illuminated electrical performance for the array. In addition, the diode IV data can be compared with computational predictions to determine PVA electrical performance degradation due to damage. Predictions are made for an undamaged array string and for strings with a variety of damage modes, such as bypass diode short-circuits, as shown in the following graph for an International Space Station PVA string. Using this information, program managers can make a firm decision to either proceed with spacecraft integration or send the PVA back to the supplier for the necessary repairs.

Dark forward electrical testing was successfully utilized in July 1995 to



Dark forward electrical testing.



Dark forward current-voltage response with bypass diode shorts.

verify the performance of the Mir Cooperative Solar Array following its shipment to the United States from Russia. This testing helped to assure program managers that the Mir Cooperative Solar Array was ready for integration with the space shuttle as part of the payload for mission STS-74 to the Russian Mir space station. A feasibility study was also performed to assess dark test capabilities in verifying International Space Station PVA performance prior to launch. Since the trend in geosynchronous communication satellites is toward larger, higher power PVA's, dark forward electrical testing may become a key part of commercial spacecraft integration and checkout processing. Dark testing offers high-power, commercial satellite manufacturers an innovative tool to help contain costs and maintain tight launch schedules.

These are among the key elements for maintaining marketplace competitive advantage.

**Find out more about Mir Cooperative Array dark testing on the World Wide Web:** <http://godzilla.lerc.nasa.gov/pspo/csa.html>

### **Bibliography**

Kerslake, T.W.; Scheiman, D.A.; and Hoffman, D.J.: Pre-Flight Dark Forward Electrical Testing of the Mir Cooperative Solar Array. NASA TM-107496, 1997. Available online: <http://letrs.lerc.nasa.gov/cgi-bin/LeTRS/browse.pl?1997/TM-107496.html>

Kerslake, T.W.; Scheiman, D.A.; and Hoffman, D.J.: Dark Forward Electrical Testing of the Mir Cooperative Solar Array. Research & Technology 1996, NASA TM-107350, 1997, pp. 157-158. Available online: <http://www.lerc.nasa.gov/WWW/RT1996/6000/6920k.htm>, or <http://letrs.lerc.nasa.gov/cgi-bin/LeTRS/browse.pl?1997/TM-107350.html>

### **Lewis contacts:**

Thomas W. Kerslake, (216) 433-5373, [Thomas.W.Kerslake@lerc.nasa.gov](mailto:Thomas.W.Kerslake@lerc.nasa.gov); David A. Scheiman, (216) 433-6756, [David.A.Scheiman@lerc.nasa.gov](mailto:David.A.Scheiman@lerc.nasa.gov); and David J. Hoffman (216) 433-2445, [David.J.Hoffman@lerc.nasa.gov](mailto:David.J.Hoffman@lerc.nasa.gov)

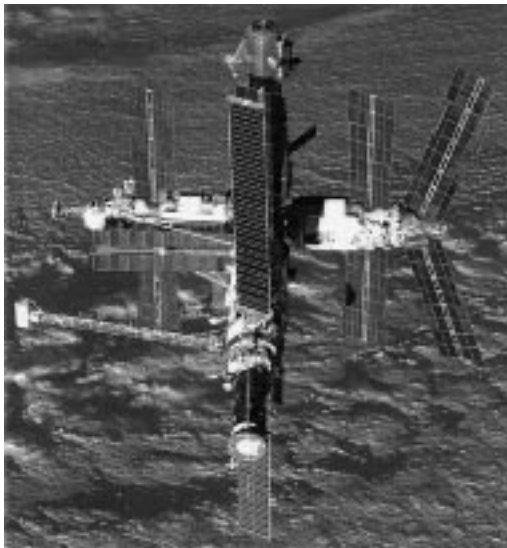
**Authors:** Thomas W. Kerslake, David A. Scheiman, and David J. Hoffman

**Headquarters program office:** OSF

### **Programs/Projects:**

STS-74, ISS, Mir, MCSA

## **On-Orbit Electrical Performance of a Mir Space Station Photovoltaic Array Predicted**



*MCSA (foreground) deployed on Mir.*

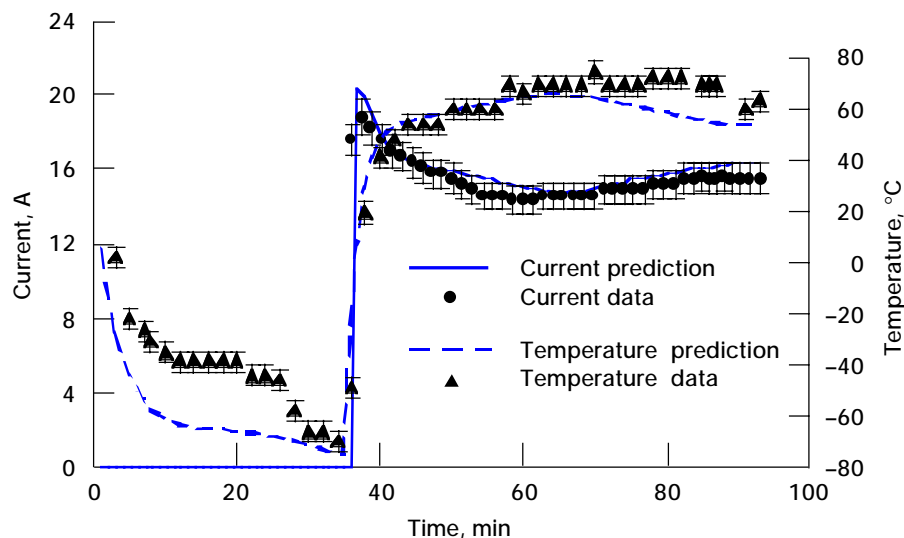
mentation on the ISS. Initial, on-orbit electrical performance and temperature data were measured in June and December of 1996.

To better interpret the MCSA flight data, NASA Lewis Research Center's programmers developed a dedicated FORTRAN computer code to predict the detailed thermal-electrical performance of the MCSA. Computational modeling covers orbit mechanics, vehicle flight attitudes, photovoltaic array pointing, heat transfer, photovoltaic array current-voltage response, environmental degradation, albedo current augmentation, power collection and distribution cabling resistance, and array voltage regulation. This code was a modified version of the premier spacecraft electrical power system analysis code SPACE (System Performance Analysis for Capability

The Mir Cooperative Solar Array (MCSA) was developed jointly by the United States and Russia to provide approximately 6 kW of photovoltaic power to the Russian space station Mir. The MCSA was launched to Mir in November 1995 and installed on the Kvant-1 module in May 1996, where it has been performing well to date. Since the MCSA panels are nearly identical to those of the International Space Station (ISS), MCSA operation offered an opportunity to gather multiyear performance data on this technology prior to its implementation on the ISS.

Evaluation) developed at NASA Lewis (ref. 1). Predictions from SPACE are used by the ISS Program Office to assess and verify planned ISS operational scenarios.

As shown in the graph, the flight data compared very favorably with computational performance predictions (ref. 2). Current predictions matched the data within 5-percent measurement error, and temperature predictions were within 10 °C of measured values during most of the orbital insolation period. This favorable comparison indicated that the MCSA's electrical performance was fully meeting preflight expectations. After 7 months of operation on orbit, there were no measurable indications of unexpected or precipitous MCSA performance degradation due to contamination or other causes. The strong correlation between experimental and computational results further bolsters our confidence in performance codes, such as SPACE, that are used in critical ISS electric power forecasting.



Generator 6 current and panel 10 temperature predictions versus data for 92-min Mir orbit.

More information about SPACE and the Mir Cooperative Array is available on the World Wide Web:

<http://godzilla.lerc.nasa.gov/ppo/space.html>

<http://godzilla.lerc.nasa.gov/ppo/csa.html>

## References

1. Hojnicki, J.S., et al.: Space Station Freedom Electrical Performance Model. NASA TM-106395, 1993.
2. Kerslake, T.W.; and Hoffman, D.J.: Mir Cooperative Solar Array Flight Performance Data and Computational Analysis. NASA TM-107502, 1997. Available online: <http://letrs.lerc.nasa.gov/cgi-bin/LeTRS/browse.pl?1997/TM-107502.html>

## Lewis contacts:

Thomas W. Kerslake, (216) 433-5373, [Thomas.W.Kerslake@lerc.nasa.gov](mailto:Thomas.W.Kerslake@lerc.nasa.gov); David J. Hoffman (216) 433-2445, [David.J.Hoffman@lerc.nasa.gov](mailto:David.J.Hoffman@lerc.nasa.gov); and Jeffrey S. Hojnicki, (216) 433-5393, [Jeffrey.S.Hojnicki@lerc.nasa.gov](mailto:Jeffrey.S.Hojnicki@lerc.nasa.gov)

**Authors:** Thomas W. Kerslake, David J. Hoffman, and Jeffrey S. Hojnicki

**Headquarters program office:** OSF

**Programs/Projects:** ISS, Mir, MCSA

## Radiation Heat Transfer Modeling Improved for Phase-Change, Thermal Energy Storage Systems

Spacecraft solar dynamic power systems typically use high-temperature phase-change materials to efficiently store thermal energy for heat engine operation in orbital eclipse periods. Lithium fluoride salts are particularly well suited for this application because of their high heat of fusion, long-term stability, and appropriate melting point. Considerable attention has been focused on the development of thermal energy storage (TES) canisters that employ either pure lithium fluoride (LiF), with a melting point of 1121 K, or eutectic composition lithium-fluoride/calcium-difluoride (LiF-20CaF<sub>2</sub>), with a 1040 K melting point, as the phase-change material. Primary goals of TES canister development include maximizing the phase-change material melt fraction, minimizing the canister mass per unit of energy storage, and maximizing the phase-change material thermal charge/discharge rates within the limits posed by the container structure.

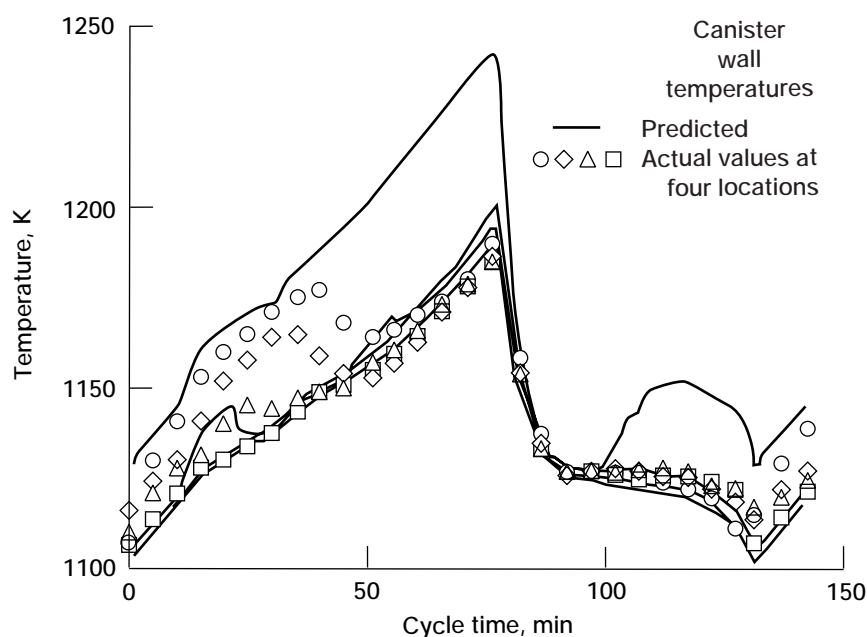
One key element for achieving these canister development goals is an accurate computational model of canister phase change heat transfer. An important, but heretofore understudied, aspect of the canister phase change problem is thermal radiation heat transfer. Radiation is the primary mode of heat transfer through salt-vapor-filled voids within the canister. These voids grow and shrink as the salt undergoes a 20- to 30-percent volume change during melting and freezing. In addition, the liquid salts are

nearly transparent to radiation with wavelengths less than 5.5  $\mu\text{m}$ , which encompasses fully three quarters of the spectral emissive power of a black body at LiF's melting temperature.

Cleveland State University (ref. 1) and the NASA Lewis Research Center developed such a canister heat transfer computational model. Building on Lewis' existing computational tools, Cleveland State developed an integrated model describing the canister's two- or three-dimensional conduction heat transfer with phase change, void behavior, and radiation heat transfer with participating media. Various combinations of radiation heat transfer modeling within the void



and liquid salt were investigated. Computational results were compared with canister data obtained from both ground experiments (ref. 2) and space shuttle flight experiments (ref. 3). The graph shows one such comparison of predicted canister wall temperatures versus measured wall temperatures for the TES-1 flight experiment (ref. 4). Although the predicted temperatures of the four radiation model cases indicate substantial differences in canister heat transfer rates, all the cases reproduce important features in the experimental temperature set during the phase-change material solid sensible energy phase, liquid sensible energy phase, and thermal arrest periods. Computational results such as these could be used to optimize TES canister designs for minimum mass or maximum heat transfer rate and, thus, improve solar dynamic power system heat receiver designs. This kind of radiation heat transfer analysis tool could also find use in assessing other engineering problems such as combustion processes, furnace design, and radiant heater design.



*Canister wall temperature predictions for four cases of radiation modeling versus TES-1 flight experiment measured wall temperatures at four stations around the perimeter of the cylindrical canister.*

**Find out more about the TES flight experiments on the World Wide Web:**  
<http://zeta.lerc.nasa.gov/expr/tes.htm>

## References

1. Thermal Analysis for Melting and Freezing of Materials in a Metallic Canister. NASA Lewis Research Center Grant NAG3-1756, 1997.
2. Kerslake, T.W.: Experiments With Phase Change Thermal Energy Storage Canisters for Space Station Freedom. NASA TM-104427, 1991.
3. Namkoong, D.; Jacqmin, D.; and Szaniszló, A.: Effect of Microgravity on Material Undergoing Melting and Freezing—The TES Experiment. NASA TM-106845, 1995.
4. Ibrahim, M., et al.: Experimental and Computational Investigations of Phase Change Thermal Energy Storage Canisters. Vol. 1, NASA TM-107382, 1996.

## Lewis contacts:

Thomas W. Kerslake, (216) 433-5373,  
 Thomas.W.Kerslake@lerc.nasa.gov, and  
 Dr. David A. Jacqmin, (216) 433-5853,  
 David.A.Jacqmin@lerc.nasa.gov

**Authors:** Thomas W. Kerslake and  
 Dr. David A. Jacqmin

**Headquarters program office:** OSF

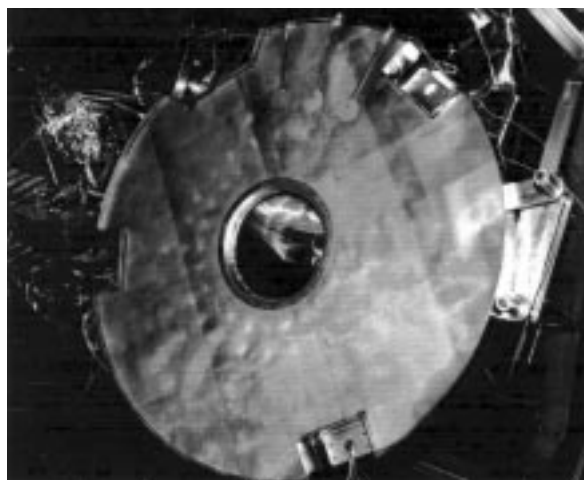
**Programs/Projects:** HEDS, ISS

# High-Temperature, High-Flux Multifoil Shield Developed for Space Applications

Spacecraft employing solar dynamic power systems typically use parabolic, point focus concentrators to collect solar power and direct it to the aperture of a heat receiver. Solar fluxes several thousand times the intensity of one solar constant are typically produced in the focal plane of such concentrators. Under heat loading this severe, passively cooled surfaces constructed of most engineering materials would rapidly melt. Therefore, high-temperature shielding is required to protect heat receiver surfaces and other spacecraft surfaces that may be exposed to high flux.

To meet this challenge for the joint U.S./Russian Solar Dynamic Flight Demonstration Program, AlliedSignal Aerospace (ref. 1) and the NASA Lewis Research Center developed a high-temperature, high-flux multifoil shield tolerant of extreme heat loading conditions in a vacuum environment. The shield is passively cooled, obviating the need for pumped fluid loops and/or heat pipe cooling systems with their attendant cost, mass, complexity, and reliability issues.

Only 1 m in diameter, the shield comprises a series of refractory metal foil layers separated by refractory metal screens in the hottest region (closest to the concentrator) and ceramic spaces in the cooler regions (ref. 2). In the hottest outer layers, the foil layers (40 total) and screens are made from tungsten, and the cooler inner layers, from molybdenum. The foil stackup is mounted to a stainless steel backplate that provides for assembly and for structural support for launch loads. The layers are stitched together and mounted to the support plate with tungsten attachment wire. A center supporting ring, 0.24-m in diameter and made of tungsten/25 vol % rhenium, adds structure to the foil stackup and defines the

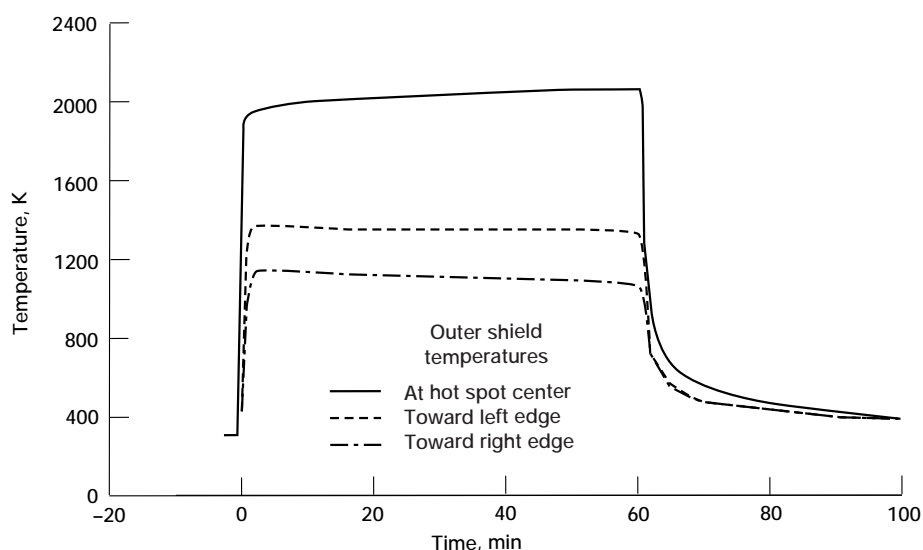


*Aperture shield test article.*

receiver aperture. For thermal growth and fabrication ease, the ring is segmented into eight circumferential sections. The top of the stackup is enclosed by a tungsten screen, which provides support for the attachment wires. At the outer circumference, a stainless steel skirt encloses the outer edges of the foil layers.

The aperture shield shown in the photo was built and successfully tested at Lewis' Tank 6 thermal-vacuum test facility. This shield survived 1-hr exposures to concentrated solar fluxes up to 800,000 W/m<sup>2</sup>. Although a peak temperature of 2072 K was reached, no signs of structural damage were observed after two separate tests. The graph shows outer shield temperatures in the hot spot center and toward its right and left edges during a 1-hr test in Tank 6.

On the basis of the outstanding test results and supporting thermal-structural analyses, we believe this shield design is tolerant of heat flux levels many factors higher than those tested. Such



*Aperture shield temperature data during high-flux, thermal vacuum testing at NASA Lewis.*

high-temperature, multifoil shield designs are not only promising for solar dynamic power system applications but also for solar thermal propulsion, planetary aerobraking systems, and solar probe missions. In all these applications, high-temperature, high-flux, vacuum-compatible shields with low mass, high reliability, and high launch load durability are required.

**Find out more about solar dynamic testing at Lewis on the World Wide Web:**  
<http://powerweb.lerc.nasa.gov/soldyn/DOC/SDGTD.html>

## References

1. Strumpf, H.J.; Krystkowiak, C.; and Klucher, B.A.: Design of the Heat Receiver for the U.S./Russia Solar Dynamic Power Joint Flight Demonstration. NASA CR-202542 (NASA Lewis contract NAS3-26970), 1996.
2. Strumpf, H.J., et al.: Design and Analysis of the Aperture Shield for a Space Solar Receiver. NASA TM-107500, 1997.
3. Kerslake, T.W.; Mason, L.S.; and Strumpf, H.J.: High-Flux, High-Temperature Thermal Vacuum Qualification Testing of a Solar Receiver Aperture Shield. NASA TM-107505, 1997. Available online: <http://letrs.lerc.nasa.gov/cgi-bin/LeTRS/browse.pl?1997/TM-107505.html>

## Lewis contacts:

Thomas W. Kerslake, (216) 433-5373,  
[Thomas.W.Kerslake@lerc.nasa.gov](mailto:Thomas.W.Kerslake@lerc.nasa.gov), and  
Lee S. Mason, (216) 977-7106,  
[Lee.S.Mason@lerc.nasa.gov](mailto:Lee.S.Mason@lerc.nasa.gov)

**Authors:** Thomas W. Kerslake and  
Lee S. Mason

**Headquarters program office:** OSF

## Programs/Projects:

HEDS, U.S./Russian Solar Dynamic  
Flight Demonstration, Mir, ISS

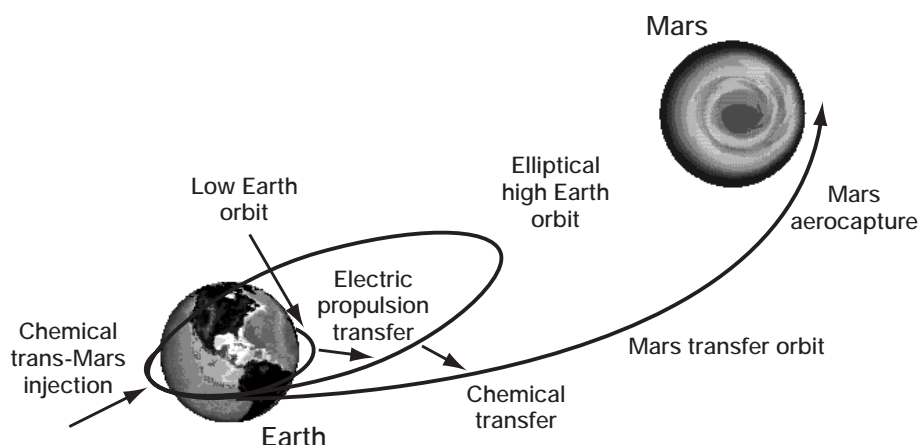
# Solar Electric Propulsion for Mars Exploration

Highly propellant-efficient electric propulsion is being combined with advanced solar power technology to provide a nonnuclear transportation option for the human exploration of Mars. By virtue of its high specific impulse, electric propulsion offers a greater change in spacecraft velocity for each pound of propellant than do conventional chemical rockets. As a result, a mission to Mars based on solar electric propulsion (SEP) would require fewer heavy-lift launches than a traditional all-chemical space propulsion scenario would. Performance, as measured by mass to orbit and trip time, would be comparable to the NASA design reference mission for human Mars exploration, which utilizes nuclear thermal propulsion; but it would avoid the issues surrounding the use of nuclear reactors in space.

The mission concept for SEP is illustrated in the following figure. First, the Mars payload, an SEP stage, and a chemical trans-Mars injection stage are placed into low Earth orbit via one or more launches from a chemical rocket of the 80 metric-tonne payload size. Over the next 6 to 9 months, the SEP system slowly raises the vehicle into a highly elliptical, high Earth orbit. This orbit, with an apogee altitude similar to that of a geosynchronous-transfer orbit, prepares the vehicle for trans-Mars injection with an energy change only a fraction of what would be required from low Earth orbit. Once in the desired high Earth orbit, the SEP stage separates from the remainder of the vehicle and the chemical trans-Mars injection stage is fired, sending the payload on to Mars. Because of the reduced velocity changes required for this maneuver, a relatively modest trans-Mars injection stage of the Centaur class can be used. When a crew is part of the Mars payload, they are shuttled to high Earth orbit for a rendezvous with the vehicle just prior to SEP stage separation and trans-Mars injection. In this way, the crew is not exposed to the high-radiation environment of

Earth's Van Allen belts during the long, slow spiral from low Earth orbit to high Earth orbit. It is anticipated that the so-called crew taxi would be based on the X-38 space shuttle replacement.

For the size of payloads required for a human Mars mission, when optimized for least mass launched to low Earth orbit, the electric propulsion system consumes 600 to 800 kW of power. Thrusters optimally have a specific impulse of 2000 to 2500 sec, which corresponds closely with the characteristics of high-power Hall thrusters currently under development. An SEP system consisting of multiple 50- to 100-kW thrusters is envisioned. High output, lightweight, deployable solar electric power technologies with specific power in the 10- to 15-kW/kg range are considered critical to the viability of the SEP concept.



*SEP concept for Mars exploration.*

The SEP concept for Mars exploration was developed in-house at the NASA Lewis Research Center by members of the Power and Propulsion Office and the Systems Engineering Division in direct support of the Exploration Office at the NASA Johnson Space Center. The SEP concept has been received favorably by Johnson and NASA Headquarters; it is presently being evaluated in greater detail as an alternative to the design reference mission by an engineering team from Lewis, Johnson, NASA Marshall Space Flight Center, and NASA Langley Research Center.

**Lewis contact:**

Kurt J. Hack, (216) 977-7060,  
Kurt.J.Hack@lerc.nasa.gov

**Author:** Kurt J. Hack

**Headquarters program office:** OSF

**Programs/Projects:** HEDS

## Space Station Radiator Test Hosted by NASA Lewis at Plum Brook Station



In April of 1997, the NASA Lewis Research Center hosted the testing of the photovoltaic thermal radiator that is to be launched in 1999 as part of flight 4A of the International Space Station. The tests were conducted by

Lockheed Martin Vought Systems of Dallas, who built the radiator. This radiator, and three more like it, will be used to cool the electronic system and power storage batteries for the space station's solar power system. Three of the four units will also be used early on to cool the service module.

This test involved multiple deployments (extension and retraction) of the 50-ft-long radiator, thermal cycling using infrared lamps as a heat source, and proof of performance—including flowing liquid ammonia through the radiator and viewing it with an infrared imaging system, and taking thermocouple readings. All tests were performed in the Space Power Facility at Lewis' Plum Brook Station facility. The Space Power Facility is the

largest vacuum tank in the world: 120 ft in height and 100 ft in diameter. It was outfitted with a Lewis-designed cryogenic enclosure, or cryoshroud, over 22-ft high with a 40- by 78-ft floor area. The cryoshroud used gasified liquid nitrogen to achieve temperatures as low as  $-250^{\circ}\text{F}$  in its interior. In combination, the cryoshroud and tank provided a simulated space environment for these tests. Vacuums in the  $10^{-6}$  torr range and temperatures lower than  $-230^{\circ}\text{F}$  were achieved. Since the radiator is designed to exist in the weightlessness of orbit, it was necessary to support it on a set of rails for these tests, so that deployment in Earth's gravity would not harm it. Also tested was the manual deployment crank, which would be used by an astronaut if the motor system failed.

In addition, under stringent time, money, and safety constraints, Lewis designed and built a remote-controlled ammonia handling system to furnish the large amount of liquid ammonia needed for the test. Most of the handling system was built at Lewis in an enclosure about the size of a medium-sized house trailer. It was shipped to Plum Brook for final integration into the test. Because of safety considerations, this system was mounted outdoors and was operated entirely by computer control, monitored by television. Liquid ammonia was supplied at controlled temperatures in two separately controlled flow loops.

The series of tests proved the photovoltaic radiator's readiness for its mission, showed compliance with thermal and hydraulic performance requirements, and verified the performance model correlations, the thermal time constants of the components, and the passive thermal model correlations.

**Lewis contact:**

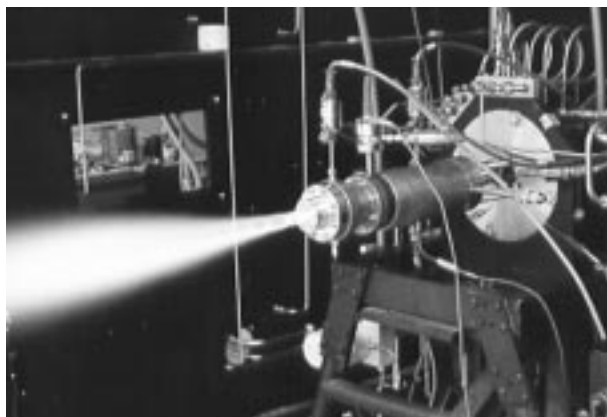
Randall C. Speth, (216) 433-8617,  
Randall.C.Speth@lerc.nasa.gov

**Author:** Randall C. Speth

**Headquarters program office:** OSF

**Programs/Projects:** HEDS, ISS

## Improving Safety and Reliability of Space Auxiliary Power Units



*Ethanol-oxygen APU combustor tests.*

provide electrical power for flight control actuators and other vehicle subsystems. Vehicle designers and mission managers have identified safety, reliability, and maintenance as the primary concerns for space APU's. In 1997, the NASA Lewis Research Center initiated an advanced technology development program to address these concerns.

The initial focus of this program is the development of technologies that will lead to a new APU that could be used in the space shuttles as early as 2003. A primary objective of this phase of the Space APU Advanced Technology Program is to eliminate the use of hydrazine fuel for the shuttle

Auxiliary Power Units (APU's) play a critical role in space vehicles. On the space shuttle, APU's provide the hydraulic power for the aerodynamic control surfaces, rocket engine gimbaling, landing gear, and brakes. Future space vehicles, such as the Reusable Launch Vehicle, will also need APU's to

APU. Hydrazine's handling requirements are a significant contributor to the costs and time for preparing the shuttle for flight. Specially trained personnel and special equipment are needed because of the volatility, toxicity, and the caustic nature of hydrazine. Replacement of hydrazine with a nontoxic fuel would significantly reduce shuttle operation costs while enabling increased flight rates.

NASA has selected ethanol and oxygen as a candidate fuel mixture for replacing hydrazine fuel on the shuttle. Ethanol and oxygen have been used in the past for propulsion engines, and these fuels are considered to be nontoxic. Their use to fuel a turbine combustor is unique, however, and requires the development of new combustor components and control techniques.



As part of this technology development effort, Lewis designed and conducted tests on an experimental ethanol and oxygen combustor. These tests are critical in determining the feasibility and performance characteristics of various design options to upgrade the shuttle APU. Combustion efficiency and soot generation were measured, and the reliability of ignition and control options were assessed. Lewis' expertise in turbomachinery and combustion, as well as its unique facilities, contributed to the success of this initial test program.

Initial test results demonstrated good combustion efficiency along with minimal soot generation and confirmed the viability of several ignition and fuel control options. In addition to this experimental test program, NASA Lewis and industry are developing analysis models and are assessing the state of the fuel and the overall thermal management of the APU system. Analytical models have also been developed to evaluate combustion chemical kinetics and preliminary designs for heat exchangers.

**Lewis contacts:**

Dr. Larry A. Viterna, (216) 433-5398,  
Larry.A.Viterna@lerc.nasa.gov, and  
Mark D. Klem, (216) 977-7474,  
Mark.D.Klem@lerc.nasa.gov

**Author:** Dr. Larry A. Viterna

**Headquarters program office:** OSF

**Programs/Projects:** HEDS, STS, RLV,  
Space APU Advanced Technology

# Engineering and Technical Services

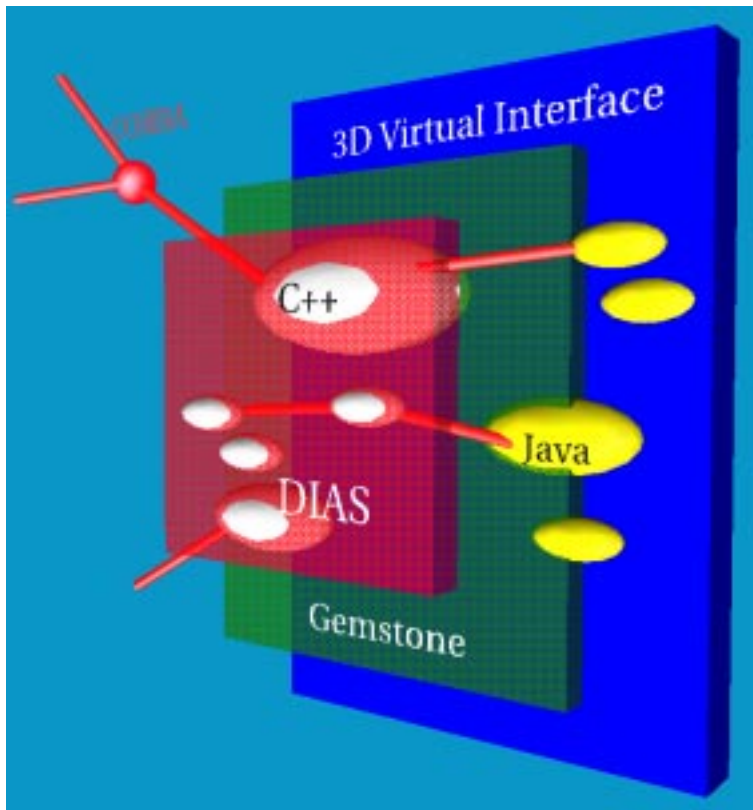


# Computer Services

## Antiterrorist Software

In light of the escalation of terrorism, the Department of Defense spearheaded the development of new antiterrorist software for all Government agencies by issuing a Broad Agency Announcement to solicit proposals. This Government-wide competition resulted in a team that includes NASA Lewis Research Center's Computer Services Division, who will develop the graphical user interface (GUI) and test it in their usability lab. The team launched a program entitled Joint Sphere of Security (JSOS), crafted a design architecture (see the following figure), and is testing the interface. This software system has a state-of-the-art, object-oriented architecture, with a main kernel composed of the Dynamic Information Architecture System (DIAS) developed by Argonne National Laboratory. DIAS will be used as the software "breadboard" for assembling the components of explosions, such as blast and collapse simulations.

Embedded in DIAS are C++ objects that represent state-of-the-art simulations developed at sundry laboratories with various areas of expertise. DIAS uses Gemstone, a middleware product that facilitates the use of CORBA and Java. CORBA allows distributed applications to talk across networks irrespective of language or operating system. Java applications and applets process queries and results from DIAS objects and display the results on the virtual interface. The Virtual Reality Modeling Language VRML2 is the outer software "wrapper" that allows simulations to be visualized in a full three-dimensional, interactive and intuitive interface.



*JSOS object-oriented architecture.*

Designed to be used by security officials who must deal with the threat of explosions, the JSOS interface can currently model blasts. A prototype scenario is depicted in the screen capture from JSOS (shown on the opposite page; figures are shown in color in the online version of this article: [http://www.lerc.nasa.gov/WWW/RT1997/7000/7100 clark1.htm](http://www.lerc.nasa.gov/WWW/RT1997/7000/7100%20clark1.htm)).

Menu choices lead users from categories of threats to specific threats. Users then define the scene by either selecting thumbnail photos that represent specific locations or by progressively zooming into a three-dimensional virtual world. The large database of sites available can be expanded to fit an agency's or center's needs after its requirements are analyzed. Global positioning systems (GPS's) can be used to assist in pinpointing locations. Once a scene is defined, the user positions a particular threat in the virtual environment. Because JSOS immerses users in the scene, this interface will be intuitive and natural for trial-and-error exercises, briefings, and presentations.

After defining the threat scene, the user can precipitate the destructive action by selecting the *detonate* button, whereby calculations are performed and results are illustrated (see the damage analysis from JSOS at the bottom of the next page).

The inner circle represents the region where death would occur, and the outer circle represents the region where there would be injury (e.g., due to window breakage). Audio prompts help users explore the scene. Currently the project is

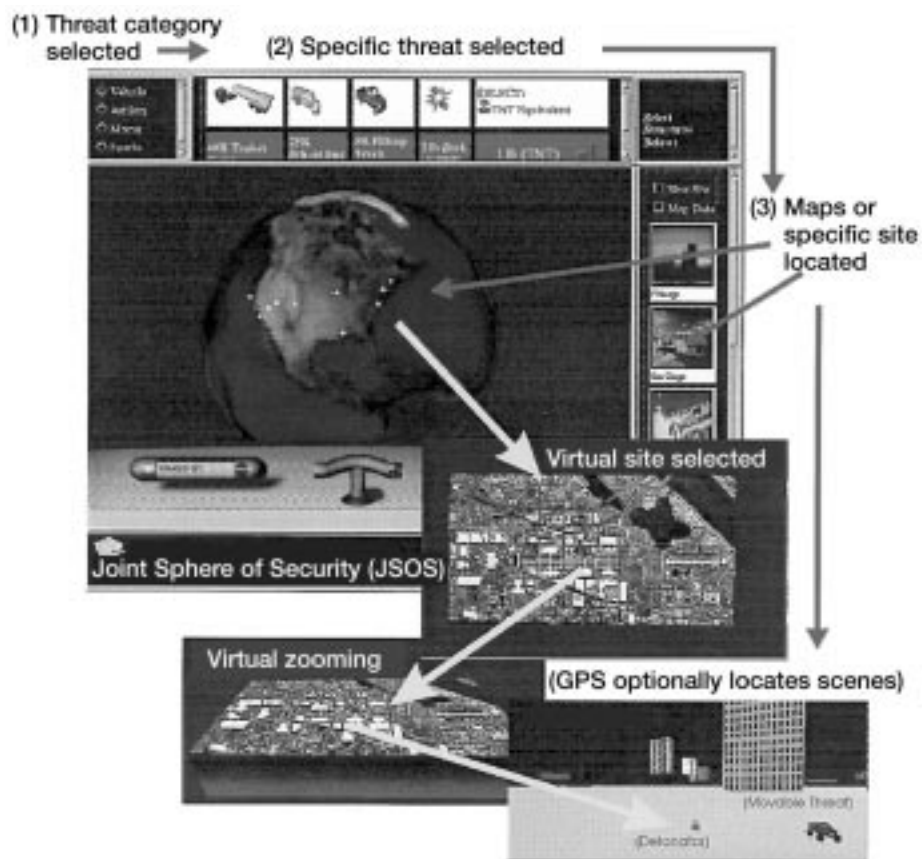
being developed to operate with an Internet browser to facilitate an application-on-demand paradigm (i.e., Java applets).

**Lewis contact:**

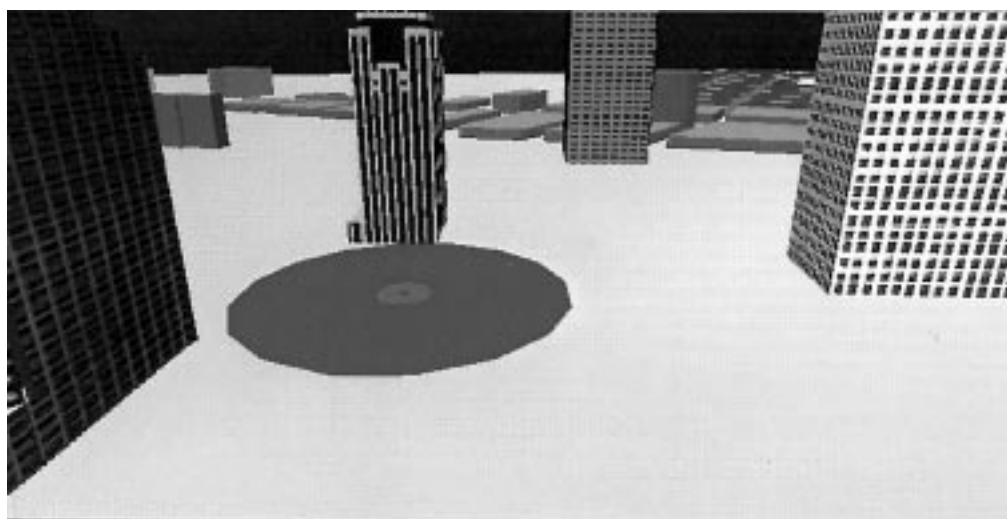
David A. Clark, (216) 433-5914,  
David.A.Clark@lerc.nasa.gov

**Author:** David A. Clark

**Headquarters program office:**  
Army Research Laboratory



Prototype scenario.



JSOS damage analysis.

# Worldwide Research, Worldwide Participation: Web-Based Test Logger

Thanks to the World Wide Web, a new paradigm has been born. ESCORT (steady state data system) facilities can now be configured to use a Web-based test logger, enabling worldwide participation in tests.

NASA Lewis Research Center's new Web-based test logger for ESCORT automatically writes selected test and facility parameters to a browser and allows researchers to insert comments. All data can be viewed in real time via Internet connections, so anyone with a Web browser and the correct URL (universal resource locator, or Web address) can interactively participate. As the test proceeds and ESCORT data are taken, Web browsers connected to the logger are updated automatically.

The use of this logger has demonstrated several benefits. First, researchers are free from manual data entry and are able to focus more on the tests. Second, research logs can be printed in report format immediately after (or during) a test. And finally, all test information is readily available to an international public.

This test logging system was recently demonstrated in Lewis' 10- by 10-Foot Supersonic Wind Tunnel. Wind tunnel data for a High Speed Research project inlet was automatically logged during a test, allowing researchers to concentrate on research activities instead of data entry.

Because the test was in a secure facility, only computers within the facility's secure intranet were able to connect during the test. Nevertheless, after

testing was completed, the data were moved to a secure Internet server. Select users could log in by user ID and password, and view encrypted logs and comments of the previous night's data. This test logger is being generalized into an updated (Java-based) Lewis-wide product that will be available to all Lewis test facilities.

**A limited demo is available on the World Wide Web:**

<http://predator.lerc.nasa.gov/~fsdcdc/2dinlet/>

**Lewis contact:**

David A. Clark, (216) 433-5914,  
[David.A.Clark@lerc.nasa.gov](mailto:David.A.Clark@lerc.nasa.gov)

**Author:** David A. Clark

**Headquarters program office:** OASTT

**Programs/Projects:** HSR, broad Government applications

A split screen is available:

## Upper section

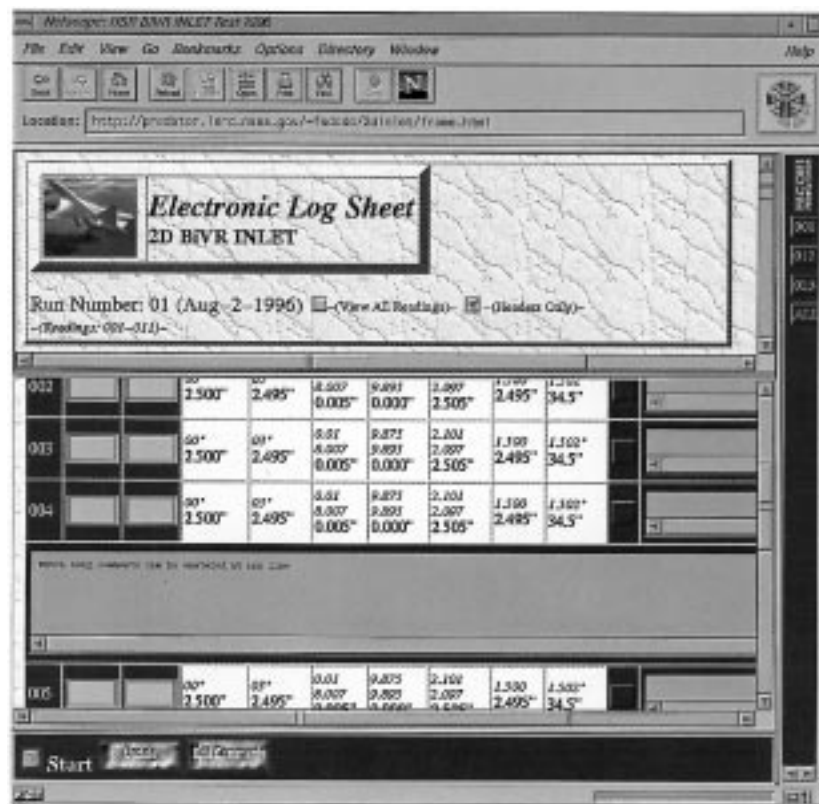
- Viewing data
- Printing data
- Sorting, etc.

## Lower section

- Entering notes
- Making addendums
- Changing text

## Extreme right

- Speed bar (quick reference for specific data points)





# Real-Time, Interactive Echocardiography Over High-Speed Networks: Feasibility and Functional Requirements



*Cleveland Clinic Foundation staff members conduct an echocardiographic examination at the NASA Lewis Research Center in Cleveland, Ohio, and transmit the live video and audio through the NASA Research and Education Network (NREN) to the NASA Ames Research Center in Mountainview, California, where the examination is remotely interpreted by another cardiologist.*

*Real-time, Interactive Echocardiography Over High Speed Networks: Feasibility and Functional Requirements* is an experiment in advanced telemedicine being conducted jointly by the NASA Lewis Research Center, the NASA Ames Research Center, and the Cleveland Clinic Foundation. In this project, a patient undergoes an echocardiographic examination in Cleveland while being diagnosed remotely by a cardiologist in California viewing a real-time display of echocardiographic video images transmitted over the broadband NASA Research and Education Network (NREN). The remote cardiologist interactively guides the sonographer administering the procedure through a two-way voice link between the two sites.

Echocardiography is a noninvasive medical technique that applies ultrasound imaging to the heart, providing a "motion picture" of the heart in action. Normally, echocardiographic examinations are performed by a sonographer and cardiologist who are located in the same medical facility as the patient. The goal of telemedicine is to allow medical specialists to examine patients located elsewhere, typically in remote or medically underserved geographic areas. For example, a small, rural clinic might have access to an echocardiograph machine but not a cardiologist. By connecting this clinic to a major metropolitan medical facility through a communications network, a minimally trained technician would be able to carry out the procedure under the supervision and guidance of a qualified cardiologist.

Although many telemedicine requirements can be satisfied by the transmission of still images (e.g., x-ray photographs and mammograms), the challenge of procedures like echocardiography is that high-resolution,

moving images must be transmitted in real time.

The main problem is bandwidth. The analog video signal produced by an echocardiograph machine requires a digital transmission bandwidth of just over 200 megabits per second (Mbps), and future three-dimensional echocardiograph equipment may require even more. Although it is possible to obtain sufficiently large telecommunications links, they can be prohibitively expensive. More importantly, they are simply not available in many parts of the world, including parts of North America. In fact, in most underdeveloped regions, it is difficult to find links approaching even 1 Mbps.

Since a major goal of telemedicine is to bring high-quality health care to underdeveloped areas, there is a need to transmit medical image data from outlying clinics to major health care facilities using whatever telecommunications links might be available—almost certainly far below the range of 200 Mbps! For moving images, such as echocardiographs, this requires the use of image compression techniques to squeeze the image data stream down to a manageable size while at the same time ensuring that the color, resolution, motion, and overall diagnostic quality of the image remain relatively unimpaired. In addition, since a compressed video stream is, in general, more easily degraded by transmission errors than an uncompressed stream, the interaction between the type of compression used and the link over which the compressed image is carried becomes extremely important. The NASA/Cleveland Clinic NREN test examined the interaction between a specific

compression algorithm (MPEG-2) and a specific type of communications protocol (asynchronous transfer mode, or ATM).

In this demonstration, the fiber-optic-based NREN provided a controlled engineering testbed for assessing the clinical feasibility of remote echocardiography. The research team was able to adjust MPEG-2 compression ratios along with ATM quality-of-service parameters (cell loss ratio, cell error ratio, and cell delay variation) to examine their effects on the diagnostic quality of the received image. Future experiments will use NREN to examine other compression techniques, such as wavelet compression, and different types of hybrid network architectures and protocols.

**Find out more on the World Wide Web:** <http://www.lerc.nasa.gov/WWW/ant/01projects.html>

**Lewis contact:**

David A. Foltz, (216) 433-5077,  
David.A.Foltz@lerc.nasa.gov

**Author:** Eric A. Bobinsky

**Headquarters program office:** OASTT

**Programs/Projects:** NREN, Next Generation Internet Architecture, Space Station Echocardiography, Telemedicine

## Manufacturing Engineering

### Electron Beam Welder Used to Braze Sapphire to Platinum

A new use for electron beam brazing was recently developed by NASA Lewis Research Center's Manufacturing Engineering Division. This work was done to fabricate a fiber-optic probe (developed by Sentec Corporation) that could measure high temperatures ( $<600^{\circ}\text{C}$ ) of vibrating machinery, such as in jet engine combustion research. Under normal circumstances, a sapphire fiber would be attached to platinum by a ceramic epoxy. However, no epoxies can adhere ceramic fibers to platinum under such high temperatures and vibration. Also, since sapphire and platinum have different thermal properties, the epoxy bond is subjected to creep over time. Therefore, a new method had to be developed that would permanently and reliably attach a sapphire fiber to platinum.

The fiber-optic probe assembly consists of a 0.015-in.-diameter sapphire fiber attached to a 0.25-in.-long, 0.059-in.-diameter platinum shell. Because of the small size of this assembly, electron beam brazing was chosen

instead of conventional vacuum brazing. The advantage of the electron beam is that it can generate a localized heat source in a vacuum. Gold reactive braze was used to join the sapphire fiber and the platinum. Consequently,

the sapphire fiber was not affected by the total heat needed to braze the components together.

First, a copper fixture that acted as a holding and centering device was fabricated. Then two 0.015-in.-diameter rings of gold braze were placed around the sapphire fiber, and the fiber was inserted into the platinum shell. The fixture was then placed in an electron beam welder with a vacuum atmosphere of  $10^{-4}$  Torr. A power setting of 1 mA at 55 kV was used to create a broad beam sufficient to melt and cause the gold wire to flow into the joint. The total time required for the braze was approximately 5 seconds.

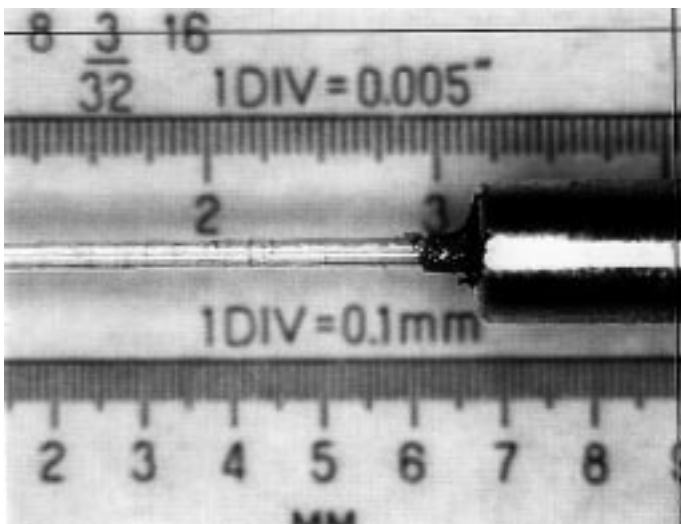
**Lewis contacts:**

Dr. Margaret L. Tuma, (216) 433-8665,  
Margaret.L.Tuma@lerc.nasa.gov;  
Walter A. Wozniak, (216) 433-2405,  
Walter.A.Wozniak@lerc.nasa.gov; and  
David Kowalski, (216) 433-2099,  
David.Kowalski@lerc.nasa.gov

**Authors:** Roger C. Forsgren and  
Thomas Vannuyen

**Headquarters program office:** OASTT

**Programs/Projects:** Aeronautics Base R&T, Fiber Optic Temperature Sensor



*Brazing a sapphire fiber to a platinum shell.*

# Facilities and Test Engineering

## New Spray Bar System Installed in NASA Lewis' Icing Research Tunnel

NASA Lewis Research Center's Icing Research Tunnel (IRT) is the world's largest refrigerated wind tunnel dedicated to the study of aircraft icing. In the IRT, natural icing conditions are duplicated to test the effects of in-flight icing on actual aircraft components and on scale models of airplanes and helicopters. The IRT's ability to reproduce a natural icing cloud was significantly improved with the recent installation of a new spray bar system. It is the spray bar system that transforms the low-speed wind tunnel into an icing wind tunnel by producing microscopic droplets of water and injecting them into the wind tunnel air stream in order to accurately simulate cloud moisture.

The spray bars and supporting mechanical and electrical systems were designed in-house by Lewis' Engineering Design and Analysis Division and Lewis' Facilities and Test Engineering Division. Accurate Machine Tool Company of Cleveland, Ohio, fabricated and assembled the spray bars, and North Bay Construction, Inc., also of Cleveland, installed the spray bars and the supporting mechanical system. The electrical system was installed in-house by Lewis' Facilities and Test Engineering Division and Lewis' Test Installation Division.

The spray bars are located in the wind tunnel settling chamber upstream of the test section. There are a total of 10 spray bars, which hold a total of approximately 130 air-assist atomizing water nozzles. In each of the 10 spray bars, there are two water headers that feed the water nozzles;

every header can be independently pressurized. This allows for step-function-type changes in the liquid water content of the icing cloud. At every nozzle location, solenoid valves control the water flow to the headers for that particular water nozzle. Each spray bar has an external cover that is an aerodynamically shaped fairing with a removable trailing edge. This feature allows for easy maintenance of the interior mechanical and electrical components.

Measurable improvements associated with the new system include an order-of-magnitude decrease in the time required to achieve a uniform icing cloud in the test section (from approximately 1 minute to less than 10 seconds), a greater than 100 percent increase in the size of the uniform cloud (from

15 to more than 30 ft<sup>2</sup>), and the creation of ice shapes similar to those produced by the previous spray bar system. After installation of the new spray bar system, test section aerodynamic calibrations and icing cloud calibrations—including the important parameters of icing cloud uniformity, droplet size distribution, liquid water content, and ice shape comparisons—were successfully completed.

The improved performance characteristics associated with the new spray bar system ensure the IRT's capability to re-create in-flight icing conditions, thus guaranteeing that the facility will continue to contribute to its primary goals, including computer simulation validation, ice accretion shape generation, ice protection system research and development testing, and aircraft ice protection system certification.

**Find out more about the IRT on the World Wide Web:**

<http://www.lerc.nasa.gov/WWW/IRT/>

**Lewis contact:**

Thomas B. Irvine, (216) 433-5369, [Thomas.B.Irvine@lerc.nasa.gov](mailto:Thomas.B.Irvine@lerc.nasa.gov)

**Author:** Thomas B. Irvine

**Headquarters program office:** OASTT

**Programs/Projects:** Aeronautics Base R&T



*New spray bar system for Lewis' Icing Research Tunnel as seen from the test section.*

## Luminescent Paints Used for Rotating Temperature and Pressure Measurements on Scale-Model High-Bypass-Ratio Fans

NASA Lewis Research Center is a leader in the application of temperature- and pressure-sensitive paints (TSP and PSP) in rotating environments. Tests were recently completed on several scale model, high-bypass-ratio turbofans in Lewis' 9- by 15-Foot Low-Speed Wind Tunnel. Two of the test objectives were to determine the aerodynamic and acoustic performance of the fan designs. Using TSP and PSP, researchers successfully achieved full-field aerodynamic loading profiles. The visualized loading profiles may help researchers identify factors contributing to the fans' performance and to the acoustic characteristics associated with the flow physics on the surface of the blades.

TSP and PSP were applied to individual blades 180° opposed on the fan rig. The painted blades were illuminated with multiple optically filtered high-speed strobes mounted in the test section wall. A rig-speed signal routed through an electronic shaft encoder controlled the firing of the strobes so that they would always "stop" the motion of the blades in the same location independent of the rig speed. Light emitted from the painted blades was detected with a cooled, digital, scientific-grade CCD (charge couple discharge) camera whose shutter was open for a controlled

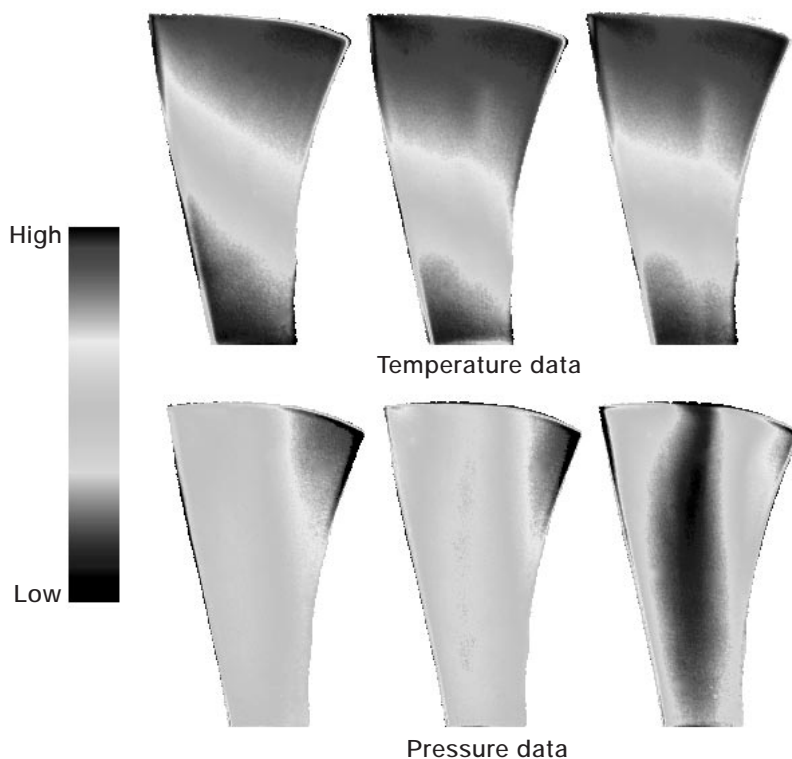
number of strobed revolutions. Temperature and pressure images were acquired sequentially with the same camera and optic filters.

Wind-off reference images and wind-on data images were needed for both TSP and PSP blades. Taking the ratio of the reference and data images enable corrections for nonuniform illumination and paint application. A general calibration supplied by the paint manufacturer was used for the normalized temperature and pressure images. Then, temperature dependence information from the paint supplier and acquired TSP data were used to correct the PSP images.





*Fan rig mounted in Lewis' 9- by 15-Foot Low-Speed Wind Tunnel. Blades are painted with TSP and PSP.*



**Lewis contacts:**

Timothy J. Bencic, (216) 433-5690,  
Timothy.J.Bencic@lerc.nasa.gov, and  
E. Brian Fite, (216) 433-3892,  
E.B.Fite@lerc.nasa.gov

**Author:** Timothy J. Bencic

**Headquarters program office:** OASTT

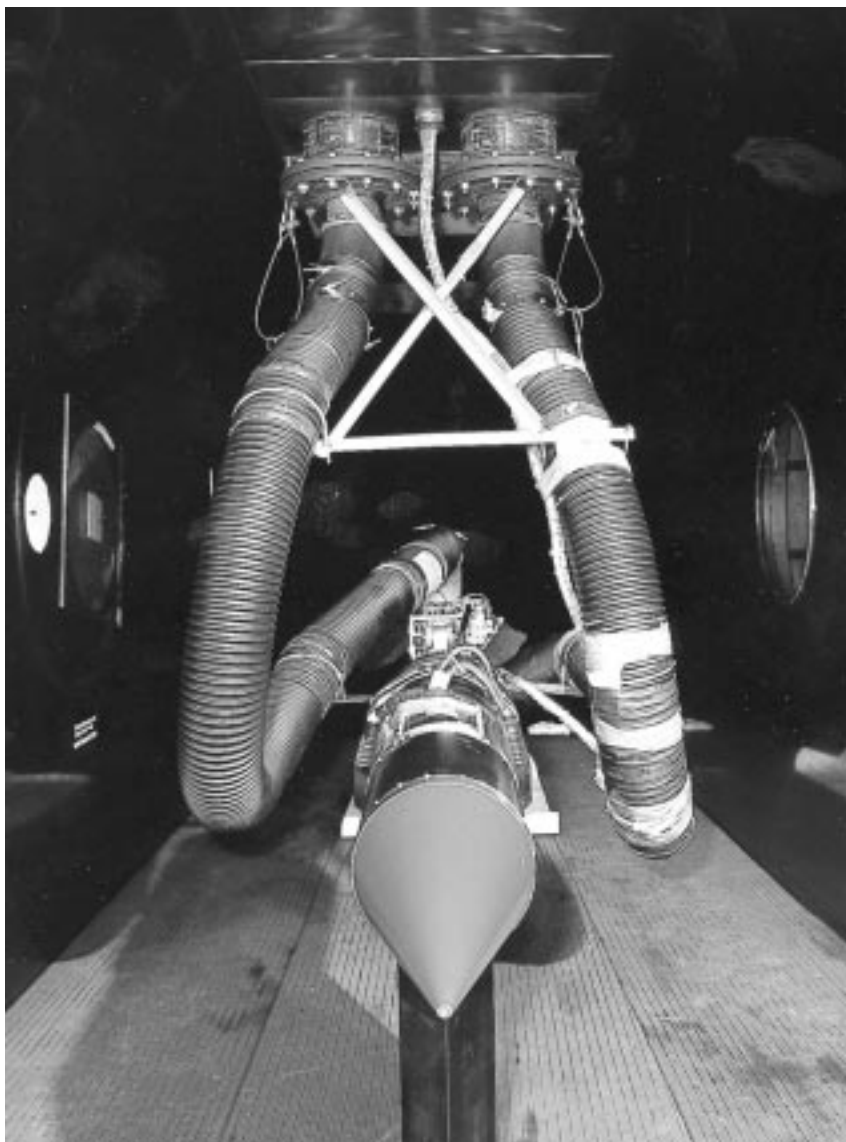
**Programs/Projects:**

Aeronautics Base R&T, AST

*Sequence of temperature and pressure images for a fan blade at constant speed but with varied aerodynamic loading.*



## New Model Exhaust System Supports Testing in NASA Lewis' 10- by 10-Foot Supersonic Wind Tunnel



*New model exhaust system supporting testing in Lewis' 10- by 10-Foot Supersonic Wind Tunnel.*

In early 1996, the ability to run NASA Lewis Research Center's Abe Silverstein 10- by 10-Foot Supersonic Wind Tunnel (10×10) at subsonic test section speeds was reestablished. Taking advantage of this new speed range, a subsonic research test program was scheduled for the 10×10 in the fall of 1996. However, many subsonic aircraft test models require an exhaust source to simulate main engine flow, engine bleed flows, and other phenomena. This was also true of the proposed test model, but at the time the 10×10 did not have a model exhaust capability. So, through an in-house effort over a period of only 5 months, a new model exhaust

system was designed, installed, checked out, and made ready in time to support the scheduled test program.

The system is designed to provide two lines of altitude exhaust, each capable of supplying up to 10 lb/sec of flow that can be connected to models in the 10×10. Flexible 8-in.-diameter hoses connecting the exhaust system to the model in the test section allow the model to be moved to desired pitch and yaw angles for research testing. Downstream of each hose, a 12-in.-diameter exhaust pipeline contains a flow measurement station (orifice plate and pressure transducers) and an electrohydraulic flow-control butterfly valve. The model exhaust system can be connected through valving to either of two exhaust sources—the tunnel exhausters or the lab central altitude exhaust system. Control for the exhaust system comes from the Westinghouse WDPF (Westinghouse Distributed Process Family) tunnel control system. This system can automatically control to an entered flow set point for each exhaust line.

**Find out more about the Abe Silverstein 10- by 10-Foot Supersonic Wind Tunnel on the World Wide Web:** <http://www.lerc.nasa.gov/WWW/AFED/facilities/10x10.html>

### **Lewis contacts:**

James W. Roeder, Jr., (216) 433-5677, [James.W.Roeder@lerc.nasa.gov](mailto:James.W.Roeder@lerc.nasa.gov), and Gary A. Klann, (216) 433-5715, [Gary.A.Klann@lerc.nasa.gov](mailto:Gary.A.Klann@lerc.nasa.gov)

**Author:** James W. Roeder, Jr.

**Headquarters program office:** OASTT

**Programs/Projects:**

Aeronautics Base R&T, AST, HSR

## Process Developed for Forming Urethane Ice Models

A new process for forming ice shapes on an aircraft wing was developed at the NASA Lewis Research Center. The innovative concept was formed by Lewis' Icing Research Tunnel (IRT) team, and the hardware was manufactured by Lewis' Manufacturing Engineering Division. This work was completed to increase our understanding of the stability and control of aircraft during icing conditions. This project will also enhance our evaluation of true aerodynamic wind tunnel effects on aircraft. In addition, it can be used as a design tool for evaluating ice protection systems.

Previously, the lost bee's wax method was used to fabricate ice models on aircraft wing sections. This method involved making a beeswax mold and filling it with plaster to form the ice models. After the plaster dried, the beeswax was melted off the plaster ice mold.

This ice modeling process has several disadvantages: (1) during fabrication, some definition of the ice model is lost because of handling; (2) the models tend to be brittle and break off easily because they are made of plaster; and (3) only one model can be fabricated at a time. Lewis' new procedure for forming urethane ice models solves all these drawbacks. With this new process, no definition is lost, the models are much more durable, and mass production is readily available.



*Left to right: Urethane ice model, wing shape model, and pliable silicone rubber RTV 1000A&B mold.*

For urethane ice models, a hard room-temperature vulcanizing (RTV) silicone rubber mold is formed of an actual ice shape in the Icing Research Tunnel. Then, an exact model is made of the wing shape that the ice came from, and a plywood box is constructed to contain both the hard RTV silicone rubber and wing shape. Release agents are applied to the hard rubber mold and wing shapes, and a two-part urethane casting material is poured into the mold to create the actual ice shape. Since the original hard rubber mold (RTV 3110) is destroyed when the cured urethane ice shape is removed, a softer, more pliable silicone rubber mold (RTV 1000A&B) must be formed around the urethane cast of the ice shape. After the pliable rubber mold solidifies, an unlimited number of identical ice shapes can be cast.

**Lewis contacts:**

David W. Sheldon, (216) 433-5662, David.W.Sheldon@lerc.nasa.gov; Daniel V. Gura, (216) 433-3363, Daniel.V.Gura@lerc.nasa.gov; and Robert J. Reminder, (216) 433-3363, Robert.J.Reminder@lerc.nasa.gov

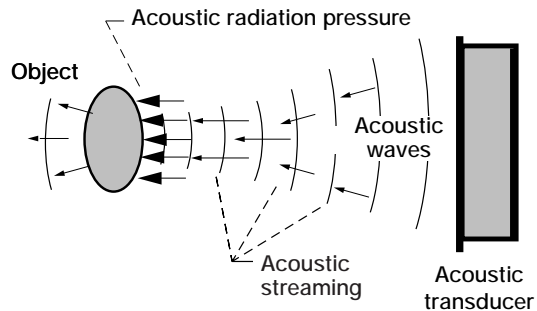
**Author:** Thomas Vannuyen

**Headquarters program office:** OASTT

**Programs/Projects:** Aeronautics Base R&T, Modern Airfoil Section Project, Tail Plane Icing Project

# Engineering Design and Analysis

## Manipulating Liquids With Acoustic Radiation Pressure Phased Arrays

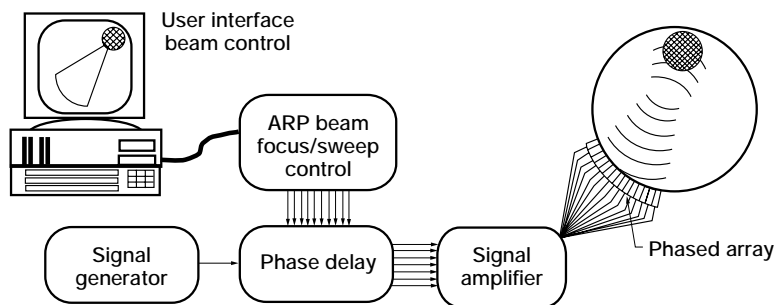


*Acoustic Radiation Pressure.*

High-intensity ultrasound waves can produce the effects of "Acoustic Radiation Pressure" (ARP) and "acoustic streaming." These effects can be used to propel liquid flows and to apply forces that can be used to move or manipulate floating objects or liquid surfaces. NASA's interest

in ARP includes the remote-control agitation of liquids and the manipulation of bubbles and drops in liquid experiments and propellant systems.

A high level of flexibility is attained by using a high-power acoustic phased array to generate, steer, and focus a beam of acoustic waves. This is called an Acoustic Radiation Pressure Phased Array, or ARPPA. In this approach, many acoustic transducer elements emit wavelets that converge into a single beam of sound waves. Electronically coordinating the timing, or "phase shift," of the acoustic waves makes it possible to form a beam with a predefined direction and focus. Therefore, a user can direct the ARP force at almost any desired point within a liquid volume.



*Acoustic Radiation Pressure Phased Array (ARPPA) system.*

ARPPA lets experimenters manipulate objects anywhere in a test volume. This flexibility allows it to be used for multiple purposes, such as to agitate liquids, deploy and manipulate drops or bubbles, and even suppress sloshing in spacecraft propellant tanks.

NASA Lewis Research Center's ARPPA technique uses an all-digital form of phase shifting to achieve the desired beam steering and focusing. Instead of using expensive phase shift circuits to control the acoustic waves and the beam shape, ARPPA forms the beam as a series of digital words in computer memory. A simple algorithm is used to calculate the desired beam focus and steering angle. Then, an off-the-shelf digital word generator is used with a reference frequency source to clock the pattern at the desired frequency. The signal is amplified from logic-level voltages to well over 100 V. The high-voltage signals are used to drive the acoustic phased

array. Each channel has a separate amplifier to drive each individual array element. Users can operate the system interactively by using a computer mouse or similar input device. When complete, the system should be able to track an object and apply the ARP force to manipulate its position and behavior in real time.

Because this system is nonintrusive, users can manipulate liquids or objects without opening the containers, making it possible to safely handle many toxic or reactive chemicals. Consequently, ARPPA has many potential ground-based applications in the handling and agitation of liquid slurries in the production of chemicals and paints.

The technique can also be used to create standing surface waves like those used for applying coatings and solders to electronic circuit boards. The ability to alter the surface wave on command may make it possible to eliminate masking operations. This, in turn, would reduce tooling costs and chemical waste products.

This ongoing work is being done entirely in-house by research engineers at NASA Lewis. Funding is being provided by the Lewis Director's Discretionary Fund.

### **Lewis contact:**

Richard C. Oeftering, (216) 433-2285,  
Richard.C.Oeftering@lerc.nasa.gov

**Author:** Richard C. Oeftering

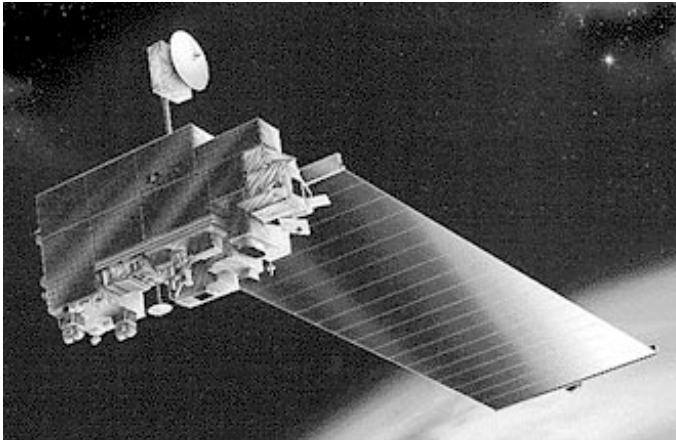
### **Headquarters program office:**

Lewis Director's Discretionary Fund

### **Programs/Projects:** Microgravity

Science, broad-based technology development for ground or space use

# Statistical Treatment of Earth Observing System Pyroshock Separation Test Data



*EOS spacecraft.*

The Earth Observing System (EOS) AM-1 spacecraft for NASA's Mission to Planet Earth is scheduled to be launched on an Atlas IAS vehicle in June of 1998. One concern is that the instruments on the EOS spacecraft are sensitive to the shock-induced vibration produced when the spacecraft separates from the launch vehicle. By employing unique statistical analysis to the available ground test shock data, the NASA Lewis Research Center found that shock-induced vibrations would not be as great as the previously specified levels of Lockheed Martin.

The EOS pyroshock separation testing, which was completed in 1997, produced a large quantity of accelerometer data to characterize the shock response levels at the launch vehicle/spacecraft interface. Thirteen pyroshock separation firings of the EOS and payload adapter configuration yielded 78 total measurements at the interface. The multiple firings were necessary to qualify the newly developed Lockheed Martin six-hardpoint separation system.

Because of the unusually large amount of data acquired, Lewis developed a statistical methodology to predict the maximum expected shock levels at the interface between the EOS spacecraft and the launch vehicle. Then, this methodology, which is based on six shear plate accelerometer measurements per test firing at the spacecraft/launch vehicle interface, was used to determine the shock endurance specification for EOS.

Each pyroshock separation test of the EOS spacecraft simulator produced its own set of interface accelerometer data. Probability distributions, histograms, the median, and higher order moments (skew and kurtosis) were analyzed. The data were found to be lognormally distributed, which is consistent with NASA pyroshock standards. Each set of lognormally transformed test data produced was analyzed to determine if the data should be combined statistically. Statistical testing of the data's standard deviations and means ( $F$  and  $t$  testing, respectively) determined if data sets were significantly different at a 95-percent confidence level. If two data sets were found to be significantly different, these families of data were not combined for statistical purposes.

This methodology produced three separate statistical data families of shear plate data. For each population, a P99.1/50 (probability/confidence) per-separation-nut firing level was calculated. By using the binomial distribution, Lewis researchers determined that this per-nut firing level was equivalent to a P95/50 per-flight confidence level. The overall envelope of the per-flight P95/50 levels led to Lewis' recommended EOS interface shock endurance specification. A similar methodology was used to develop Lewis' recommended EOS mission assurance levels.

The available test data for the EOS mission are significantly larger than for a normal mission, thus increasing the confidence level in the calculated expected shock environment. Lewis significantly affected the EOS mission by properly employing statistical analysis to the data. This analysis prevented a costly requalification of the spacecraft's instruments, which otherwise would have been exposed to significantly higher test levels.

## Find out more on the World Wide

**Web:** <http://eosps0.gsfc.nasa.gov>  
<http://www.hq.nasa.gov/office/mtpe>

## Bibliography

Hughes, W.O.; and McNelis, A.M.: Statistical Analysis of a Large Sample Size Pyroshock Test Data Set. Proceedings of the 68th Shock and Vibration Symposium, Hunt Valley, MD, Nov., 1997.

## Lewis contacts:

Anne M. McNelis, (216) 433-8880, [Anne.M.McNelis@lerc.nasa.gov](mailto:Anne.M.McNelis@lerc.nasa.gov), and William O. Hughes, (216) 433-2597, [William.O.Hughes@lerc.nasa.gov](mailto:William.O.Hughes@lerc.nasa.gov)

**Authors:** Anne M. McNelis and William O. Hughes

**Headquarters program office:** MTPE  
**Programs/Projects:** MTPE, EOS



# New Test Section Installed in NASA Lewis' 1- by 1-Foot Supersonic Wind Tunnel

NASA Lewis Research Center's 1- by 1-Foot Supersonic Wind Tunnel (1×1) is a critical facility that fulfills the needs of important national programs. This tunnel supports supersonic and hypersonic research test projects for NASA, for other Government agencies, and for industry, such as the High Speed Research (HSR) and Space Transportation Technologies (STT) programs. The 1×1, which is located in Lewis' Building 37, Cell 1NW, was built in 1954 and was upgraded to provide Mach 6.0 capability in 1989. Since 1954, only minor improvements had been made to the test section.

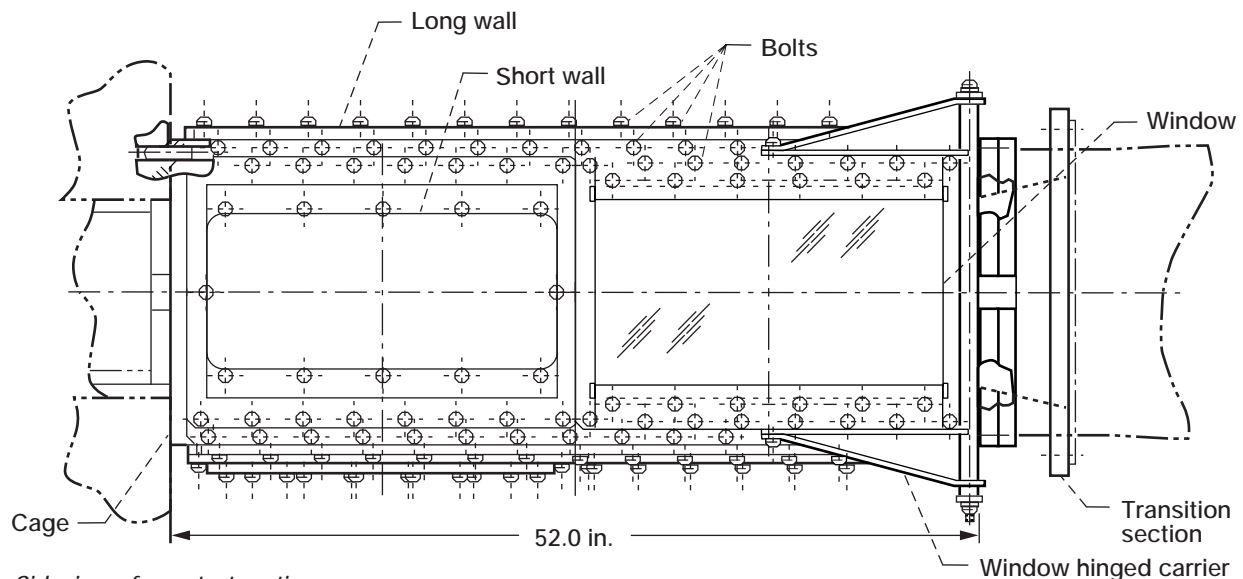
To improve the 1×1's capabilities and meet the needs of these programs, Lewis recently redesigned and replaced the test section. The new test section has interchangeable window and wall inserts that allow easier and faster test configuration changes, thereby improving the adaptability and productivity of this highly utilized facility. In addition, both the wall and window areas are much larger. The larger walls provide more flexibility in how models are mounted and instrumented. The new window design vastly increases optical access to the research test hardware, which makes the use of advanced flow-visualization systems more effective.

The new test section consists of a central frame, called the cage, which provides four identically sized, full-length openings in each of its four sides. This feature permits long walls to be interchangeably located in any position. The addition of a center frame, which divides any full-length cage opening into two identical openings and complements the structural integrity of the complete test section assembly, allows window or short wall inserts to be interchangeably located. Windows can be mounted tandem or across from one another, but not adjacent to (share a corner with) each other. Otherwise, any mounting combination of inserts is possible. To provide uniform and flush flow-walls, which are critical to high-speed research testing, and to ensure interchangeability without individual alignment or shimming, we held the dimensional tolerances of all parts very tight. All

the inserts were designed to maximize the wall panel and/or window area and to provide research engineers with the greatest amount of versatility.

The new windows provide 40 percent more area and are designed for use at all test conditions, including the hypersonic operating range through Mach 6.0. The window glass is made from a high-quality fused silica material that is transparent both for direct viewing and to advanced research flow-visualization instruments that use lasers and other special imaging techniques.

The long wall is of particular interest to research customers of the facility. Because it fills one full-length opening in the cage, the long wall offers unprecedented flexibility in both the mounting of models and the installation of special instrumentation. The long wall panel is a relatively simple and inexpensive part that can be used by customers to assemble and prepare their research test hardware in



*Sideview of new test section.*



advance, outside of the tunnel test section. Now that the new test section is fully operational, many tests have been planned that will fully utilize the 1×1's unique, enhanced features.

**Find out more about Lewis' 1- by 1-Foot Supersonic Wind Tunnel on the World Wide Web:**

<http://www.lerc.nasa.gov/WWW/AFED/facilities/1x1.html>

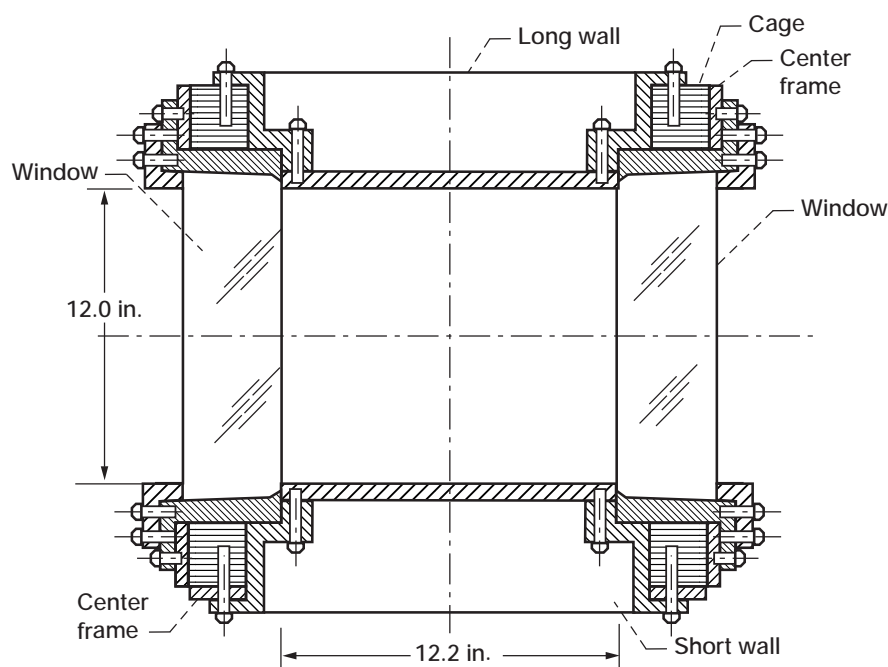
**Lewis contacts:**

Steven W. Bauman, (216) 433-3826, Steven.W.Bauman@lerc.nasa.gov, and Gary A. Klann, (216) 433-5715, Gary.A.Klann@lerc.nasa.gov

**Author:** Steven W. Bauman

**Headquarters program office:** OASTT

**Programs/Projects:** Propulsion Systems R&T, HSR, AST, STS



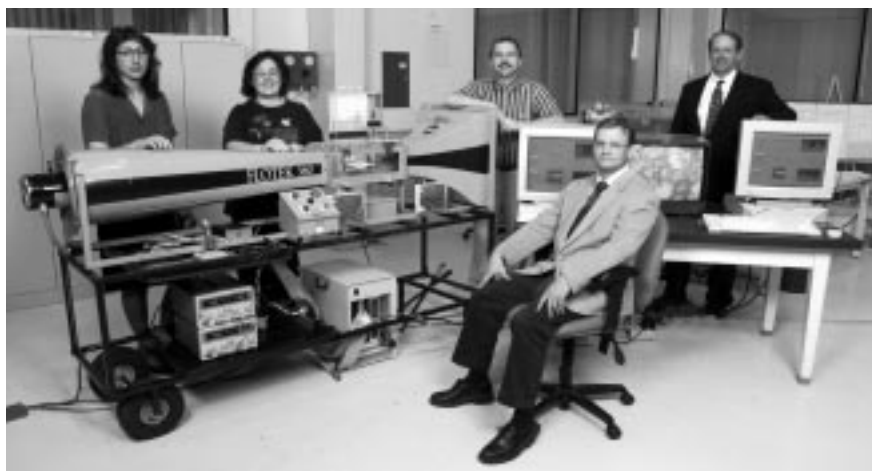
*Typical cross section of new test section.*

## Embedded Web Technology: Internet Technology Applied to Real-Time System Control

The NASA Lewis Research Center is developing software tools to bridge the gap between the traditionally non-real-time Internet technology and the real-time, embedded-controls environment for space applications. Internet technology has been expanding at a phenomenal rate. The simple World Wide Web browsers (such as earlier versions of Netscape, Mosaic, and Internet Explorer) that resided on personal computers just a few years ago only enabled users to log into and view a remote computer site. With current browsers, users not only view but also interact with remote sites. In

addition, the technology now supports numerous computer platforms (PC's, MAC's, and Unix platforms), thereby providing platform independence.

In contrast, the development of software to interact with a micro-processor (embedded controller) that is used to monitor and control a space experiment has generally been a unique development effort. For each experiment, a specific graphical user interface (GUI) has been developed. This procedure works well for a single-user environment. However, the interface for the International Space Station (ISS) Fluids and Combustion Facility will have to enable scientists throughout the world and astronauts onboard the ISS, using different computer platforms, to interact with their experiments in the Fluids and Combustion Facility.



*Small wind tunnel (6- by 6-in. test section) controlled over the Internet.*

Developing a specific GUI for all these users would be cost prohibitive. An innovative solution to this requirement, developed at Lewis, is to use Internet technology, where the general problem of platform independence has already been partially solved, and to leverage this expanding technology as new products are developed. This approach led to the development of the Embedded Web Technology (EWT) program at Lewis, which has the potential to significantly reduce software development costs for both flight and ground software. However, applying this solution to the Fluids and Combustion Facility, or any other embedded control, would require technological breakthroughs.

The Lewis team proceeded to develop the first real-time embedded hypertext transfer protocol server software designed for space flight. This software, when loaded into a control processor, allows the processor to act as a "remote site." Authorized users, using a browser, can interact with the control processor to retrieve data and control the experiment. Another innovation is to serve Java applets (executable programs written in Java and embedded in Web pages). When users download the desired applets to their browsers, the applet produces a graphic of the sensor and the current sensor reading. Users can thus develop their own GUI's. This innovation alone has the potential for enormous cost savings over the alternative of developing many specific GUI's, and it is directly applicable to our original problem of how to support many undefined users on multiple platforms.

The Embedded Web Technology program also has commercial and non-space applications in products where a microprocessor is used for control. The developed software has been loaded into a control computer for a

small wind tunnel. The wind tunnel, which is controlled via the Internet, will demonstrate the technology at an Embedded Web Technology workshop sponsored by the Great Lakes Industrial Technology Center, a NASA Technology Center managed by Batelle. The workshop will foster technology transfer to commercial businesses in the Great Lakes Region.

**More information is available on the World Wide Web:**

<http://fcfsrv1.lerc.nasa.gov/public/>  
<http://zeta.lerc.nasa.gov/fcfwww/index.htm>

**Lewis contacts:**

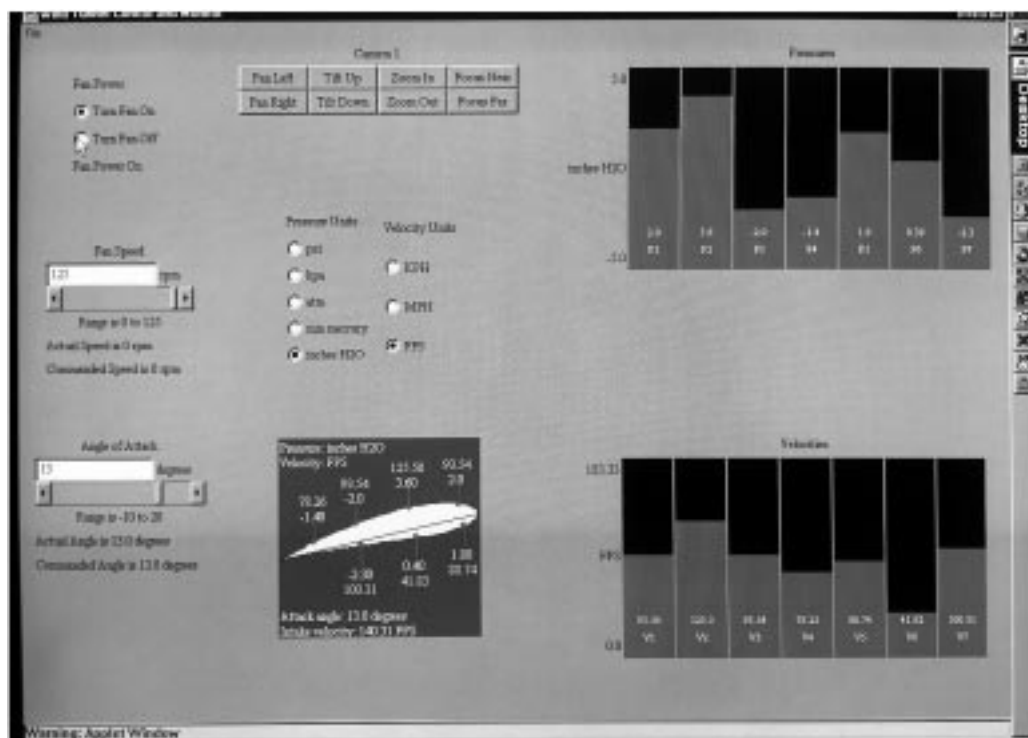
Carl J. Daniele, (216) 433-5325,  
 Carl.J.Daniele@lerc.nasa.gov;  
 Richard A. Tyo, (216) 433-8619,  
 Richard.A.Tyo@lerc.nasa.gov; and  
 David W. York, (216) 433-3162,  
 David.W.York@lerc.nasa.gov

**Author:** Carl J. Daniele

**Headquarters program office:** OLMSA

**Programs/Projects:**

Microgravity Science, ISS, EWT



Graphical user interface screen developed using Java applets for controlling the small wind tunnel.

# Commercial Technology



# NASA Lewis Helps Company With New Single-Engine Business Turbojet



*Century Aerospace single-engine business turbojet. (Copyright Century Aerospace Corporation; used with permission.)*

Century Aerospace Corporation, a small company in Albuquerque, New Mexico, is developing a six-seat aircraft powered by a single turbofan engine for general aviation. The company had completed a preliminary design of the jet but needed analyses and testing to proceed with detailed design and subsequent fabrication of a prototype aircraft. NASA Lewis Research Center used computational fluid dynamics (CFD) analyses to ferret out areas of excessive curvature in the inlet where separation might occur. A preliminary look at the results indicated very good inlet performance; and additional calculations, performed with vortex generators installed in the inlet, led to even better results. When it was initially determined that the airflow distortion pattern at the compressor face fell outside of the limits set by the engine manufacturer, the Lewis team studied possible solutions, selected the best, and provided recommendations. CFD results for the inlet system were so good that wind tunnel tests were unnecessary.

Lewis' Inlet Branch uses various NASA CFD codes to aid in the design of aircraft inlets. Members of this branch conducted initial CFD design assistance on Century Aerospace's engine inlet and also provided computational fluid dynamics software and training. After additional CFD runs verified design recommendations, Century Aerospace obtained agreement from the engine manufacturer and incorporated the changes in the design.

Century Aerospace now expects to meet 1999 production goals for its new business turbojet, creating 400 new jobs in the process. A market study shows that as many as 708 aircraft (at roughly \$1.85 million each) could be sold over a 10-year period.

**Lewis contacts:**

Commercial Technology Office,  
(216) 433-5568, and John M. Abbott,  
(216) 433-3607,  
[John.M.Abbott@lerc.nasa.gov](mailto:John.M.Abbott@lerc.nasa.gov)

**Author:** Commercial Technology Office

**Headquarters program office:** OASTT

**Programs/Projects:**  
Technology Transfer

## NASA Lewis Helps Develop Advanced Saw Blades for the Lumber Industry

NASA Lewis Research Center's Structures and Material Divisions are centers of excellence in high-temperature alloys for aerospace applications such as advanced aircraft and rocket engines. Lewis' expertise in these fields was enlisted in the development of a new generation of circular sawblades for the lumber industry to use in cutting logs into boards.

The U.S. Department of Agriculture's (USDA) Forest Products Laboratory and their supplier had succeeded in developing a thinner sawblade by using a nickel-based alloy, but they needed to reduce excessive warping due to residual stresses. They requested assistance from Lewis' experts, who successfully eliminated the residual stress problem and increased blade strength by over 12 percent. They achieved this by developing an innovative heat treatment based on their knowledge of nickel-based superalloys used in aeropropulsion applications.

**Lewis contacts:**

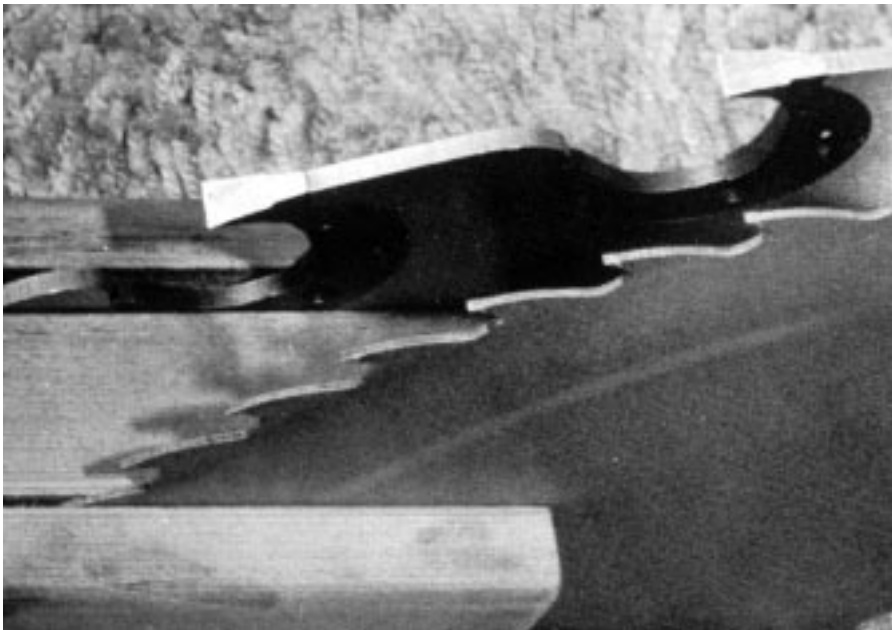
Commercial Technology Office,  
(216) 433-5568, and  
Dr. Paul A. Bartolotta, (216) 433-3338,  
Paul.A.Bartolotta@lerc.nasa.gov

**Author:** Commercial Technology Office

**Headquarters program office:** OASTT

**Programs/Projects:** Technology  
Transfer, Aeronautics Base R&T, HOST

**Special recognition:** Space Act Award



*Advanced saw blade compared with older blade.*

At this time, it appears that the scope of the impact of this joint effort between the USDA and NASA will extend far beyond the commercial benefits to the blade manufacturer. The new thinner blades are expected to increase the amount of usable lumber gained from each log by 5 percent, which could lead to over 2 million trees saved each year and to a 4- to 5-percent cost reduction in new housing costs. In turn, the reduction in new housing costs could lead to increased new housing starts and increased demand for additional consumer products. In short, the new blades could mean that 1 billion board feet of lumber will be recovered from what otherwise would be sawdust and waste wood—benefiting our environment and our economy.



# Modeling Code Is Helping Cleveland Develop New Products



*Lewis researcher Dale Hopkins and Master Builders engineer Steve Tysl discuss ICAN models and computations of performance properties for cement-based materials.*

Master Builders, Inc., is a 350-person company in Cleveland, Ohio, that develops and markets specialty chemicals for the construction industry. Developing new products involves creating many potential samples and running numerous tests to characterize the samples' performance. Company engineers enlisted NASA's help to replace cumbersome physical testing with computer modeling of the samples' behavior. Since the NASA Lewis Research Center's Structures Division develops mathematical models and associated computation tools to analyze the deformation and failure of composite materials, its researchers began a two-phase effort to modify Lewis' Integrated Composite Analyzer (ICAN) software for Master Builders' use. Phase I has been completed, and Master Builders is pleased with the results. The company is now working to begin implementation of Phase II.

Structures Division researchers adapted ICAN to model concrete micro-structures and predict mechanical performance under structural loads. (ICAN was originally developed to model the behavior of fiber-reinforced polymer matrix composites.) Lewis delivered the code in a format compatible for desktop personal computers (PC's) and provided data from a validation test case, as well as preliminary user instructions for the company's independent evaluation and use of the software. In addition, Lewis will be able to use the modified software for its own jet engine research.

The modified NASA software has already allowed Master Builders to improve the productivity of its batch testing by 200 percent and to save an estimated \$25,000 to \$100,000. The completed project will enable this company to create its specialty products more quickly and economically, as well as to increase the number of new products it can develop.

**Lewis contacts:**

Commercial Technology Office,  
(216) 433-5568, and  
Dale A. Hopkins, (216) 433-3260,  
Dale.A.Hopkins@lerc.nasa.gov

**Author:** Commercial Technology Office

**Headquarters program office:** OASTT

**Programs/Projects:** Aeronautics Base  
R&T, Technology Transfer

**Special recognition:**

NASA Team Achievement Award

## Electronics Manufacturer Provided With Testing and Evaluation Data Necessary to Obtain Additional Orders



*Cellular phone antenna tested by Lewis.*

Without Lewis' technical assistance in obtaining test data confirming the antenna's performance, this company would not have been awarded the contract. As a result of Lewis' interaction, Sterling has been successful in obtaining additional contracts, which have enabled them move to a larger location and to stabilize the number of employees in their workforce.

**Lewis contacts:**

Commercial Technology Office,  
(216) 433-5568, and  
Richard R. Kunath, (216) 433-3490,  
Richard.R.Kunath@lerc.nasa.gov

**Author:** Commercial Technology Office

**Headquarters program office:** OSS

**Programs/Projects:**  
Technology Transfer

A local electronics manufacturer, the Sterling Manufacturing Company, was presented with the opportunity to supply 30,000 automotive cellular antennas to a European subsidiary of a large U.S. auto manufacturer. Although the company built an antenna that they believed would meet the auto manufacturer's specifications, they were unable to conduct the necessary validation tests in-house. They decided to work with NASA Lewis Research Center's Space Electronics Division, which, as part of its technology development program, evaluates the performance of antennas in its Microwave Systems Lab to assess their capabilities for space communications applications. Data measured in Lewis' Microwave Systems Lab proved that Sterling's antenna performed better than specified by the auto manufacturer.

## NASA Lewis' Icing Research Tunnel Works With Small Local Company to Test Coatings



*Dynamic Coatings race car coated with new product.*

Dynamic Coatings, Inc., wanted to test coating products that would enable the company to approach new markets. A Space Act Agreement with NASA Lewis Research Center afforded them this opportunity. They used Lewis' Icing Research Tunnel to test coating products for reduced ice adhesion, industrial and aerospace lubrication applications, a tire-mold release coating now used in the production of tires for the Boeing 777, and a product that solidifies asbestos fibers (which is being tested as an insulator in a power plant in Iowa). Not only was the testing a success, but during these activities, Dynamic Coatings met another coating company with whom they now have a joint venture offering a barnacle-repellent coating for marine applications, now on the market in Florida.

The company has grown to \$100,000 per year in sales and is poised for further expansion. Projected sales for the solidification product, if a full test in a power plant is successful, are \$10 million per month. Three new or improved products are directly associated with Dynamic Coatings' interaction with Lewis.

**Lewis contacts:** Commercial Technology Office, (216) 433-5568, and Stephen M. Riddlebaugh, (216) 433-5565, [Stephen.M.Riddlebaugh@lerc.nasa.gov](mailto:Stephen.M.Riddlebaugh@lerc.nasa.gov)

**Author:** Commercial Technology Office

**Headquarters program office:** OASTT

**Programs/Projects:** Aeronautics Base R&T, Boeing 777, Technology Transfer

## NASA Lewis and Ohio Company Hit Hole in One

Ben Hogan Company's Golf Ball Division, which is based in Elyria, Ohio, had developed concepts and prototypes for new golf balls but was unable to determine exact performance characteristics. Specifically, the company's R&D department wanted to measure the spin rates of experimental golf balls. After the Golf Ball Division requested assistance, researchers and technicians from the NASA Lewis Research Center went to Elyria and conducted several days worth of tests. Ben Hogan is using the test results to improve the spin characteristics of a new ball it plans to introduce to the market. This company has requested additional NASA testing of its golf balls, so another project is being planned.

The Lewis Imaging Technology Center's (ITC) Scientific Imaging Group's state-of-the-art, high-speed digital imaging equipment gathers high-quality digital imagery to measure, analyze, and obtain accurate data for numerous applications. The technology had been used to improve and/or develop the next generation of aircraft engine inlet ducts. For its work with Ben Hogan, ITC measured the spin rates of seven types of balls—four of which were experimental—by marking the golf balls with data analysis control points, hitting three balls of each type with four different golf clubs, capturing images of the balls in flight with high-speed digital imaging equipment, archiving the imaging data, and analyzing the data via computer to determine spin rates and velocities. The spin rate calculations helped Ben Hogan engineers to evaluate the ball designs and further the development of a new golf ball.

The company estimates that Lewis' assistance could increase sales by 30 percent and employment by 20 percent when introduction and production begins, which is planned for the coming year.

**Lewis contacts:**

Commercial Technology Office,  
(216) 433-5568, and  
Jay C. Owens, (216) 433-5976,  
Jay.C.Owens@lerc.nasa.gov

**Author:** Commercial Technology Office

**Programs/Projects:**

Technology Transfer, golf balls



*Flight testing of golf balls.*

# New Research Methods Developed for Studying Diabetic Foot Ulceration

Dr. Brian Davis, one of the Cleveland Clinic Foundation's researchers, has been investigating the risk factors related to diabetic foot ulceration, a problem that accounts for 20 percent of all hospital admissions for diabetic patients. He had developed a sensor pad to measure the friction and pressure forces under a person's foot when walking. As part of NASA Lewis Research Center's Space Act Agreement with the Cleveland Clinic Foundation, Dr. Davis requested Lewis' assistance in visualizing the data from the sensor pad. As a result, Lewis' Interactive Data Display System (IDDS) was installed at the Cleveland Clinic. This computer graphics program is normally used to visualize the flow of air through aircraft turbine engines, producing color two- and three-dimensional images.

Using IDDS, Dr. Davis can now map data onto a grid and then map the outline of a patient's foot over the data. The information that the sensor pad and IDDS provide will help improve our understanding of the factors that lead to skin breakdown, and should ultimately improve the quality of life for diabetic patients.

## Bibliography

Stegeman, J.D.: User's Manual for Interactive Data Display System (IDDS). NASA TM-105572, 1992.

## Lewis contacts:

Commercial Technology Office,  
(216) 433-5568, and  
James D. Stegeman, (216) 433-3389,  
James.D.Stegeman@lerc.nasa.gov

**Author:** Commercial Technology Office

**Headquarters program office:** OASTT

**Programs/Projects:** Aeronautics Base  
R&T, Technology Transfer

**Special recognition:** Cosmic Award

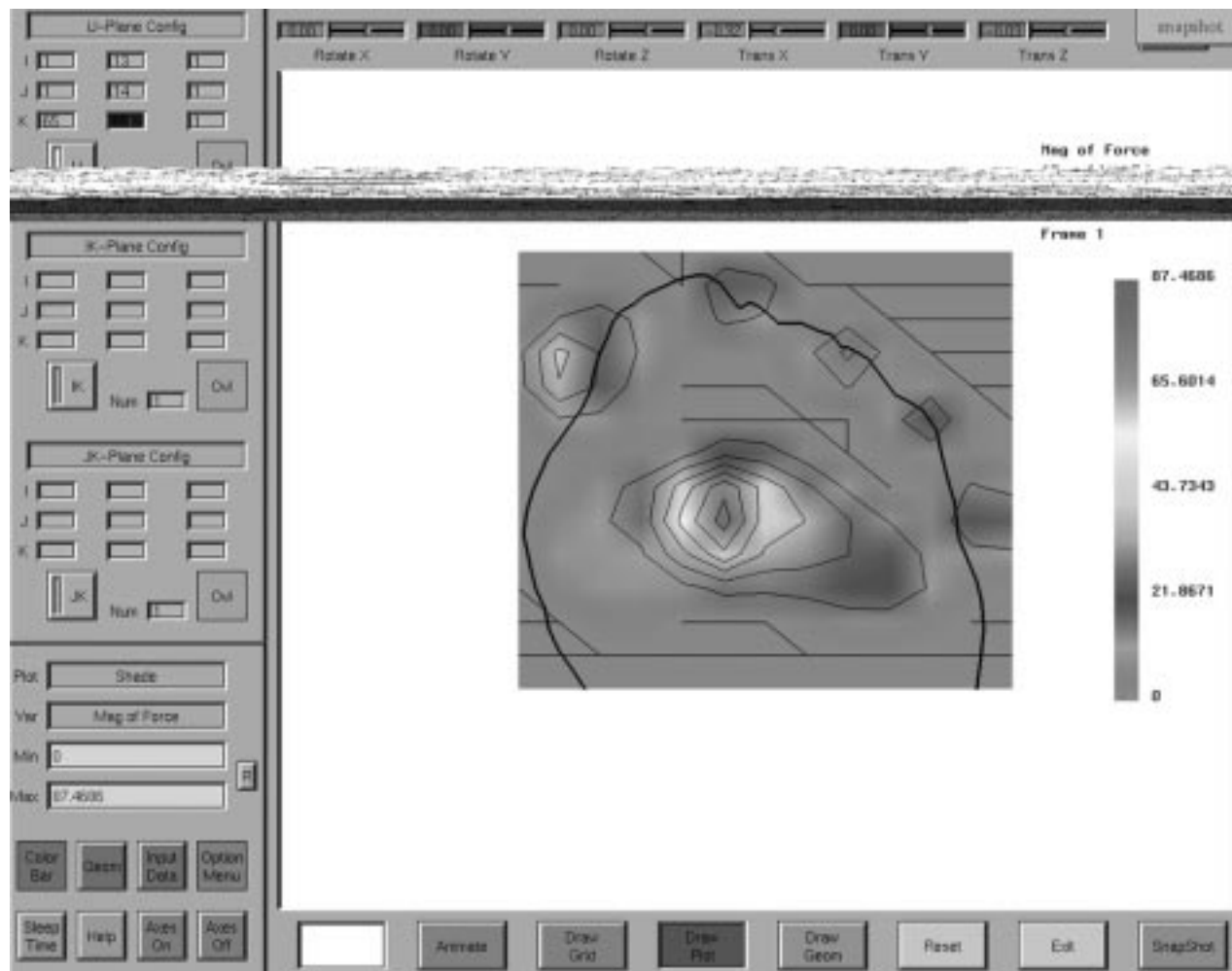


Image of foot contour from sensor pad displayed on IDDS.



# NASA Headquarters Program Offices

<b>ARL</b>	Army Research Laboratory
<b>DoD</b>	Department of Defense
<b>OASTT</b>	Office of Aeronautics and Space Transportation Technology
<b>OLMSA</b>	Office of Life & Microgravity Sciences & Applications
<b>OMTPE</b>	Office of Mission to Planet Earth
<b>OSF</b>	Office of Space Flight
<b>OSMA</b>	Office of Safety and Mission Assurance
<b>OSS</b>	Office of Space Science
<b>USAF</b>	United States Air Force

# Programs and Projects That Support or Will Benefit From This Research

<b>ACTS</b>	Advance Communication Technology Satellite
<b>AEAP</b>	Atmospheric Effects of Aviation Project
<b>AITP</b>	Aerospace Industry Technology Program
<b>APU</b>	Auxilliary Power Units
<b>ART</b>	Advanced Reusable Technologies
<b>ASCOT</b>	Airframes Systems Concept to Test (NASA Langley Research Center)
<b>ASCR</b>	Advanced Subsonic Combustor Rig
<b>AST</b>	Advanced Subsonic Technology
<b>ATM</b>	Asynchronous Transfer Mode
<b>ATMS</b>	Advanced Technology & Mission Studies
<b>AXAF</b>	Advanced X-Ray Astrophysics Facility
<b>CARES</b>	Ceramics Analysis and Reliability Evaluations of Structures
<b>CM-1</b>	Combustion Module-1
<b>EO-1</b>	Earth Observer-1 spacecraft
<b>EOS</b>	Earth Observing System
<b>EPM</b>	Enabling Propulsion Materials
<b>EWT</b>	Embedded Web Technology
<b>FQE</b>	Fast Quiet Engine
<b>FSDC</b>	Fiber Supported Droplet Combustion
<b>GIBN</b>	Global Interoperability for Broadband Networks
<b>HEDS</b>	Human Exploration and Development of Space
<b>HISTEC</b>	High Stability Engine Control
<b>HITEMP</b>	Advanced High Temperature Engine Materials Technology Program
<b>HOSS</b>	Hydrogen On-Orbit Storage and Supply Experiment
<b>HOST</b>	Turbine Engine Hot Section Technology
<b>HPCCP</b>	High Performance Computing and Communications
<b>HSCT</b>	High Speed Civil Transport
<b>HSR</b>	High Speed Research
<b>HST</b>	Hubble Space Telescope
<b>IHPTET</b>	Integrated High Performance Turbine Engine Technology
<b>In-STEP</b>	In-Space Technology Experiments Program
<b>ISS</b>	International Space Station
<b>ISUS</b>	Integrated Solar Upper Stage
<b>JSF</b>	Joint Strike Fighter
<b>LPT</b>	Low Pressure Turbine
<b>MCSA</b>	Mir Cooperative Solar Array
<b>Mir</b>	Russian space station Mir
<b>MSL</b>	Microgravity Science Laboratory
<b>MSL-1R</b>	Microgravity Science Laboratory-First Reflight
<b>MTPE</b>	Mission to Planet Earth
<b>NASP</b>	National Aerospace Plane
<b>NCC</b>	National Combustion Code
<b>NCP</b>	National Cycle Program
<b>NII/GII</b>	National and Global Information Infrastructure
<b>NPSS</b>	Numerical Propulsion System Simulation
<b>NREN</b>	NASA Research and Education Network
<b>OBP</b>	On-Board Propulsion
<b>PHSV</b>	Propulsion for Highly Survivable Vehicles
<b>P&amp;PM</b>	Physics and Process Modeling

<b>PPT</b>	Pulsed Plasma Thruster
<b>ReCAT</b>	Reduced Cost of Air Travel
<b>RLV</b>	Reusable Launch Vehicles
<b>SGE</b>	Smart Green Engine
<b>SSE</b>	Shooting Star Experiment
<b>STS</b>	Space Transportation System
<b>USAF</b>	United States Air Force
<b>USML</b>	United States Microgravity Laboratory
<b>USMP</b>	United States Microgravity Payload
<b>VTRE</b>	Vented Tank Resupply Experiment
<b>X2000</b>	Deep Space Development Program
<b>X-33</b>	Replacement for space shuttles

# Index of Authors and Contacts

Both authors and contacts are listed in this index. Articles start on the page numbers following the names.

- A**  
Abbott, John M. 168  
Allen, Jeffrey S. 132  
Alston, Dr. William B. 24  
Anderson, Robert C. 75
- B**  
Baez, Anastacio N. 41  
Banks, Bruce A. 48  
Barnhart, Paul J. 4, 5  
Bartolotta, Dr. Paul A. 169  
Bauman, Steven W. 164  
Bencic, Timothy J. 158  
Berton, Jeffrey J. 3  
Biesiadny, Tom J. 85  
Bobinsky, Eric A. 155  
Bright, Michelle M. 60  
Brindley, Dr. William J. 25  
Britton, Doris L. 35  
Brown, Dr. Gerald V. 112, 115, 117
- C**  
Carlisle, Karen L. 131  
Castelli, Michael G. 100  
Castner, Raymond S. 89  
Chato, David J. 91, 93  
Choi, Dr. Benjamin B. 112  
Choi, Dr. Sung R. 102, 103  
Clark, David A. 152, 154  
Colantonio, Dr. Renato O. 124  
Commercial Technology Office 168–174  
Concus, Paul 130  
Curran, Dr. Frank M. 136  
Cuy, Michael D. 53
- D**  
Dalton, Penni J. 138  
Daniele, Carl J. 165  
de Groh, Kim K. 43  
de Groot, Dr. Wim A. 38  
Decker, Dr. Arthur J. 58  
DeLaat, John C. 61  
Delvigs, Dr. Peter 23  
Dever, Joyce A. 44  
Doherty, Michael P. 128  
Donovan, Richard M. 49  
Draper, Susan L. 12
- E**  
Eldridge, Dr. Jeffrey I. 19  
Ellis, David L. 13  
Ellis, Rod 108  
Ensworth, Clint B., III 139
- F**  
Ferguson, B.L. 25  
Ferguson, Dr. Dale C. 31  
Finn, Robert 130  
Fite, E. Brian 58, 158  
Foltz, David A. 155  
Forsgren, Roger C. 156  
Fralick, Gustave C. 52  
Freborg, A.M. 25  
Fusaro, Robert L. 114
- G**  
Gabb, Dr. Timothy P. 13  
Garg, Dr. Anita 13  
Gayda, Dr. John 13, 15  
Goldsby, Dr. Jon C. 16  
Gura, Daniel V. 161  
Gyekenyesi, Dr. John P. 103
- H**  
Hack, Kurt J. 146  
Haggard, John 122  
Harrington, Douglas E. 86  
Hawersaat, Bob W. 131  
Hicks, Dr. Yolanda R. 75  
Hoberecht, Mark A. 36  
Hoffman, David J. 140, 142  
Hojnicki, Jeffrey S. 142  
Holdeman, Dr. James D. 77  
Hopkins, Dale A. 97, 98, 170  
Hughes, William O. 163  
Hurst, Janet B. 17  
Hwang, Dr. Danny P. 85
- I**  
Irvine, Thomas B. 157  
Ivancic, William D. 65
- J**  
Jacobson, Dr. Nathan S. 27  
Jacqmin, Dr. David A. 143  
Jadaan, Osama M. 110  
Jankovsky, Robert S. 40
- Janosik, Lesley A. 104, 109, 110  
Jaworske, Dr. Donald A. 46  
Johns, Albert L. 87  
Johnson, Dr. Dexter 112, 115  
Johnston, Dr. J. Christopher 28  
Jules, Kenol 4
- K**  
Kannmacher, Kevin 24  
Kascak, Albert F. 117  
Kautz, Harold E. 105  
Kerslake, Thomas W. 140, 142, 143, 145  
Klann, Gary A. 160, 164  
Klem, Mark D. 148  
Kolecki, Joseph C. 32  
Kowalski, David 156  
Kunath, Richard R. 171  
Kurkov, Dr. Anatole P. 118
- L**  
Lam, David W. 88  
Landis, Geoffrey A. 34  
Lawrence, Dr. Charles 6  
Lee, Dr. Chi-Ming 78  
Lee, Dr. Richard Q. 69  
Lee, Ho-Jun 98  
Lei, Dr. Jih-Fen 53  
Lekan, Jack F. 132, 134  
Lerch, Brad A. 108  
Ling, Jerri S. 128  
Lissenden, Cliff J. 108  
Liu, Dr. Nan-Suey 73, 74  
Locke, Dr. Randy J. 75
- M**  
Macosko, Robert P. 49  
Macri, Frank 24  
Manthey, Lori A. 2  
Manzo, Michelle A. 37  
Mason, Lee S. 145  
May, James E. 62  
McKissock, David B. 139  
McNelis, Anne M. 163  
McNelis, Nancy B. 94  
Meador, Dr. Mary Ann B. 28  
Meador, Dr. Michael A. 23  
Mehmed, Oral 58, 115, 118  
Melis, Matthew E. 6, 99

Miller, Dr. Robert A. 30  
Miller, Thomas B. 37  
Miranda, Dr. Félix A. 67  
Morscher, Gregory N. 18

## **N**

Nadell, Shari-Beth 5  
Nathal, Dr. Michael V. 12  
Nayagam, Dr. Vedha 122, 124  
Nemeth, Noel N. 109  
Neudeck, Dr. Philip G. 54, 56  
Neumann, Eric S. 134  
Nguyen, Dr. Quang-Viet 79

## **O**

Oeftering, Richard C. 162  
Owens, Jay C. 173

## **P**

Paduano, James D. 60  
Palaszewski, Bryan A. 80, 82  
Patnaik, Dr. Surya N. 97  
Patterson, Richard L. 47  
Paxson, Daniel E. 70  
Pepper, Dr. Stephen V. 20  
Pereira, Dr. J. Michael 12, 99  
Peterson, Todd T. 136  
Petrus, G.J. 25  
Powell, J. Anthony 57  
Powers, Lynn M. 109, 110

## **R**

Raju, Dr. Manthena S. 73, 74  
Raman, Dr. Ganesh 90  
Reminder, Robert J. 161  
Revilock, Duane M. 99  
Richard, Jacques 52  
Riddlebaugh, Stephen M. 172  
Roberts, Dr. Gary D. 99  
Roeder, James W., Jr. 160  
Romanofsky, Robert R. 67  
Ronney, Prof. Paul 127  
Roth, Dr. Don J. 111  
Rutledge, Sharon K. 48

## **S**

Salem, Jonathan A. 102  
Saravanos, Dimitrios A. 98  
Scheiman, David A. 140  
Shaw, Dr. Robert J. 2  
Sheldon, David W. 161  
Shyne, Rickey J. 72  
Siebert, Mark W. 32  
Smith, Timothy D. 95

Sohn, Dr. Ki-Hyeon 72  
Soltis, James V. 42  
Spakovzsky, Zoltan 60  
Spees, John A. 24  
Speth, Randall C. 147  
Steffen, Christopher J. 95  
Stegeman, James D. 174  
Steinetz, Dr. Bruce M. 119  
Strazisar, Dr. Anthony J. 60  
Sutter, Dr. James K. 24

## **T**

Taghavi, Dr. Ray 90  
Thompson, Dennis M. 134  
Thorp, Scott A. 58  
Tomsik, Thomas M. 94  
Truong, Long V. 51  
Tuma, Dr. Margaret L. 156  
Tyo, Richard A. 165

## **U**

Urban, Dr. David L. 125

## **V**

Vannucci, Raymond D. 23  
Vannuyen, Thomas 156, 161  
Veres, Joseph P. 8  
Viterna, Dr. Larry A. 148  
von Deak, Thomas C. 66

## **W**

Weigl, Harald J. 60  
Weiland, Dr. Karen J. 127  
Weislogel, Mark M. 130  
Welch, Dr. Gerard E. 70  
Wernet, Dr. Mark P. 59  
Wey, Dr. Chowen C. 84  
Wilson, Jack 70  
Wnuk, Stephen P. 53  
Wolter, John D. 89  
Wozniak, Walter A. 156

## **Y**

York, David W. 165  
Yungster, Dr. Shaye 95

## **Z**

Zakrajsek, June F. 64  
Zaller, Michelle M. 75  
Zaman, Dr. Afroz J. 69  
Zaman, Dr. Khairul 90  
Zehe, Dr. Michael J. 22  
Zhu, Dongming 30



REPORT DOCUMENTATION PAGE			Form Approved OMB No. 0704-0188	
Public reporting burden for this collection of information is estimated to average 1 hour per response, including the time for reviewing instructions, searching existing data sources, gathering and maintaining the data needed, and completing and reviewing the collection of information. Send comments regarding this burden estimate or any other aspect of this collection of information, including suggestions for reducing this burden, to Washington Headquarters Services, Directorate for Information Operations and Reports, 1215 Jefferson Davis Highway, Suite 1204, Arlington, VA 22202-4302, and to the Office of Management and Budget, Paperwork Reduction Project (0704-0188), Washington, DC 20503.				
1. AGENCY USE ONLY (Leave blank)		2. REPORT DATE April 1998		3. REPORT TYPE AND DATES COVERED Technical Memorandum
4. TITLE AND SUBTITLE  Research & Technology 1997			5. FUNDING NUMBERS  None	
6. AUTHOR(S)				
7. PERFORMING ORGANIZATION NAME(S) AND ADDRESS(ES)  National Aeronautics and Space Administration Lewis Research Center Cleveland, Ohio 44135-3191			8. PERFORMING ORGANIZATION REPORT NUMBER  E-10948	
9. SPONSORING/MONITORING AGENCY NAME(S) AND ADDRESS(ES)  National Aeronautics and Space Administration Washington, DC 20546-0001			10. SPONSORING/MONITORING AGENCY REPORT NUMBER  NASA TM-98-206312	
11. SUPPLEMENTARY NOTES  Responsible person, Walter S. Kim, organization code 9400, (216) 433-3742.				
12a. DISTRIBUTION/AVAILABILITY STATEMENT  Unclassified-Unlimited Subject Categories: 01 and 31  This publication is available from the NASA Center for AeroSpace Information, (301) 621-0390.			12b. DISTRIBUTION CODE	
13. ABSTRACT (Maximum 200 words)  This report selectively summarizes the NASA Lewis Research Center's research and technology accomplishments for fiscal year 1997. It comprises 134 short articles submitted by the staff scientists and engineers. The report is organized into five major sections: Aeronautics, Research and Technology, Space, Engineering and Technical Services, and Technology Transfer. A table of contents and an author index have been included to assist the reader in finding articles of special interest. This report is not intended to be a comprehensive summary of all research and technology work done over the past fiscal year. Most of the work is reported in Lewis-published technical reports, journal articles, and presentations prepared by Lewis staff and contractors (for abstracts of these Lewis-authored reports (as well as some complete reports), visit the Lewis Technical Report Server (LeTRS) on the World Wide Web— <a href="http://letrs.lerc.nasa.gov/LeTRS/">http://letrs.lerc.nasa.gov/LeTRS/</a> ). In addition, university grants have enabled faculty members and graduate students to engage in sponsored research that is reported at technical meetings or in journal articles. For each article in this report, a Lewis contact person has been identified, and where possible, reference documents are listed so that additional information can be easily obtained. The diversity of topics attests to the breadth of research and technology being pursued and to the skill mix of the staff that makes it possible. For more information about Lewis' research, visit us on the World Wide Web ( <a href="http://www.lerc.nasa.gov">http://www.lerc.nasa.gov</a> ). Also, this document is available on the World Wide Web ( <a href="http://www.lerc.nasa.gov/WWW/RT/">http://www.lerc.nasa.gov/WWW/RT/</a> ).				
14. SUBJECT TERMS  Aeronautics; Aerospace engineering; Space flight; Space power; Materials; Structures; Electronics; Space experiments; Technology transfer			15. NUMBER OF PAGES 193	
			16. PRICE CODE A09	
17. SECURITY CLASSIFICATION OF REPORT  Unclassified	18. SECURITY CLASSIFICATION OF THIS PAGE  Unclassified	19. SECURITY CLASSIFICATION OF ABSTRACT  Unclassified	20. LIMITATION OF ABSTRACT	